1-1-2012

Understanding the gender-based mechanism of mso in als mice: a metabolic characterization of the sod1-g93a mouse model

Monica Ann Bame
Wayne State University,

UNDERSTANDING THE GENDER-BASED MECHANISM OF MSO TREATMENT IN ALS MICE: A METABOLIC CHARACTERIZATION OF THE SOD1-G93A MOUSE MODEL

by

MONICA A. BAME

DISSERTATION

Submitted to the Graduate School

of Wayne State University,

Detroit, Michigan

in partial fulfillment of the requirements

for the degree of

DOCTOR OF PHILOSOPHY

2012

MAJOR: BIOCHEMISTRY AND
MOLECULAR BIOLOGY

Approved by:

_____

Advisor Date

_____

_____

_____

TABLE OF CONTENTS

List of Figures……iv

List of Tables……vii

CHAPTER 1 – INTRODUCTION……1

1.1 Biology of the Nervous System……1

1.2 Amyotrophic Lateral Sclerosis……7

1.2.1 Amyotrophic Lateral Sclerosis in General……7

1.2.2 Causes of ALS……9

1.2.3 Molecular Mechanisms Underlying ALS Pathogenesis……18

1.2.3.1 Glutamate Excitotoxicity……19

1.2.3.2 Mitochondrial Dysfunction and Oxidative Stress……23

1.2.3.3 Dysfunctional Protein Quality Control Mechanisms……26

1.2.3.4 Aberrant mRNA Processing……31

1.2.3.5 Neurotrophic Factor Dysregulation……35

1.2.3.6 Neuroinflammation……36

1.2.4 Diagnosis and Treatments of ALS……44

1.3 Models of ALS……47

1.4 Purpose of the Study……57

CHAPTER 2 – THE GENDER-SPECIFIC EFFECT OF MSO ON SURVIVAL……60

2.1 Introduction……60

2.1.1 Glutamine Synthetase……60

2.1.2 L-Methionine Sulfoximine……63

2.1.3 Effect of Gender on Lifespan, Disease Progression, and the Response to Methionine Sulfoximine……68

2.2 Materials and Methods……69

2.3 Results……...72

2.4 Discussion……87

CHAPTER 3 – THE BIOCHEMICAL EFFECTS OF MSO TREATMENT ON ALS MICE……92

3.1 Introduction……92

3.1.1 Amino Acid Metabolism……92

3.1.2 L-Glutamine and Nitrogen Metabolism……97

3.1.3 The Effects of Gender and MSO Treatment on Nitrogen Metabolism in SOD1 G93A mice……100

3.2 Materials and Methods……105

3.3 Results……111

3.3.1 Glutamine Synthetase Activity in the CNS……111

3.3.2 Glutaminase Activity in the Brain……128

3.3.3 Plasma Metabolite Analysis……137

3.3.4 Nitrogen Metabolism in the Liver……158

3.3.5 The Effects of Ovariectomization on Enzyme Activity and Plasma Metabolites……172

3.4 Discussion……177

3.4.1 Glutamine Synthetase Activity in the CNS……177

3.4.2 Glutaminase Activity in the Brain……180

3.4.3 Plasma Metabolite Analysis……180

3.4.3.1 Plasma Ammonia Levels……180

3.4.1.2 Plasma Metabolites in 50 Day Untreated Mice……181

3.4.1.3 Plasma Metabolites in 70 Day Saline-treated Mice……185

3.4.1.4 Plasma Metabolites in 70 Day MSO-treated Mice……187

3.4.1.5 Nitrogen Metabolism in the Liver……191

3.4.1.6 The Effects of Ovariectomization on Enzyme Activity and plasma metabolites……194

3.5 Future Experiments……..……...195

APPENDIX A – 50 DAY PLASMA METABOLITE COMPARISONS……..198

APPENDIX B – 70 DAY SALINE-TREATED PLASMA METABOLITE COMPARISONS……..203

APPENDIX C – 70 DAY MSO-TREATED PLASMA METABOLITE COMPARISONS…….208

APPENDIX D – THE EFFECTS OF OVARIECTOMIZATION ON PLASMA METABOLITES…….214

References…..…….215

Abstract…...……..260

Autobiographical Statement……..……263

LIST OF FIGURES

Figure 1.1.1	Overview of spinal cord structure and spinal nerves	2
Figure 1.1.2	Basic cellular interactions in the central nervous system	4
Figure 1.2.2.1	Amino acid sequence of the SOD-1 protein	13
Figure 1.2.3.1	Glutamatergic signaling in the central nervous system	21
Figure 2.1.2.1	Chemical structure of MSO and analogous compounds	65
Figure 2.3.1	Kaplan-Meier survival curves for MSO's effect on the lifespan of SOD1 G93A mice	73
Figure 2.3.2	Kaplan-Meier survival curves for MSO's effect on the longevity of each gender	76
Figure 2.3.3	Hang-time data for female and male mice treated with saline and 20 mg/kg MSO	78
Figure 2.3.4	Kaplan-Meier hang-time competence curves using zero hang-time (complete inability to hang on to a wire grid) as the terminal event	79
Figure 2.3.5	Kaplan-Meier survival curves of MSO's effect on longevity in the absence of sex hormones	82
Figure 2.3.6	Kaplan-Meier hang-time competence curves (using zero hang-time as hang-time as the terminal event) for gonadectomized mice	83
Figure 2.3.7	Kaplan-Meier survival plots comparing the longevity of saline-treated mice with intact gonads to those that have undergone gonadectomy	85
Figure 2.3.8	Kaplan-Meier hang-time competence plots comparing saline-treated mice with intact gonads to those that have undergone gonadectomy	86
Figure 3.1.1.1	The common amino acids	94
Figure 3.1.1.2	The γ-glutamyl cycle of amino acid uptake	96
Figure 3.1.2.1	The urea cycle	99
Figure 3.3.1.1	Brain glutamine synthetase activity in wild-type and SOD1 mice	113
Figure 3.3.1.2	Spinal cord glutamine synthetase activity in wild-type and SOD1 mice	115
Figure 3.3.1.3	Brain glutamine synthetase activity broken down by gender and genotype	117

Figure 3.3.1.4 Spinal cord glutamine synthetase activity broken down by gender and genotype……...119

Figure 3.3.1.5 Brain glutamine synthetase activity in saline and MSO-treated mice……...121

Figure 3.3.1.6 Spinal cord glutamine synthetase activity in saline and MSO treated mice……..123

Figure 3.3.1.7 Brain glutamine synthetase activity broken down by gender and genotype……...125

Figure 3.3.1.8 Spinal cord glutamine synthetase activity broken down by gender and genotype……...127

Figure 3.3.2.1 Specific activity of brain glutaminase in wild-type and SOD1 mice…….130

Figure 3.3.2.2 Brain glutaminase activity broken down by gender and genotype……..132

Figure 3.3.2.3 The effects of MSO treatment on glutaminase activity……134

Figure 3.3.2.4 Brain glutaminase activity of saline and MSO-treated mice broken down by gender and genotype……..136

Figure 3.3.3.1 Plasma ammonia concentrations in wild-type and SOD1 mice……...139

Figure 3.3.3.2 Plasma ammonia concentrations broken down by gender and genotype……...141

Figure 3.3.3.3 The effects of MSO treatment on plasma ammonia levels……...143

Figure 3.3.4.1 Specific activity of liver CPSI in wild-type and SOD1 mice……..160

Figure 3.3.4.2 Specific activity of liver CPSI broken down by gender and genotype……...162

Figure 3.3.4.3 The effects of MSO treatment on CPSI activity in presymptomatic wild-type and SOD1 mice……...164

Figure 3.3.4.4 Specific activity of liver glutamine synthetase activity in wild-type and SOD1 mice……167

Figure 3.3.4.5 Specific activity of liver GS broken down by gender and genotype……169

Figure 3.3.4.6 The effects of MSO treatment on liver GS activity in presymptomatic wild-type and SOD1 mice……...171

LIST OF TABLES

Table 1.2.2.1	List of genetic mutations associated with ALS	11
Table 1.2.2.2	List of genes found to have SALS-associated mutations	16
Table 1.3.1	SOD1 mutations expressed in transgenic mouse models of ALS	54
Table 2.3.1	Summary of survival comparisons and associated statistical values	75
Table 2.3.2	Summary of hang-time competence comparisons and associated statistical values	80
Table 3.3.3.1	Plasma metabolite differences between 50 day old untreated and 70 day old saline-treated SOD1 and wild-type mice	145
Table 3.3.3.2	Plasma metabolite profiles of 50 and 70 day old mice broken down by gender	148
Table 3.3.3.3	Gender differences in plasma metabolites of wild-type and SOD1 mice	151
Table 3.3.3.4	The effects of MSO treatment on plasma metabolite levels of SOD1 mice	154
Table 3.3.3.5	Gender-specific changes in plasma metabolites with MSO treatment	156
Table 3.3.5.1	The effects of ovariectomization on enzyme activity in SOD1 females	174
Table 3.3.5.2	The effects of ovariectomization on plasma metabolite levels in SOD1 female mice	176
Table A-1	List of all mean 50 day mouse plasma metabolite values grouped by genotype and the corresponding *p* values obtained from the MANOVA	198
Table A-2	List of all mean 50 day female plasma metabolite values grouped by genotype and the corresponding *p* values obtained from the MANOVA	199
Table A-3	List of all mean 50 day male plasma metabolite values grouped by genotype and the corresponding *p* values obtained from the MANOVA	200
Table A-4	List of all mean 50 day wild-type plasma metabolite values grouped by gender and the corresponding *p* values obtained from the MANOVA	201

Table A-5 List of all mean 50 day SOD1 plasma metabolite values grouped by gender and the corresponding *p* values obtained from the MANOVA……..202

Table B-1 List of all mean 70 day saline-treated mouse plasma metabolite values grouped by genotype and the corresponding *p* values obtained from the MANOVA……..203

Table B-2 List of all mean 70 day saline-treated female mouse plasma metabolite values grouped by genotype and the corresponding *p* values obtained from the MANOVA……....204

Table B-3 List of all mean 70 day saline-treated male mouse plasma metabolite values grouped by genotype and the corresponding *p* values obtained from the MANOVA……....205

Table B-4 List of all mean 70 day saline-treated wild-type mouse plasma metabolite values grouped by gender and the corresponding *p* values obtained from the MANOVA……....206

Table B-5 List of all mean 70 day saline-treated SOD1 mouse plasma metabolite values grouped by gender and the corresponding *p* values obtained from the MANOVA……....207

Table C-1 List of all mean 70 day wild-type mouse plasma metabolite values grouped by treatment and the corresponding *p* values obtained from the MANOVA……..208

Table C-2 List of all mean 70 day SOD1 mouse plasma metabolite values grouped by treatment and the corresponding *p* values obtained from the MANOVA……..209

Table C-3 List of all mean 70 day female wild-type mouse plasma metabolite values grouped by treatment and the corresponding *p* values obtained from the MANOVA……..210

Table C-4 List of all mean 70 day female SOD1 mouse plasma metabolite values grouped by treatment and the corresponding *p* values obtained from the MANOVA……..211

Table C-5 List of all mean 70 day male wild-type mouse plasma metabolite values grouped by treatment and the corresponding *p* values obtained from the MANOVA……..212

Table C-6 List of all mean 70 day male SOD1 mouse plasma metabolite values grouped by treatment and the corresponding *p* values obtained from the MANOVA……..213

Table D-1 List of all mean 70 day saline-treated female plasma metabolite values grouped by intact or removed gonads and the corresponding *p* values obtained from the MANOVA……214

CHAPTER 1

INTRODUCTION

1.1 Biology of the Nervous System

The nervous system can be broken down into two parts, the central nervous system (CNS) which is composed of the brain and spinal cord, and the peripheral nervous system (PNS), consisting of nerves, ganglia, and the enteric nervous system which controls the gastrointestinal system (Chapman & Silkwood-Sherer 2000). These two parts of the nervous system come together where nerves enter and exit the spinal cord and the brain, in spinal and cranial nerves respectively. Spinal nerves enter and exit the spinal cord through openings between adjacent vertebrae and correspond roughly to segments of the vertebral column. Figure 1.1.1 (A) shows how the spinal cord is encased in the vertebral column and where spinal nerves join the periphery. Sensory information comes into the spinal cord from the periphery through nerves entering dorsal roots, while motor information leaves the spinal cord through nerves exiting ventral roots, sending motor signals to the periphery (Chapman & Silkwood-Sherer 2000; Squire et al 2008). Spinal nerves handle sensory and motor information from the limbs and trunk. Figure 1.1.1 (B) shows the basic structure of the spinal cord and how dorsal and ventral roots leave the spinal cord and come together to form spinal nerves. Cranial nerves, which emerge from the brain directly, deal with sensory and motor information from the head and neck (Chapman & Silkwood-Sherer 2000; McNeill 1997).

Figure 1.1.1 Overview of spinal cord structure and spinal nerves.

A. The general structure of the spinal column. The spinal cord is encased by the vertebrae with spinal nerves roughly corresponing to each vertebrae, entering the periphery through spaces between them. **B.** The general structure of the spinal cord. Grey matter is found in the center of the spinal cord and consists of neuronal cell bodies that receive sensory information that enters through dorsal roots. Motor information exits the spinal cord through ventral roots. White matter surrounds the grey matter and consists of tracts of myelinated axons that send information up and down the spinal cord.

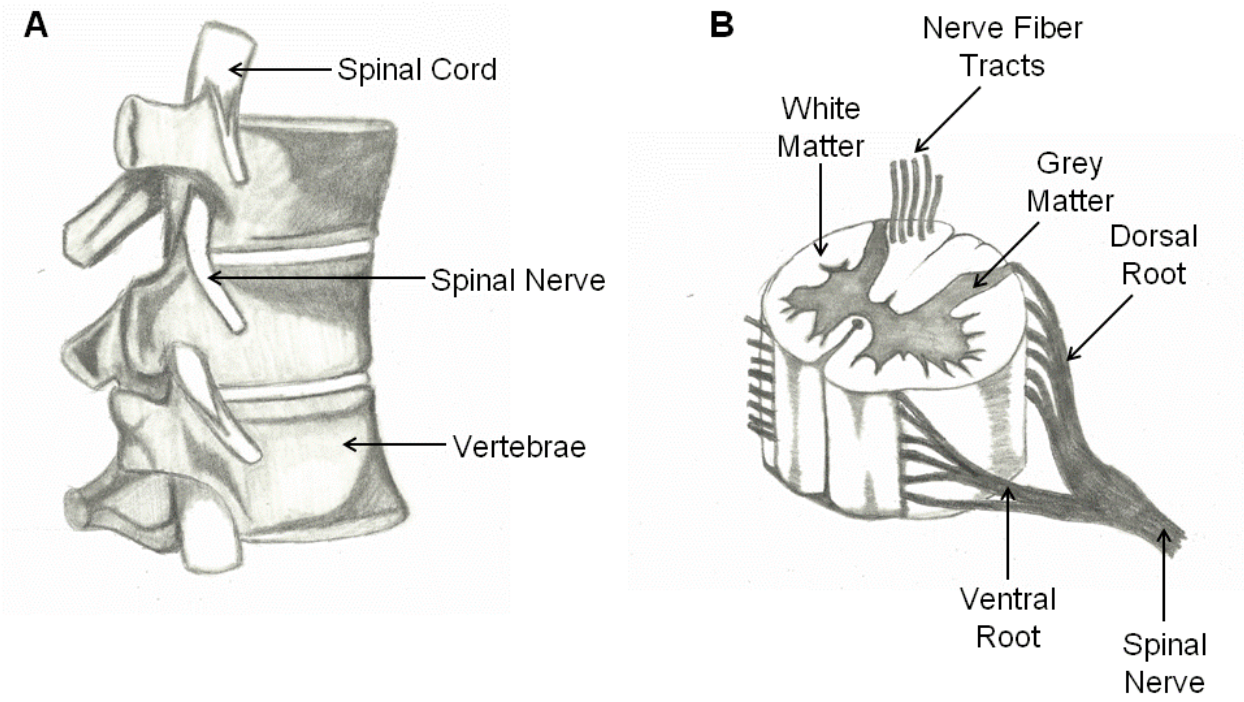

Both the CNS and the PNS are composed of a variety of cell types that work cooperatively to maintain homeostasis and allow for intercellular communication through electrochemical signaling. There are two main types of cells that make up the nervous system, neurons and glial cells.

Neurons are polarized cells that can be divided into distinct sub cellular regions, each of which carries out a different set of functions (Cooper et al 2003; Nestler et al 2001; Squire et al 2008). They come in a variety of shapes and sizes but can be broken down into a basic morphology consisting of three regions: 1) the soma (cell body), containing the nucleus and cytoplasmic organelles; 2) dendrites, which branch from the soma and vary in size, shape, and number depending upon the type of neuron; and 3) a single axon, which is rich in neurofilaments, extending a distance from the cell body to make contacts with other neurons (Cooper et al 2003; Nestler et al 2001; Squire et al 2008). These three basic compartments of a neuron can be seen in Figure 1.1.2. Dendrites, neuronal cell bodies, and unmyelinated axons make up grey matter.

Dendrites receive electrochemical signals from other neurons, which are integrated at the cell body and passed down the axon in the form of action potentials to signal other neurons or organs. In order to send these signals, neurons express a variety of ion channels and pumps to maintain an electrochemical gradient across the membrane. They also express a variety of neurotransmitter receptors coupled to ion channels, which alter the electrochemical gradient for signaling. The connections between pre- and post-synaptic neurons are dynamic, with the formation of new synapses and the removal of unused synapses occurring constantly. Maintaining and resetting electrochemical gradients after an action potential, and synaptic restructuring both require a significant amount of energy which is provided by supporting cells.

Glial cells are a broad category of cells that serve structural and supportive functions in the nervous system. In the CNS there are three main types of glia, oligodendrocytes, astrocytes,

Figure 1.1.2 Basic cellular interactions in the central nervous system.

There is a complex set of interactions that occur between neurons, astrocytes, and oligodendrocytes in the central nervous system. Astrocytes can make several connections with neurons - at the soma, at nodes of Ranvier (between myelin sheaths), and at synapses – while also making connections with blood vessels and other astrocytes. Oligodendrocytes (OL) send out several processes to myelinate multiple axons.

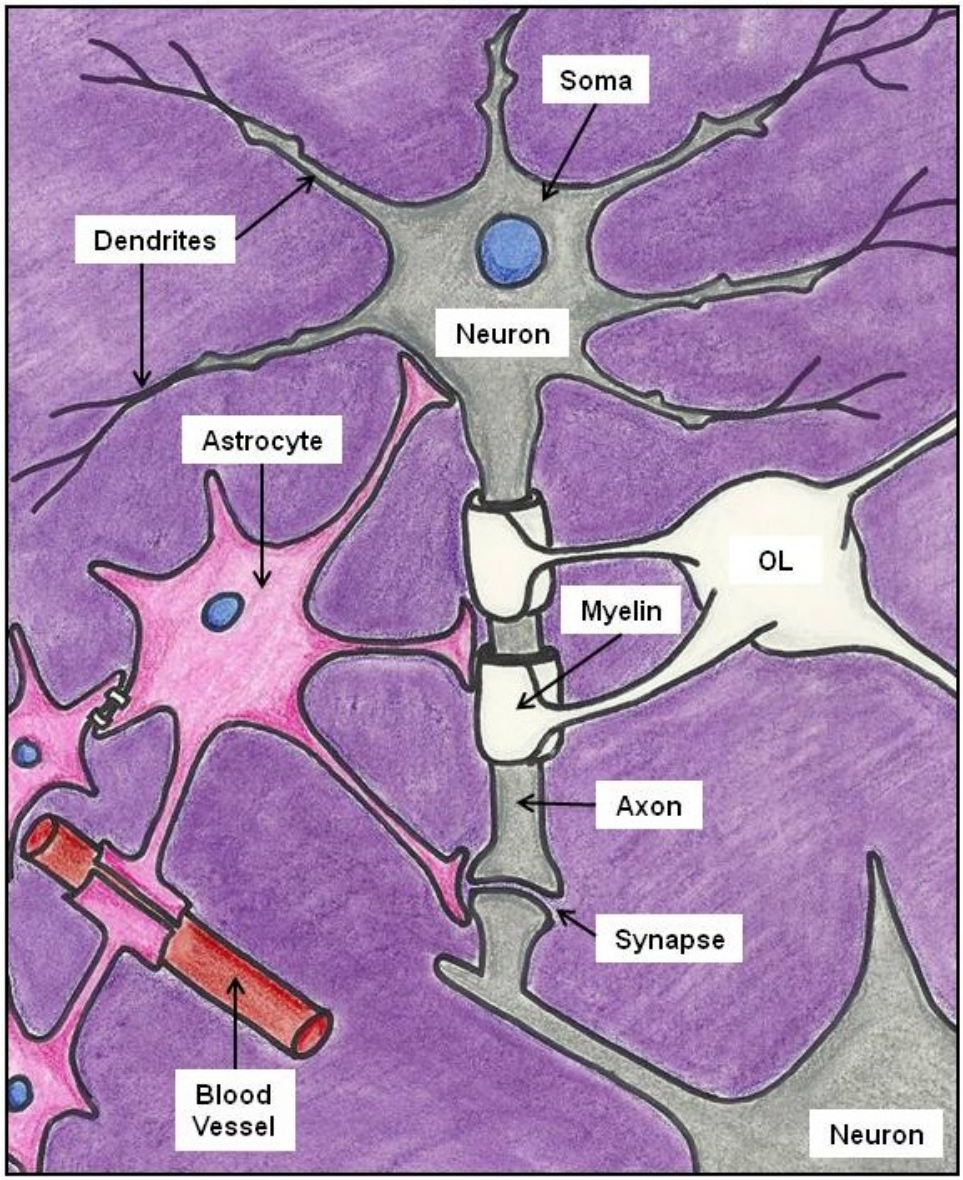

and microglia, whereas the PNS has only one major type of glial cell, Schwann cells (Chapman & Silkwood-Sherer 2000; Squire et al 2008). Both oligodendrocytes and Schwann cells synthesize myelin, a fatty substance that wraps around axons to accelerate the propagation of action potentials. Although they are similar in function, oligodendrocytes and Schwann cells have very different morphological features. Oligodendrocytes have a cell body that gives rise to several processes, each of which is composed of a long, extremely thin layer of plasma membrane that wraps around a portion of an axon to produce myelin. A single oligodendrocyte produces and maintains several myelin sheaths, myelinating segments of multiple axons. Figure 1.1.2 illustrates an oligodendrocyte myelinating an axon in the CNS. Schwann cells, on the other hand, are very thin, pancake-shaped cells that wrap their entire cell body around a single axon segment to produce myelin. As a result, it takes multiple Schwann cells to myelinate a single axon in the PNS. Axons are myelinated in small segments, with gaps called nodes of Ranvier between segments of myelin (Chapman & Silkwood-Sherer 2000; Nestler et al 2001; Squire et al 2008). Myelinated axons have a characteristic white color and make up the portion of the CNS referred to as white matter.

Astrocytes and microglia are two very different types of cells that also serve supporting roles in the CNS. In most areas of the brain, astrocytes make up 20-50% of the volume (Squire et al 2008). They are star-shaped cells, and like oligodendrocytes, extend several processes from their cell bodies. These processes branch out and serve a variety of structural and supportive functions throughout the CNS, and are extremely important in maintaining homeostasis and supporting neuron function (Squire et al 2008). They help form barriers within the CNS, the glia limitans (Squire et al 2008) as well as the blood-brain, blood-cerebrospinal fluid, and blood-spinal cord barriers (BBB, BCSFB, and BSCB respectively), providing protection from pathogens and other types of insults (Abbott 2002; Engelhardt & Coisne 2011). They also extend processes to nodes of Ranvier, synapses, dendrites, and neuronal cell bodies where

they help to buffer ion fluxes during action potentials, remove excess neurotransmitters, and provide much needed metabolic intermediates to active neurons (Fields & Stevens-Graham 2002; Prebil et al 2011; Squire et al 2008; Turner & Adamson 2011). Astrocytes are connected to one another by gap junctions, which allows for the movement of small molecules and ions across the brain parenchyma. Figure 1.1.2 shows some of the interactions that astrocytes can make within the CNS. Astrocytes also produce growth factors and extracellular matrix proteins which act to regulate survival, proliferation, differentiation, and the morphology of other cell types in the nervous system. In addition, astrocytes have the potential to become activated and produce cytokines during injury and infection playing an immunological role as well (Dong & Benveniste 2001; Squire et al 2008).

Microglia are considered to be the resident macrophages of the CNS, which has traditionally been thought of as an immunologically privileged tissue (Murphy et al 2008). The physical barriers produced by astrocytes make it difficult for antibodies and peripheral immune cells, such as natural killer cells, T-cells, and macrophages, to infiltrate the CNS to fight infection. Microglia, which develop from monocytes derived from bone-marrow, have the ability to phagocytose apoptotic cells (Murphy et al 2008; Nicklin et al 2009) and provide the first line of defense during infection. In the case of injury or infection, microglia become reactive, changing their morphology and upregulating molecules involved in immune responses. They can divide and behave like macrophages, secrete cytokines and growth factors, and present antigens to T-cells (Murphy et al 2008; Squire et al 2008; Town et al 2005). Microglia react quickly in response to alterations in their environment and can act in conjunction with astrocytes to regain homeostasis.

In the healthy nervous system, there is a delicate interplay between all of the various cell types which allows for rapid transmission of signals between neurons and a quick response of the person to environmental factors. Astrocytes maintain barriers which separate the CNS from

the circulating blood, selectively allowing the entry of nutrients and peripheral immune cells and the exit of waste, while blocking the entry of pathogens (Abbott 2002; Engelhardt & Coisne 2011; Fields & Stevens-Graham 2002; Redzic 2011; Squire et al 2008). Neurons with myelinated axons communicate quickly with each other through electrochemical signals, which are regulated by astrocytes. During neuronal signaling, astrocytes maintain ion homeostasis at the nodes of Ranvier and at synapses, where they also aid in the removal of excess neurotransmitter to prevent over-signaling (Nestler et al 2001; Squire et al 2008). They are capable of interacting with neurons by expressing neurotransmitter receptors that detect signals from neurons, allowing them to adjust their metabolism accordingly to keep active neurons functioning efficiently (Nestler et al 2001; Prebil et al 2011). Astrocytes, with the help of microglia, monitor the environment and respond accordingly to maintain homeostasis. Neurons are delicate cells and when this homeostasis is disrupted by chemical insult, pathogen infiltration, or other injuries, a cascade of events can occur that result in neuron death, inflammation, and overall dysfunction within the nervous system.

1.2 Amyotrophic Lateral Sclerosis

1.2.1 Amyotrophic Lateral Sclerosis in General

Amyotrophic Lateral Sclerosis (ALS) is a devastating neurodegenerative disease in which the primary target is the motor neuron. Amyotrophy refers to the atrophy of skeletal muscle fibers that occurs when motor neurons die and muscle innervation is lost. Lateral sclerosis refers to the degeneration of neurons in the anterior horn and lateral corticospinal tracts and the gliosis that accompanies this (Wijesekera & Leigh 2009). The disease is commonly referred to as Lou Gehrig's disease after New York Yankee, Lou Gherig, who died of the disease in 1941. The axons of motor neurons gradually die back from the skeletal muscles they innervate, leading to a loss of neuromuscular connections and muscle atrophy. Patients experience

muscle weakness which rapidly turns into paralysis, and eventually succumb to respiratory complications within one to five years of disease onset (Bruijn et al 2004).

ALS is a relatively rare disease, with an overall incidence of about 2 in 100,000 people per year (Alonso et al 2009; Logroscino et al 2008) and a prevalence of about 5 in 100,000 people (Haverkamp et al 1995). The low incidence rate makes it difficult to collect epidemiological data from large numbers of patients, but with better diagnostic and communication technologies, data collection is improving. The incidence of the disease increases after age 40 and peaks somewhere between the late 60s and early 70s, after which the incidence seems to decline (Logroscino et al 2008). The typical age of onset of ALS is between 50 and 60 years of age (Bruijn et al 2004), but there are some rare forms with juvenile onset (Beghi et al 2007). There tends to be a slight male prevalence in the disease, with a male to female ratio of about 3:2 (Wijesekera & Leigh 2009). This gender difference decreases with increasing age and approaches a ratio of 1:1 after age 60 (Haverkamp et al 1995).

The phenotypic characterization of ALS is inconsistent across patients (Logroscino et al 2008). The symptoms of the disease vary, depending upon the area in which motor neurons are affected. Most patients, about 75%, develop early symptoms in the limbs in what is referred to as limb or spinal onset ALS. This can begin in the arms or legs, with the most common symptoms being muscle weakness and wasting. Involuntary muscle twitching and cramping can occur prior to muscle weakness (Wijesekera & Leigh 2009). When symptoms begin in the leg patients may experience some problems walking, whereas patients with arm symptoms have difficulty performing tasks requiring manual dexterity. Typically symptom onset is asymmetrical, affecting only one side of the body, however most patients eventually experience symptoms in other limbs (Wijesekera & Leigh 2009). The remaining 25% of patients have symptom onset occurring in the head or neck, which is referred to as bulbar onset ALS. These symptoms typically present themselves as difficulty swallowing or speaking, due to problems

with tongue mobility, and may progress to include facial weakness (Wijesekera & Leigh 2009). Patients with bulbar onset ALS may experience limb symptoms simultaneously, and most patients with limb onset eventually develop bulbar symptoms as well. It is important to note that there is significant heterogeneity in the symptoms of ALS (Beghi et al 2007), which makes the disease difficult to diagnose.

Patients with ALS suffer from degeneration of both upper and lower motor neurons. Upper motor neurons are neurons whose cell bodies reside in the primary motor cortex of the brain, sending their axons down the spinal cord. Lower motor neurons have axons that project into the ventral root and through a spinal nerve to innervate skeletal muscle, with their cell bodies remaining in the ventral horn of the spinal cord (Chapman & Silkwood-Sherer 2000). Upper motor neurons in the primary cortex send signals down the spinal cord and synapse on lower motor neurons, which then send signals to skeletal muscles in the periphery (Chapman & Silkwood-Sherer 2000). When either type of motor neuron is affected by the disease, there is a loss of trophic factor signaling between synapsing neurons, which can result in dying back of all of the motor neurons in the pathway leading to paralysis.

1.2.2 Causes of ALS

ALS is a heterogeneous disorder with a variety of factors, both genetic and environmental, believed to play a role in pathogenesis of the disease. Patients with ALS can be broken down into two groups, those with a hereditary form of ALS, Familial ALS (FALS), and those with no known family history of ALS, referred to as Sporadic ALS (SALS). SALS is much more common, accounting for the majority of ALS cases, while FALS accounts for only 5-10% of all cases of the disease (Bruijn et al 2004; Wijesekera & Leigh 2009). The pathological and clinical characteristics of FALS and SALS are strikingly similar, making it very difficult to distinguish between the two (Beghi et al 2007). Genetic forms of ALS show a great deal of heterogeneity, with a variety of gene mutations implicated in the cause.

Mutations in 13 genes have been found to be associated with FALS (Table 1.2.2.1). All of these genes are inherited in an autosomal dominant fashion, with the exception of three that are recessive and two with unknown inheritance patterns. The genetic loci of all of these mutations have been determined, however only seven gene products have been positively identified in ALS: 1) superoxide dismutase-1 (SOD1); 2) alsin; 3) senataxin (SETX); 4) vesicle associated protein B (VAPB); 5) angiogenin (ANG); 6) TAR-DNA binding protein-43 (TDP43); and 7) fused in sarcoma (FUS) (Beghi et al 2007; Belzil et al 2009; Bruijn et al 2004; Pasinelli & Brown 2006; Wijesekera & Leigh 2009). Two genes, with unknown products, produce a form of ALS that is associated with frontotemporal dementia (FTD) (Beghi et al 2007; Wijesekera & Leigh 2009). Mutations in chromatin-modifying protein 2B (CHMP2B; also called charged multivesicular body protein 2B) have been found in two ALS patients and seem to be primarily associated with a form of FTD accompanied by ALS, however more research must be done in order to characterize the inheritance pattern of these mutations and their involvement in the disease (Beghi et al 2007; Parkinson et al 2006). Mutations in dynactin (DCTN1), a protein involved in axonal transport, have been associated with a form of lower motor neuron disease and their presence in the genome may increase a person's susceptibility to motor neuron degeneration and the development of ALS (Beghi et al 2007; Wijesekera & Leigh 2009). Another axonal protein, microtubule-associated protein tau (MAPT), is commonly associated with FTD and may also increase the risk of developing ALS.

Table 1.2.2.1 List of genetic mutations associated with ALS

ALS Type	Gene Locus	Gene	Number of Mutations	Inheritance	Onset & Progression	Associated with SALS	Normal Protein Function
ALS1	21q	SOD-1	>100	AD & AR*	Varies with mutation, but usually late onset with fast progression	Yes	Antioxidant enzyme that removes superoxide anions
ALS2	2q33	ALSIN	10	AR	Juvenile onset with slow progression	No	GEF possibly involved in actin organization and vesicular trafficking
ALS3	18q21	TBD	10	AD	Late onset with fast progression	Unknown	Unknown
ALS4	9q34	SETX	3	AD	Early onset with chronic, slow progression	Probably Not	Believed to be a helicase involved in RNA processing
ALS5	15q15	TBD	Unknown	AR	Juvenile onset	Probably Not	Unknown
ALS6	16q21	FUS	12	AD	Late onset with fast progression	Yes	DNA/RNA-binding protein involved in transcriptional activation
ALS7	20ptel-p13	TBD	Unknown	AD	Late onset with fast progression	Unknown	Unknown
ALS8	20q13.3	VAPB	1	AD	Late onset with slow progression	No	Membrane protein found in the plasma membrane and intracellular vesicles
ALS + FTD	9q21-q22	TBD	Unknown	AD	Late onset with frontotemporal dementia	Unknown	Unknown
ALS + FTD	9p21.3	TBD	Unknown	AD	Late onset with frontotemporal dementia	Unknown	Unknown
ALS	14q11.2	ANG	6	AD	Late onset with slow progression	Yes	Protein involved in angiogenesis; May also function as a t-RNA specific ribonuclease
FTD	3	CHMP2B	2	?	Adult onset dementia with ALS; mutations may increase risk of ALS	Unknown	Part of ESCRT-III complex involved in endocytosis
ALS	9p	TDP43	>30	AD	Variable onset and progression; can occur in combination with FTD	Yes	DNA/RNA-binding protein involved in transcriptional repression, translational regulation, and pre-mRNA splicing
LMND	2p13	DCTN1	5	AD	Unknown; mutations may increase risk of ALS	Maybe	Protein involved in a complex responsible for axonal transport
FTD	17q21	MAPT	3	AD	Adult onset frontotemporal dementia; mutations may increase risk of ALS	Maybe	Microtubule-associated protein that modulates the stability of microtubules in axons

AD = autosomal dominant
AR = autosomal recessive
* The SOD1 D90A mutation is the only recessive mutation (Al-Chalabi et al 1998).
GEF = guanine nucleotide exchange factor
ESCRT-III = endosomal sorting complex required for transport-III

Of the seven positively identified genes involved in FALS, superoxide dismutase-1 (SOD1) is probably the most well studied protein, although its involvement in neurodegeneration is still a mystery. SOD1 is a ubiquitously expressed copper/zinc-binding protein that is involved in scavenging reactive oxygen species (ROS) produced during oxidative phosphorylation. Superoxide dismutase catalyzes the reaction between two molecules of superoxide and two protons to produce hydrogen peroxide and oxygen, preventing oxidative damage within the cell (Nelson & Cox 2008). Approximately 15-20% of FALS cases are associated with mutations in the gene encoding SOD1, accounting for only a small portion of all cases of ALS (Beghi et al 2007; Bruijn et al 2004; Orrell et al 1996; Wijesekera & Leigh 2009; Zoccolella et al 2006). Over 100 different ALS-associated mutations have been found in the gene encoding SOD1, most of which are autosomal dominant (Beghi et al 2007; Wijesekera & Leigh 2009). These mutations result in a variety of alterations to the protein, most of which are single-amino acid substitutions that may alter the protein structure to decrease metal binding and increase protein aggregation (Hayward et al 2002; Johnston et al 2000; Rumfeldt et al 2009; Shinder et al 2001; Tiwari & Hayward 2005). Figure 1.2.2.1 shows the amino acid sequence of the SOD1 protein, with the amino acids that can undergo mutations highlighted in green. The enzyme can be mutated in several locations throughout its sequence, including introns (Turner & Talbot 2008). The mechanism by which mutations in the SOD1 protein lead to motor neuron death remain unclear, since the enzyme appears to retain its normal function with most mutations, but are believed to involve a toxic gain of function (Harraz et al 2008; Mali & Zisapels 2008) and the combined effects of its expression in neurons, microglia, and astrocytes (Boillee et al 2006; Yamanaka et al 2008a).

Figure 1.2.2.1 Amino acid sequence of the SOD1 protein.

SOD1 mRNA consists of five exons and four introns and the final protein-product is 153 amino acids in length. The protein can undergo a wide variety of mutations and the amino acids that can be mutated are highlighted in green with the substitutions listed below them. Amino acids involved in Cu/Zn binding are indicated with red lines and the cysteine residues involved in disulfide bond formation are indicated with blue lines. Introns and the 3' untranslated region are shown in purple and the asterisks indicate those that can contain mutations.

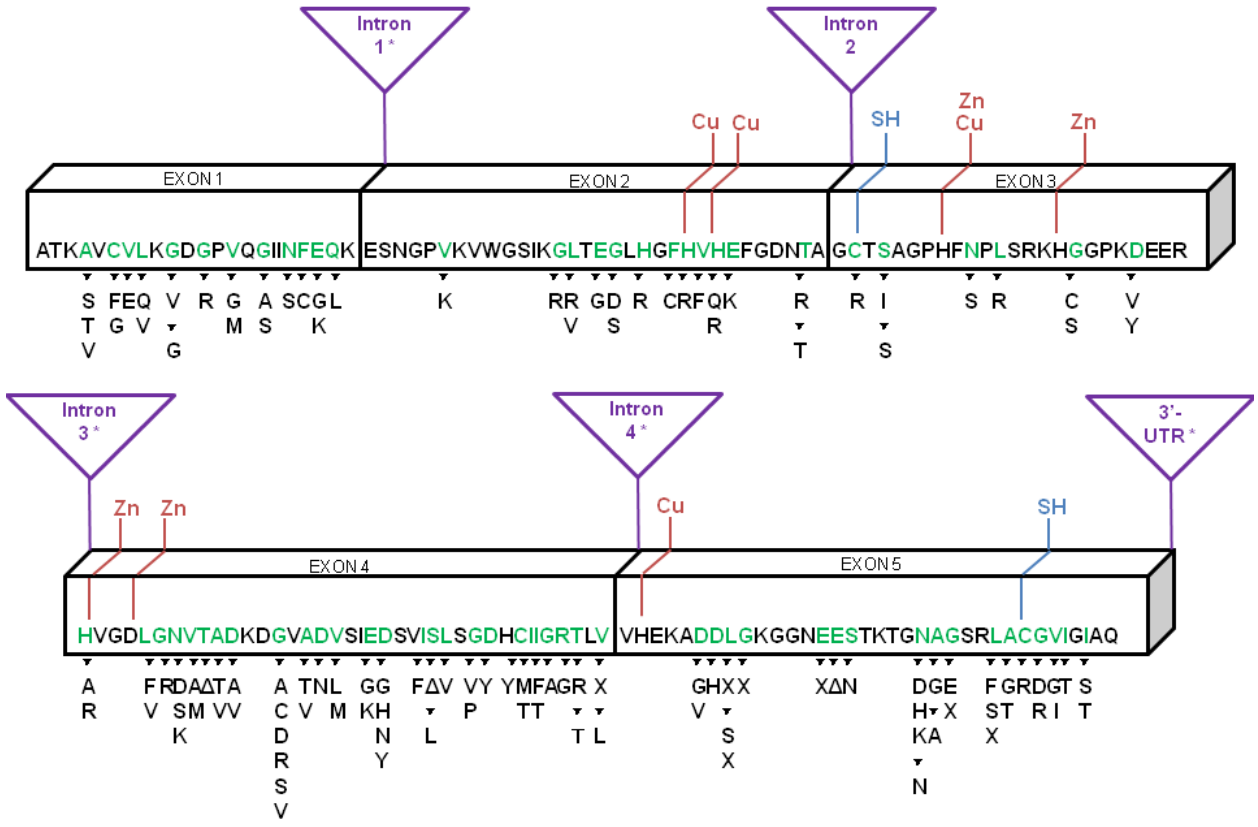

The remaining six genes involved in ALS encode an array of proteins involved in a variety of cellular processes. Alsin, a protein containing three guanine nucleotide exchange factor domains (Yang et al 2001), is a cytosolic protein capable of associating with membrane structures believed to be involved with actin cytoskeleton remodeling and vesicular trafficking (Topp et al 2004). Senataxin, which has been linked to an early onset form of ALS (Chance et al 1998), was discovered to be the ortholog of a yeast RNA helicase (Moreira et al 2004) and is believed to play a role in RNA processing in humans (Beghi et al 2007). Vesicle associated protein B (VAPB) is an integral membrane protein found on the membrane of the endoplasmic reticulum, which is believed to exert its negative effects in ALS by promoting protein aggregation and ER stress (Langou et al 2010; Moumen et al 2011; Nachreiner et al 2010). Angiogenin is a protein involved in angiogenesis that plays a variety of roles within the cell. Under normal conditions angiogenin acts as a ribonuclease, regulating rRNA transcription (Li & Hu 2010), attenuates apoptotic signals (Li et al 2012), and can bind to actin to alter polymerization (Pyatibratov & Kostyukova 2012; Pyatibratov et al 2010). TDP43 is a DNA/RNA-binding protein found in glia and neurons (Swarup et al 2011b) that plays a role in the maintenance of autophagy (Bose et al 2011), regulation of splicing RNA transcripts and the production of micro RNAs (Lee et al 2012a), and may associate with mutant forms of VAPB in ALS (Suzuki & Matsuoka 2011). Like TDP43, FUS (also called TLS for translocated in liposarcoma) is also a DNA/RNA-binding protein. It is found primarily in the nucleus of normal cells but is transported to dendritic spines and is involved in transcription, splicing, and mRNA transport from the nucleus to the cytoplasm (Fujii et al 2005; Wang et al 2008; Yang et al 1998; Zinszner et al 1997). Despite its rare occurrence and the variety of genetic factors involved, studies of FALS have offered insight into the molecular mechanisms underlying motor neuron death and provided potential therapeutic targets and biomarkers of the disease.

FALS research has been able to shed some light on SALS, as some of the mutations involved in hereditary forms of the disease have also been identified in sporadic ALS patients. Table 1.2.2.1 lists the cellular function of the proteins SOD1, ANG, TDP43, and FUS that have been found to undergo mutations and become involved in some cases of SALS. In addition to these, mutations in APEX1 (Hayward et al 1999), HFE (Goodall et al 2005; He et al 2011; Sutedja et al 2007a; Wang et al 2004b), PON (Cronin et al 2007; Slowik et al 2006; Ticozzi et al 2010; Valdmanis et al 2008), PRPH (Corrado et al 2011; Gros-Louis et al 2004; Leung et al 2004), and PGRN (Sleegers et al 2008; Talbot & Ansorge 2006) have also been found to be associated with SALS (Table 1.2.2.2). It is unknown as to whether or not these mutations cause the disease, or if their presence increases the risk of developing ALS (Schymick et al 2007). The association of certain genes with SALS provides some hope that there may be a genetic component to sporadic forms of the disease.

Table 1.2.2.2 List of genes found to have SALS-associated mutations.

Gene	Protein	Normal Protein Function	References
APEX1	Apurinic Endonuclease	DNA repair enzyme that protects against oxidative stress	Hayward *et al.* (1999)
HFE	Human Haemochromatosis Protein	Membrane protein associated with β-2 microglobulin involved in iron metabolism	Wang *et al.* (2004) Goodall *et al.* (2005) Sutedja *et al.* (2007) He *et al.* (2011)
PON	Paraoxonase	Serum enzyme responsible for removing neurotoxins and organophosphates	Slowik *et al.* (2006) Cronin *et al.* (2007) Valdmanis *et al.* (2008) Ticozzi *et al.* (2010)
PRPH	Peripherin	Intermediate filament expressed by peripheral sensory neurons and autonomic nerves	Leung *et al.* (2004) Gross-Louis *et al.* (2004) Corrado *et al.* (2011)
PGRN	Progranulin	Peptide that is secreted and cleaved to form granulin, a growth factor involved in development, wound repair, and inflammation	Talbot & Ansorage (2006) Sleegers *et al.* (2008)

There are a large number of genetic mutations associated with FALS that have the ability to alter a variety of proteins with roles in a multitude of cellular processes which lead to a significant amount of heterogeneity in the disease. To complicate matters further, the inheritance patterns of FALS genes are not strictly followed in all cases and multiple mutations can occur within the same individual (Andersen 2006; Andersen et al 1996; Orrell et al 1996). This had led to the belief that ALS develops through a complex interaction between genetic and environmental factors.

Since most cases of ALS are sporadic and have no known genetic component, exposure to environmental toxins and head injuries are believed to be potential risk factors for developing ALS. Examining patients' occupations has typically been used as a way to evaluate exposure to toxins that may be associated with development of the disease. Workplace exposure to lead, with elevated lead levels found in bone and blood of ALS patients, has been suggested to play a role in the etiology of ALS (Kamel et al 2005; Kamel et al 2002). People exposed to other chemicals commonly associated with construction work, such as paint strippers, lubricating oils, coolants, metals and metal fumes, also show an increased risk in developing ALS (Binazzi et al 2009; Fang et al 2009). One study conducted in Italy showed that professional soccer players had an increased risk of developing the disease (Chio et al 2005), suggesting that head injuries lead to an increased risk of ALS. Patients who had experienced multiple head injuries or who had been injured within a ten year period prior to diagnosis were found to have a threefold higher risk of developing ALS. It was also found that people with head injuries were more likely to have bulbar onset ALS and an earlier age of diagnosis (Chen et al 2007).

Most often the types of studies used to evaluate chemical exposures and injuries associated with ALS involve the use of questionnaires, which also take into consideration other means of exposure to toxins, such as smoking and diet. Several studies have found that smokers have an increased risk in developing ALS (Binazzi et al 2009; Nelson et al 2000;

Sutedja et al 2007b; Weisskopf et al 2004). One study determined that female smokers have a greater risk of developing ALS than male smokers (Weisskopf et al 2004), while another study detected a link between cigarette smoking and bulbar onset ALS (Binazzi et al 2009). Interestingly, an interaction between cigarette smoking and chemical exposure was also observed (Fang et al 2009). This increased risk in ALS with smoking could be directly due to the chemicals found within cigarettes, or chemicals in the cigarettes could induce the expression of metabolic enzymes that alter metabolism in such a way that smokers become more sensitive to other chemicals. With respect to diet, it was found that bulbar onset patients showed an increase in the consumption of cold cuts and a decrease in the consumption of vegetables (Binazzi et al 2009). In a small population of people in Guam, where the incidence of ALS is higher than that of Europe and North America, β-methyl-amino-L-alanine is found in low levels in the diet and has been found in brain tissue of ALS patients and is believed to play a role in the disease (Banack & Murch 2009).

1.2.3 Molecular Mechanisms Underlying ALS Pathogenesis

Genetic analyses of patients with both hereditary and sporadic forms of ALS have identified a wide variety of genes that can be involved in the development of the disease. These genes encode proteins that are involved in several different cellular processes and implicate an array of cellular mechanisms that may become dysfunctional during the disease. Understanding the molecular mechanisms behind the disease is the primary goal of ALS research, as it will aid in the development of pharmacological treatments and possibly uncover biomarkers that may allow for early detection of the disease. There are believed to be six major mechanisms underlying ALS pathogenesis: glutamate excitotoxicity; mitochondrial dysfunction and oxidative stress; dysfunctional protein quality control mechanisms; aberrant RNA processing; neurotrophic factor dysregulation; and neuroinflammation. These mechanisms

overlap to some extent and involve several different cell types. Experimental evidence suggests that these mechanisms may converge at some point to initiate the programmed cell death pathway, as the final mechanism of cell death seems to resemble apoptosis.

1.2.3.1 Glutamate Excitotoxicity

The amino acid glutamate acts as the major excitatory neurotransmitter in the central nervous system where it is released from electrically stimulated neurons in a calcium-dependent fashion (Cooper et al 2003; Nestler et al 2001; Squire et al 2008). Upon stimulation, glutamate is released from the pre-synaptic nerve terminal into the synaptic cleft where it: 1) stimulates the post-synaptic neuron by binding to glutamate receptors; 2) is taken up by astrocytes; and 3) may be taken back up by the pre-synaptic neuron for recycling (Figure 1.2.3.1). In healthy individuals, glutamate binds to a variety of glutamate receptors on post-synaptic neurons, some of which are coupled to ion channels that when stimulated, allow for an influx of calcium to induce an action potential. Since overstimulation of these receptors can lead to a massive influx of calcium resulting in apoptosis, there are mechanisms in place to remove glutamate from the synapse. Both pre-synaptic neurons and astrocytes express excitatory amino acid transporters (EAATs) which remove excess glutamate from the synapse. Glutamate taken up by pre-synaptic neurons can be repackaged into vesicles for later use or converted to aspartate by the mitochondrial enzyme aspartate transaminase (Nestler et al 2001). The majority of the glutamate in the synapse is taken up by astrocytes where it is converted to glutamine by the enzyme glutamine synthetase (GS) (Cooper et al 2003; Nestler et al 2001; Squire et al 2008). GS plays an extremely important role in the central nervous system as it not only detoxifies glutamate, but it removes ammonia as well. The glutamine produced in astrocytes is then passed back to neurons where it is converted to glutamate by mitochondrial glutaminase and then packaged into vesicles for later use. This process of astrocytic removal of glutamate, its

conversion to glutamine by GS, and the transport of glutamine back to neurons is referred to as the glutamate-glutamine cycle and its importance in the CNS is illustrated in Figure 1.2.3.1.

Figure 1.2.3.1.1 Glutamatergic signaling in the central nervous system.

Once released from the pre-synaptic neuron, there are three possible fates of glutamate in the synapse. **A.** Glutamate can interact with ionotropic glutamate receptors (NMDA, AMPA, or kainate receptors) on the post-synaptic neuron, which are coupled to ion channels and allow calcium to flow into the cell. Glutamate can also bind to metabotropic receptors which are coupled to g-proteins and produce their effects more slowly. **B.** Glutamate can be taken up by the pre-synaptic cell where it is recycled for subsequent action potentials. **C.** The majority of the glutamate is taken up by astrocytes, where glutamine synthetase (GS) converts it to glutamine. The glutamine is then transported back to the pre-synaptic neuron through SN1 transporters where it is converted back to glutamate by mitochondrial glutaminase and packaged into vesicles.

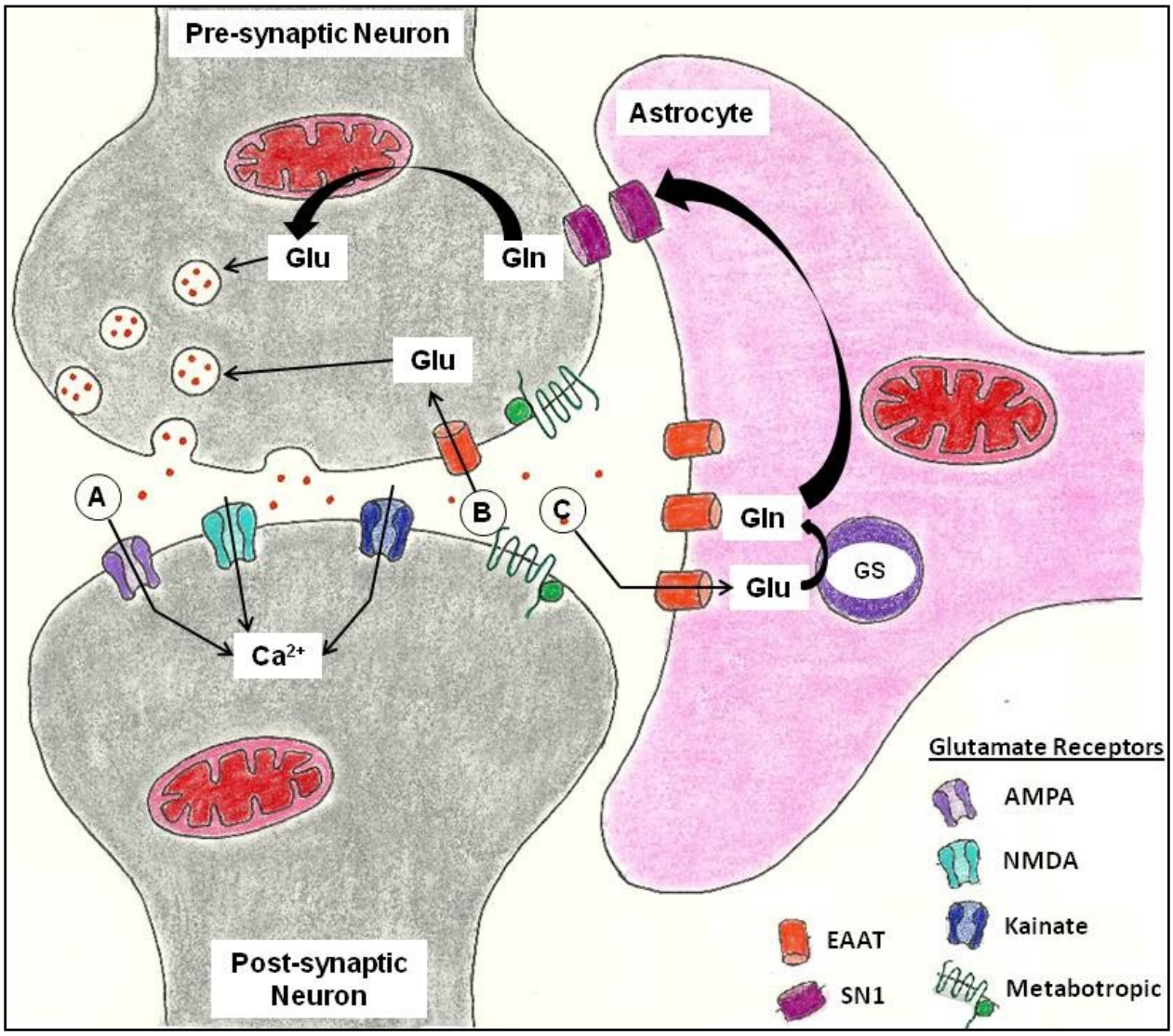

EAAT = excitatory amino acid transporter
SN1 = glutamine transporter
AMPA = α-amino-3-hydroxy-5-methyl-4-isoxazole
NMDA = N-methyl-D-aspartate

Experimental evidence suggests that the glutamate-glutamine cycle is disrupted in ALS. Glutamate levels were found to be elevated in the cerebrospinal fluid (CSF) of ALS patients (Rothstein et al 1990) and glutamate signaling defects were found in neuronal tissue from patients who had died of ALS (Rothstein et al 1992). Western blot analysis of post-mortem motor cortex tissue indicated that the major astrocytic glutamate transporter EAAT2 was significantly decreased in patients with ALS, and that a splice variant of this transporter, EAAT2b, was increased when compared to controls (Maragakis et al 2004). Immunohistochemical analysis of lumbar spinal cord samples from patients with motor neuron disease showed a decrease in EAAT2 density in the grey matter (Fray et al 1998). In a rat model of ALS, immunohistochemical analysis of spinal cord sections showed a focal loss of EAAT2 in the ventral horn region that coincided with gliosis but occurred prior to motor neuron degeneration. As the disease progressed the loss of EAAT2 and reactive gliosis increased, suggesting that these processes worsen with disease progression (Howland et al 2002).

Studies in which excitatory amino acid transporters were selectively knocked down, in both cell culture and animal models, showed that glutamate uptake was impaired and that animals developed a motor neuron syndrome that resulted in paralysis similar to ALS (Rothstein et al 1996). In mouse models of ALS, it was shown that overexpression of EAAT2 was able to slow motor neuron loss and grip strength decline (Guo et al 2003) and treatment with drugs that increase the expression of glutamate transporters also slow disease progression and increase survival (Rothstein et al 1995). Taken together, these results suggest that there may be a decrease in glutamate uptake by astrocytes due to down-regulation of transporters which in turn leads to an increase in glutamate in the CSF. Excessive glutamate in the synapse may lead to increased calcium influx into motor neurons, resulting in caspase activation and apoptosis. Caspase activation has been observed in mouse models of ALS (Li et al 2000; Pasinelli et al 2000), lending support for this method of motor neuron death. However, the order in which

these mechanisms occur during pathogenesis remains unclear as the dysfunction of other cellular mechanisms may play a role in glutamate transporter expression. For example, analysis of post-mortem spinal cord tissue collected from ALS patients indicated that mRNA levels of EAAT2 were normal (Bristol & Rothstein 1996) and aberrant EAAT2 mRNA has been detected in affected areas in ALS patients (Lin et al 1998), indicating that dysfunctional mRNA processing may lead to a decrease in transporter expression. Caspase-3 has also been shown to cleave and inhibit EAAT2 function (Boston-Howes et al 2006), suggesting that decreased transporter function may occur secondary to excitotoxic mechanisms.

1.2.3.2 Mitochondrial Dysfunction and Oxidative Stress

Mitochondria are mobile, plastic organelles that occupy a significant volume of eukaryotic cells. They are capable of associating with microtubules, which carry them to different locations within a cell and allow the mitochondria to take on unique distributions and orientations depending upon the cell type (Alberts et al 2002). Mitochondria play many roles within the cell, but they primarily function as energy producing organelles. Glycolysis alone is not sufficient to meet the energy demands of most animals and the pyruvate produced is taken up by the mitochondria (along with the carbon skeletons of fatty acids and amino acids) where it is oxidized by molecular oxygen (Alberts et al 2002; Nelson & Cox 2008). High energy electrons are produced which drive the electron transport chain to form the ATP that fuels the cell (Nelson & Cox 2008). If not channeled properly these electrons can become involved in aberrant reactions and damage cellular components, but healthy cells have mechanisms in place to help prevent oxidative damage.

In addition to their role as energy producers, mitochondria play an extensive role in calcium signaling and homeostasis. Mitochondria can store calcium and take it up from the cytosol to maintain intracellular calcium concentrations and modulate calcium signaling. They

can also interact directly with endoplasmic reticulum (ER) membranes through a structure called the mitochondria-associated ER membrane (MAM), which is involved in phospholipid exchange (Vance 1990), may play a role in the secretory pathway (Rusinol et al 1994), and also plays a role in calcium signaling (Rizzuto et al 2009). Through this interaction the ER can send calcium directly to the mitochondria to stimulate oxidative metabolism, allowing the cell to integrate signal transduction and metabolic pathways (Hayashi et al 2009). Regardless of how the calcium enters mitochondria, it can increase the production of ROS and once a calcium threshold is surpassed the intrinsic apoptotic pathway can be initiated resulting in cell death (Green 1998).

In patients with ALS, as well as in cell culture and animal models of the disease, experimental evidence suggests that at some point during disease pathogenesis mitochondria become dysfunctional and cells experience and increase in oxidative stress. In mouse models of ALS morphological abnormalities in motor neuron mitochondria, such as swelling and vacuolization, can be seen as early as two weeks of age, well before symptom onset (Bendotti et al 2001). These abnormal mitochondria can be found in the dendrites and axons of motor neurons and appear to be undergoing degeneration (Wong et al 1995). Mitochondrial vacuolization is associated with an increase in immunoreactivity for mutatant SOD1 (Bendotti et al 2001; Jaarsma et al 2000), which appears to associate with the outer mitochondrial membrane, the intermembrane space and the matrix (Higgins et al 2003; Mattiazzi et al 2002; Vijayvergiya et al 2005). Mitochondrial accumulation in the axon terminals of motor neurons is associated with an increase in ROS and RNS, and these mitochondrial show an accumulation of nitrated proteins (Martin et al 2007). Single-stranded, followed by double-stranded, DNA breaks in nuclear and mitochondrial DNA accompany morphological changes in mitochondria (Martin et al 2007). Abnormalities in mitochondrial DNA, such as alterations in gene copy

number as well as gene deletions, have been seen in spinal motor neurons of ALS patients (Keeney & Bennett 2010).

In addition to morphological changes in mitochondria, alterations in mitochondrial proteins and enzyme activities have been associated with disease pathogenesis. Mitochondria isolated from the brain and spinal cord of mouse models of ALS show an overall decrease in state three respiration, suggesting a decrease in the rate at which oxygen can be utilized for ATP synthesis in symptomatic animals (Mattiazzi et al 2002). While mitochondria isolated from the spinal cords of ALS patients showed an overall decrease in activity of all of the enzymes of the respiratory chain (Wiedemann et al 2002). When oxygen consumed by the whole animal was measured in mouse models, there was an increase in the total oxygen consumption as well as energy expenditure at rest, which was attributed to greater energy usage by the muscle (Dupuis et al 2004). These results were preceded by alterations in leptin, insulin, and corticosterone signaling prior to the development of symptoms (Dupuis et al 2004). In addition, presymptomatic mice have shown depletion of ATP in the cortex along with impaired glucose utilization in bulbospinal and corticospinal motor tracts (Browne et al 2006). Mutant SOD1 protein has been shown to interact with cytosolic malate dehydrogenase, an enzyme involved in the malate-aspartate shuttle important for transporting electrons produced during glycolysis across the mitochondrial inner membrane, in neuronal cell culture experiments (Mali & Zisapels 2008). Neuron-like cells stably expressing mutant SOD1 have shown an overall decrease in glutathione levels (D'Alessandro et al 2011), with a corresponding decrease in mitochondrial glutathione pools which make these cells more susceptible to oxidative stress (Muyderman et al 2009). In post-mortem brain tissue of SALS patients, an increase in the level of protein carbonyl groups was found suggesting an increase in oxidative damage to proteins (Bowling et al 1993). Similar results were found in mouse models of the disease, in which increased levels of oxidative damage were found in mitochondrial proteins and lipids (Mattiazzi et al 2002).

It is important to note that these alterations to mitochondria and mitochondrial proteins in ALS are not limited to motor neurons, but have been seen in liver, lymphocytes, muscle, and astrocytes. Hepatocytes from liver biopsy samples collected from ALS patients have shown defects in mitochondrial morphology, exhibiting enlarged mitochondria containing protein inclusions, that were associated with liver dysfunction (Nakano et al 1987). Mouse models of the disease also show a decrease in liver mitochondrial respiration and oxidative damage to proteins and lipids within the mitochondria at the time of symptom onset (Mattiazzi et al 2002). In circulating lymphocytes isolated from SALS patients, mitochondria showed a decrease in complex I activity and an increase in free cytosolic calcium levels (Curti et al 1996). Abnormalities in muscle mitochondrial DNA from SALS patients have been associated with decreased activity in NADH dehydrogenase and cytochrome c oxidase (Vielhaber et al 2000). In astrocytes isolated from a rat model of ALS, mitochondria showed defective respiratory function, a decrease in membrane potential, and an increase in ROS production and protein nitration. When these cells were co-cultured with motor neurons and preincubated with antioxidants and nitric oxide synthase inhibitors, motor neuron loss was prevented suggesting that dysfunctions in other cell types contribute to motor neuron death (Cassina et al 2008).

1.2.3.3 Dysfunctional Protein Quality Control Mechanisms

In healthy cells there are several quality control mechanisms in place to aid in the refolding of misfolded proteins, and quickly degrade misfolded proteins that cannot be repaired to prevent their accumulation and stress on cells. Often times when proteins are misfolded, hydrophobic amino acid residues, which are normally found inside of proteins, are exposed and signal quality control machinery to aid in protein refolding or removal. Chaperon proteins, like the heat shock protein families hsp60 and hsp70, can be found in the cytosol, mitochondria, and the ER to aid in proper protein folding (Alberts et al 2002). When proper folding cannot be

accomplished proteins are degraded through two major mechanisms, ER associated degradation and the ubiquitin-proteosome pathway, which function cooperatively to maintain homeostasis within the cell.

The endoplasmic reticulum is found in two forms within the cell, a smooth form containing a variety of enzymes and proteins which is involved in the secretory pathway and calcium homeostasis; and a rough form containing ribosomes on the cytosolic side of the membrane and different types of proteins and enzymes inside which are involved in protein synthesis, folding, post-translational modification, and transport (Alberts et al 2002). When new proteins are misfolded and accumulate within the ER, the unfolded protein response (UPR) is initiated and there is an increase in ER chaperones and enzymes that degrade misfolded proteins within the ER (Alberts et al 2002). When refolding within the ER fails, proteins can be transported back into the cytosol for degradation through the ubiquitin-proteosome pathway. Dysfunction or overloading of ER associated protein degradation machinery can lead to ER stress, disruption of protein synthesis and transport, and calcium homeostasis, resulting in mitochondrial dependent or independent forms of cell death.

There is evidence to suggest that the UPR is activated during ALS and that there are abnormalities in ER associated degradation of misfolded proteins. Spinal cords from patients with SALS also show signs of the UPR, with induction of kinases, chaperones, and other proteins involved in ER stress (Atkin et al 2008; Ilieva et al 2007; Sasaki 2010). Transgenic mouse models of ALS in which mutant SOD1 protein is overexpressed show early upregulation of ER stress markers well before symptom onset, and an ER-stress protective agent has been shown to slow progression of the disease in these animals (Saxena et al 2009). Studies using ALS mice have shown that mutant forms of SOD1 accumulate in ER lumen to form high molecular weight aggregates that interact with immunoglobulin-binding protein (BiP), an ER chaperone, in affected spinal cord regions (Kikuchi et al 2006). Mutant forms of SOD1 have

also been shown to directly interact with derlin-1, a protein component of ERAD machinery, which causes ER stress in motor neurons and leads to activation of the apoptosis-signal regulating 1 (ASK1) cell death pathway (Nishitoh et al 2008). Mutant forms of VAPB, an ER protein which has recently been associated with ALS, also show the ability to trigger ER stress and activate the UPR. In cell culture models, mutant forms of VAPB form aggregates that co-localize with other ER proteins, initiating upregulation of ER stress related proteins (Moumen et al 2011). Viral-mediated expression of mutant forms of VAPB in primary mouse motor neuron cultures also showed evidence of ER stress, as well as impaired calcium homeostasis, providing further support for ER stress in ALS pathogenesis (Langou et al 2010).

The proteosome is an ATP-dependent protease that works to degrade proteins in the cytoplasm and aids the ER in removal of improperly assembled proteins. The proteosome is a large, multisubunit complex that specifically targets, with a few exceptions, proteins that have been tagged with ubiquitin. Once inside the active site, proteins are cleaved into several short peptide fragments about seven to eight amino acids long that can then go on to be degraded further into individual amino acids. In addition to the removal of misfolded proteins, the proteosome also degrades normal proteins to regulate their concentrations within the cell and maintain homeostasis. As with ERAD, dysfunction or overloading of the proteosome can lead to increased cellular stress and result in cell death.

The presence of cytosolic protein aggregates, as well as ubiquitin-positive protein aggregates, in the spinal cords of ALS patients has provided evidence suggesting that protein aggregation and dysfunction of the proteosome play a role in disease pathogenesis (Redler & Dokholyan 2012; Wijesekera & Leigh 2009). Several different proteins have been found to aggregate in motor neurons during ALS, such as neurofilaments, mutant SOD1 protein, and TDP43. Mutations in the KSP region of the neurofilament heavy chain, a region involved in neurofilament cross-linking, have been found in patients with sporadic and familial ALS (Al-

Chalabi et al 1999; Figlewicz et al 1994; Tomkins et al 1998). In addition, peripherin, an intermediate filament found primarily in motor neurons, has been found in axonal aggregates in ALS patients and mouse models of the disease (Corbo & Hays 1992; Robertson et al 2003). The aggregation of neurofilaments in the axons of motor neurons may slow anterograde and retrograde transport of proteins and organelles, disrupt homeostasis, and alter the neuron's ability to send signals to other cells. As previously mentioned, mitochondria have been found to accumulate in axon terminals in mouse models of ALS (Martin et al 2007). This accumulation may be due to neurofilament aggregates which block the axon and prevent retrograde transport back to the cell body. In the same respect, blockage of axons may impair anterograde transport of proteins to the axon terminal and may play a role in the dysregulation of neurotrophic factor signaling. Both retrograde and anterograde transport along axons have been shown to be slowed in mouse models of ALS (Borchelt et al 1998; De Vos et al 2008; Murakami et al 2001; Williamson & Cleveland 1999).

In addition to neurofilaments, mutant forms of the SOD1 protein have been found in protein aggregates in ALS patients, mouse models, and cell culture models of the disease (Deng et al 2006; Gruzman et al 2007; Johnston et al 2000; Matsumoto et al 1996; Shibata et al 1996a; Shibata et al 1994; Shibata et al 1996b). Several studies have been conducted to examine changes in stability of the SOD1 protein with the various mutations it can undergo (Furukawa & O'Halloran 2005; Hough et al 2004; Khare et al 2006; Rodriguez et al 2005; Shaw & Valentine 2007). It has been shown that not all of the mutations that can occur within SOD1 disrupt the protein's stability (Rodriguez et al 2005), which suggests that the different mutations promote SOD1 aggregation by different mechanisms (Shaw & Valentine 2007). However, there are over 100 different mutations that can occur in SOD1 and many of them have been shown to disrupt protein stability, increase its dissociation, and increase its ability to form aggregates (Furukawa & O'Halloran 2005; Hough et al 2004; Khare et al 2006). Interestingly, mouse

models of ALS show SOD1 aggregation as early as birth and these aggregates are enriched in motor neurons (Jonsson et al 2004; Rakhit et al 2007; Zetterstrom et al 2007). Co-expression of wild-type SOD1 with certain mutant forms of the protein in animal models actually increases its ability to aggregate and exacerbates ALS phenotypes (Deng et al 2006; Fukada et al 2001; Jaarsma et al 2000; Wang et al 2009).

Aggregation of mutant SOD1 protein within motor neurons has also provided support for the hypothesis that the ubiquitin-proteosome system becomes dysfunctional during ALS pathogenesis. It has been determined that misfolded SOD1 undergoes degradation through the proteosome system (Di Noto et al 2005), and inhibition of the proteosome leads to increased aggregation of mutant SOD1 and cell death (Hoffman et al 1996; Hyun et al 2003; Puttaparthi et al 2003). Mutant forms of SOD1 have been shown to sequester proteosomal subunits, as well as ubiquitin ligases and some chaperone proteins (Hyun et al 2003; Niwa et al 2002; Watanabe et al 2001; Zetterstrom et al 2011b), and proteosomal dysfunction has been seen in animal and cell culture models of the disease (Cheroni et al 2009; Sau et al 2007). Spinal cord samples from mouse models of FALS and ALS patients test positive for ubiquitin and ubiquitin-ligase immunoreactive aggregates (Bendotti et al 2004; Leigh et al 1991; Mendonca et al 2006; Watanabe et al 2001), suggesting that proteosomal dysfunction or overloading prevents degradation of tagged proteins. These ubiquitin positive aggregates are typically found in the anterior horn of the spinal cord (Leigh et al 1991) and have been found in astrocytes as well as motor neurons (Mendonca et al 2006). TDP43 has also been found in these inclusions in affected regions in ALS patients (Arai et al 2006; Neumann et al 2006), but TDP43 positive aggregates seem to be specific to SALS patients (Tan et al 2007).

1.2.3.4 Aberrant mRNA Processing

The discovery of ALS-associated mutations in DNA/RNA-binding proteins, TDP43 and FUS, has lead to new ideas involving alterations in mRNA processing playing a role in the progression of the disease. This area of ALS research is relatively new and the normal roles of these proteins have yet to be fully characterized. TDP43 protein aggregates were first discovered in tissue from patients with FTD, and in 2006, TDP43 was identified as a major constituent of protein aggregates in tissue from patients with ALS (Arai et al 2006; Neumann et al 2006). Since then there has been an increase in research to identify mutations in the gene encoding TDP43, understand the normal cellular functions of the protein, as well as elucidate the mechanisms underlying its aggregation in ALS and FTD. Starting in 2008, several ALS-specific mutations in the gene encoding TDP43 were identified in both FALS and SALS patients (Kabashi et al 2008; Lagier-Tourenne et al 2010; Sreedharan et al 2008). During this time, mutations in the gene encoding FUS, which is functionally and structurally similar to TDP43, were also identified and associated with ALS (Kwiatkowski et al 2009; Vance et al 2009).

Under normal conditions both TDP43 and FUS are found primarily in the nucleus, with lower levels of both proteins detectable in the cytoplasm (Andersson et al 2008; Lagier-Tourenne et al 2010). Both proteins are widely expressed, capable of binding DNA and RNA and have several similarities in their sequences. TDP43 is 414 amino acids in length and consists of two RNA recognition motifs and a glycine-rich region at the C-terminus (Ayala et al 2005; Ou et al 1995; Wang et al 2004a). The first RNA recognition motif is required for RNA binding (Ayala et al 2005), but the second is not and is believed to play a role in the reorganization of chromatin (Ayala et al 2008; Buratti et al 2001). The C-terminal glycine-rich region is required for TDP43 to interact with other proteins (Ayala et al 2005; D'Ambrogio et al 2009; Wang et al 2004a) and is the primary site for ALS-associated mutations. In addition, TDP43 also contains a predicted nuclear localization sequence closer to the N-terminus and a

nuclear export sequence within the second RNA recognition motif (Lagier-Tourenne et al 2010). These sequences are believed to be involved in the shuttling of the protein between the nucleus and the cytoplasm. The FUS protein is 526 amino acids in length and consists of an N-terminal sequence rich in glutamine, glycine, serine and tyrosine residues (called the QGSY-region), a region of multiple arginine-glycine-glycine repeats, a zinc-finger motif at the C-terminus, and like TDP43, a glycine-rich region and an RNA recognition motif (Crozat et al 1993; Iko et al 2004; Morohoshi et al 1998; Prasad et al 1994). Most of the FUS mutations that are associated with ALS are found clustered in the glycine-rich region of the protein, however the C-terminal portion of the protein, which is believed to contain a nuclear localization sequence, can also become mutated (Lagier-Tourenne et al 2010). Like TDP43, FUS also contains a predicted nuclear export sequence in the RNA recognition sequence.

The exact roles of these two proteins have yet to be elucidated and there is no evidence to suggest that TDP43 and FUS interact with each other directly despite their structural similarities (Lagier-Tourenne et al 2010), but they may have roles in the same pathway (Kabashi et al 2011). Under normal conditions, TDP43 is involved in the regulation of transcription, alternative RNA splicing, RNA stabilization, and plays a role in the metabolism of micro RNA (Buratti & Baralle 2008; Buratti et al 2010). TDP43 is capable of regulating its own mRNA levels by binding to its own transcript (in an intron found in the 3'-untranslated region) and enhancing splicing (Ayala et al 2011; Polymenidou et al 2011). Variations have been found in the sequence of the 3'-UTR in patients with FTD (Gitcho et al 2009) corresponding with increased TDP43 protein expression (Gitcho et al 2009; Mishra et al 2007), suggesting that mutations in this region of the protein lead to enhanced splicing and increased protein levels during disease progression. TDP43 has been found to be abnormally truncated in tissue collected from patients, with C-terminal fragments found in brain and both N- and C-terminal fragments found in spinal cord samples of FTD and ALS patients (Igaz et al 2008). In addition to truncation,

TDP43 has found to be hyperphosphorylated and ubiquitinated (Arai et al 2006; Neumann et al 2006). Most of the TDP43 aggregates found in patients occur within the cytoplasm or neurites of affected cells and correspond with an overall depletion of nuclear TDP43 (Arai et al 2006; Cairns et al 2007; Neumann et al 2006). This mislocalization is a pathological hallmark of the disease in patients with TDP43 mutations and it is unclear if it is due to mutations in the nuclear localization sequence itself or mutations in the C-terminal glycine rich region which is involved in interactions with other proteins. Several models of the disease, including mouse, *D. melanogaster,* and *C. elegans,* all show severe motor symptoms upon overexpression of wild-type and mutant forms of TDP43, with wild-type TDP43 found mainly in nuclei and mutant TDP43 accumulating in the cytoplasm (Ash et al 2010; Hanson et al 2010; Kabashi et al 2010; Li et al 2010b; Shan et al 2010; Swarup et al 2011a; Voigt et al 2010; Wils et al 2010; Xu et al 2010). However, mouse models of ALS that overexpress wild-type human TDP43 containing mutations in the predicted nuclear localization sequence do not show reduced levels of human or mouse TDP43 in the nucleus when compared to controls (Igaz et al 2011), suggesting that TDP43 pathology in mouse models may differ from that of ALS patients.

The fused in sarcoma (FUS) protein, also called translocation in liposarcoma (TLS), was originally identified in cancer patients where the gene encoding FUS had undergone a chromosomal translocation leading to the production of fusion proteins (Crozat et al 1993; Rabbitts et al 1993). The gene encoding FUS is constitutively activated and ubiquitously expressed in almost all human tissues and cell lines under normal conditions (Aman et al 1996; Andersson et al 2008; Morohoshi et al 1996). Expression levels of the protein vary between tissues, but expression seems to be downregulated in differentiated cells and upregulated in certain cancers suggesting it may play a role in proliferation (Andersson et al 2008; Mills et al 2000). FUS is primarily nuclear, except in hepatocytes where it is found in the cytosol, and when cells are exposed to environmental stressors it can be found in cytoplasmic aggregates

that localize with stress granules containing translationally silenced mRNA and micro RNAs (Andersson et al 2008). Neurons and glial cells contain cytoplasmic aggregates that stain positive for FUS in postmortem CNS tissue isolated from patients with mutations in the gene (Corrado et al 2010; Kwiatkowski et al 2009; Vance et al 2009). FUS can interact with a variety of molecules as it has two functional domains, an N-terminal domain rich in glutamine, glycine, serine, and tyrosine residues that functions as a transcriptional activation domain and a domain near the C-terminus for DNA/RNA binding (Yang et al 2010).

FUS binds to pre-mRNA as a component of the heterogeneous nuclear ribonucleoprotein (hnRNP) H complex (Calvio et al 1995) and it takes part in pre-mRNA splicing by forming a complex with other hnRNPs, specifically A1 and C1/C2 (Zinszner et al 1994). FUS is also believed to form a complex with RNA that interacts with RNA polymerase II, as it accumulates in the cytoplasm upon inhibition of RNA polymerase II (Zinszner et al 1997). It has also been found to be part of the Drosha complex and may have a role in micro RNA processing (Strong 2010). In neurons FUS is believed to play a role in the reformation of actin and maintenance of dendritic spine shape, as it has been found localized with a protein complex involved in transporting actin-related mRNA to dendrites (Fujii et al 2005; Fujii & Takumi 2005). In addition to its role in RNA processing, FUS is believed to play a role in maintaining the integrity of the genome through its ability to promote annealing of DNA (Baechtold et al 1999) and acts as a transcriptional regulator through its interactions with DNA, nuclear receptors, and transcription factors (Amoresano et al 2010; Kaczynski et al 2003; Law et al 2006; Li et al 2010a). Exactly how ALS associated mutations in FUS disrupt its normal function and lead to its aggregation are not entirely clear, however mutations have been found in exons that make up the N-terminal QGSY and glycine-rich regions, as well as in the C-terminal region involved in DNA/RNA binding (Lagier-Tourenne et al 2010). Due to the locations of these mutations, it is not unreasonable to believe that they may disrupt protein transport (shuttling of FUS to and from

the nucleus), DNA/RNA binding, and some of the interactions between FUS and other proteins involved in forming the various complexes that take part in RNA processing and transcriptional regulation.

1.2.3.5 Neurotrophic Factor Dysregulation

Neural networks are dynamic entities that are capable of changing over time in response to molecular cues secreted by cells within the nervous system and by skeletal muscle. Neurotrophic factors are peptides that act as these molecular cues, and when secreted, influence the cell cycle, growth, differentiation, and survival of neurons and glia (Nestler et al 2001). They are produced in the cell body and sent to areas where they will be secreted. It has been suggested that neurotrophic factor signaling is dysfunctional in ALS and that motor neuron death results from withdrawal of these molecules. Studies with mouse models have supported this idea by showing that knocking out ciliary neurotrophic factor (CNTF) resulted in motor neuron death and loss of muscular strength (Masu et al 1993). ALS mouse models in which CNTF had been knocked out showed earlier onset of symptoms, which correlated with early onset seen in human FALS patients expressing mutations in the gene for CNTF, in addition to mutations in SOD1 (Giess et al 2002). Despite these findings, neurotrophic factor deficits have not been seen in human ALS patients. CNTF, hepatocyte growth factor (HGF), and gial-cell derived neurotrophic factor (GDNF) were found to be upregulated in spinal cord samples of ALS patients (Jiang et al 2005), and GDNF levels in CSF and GDNF mRNA levels in muscle biopsies were found to be elevated in ALS patients (Grundstrom et al 1999; Grundstrom et al 2000; Yamamoto et al 1999). The upregulation of these factors in ALS patients may be secondary to other dysfunctional cellular processes and reflect a defense mechanism attempting to aid in motor neuron survival.

Vascular endothelial growth factor (VEGF) and angiogenin (ANG) are proteins involved in vasculogenesis and angiogenesis that have been found to play roles in the CNS and have been implicated in ALS. VEGF has been found to act as a neurotrophic factor, promoting neurite outgrowth and increasing neuron survival in cell culture (Sondell et al 1999) and decreased expression in mice leads to neurodegeneration (Oosthuyse et al 2001). VEGF levels have been found to be decreased in the CSF of ALS patients (Devos et al 2004). ANG has been found to play a role in directing the path of neurite outgrowth (Subramanian & Feng 2007), and expression of ALS-associated ANG mutants leads to compromised neurite outgrowth and cytotoxicity in neuron cultures (Subramanian et al 2008). The roles of VEGF and ANG in the pathogenesis of ALS remain unclear, as their primary roles in the body are to promote *de novo* blood vessel formation, as well as blood vessel formation from pre-existing vessels. In addition to motor neuron degeneration, ALS patients exhibit decreased cerebral blood flow (Kobari et al 1996; Waldemar et al 1992) and mouse models of ALS show breakdown of the blood-spinal cord barrier (Zhong et al 2008), suggesting that VEGF and ANG may actually play roles vascular growth.

1.2.3.6 Neuroinflammation

Motor neurons are the primary cell target of ALS, but in many ALS models in which mutant proteins are overexpressed, such as SOD1, these proteins are not expressed solely in motor neurons, but in all cells of the CNS as well as other organs. So why do motor neurons undergo selective cell death? Several studies of ALS suggest that the disease is non-cell autonomous, involving a variety of cell types both within and outside of the CNS. Animal models suggest that motor neuron-specific expression of mutatant SOD1 is not sufficient to cause neurodegeneration (Pramatarova et al 2001), suggesting that aberrant interactions with other cell types are necessary to cause motor neuron death. The CNS is set up in such a

manner that even though neurons may appear to be the most important cell type (as their rapid signaling abilities play a vital role in all life processes), they cannot function without the aid of a variety of supporting cells. Astrocytes, oligodendrocytes/Schwann cells, and microglia are indispensable pieces of the nervous system, each of which play an important role in maintaining homeostasis and proper neuronal function.

During the pathogenesis of ALS, inflammatory processes occur that involve supportive cells within the CNS, as well as peripheral immune cells that infiltrate the CNS, resulting in a variety of cellular interactions that lead to motor neuron death. Studies of postmortem tissue from ALS patients suggest that neuroinflammation is an important part of the disease, however the progression of these processes are difficult to study in human patients as most human data comes from end stage patients. As a result, several studies have focused on animal models of ALS where early events in neuroinflammatory processes can be monitored. Both human and animal models of ALS show that astrocytes become activated, microglia become reactive, and peripheral immune cells enter the CNS to take part in inflammation. Although data are not necessarily consistent across animal and human studies of the disease, research also shows that a variety of cytokines and chemokines are released by activated cells within the nervous system, and can be beneficial or deleterious to the disease process.

It is not fully understood how myelinating cells (oligodendrocytes in the CNS and Schwann cells in the PNS) contribute to the pathogenesis of ALS, but studies aimed at characterizing other roles of these cells, suggest that they may be important players in disease progression. When mitochondrial cytochrome C oxidase is conditionally knocked down in oligodendrocytes and Schwann cells of mice, animals undergo severe neuropathy that includes defective myelination, muscle atrophy, and paralysis and a corresponding increase in brain lactate concentrations compared to control animals (Funfschilling et al 2012). These results suggest that there is some kind of metabolic coupling between myelinating cells and axons and

that myelinating cells, much like astrocytes, may play multiple roles in the nervous system. Further experimental evidence supports this idea, as it has been shown that disruption of monocarboxylate transporter 1 (MCT1; the major lactate transporter in the brain which is enriched in oligodendrocytes) leads to axonal damage and neuron death in cell culture and animal models (Lee et al 2012b). Tissue from ALS patients shows a reduction in the expression of this transporter and SOD1 mouse models support these data, showing transporter down regulation in spinal cord tissue of early symptomatic and end stage mice (Lee et al 2012b). It is possible that expression of the mutant SOD1 protein disrupts cell processes within myelinating cells, as well as neurons, leading to a decline in metabolic support. Mutant misfolded SOD1 protein aggregates have been found in the nuclei of oligodendrocytes (Forsberg et al 2011) and the complement proteins C3d and C4d have been found associated with oligodendrocytes (Kawamata et al 1992) in CNS tissue from ALS patients. Studies focusing on Schwann cell involvement in ALS progression have produced conflicting results. When Schwann cell expression of mutant SOD1 protein was reduced in transgenic mice, disease onset was not affected but disease progression was accelerated and the average lifespan was decreased (Lobsiger et al 2009). However, when mutant SOD1 protein expression was targeted to Schwann cells of mice, animals did not develop paralysis and no motor neuron degeneration was observed. In addition, further increasing the expression of mutant SOD1 protein in Schwann cells of transgenic mice did not accelerate disease progression (Turner et al 2010).

Astrocytes, which also provide neurons with metabolic support and maintain an environment suitable for synaptic signaling, become activated during the course of ALS, increasing in size and the number of processes extending from the cell body (Boillee et al 2006). Postmortem tissue from ALS patients shows increased glial fibrillary acidic protein (GFAP) and phosphotungstic acid hematoxylin (PTAH) reactivity suggestive of astrocyte activation and the number of reactive astrocytes near sites of neuron loss is inversely

proportional to the number of motor neurons remaining (Schiffer et al 1996). Astrocytes in tissue from mouse models of the disease show similar characteristics upon activation (Garbuzova-Davis et al 2007b) and those near capillaries in the brainstem show swollen end-foot processes that may contribute to the breakdown of the BBB (Garbuzova-Davis et al 2007a). Although reactivity may be a normal response to pathogens or stress within the CNS, normal homeostatic functions of astrocytes may become impaired upon activation and ultimately impair neuron function.

In cell culture models, normal and mutant SOD1-expressing motor neurons plated on an astrocyte monolayer expressing mutant SOD1 protein showed an increase in motor neuron death, suggesting a toxic interaction between the two cell types that involves mutant protein expression in astrocytes (Nagai et al 2007). Culturing normal and mutant SOD1-expressing neurons in conditioned cell culture media obtained from astrocytes expressing mutant SOD1 protein also resulted in motor neuron death, suggesting that astrocytes secrete a factor that is toxic to motor neurons (Nagai et al 2007). However, motor neurons have been found to release factors that may contribute to activation of astrocytes and their own demise. Fibroblast growth factor 1 (FGF-1), which is highly expressed in motor neurons, has been shown to be released from stressed motor neurons expressing mutant SOD1 protein in culture. When these cells are co-cultured with astrocytes, the astrocytes become activated and motor neuron survival decreases (Cassina et al 2005). Chemically activated astrocytes isolated from ALS rats show increased expression of mGluR5 (Vermeiren et al 2006), a metabotropic glutamate receptor involved in regulation of astrocyte activity and proliferation (Miller et al 1995), and modulation of excitatory synaptic transmission (Aronica et al 2003). These cells also show impaired glutamate uptake (Vermeiren et al 2006), suggesting that reactive astrocytes may be less capable of carrying out their normal supportive roles. It is not clear as to when astrocytes become reactive and ALS pathogenesis cannot be explained solely by aberrant interactions between motor

neurons and astrocytes. In an ALS mouse model utilizing an astrocyte-specific deletable mutant SOD1 gene, the removal of mutant SOD1 from astrocytes did not affect the onset of the disease, but progression was slowed and microglial activation was delayed (Yamanaka et al 2008b). These results suggest a more complex interaction of cells in the CNS and that astrocytes may become activated first and contribute to microglial activation.

Microglia, which interact closely with both astrocytes and neurons, are considered to be the resident macrophages of the nervous system, providing the first line of defense against insults to the CNS. Although they are typically regarded as macrophage-like cells, they can be activated by a variety of signals to produce an array of activated phenotypes. These phenotypes range from phagocytic activity characteristic of innate immunity to antigen presentation characteristic of adaptive immunity (Town et al 2005). Once activated, microglial morphology changes and these cells become more mobile in order to travel to sites of infection. In addition to gaining mobility, microglia secrete a variety of pro-inflammatory molecules including nitric oxide and superoxide to kill pathogens, and interferon γ and tumor necrosis factor α to continue stimulating an immune response (Philips & Robberecht 2011). Microglia can also release anti-inflammatory cytokines (interleukins 4 and 10), as well as trophic factors (insulin-like growth factor 1), to help stop inflammatory responses and initiate repair. The factors secreted are influenced by surrounding cells and the local environment, resulting in either deleterious or benign effects of microglial activation.

Experimental evidence from both ALS patients and animal models of the disease indicates that microglial activation is part of the disease process. Activated microglia have been found in both brain and spinal cord tissue of ALS patients, specifically in areas undergoing significant motor neuron death (Kawamata et al 1992; Moisse & Strong 2006). The exact time point at which microglia become activated during the progression of ALS is unclear, but studies using animal models of the disease suggest that it occurs near the end stage of the disease

succeeding astrocyte activation (Hall et al 1998). However, some studies using animal models of ALS have found microglial activation to occur in presymptomatic mice as early as 60 days of age (Dibaj et al 2011), suggesting that microglial activation may have an early and a late phase or it may be model-specific. New techniques utilizing a specific ligand of the peripheral benzodiazepine binding site expressed by mitochondria of activated microglia and positron emission tomography allow for the *in vivo* detection of activated cerebral microglia in ALS patients (Turner et al 2004) and may become a useful tool for studying the time course of microglial activation in humans, provided the discovery of earlier methods of disease detection and diagnosis.

The phenotype of activated microglia in animal models and human ALS patients appears to be primarily pro-inflammatory in nature. In human studies, monocyte chemoattractant protein-1 (MCP-1), a chemokine involved in the recruitment of peripheral immune cells, was found to be elevated in both the serum and CSF of ALS patients. However, its expression was not limited to microglia, but was also detected in neurons and astrocytes in post-mortem spinal cord tissue (Baron et al 2005). Primary microglia cultures prepared from ALS mice show increased release of MCP-1 upon stimulation with lipopolysaccharide (LPS) compared nontransgenic primary microglia cultures (Sargsyan et al 2009), supporting human data. Studies using animal models of ALS have also found mRNA levels of TNFα, IFNγ, and TGFβ-1 and 2 are elevated in spinal cord tissue with a corresponding increase in protein levels of TNFα, IL-6, IFNγ, and some chemokines (Hensley et al 2003). TNFα mRNA expression has been shown to occur prior to symptom onset and increase until the end stage of the disease (Elliott 2001), suggesting that it may be the main cytokine driving neuroinflammation and possibly motor neuron death. Microglia have been shown to express neurotransmitter receptors, such as ionotropic and metabotropic glutamate receptors, that under normal conditions may help them monitor their local environment. These receptors, however, may also play a role in modulating

the release of certain cytokines from activated microglia when neurons become stressed (Pocock & Kettenmann 2007). Animal models of the disease in which mutant SOD1 protein expression was reduced in microglia have shown no changes in disease onset; however disease progression was slowed (Boillee et al 2006). In mice where reactive microglia have been significantly reduced, motor neuron degeneration continues at the same rate (Gowing et al 2008), suggesting that microglia alone are not responsible for motor neuron death.

In mouse models of ALS, it has been shown that both the blood-brain and blood-spinal cord barriers begin to break down early in the disease (Garbuzova-Davis et al 2007a; Garbuzova-Davis et al 2007b). Data from ALS patients corroborate these findings as albumin, immunoglobulin G (IgG), and the complement component C3c have been detected in cerebrospinal fluid (CSF), and IgG has been found in motor neurons of the spinal cord (Annunziata & Volpi 1985; Engelhardt et al 2005; Leonardi et al 1984; Meucci et al 1993). In addition, both human patients and animal models of the disease show peripheral immune cell infiltration into the CNS, further supporting the evidence that the barriers of the CNS are compromised during the disease (Beers et al 2008; Chiu et al 2008; Troost et al 1989).

Astrocytes and microglia work together to create an environment that allows for the infiltration of peripheral immune cells into the CNS. Astrocytes help form the blood-brain barrier and the blood-spinal cord barrier, which are compromised during ALS and both astrocytes and microglia release MCP-1 to attract circulating immune cells to sites of injury. As a result, a variety of immune cells which normally cannot enter the nervous system, have been detected in the CNS of ALS patients and animal models. Cytotoxic (CD8+) and helper (CD4+) T cells have been found lining the walls of capillaries and venules and extending into affected areas (corticospinal tracts, motor nuclei of the brainstem, and the primary motor cortex) of the CNS in postmortem tissue from ALS patients (Kawamata et al 1992). Animal models of ALS show a similar pattern of peripheral immune cell infiltration, with CD4+ and CD8+ T cells, and natural

killer cell populations found in spinal cord tissue prior to symptom onset (Chiu et al 2008). Peripheral macrophages have also been shown to enter the spinal cords of ALS patients, surrounding and possibly engulfing motor neurons (Graves et al 2004). It is unclear as to whether or not these T cells are attracted to areas of motor neuron degeneration by chemokines or if they are part of an antigen-driven immune response (Holmoy 2008). In animal models of ALS in which the primary T cell receptor was knocked out disease progression was accelerated, suggesting a potentially protective role for T cells in the disease process (Chiu et al 2008). Specifically, helper (CD4+) T cells have been shown to have a neuroprotective effect in mouse models of ALS (Beers et al 2008).

It has been suggested that a toxic form of SOD1 may be involved in triggering an immune response in ALS and may possibly act as an antigen to activate immune cells (Brotherton et al 2012). Misfolded SOD1 protein has been found in the CSF of ALS patients suffering from both sporadic and familial ALS (Frutiger et al 2008; Zetterstrom et al 2011a) and an antibody that can differentiate between pathologically affected cells in tissue from human and animal models carrying SOD1 mutations has been discovered (Brotherton et al 2012) providing evidence for the presence of a toxic form of the protein. The presence of misfolded SOD1 protein in CSF, in the absence of disease-causing SOD1 mutations, suggests that there is probably something else going on in patients leading to motor neuron degeneration. There is a clear immune component to ALS and more work needs to be done to characterize the immune response and identify potential antigens that may activate immune cells and exacerbate disease progression.

Several studies have identified a range of cellular processes that become dysfunctional during the progression of ALS – glutamate excitotoxicity, mitochondrial dysfunction and oxidative stress, dysfunctional protein quality control, aberrant mRNA processing, neurotrophic factor dysregulation, and neuroinflammation – and all of these mechanisms may contribute to

the development of the disease. It is clear that certain mutations contribute to the disease, but the overlap of dysfunctional cellular processes in transgenic animal models suggests that ALS pathogenesis is much more complex than a single gene mutation can account for. Although these studies help to identify potential therapeutic targets by dissecting out specific disease-associated mechanisms, treating the disease still remains a hurdle due to its difficulty to diagnose and its rapid progression.

1.2.4 Diagnosis and Treatment of ALS

ALS is an extremely difficult disease to diagnose. There is no individual test or procedure that can lead to a definitive diagnosis of the disease and no diagnostic biomarkers for the disease have been identified (Turner et al 2009). Part of the difficulty in diagnosing the disease is due to the wide range of symptoms exhibited by ALS patients and the overlap of these symptoms with those of other motor neuron diseases, such as spinal muscular atrophy. Clinicians carefully monitor symptoms and typically conduct a range of diagnostic tests to rule out other diseases in order to diagnose patients with ALS. As a result it can take a significant amount of time, up to a year from symptom onset, to obtain a positive diagnosis of ALS (Turner et al 2009). By the time symptoms become apparent, a significant number of the motor neurons in the anterior horn of the spinal cord are thought to have died and these cells do not have the ability to proliferate and replace themselves. To be able to effectively treat ALS patients and prevent motor neuron damage, early diagnosis is critical.

The difficulty in diagnosing ALS and the need for early diagnosis lead clinicians and scientists to convene at a workshop in 1990 where a set of diagnostic criteria were drafted. In 1994 the first set of internationally acceptable criteria for the diagnosis of ALS, resulting from this meeting, were published in the *Journal of the Neurological Sciences* (Brooks 1994). The *El*

Escorial World Federation of Neurology Criteria for the Diagnosis of Amyotrophic Lateral Sclerosis read as follows:

> The diagnosis of ALS ***requires*** the ***presence*** of
> (1) signs of lower motor neuron (LMN) degeneratioin by clinical, electrophysiological or neuropathologic examination,
> (2) signs of upper motor neuron (UMN) degeneration by clinical examination, and
> (3) progressive spread of signs within a region or to other regions,
> together with the ***absence*** of
> (1) electrophysiological evidence of other disease processes that might explain the signs of LMN and/or UMN degeneration, and
> (2) neuroimaging evidence of other disease processes that might explain the observed clinical and electrophysiological signs. (Brooks 1994)

In addition to basic diagnostic criteria for ALS, this guide also provided a list of steps for clinicians to follow to diagnose the disease which read as follows:

> The diagnosis of ALS is made possible by
> (1) history, physical and appropriate neurological examinations to ascertain clinical findings which may suggest **suspected, possible, probable** or **definite ALS**,
> (2) electrophysiological examinations to ascertain findings which confirm LMN degeneration in clinically involved regions, identify LMN degeneration in clinically uninvolved regions and exclude other disorders,
> (3) neuroimaging examinations to ascertain findings which may exclude other disease processes,
> (4) clinical laboratory examinations, determined by clinical judgment, to ascertain possible ALS-related syndromes,
> (5) neuropathologic examinations, where appropriate to ascertain findings which may ***confirm*** or ***exclude*** **sporadic ALS, coexistent sporadic ALS, ALS-related syndromes** or **ALS variants**,
> (6) repetition of clinical and electrophysiological examinations at least six months apart to ascertain evidence of progression. (Brooks 1994)

The *El Escorial World Federation of Neurology Criteria for the Diagnosis of Amyotrophic Lateral Sclerosis* also included a thorough description of clinical signs of the disease, a list of disorders related to ALS, and defined the different types of ALS. Developing a set of internationally acceptable diagnostic criteria for ALS was a breakthrough for diagnosing the disease, and these criteria have been built upon over the years to accommodate new technologies and to include guidelines for clinical trials.

Despite the continual evolution of diagnostic criteria for ALS, as well as an increased understanding in molecular mechanisms underlying disease progression, there is still a need for drugs that can slow progression of the disease and help increase patients' quality of life. Currently, the only drug approved to treat ALS in most countries is riluzole, which has a modest effect on the lifespan of patients (Miller et al 2007). Riluzole is believed to target excitotoxicity in ALS patients, as it has been found to prevent the release of neurotransmitters stimulated by excitatory amino acids, like glutamate (Barbeito et al 1990; Benavides et al 1985; Hubert & Doble 1989). Riluzole has been shown to block NMDA and kainic acid initiated currents in Xenopus oocytes (Debono et al 1993), but radioligand binding studies failed to demonstrate its ability to bind with glutamate receptors (Benavides et al 1985; Debono et al 1993), suggesting that riluzole targets excitotoxicity in an indirect fashion. The drug has also been shown to inhibit basal and synaptically stimulated glutamate release (Cheramy et al 1992; Hubert & Doble 1989; Martin et al 1993) and appears to exhibit its indirect effects on excitotoxicity through its ability to block tetrodotoxin-sensitive sodium channels expressed on damaged neurons, preventing glutamate release by reducing calcium influx into the presynaptic neuron (Song et al 1997). Riluzole has also been shown to enhance the Wnt pathway (Biechele et al 2010), which has recently been implicated in ALS (Chen et al 2012). Even though riluzole has been shown to target multiple pathways involved in ALS it only extends the median survival by about two to three months (Miller et al 2007), and by the time it is administered motor neurons have undergone a significant amount of damage that cannot be reversed. The issues with diagnosing the disease combined with a lack of treatment options, makes slowing the progression of ALS with early treatment a serious problem.

1.3 Models of ALS

ALS is a complicated disease that is not fully understood. A wide array of gene mutations have been implicated as causative factors for developing the disease, and a number of molecular mechanisms are believed to play a role in the death of motor neurons. Much has been learned about the pathogenesis of the disease due to the development of ALS animal models. However, it has been difficult to link all of the molecular mechanisms with gene mutations to gain a full understanding of the initial steps leading to motor neuron death, creating the need to continue studying ALS and developing better disease models. There are a variety of ways in which ALS can be modeled in the laboratory, from single-cell systems to whole animal models, each of which have a variety of advantages and disadvantages.

Single-cell models of ALS, such as *Saccharomyces cerevisiae* and mammalian cell cultures of neurons, astrocytes, and microglia, are easily manipulated genetically and pharmacologically and allow for rapid data collection. *S. cerevisiae* is a simple eukaryotic organism that shares several protein quality control mechanisms with many higher eukaryotes and is a useful system for studying the protein misfolding that occurs as a consequence of expressing mutations in proteins such as SOD1, TDP43, and FUS (Bastow et al 2011). In addition, *S. cerevisiae* can be used to study oxidative stress associated with SOD1 mutations, as well as a variety of different protein-protein interactions (heat shock and chaperone proteins, and DNA/RNA binding proteins) that may occur during ALS pathogenesis (Bastow et al 2011). Like yeast, mammalian cell culture models can also be used to gain insight into the molecular mechanisms behind ALS, however, these cells can provide a clearer picture of exactly what is happening in a single cell type during the disease. For example, fluorescently-tagged proteins can be expressed in these systems and intracellular trafficking can be monitored directly using live cell imaging, to gain a greater understanding of ER stress or aggregation of mutant proteins. In addition, co-culturing of neurons and other cell types such as astrocytes can provide insight

into cell-cell interactions that may become toxic during the progression of ALS. These single-cell model systems of ALS are valuable tools for understanding the molecular mechanisms behind the disease, but they only tell a small part of the story. *S. cerevisiae* may have some similarities to human cells, but they are not human and therefore do not express all of the same proteins, nor do they mimic the cell-cell interactions that occur within higher organisms. Mammalian cell culture systems may model the molecular mechanisms of ALS more accurately than yeast, but these cells do not behave in culture exactly as they do in the body. In single cell culture systems cell-cell interactions that occur in the body (neuron-astrocyte, neuron-muscle, and neuron-oligodendrocyte) are lost, while in co-culture systems interactions may be regained to some extent, but again are not the same as in the human body.

Small, multicellular organisms provide a slightly better model of the disease, as these systems maintain the cellular interactions that are lost in single-cell systems. *Caenorhabditis elegans*, *Drosophilia melanogaster,* and zebrafish have all been used as small model systems to study ALS (Joyce et al 2011). *C. elegans* and *D. melanogaster* are small multicellular organisms that are easy to manipulate genetically and grow in the lab. Both organisms have a short life cycle and are capable of rapidly reproducing in large numbers, which allows for rapid collection of data. *C. elegans* is a simple organism that has been studied extensively. It is a transparent nematode containing less than 1000 cells, the lineage of which can be traced back to the egg (Muller & Grossniklaus 2010). The adult nematode contains 302 neurons that can be broken down into classes based on their function – chemosensory, mechanosensory, and thermosensory. *C. elegans* has been so thoroughly studied that the complete pattern of synaptic connections within its nervous system has been mapped and all of the neuronal subtypes have been identified down to the neurotransmitter secreted and the area innervated (Gama Sosa et al 2012). The transparent nature of *C. elegans* allows for proteins to be fluorescently tagged, and specific cells and intracellular processes can then be visualized within

living nematodes. In addition, genetic manipulations in which genes are targeted to specific cells or turned on at specific times can be performed in *C. elegans.* Several proteins involved in vesicle formation, trafficking, and release at the synapse, are highly conserved, which allows *C. elegans* to be used as a model for neurodegenerative diseases (Teschendorf & Link 2009). In ALS research *C. elegans* has been used to examine the effects of neuron-specific expression of various human SOD1 and TDP43 mutations, as well as the effects of muscle-specific expression of human SOD1 mutations, on protein aggregation, movement, and lifespan (Joyce et al 2011).

D. melanogaster is slightly more complex than *C. elegans*, but the adult fly brain and the eye have been utilized extensively to study mechanisms of neurodegeneration (Jeibmann & Paulus 2009). *D. melanogaster* expresses both neurons and glial cells in the developing CNS, that grow to produce the adult brain which contains association areas used for olfactory learning and memory called mushroom bodies (Gama Sosa et al 2012). Neurons in the complex eye develop in a stereotypical fashion with sequential differentiation of photoreceptors. Like *C. elegans*, the fruit fly has some mammalian homologs and can be used to understand the normal biological functions of genes, as well as dysfunctions that lead to neuronal death upon mutation (Bonini & Fortini 2003; Gama Sosa et al 2012; Muqit & Feany 2002). *D. melanogaster* can be manipulated in such a way that gene expression can be targeted to specific regions of the body (such as the eye or mushroom bodies) or induced at specific times using hormone inducible gene expression, or Tet-On/Tet-Off inducible systems (Gama Sosa et al 2012). The beauty of the fruit fly as a model system is that it can be used to perform forward genetic screens in which phenotypes are assessed and selected for through breeding to identify the genes responsible for causing certain traits. As a result, large-scale genetic screens can be performed in a relatively short period of time and used to dissect out the cell-signaling pathways involved in disease. *D. melanogaster* has been used to examine the effects of tissue-specific expression of

human wild-type and mutated forms of SOD1 and TDP43 on protein aggregation, glial cell stress, motor dysfunction, cell death, and lifespan (Joyce et al 2011).

The zebrafish (*Danio rerio*), an inexpensive vertebrate, has increased in popularity as a model organism. It is somewhat more difficult to work with in the lab than fruit flies and nematodes, as it requires more space (for aquariums) and has a longer life cycle, but it can reproduce rapidly and is fairly easy to breed and maintain (Gama Sosa et al 2012). Zebrafish share a close evolutionary relationship with mammals and the overall organization of the brain is similar to that of humans. The zebrafish brain consists of a forebrain, a midbrain, and a hindbrain which contains a diencephalon, telencephalon, and a cerebellum. Their peripheral nervous system has motor and sensory components, similar to humans, and they exhibit higher order behaviors that are not present in invertebrate systems (Gama Sosa et al 2012; Lieschke & Currie 2007). Zebrafish are easy to manipulate genetically and there are a variety of techniques that can be employed to generate transgenic zebrafish models of disease. Plasmid DNA can be inserted into the cytoplasm of fertilized eggs through microinjection or electroporation, sperm can be genetically modified, retroviral systems can be used to deliver genetic material, and genes can be knocked down using morpholino technology (Gama Sosa et al 2012). Gene expression can be regulated in a cell type-specific manner or temporally using similar systems utilized in fruit fly models. During the larval stage of development, the brain and skull of the zebrafish are transparent which allows for fluorescence imaging of cells *in vivo* (Cheng et al 2011). Dyes can be injected into cells, and transgenic fish expressing genetically coded calcium indicators in specific neurons have been developed, allowing for the imaging of neural activity by monitoring calcium changes that occur during action potentials (Wilms & Hausser 2009). The adult zebrafish develops stripes and is no longer transparent making *in vivo* imaging in the adult fish difficult, however cancer researchers recently developed a new strain of the species (called Casper) that remains transparent as an adult (White et al 2008), which may be

used to visualize cells involved in neurodegeneration. In addition to the ease with which cells can be visualized in zebrafish, this model can also be used to perform forward genetic screens, as well as reverse genetic screens in which genes are manipulated (mutated, inserted, or knocked down) and corresponding phenotypes assessed to identify genes with the potential to cause neurodegeneration. Mutations in the zebrafish SOD1 gene have been used to study motor neuron loss and muscle atrophy, and the motor defects that accompany these phenomena during ALS. Human wild-type and mutant TDP43 mRNA have also been expressed in zebrafish embryos as a model for ALS (Joyce et al 2011).

C. elegans, *D. melanogaster*, and *D. rerio*, have been useful models in gaining an understanding of the molecular mechanisms behind the pathogenesis of neurodegenerative disorders, but they are not the best models for human diseases. Both *C. elegans* and *D. melanogaster* lack an immune system, which is a major disadvantage when studying neurodegeneration. These organisms also lack mylenated axons and as a result are missing an important cell-cell interaction (that of neurons and oligodendrocytes or Schwann cells), as the motor neurons undergoing degeneration in human ALS are myelinated (Gama Sosa et al 2012). Microglial activation, peripheral immune cell infiltration into the CNS, and interactions between neurons and myelinating cells play significant roles in the progression of ALS, as previously discussed, and the inability of these organisms to mimic these processes limits the usefulness of data collected from invertebrate models. Zebrafish are a slightly more useful model of ALS because they have an immune system that functions similar to that of humans, and have even been used as models for immune function during other types of infection. In addition, this model also expresses many of the same CNS cell types seen in humans and mimics human anatomy and physiology better than invertebrate models. The use of fish as a model system does have its disadvantages. The gene targeting technology available for the zebrafish model is limited and a greater range of gene targeting exists for mouse models (Gama Sosa et al 2012).

Zebrafish also live in a very different environment than humans, which may be a disadvantage when studying diseases like ALS that may have an environmental component.

The best organisms for models of human diseases are those that most closely resemble humans (with respect to organ structure and function, and genetics) and can mimic human diseases. Several mammalian models of ALS are currently being used to study the disease, and research is ongoing to produce better mammalian models that exhibit the same hallmarks of the disease seen in humans. Currently there are a wide variety of mouse models of ALS and there are a few rat models of the disease. There is even a naturally occurring SOD1 mutation that produces a neurodegenerative disorder in dogs that can be used as a model for ALS (Awano et al 2009; Joyce et al 2011). All of these models have been invaluable tools for studying the disease, but they do not exhibit the same symptoms and they do not always show the same pathological hallmarks of the disease as human patients. As a result, researchers have been working on better models of the disease and have recently produced a non-human primate model of ALS (Uchida et al 2012).

The mouse is probably the most common and well-studied mammalian model of human disease. The first genetically modified mouse was created in 1974 when DNA inserted into a mouse embryo showed that the gene insert was present in all of the animal's cells, but was unable to be passed to offspring (Jaenisch & Mintz 1974). The first transgenic mice capable of passing exogenous DNA to offspring were later produced in 1981. This was accomplished by injecting purified DNA into a single-cell mouse embryo (Costantini & Lacy 1981; Gordon & Ruddle 1981). Since then, the technology used to genetically manipulate mice has been vastly improved and applied to other animals creating an entire industry devoted to transgenic animal models of human disease.

The first transgenic mouse model overexpressing the human SOD1 gene was produced in the 1980s and was used to examine the effects of increased dosage of the protein

in Down syndrome (Epstein et al 1987). In 1994 the first transgenic mouse model overexpressing a mutant form of SOD1 associated with ALS, the G93A mutation, was found to exhibit motor neuron degeneration similar to that seen in ALS patients (Gurney et al 1994). Since this time, a variety of SOD1 mutations, both artificial and those found in ALS patients, have been expressed in mice to discern how alterations in the protein's structure contribute to disease onset and progression (Joyce et al 2011). Table 1.3.1 lists the SOD1 mutations that have been expressed in mouse models, as well as the age of disease onset and survival time for these animals. Interestingly, the SOD1-A4V mutation, which is the most commonly occurring SOD1 mutation in human ALS (Deng et al 1993; Siddique & Deng 1996), does not cause motor neuron degeneration when expressed alone in transgenic mice, but must be co-expressed with human wild-type SOD1 in order to produce a disease phenotype (Deng et al 2006). The G93A mutation, which is much less common in human ALS, is probably the most commonly studied mutation thanks to its use in transgenic mouse models of the disease.

Table 1.3.1 SOD1 mutations expressed in transgenic mouse models of ALS.

SOD1 Mutation	Age of Onset (Weeks)	Survival (Weeks)
hSOD1-A4V[a]	35	48
hSOD1-G37R	15-17	25-29
hSOD1-H46R	20	24
hSOD1-H46R/H48Q[b]	17-26	ND
hSOD1-H43R/H48Q/H63G/H120G[b]	35-52	ND
hSOD1-L84V	21-26	26-30
hSOD1-G85R	35-48	37-54
mSOD1-G86R[c]	13-17	17
hSOD1-D90A	52	61
hSOD1-G93A[d]	13-26	17-50
hSOD1-T116X[e]	41	43
hSOD1-L126X	28-44	47
hSOD1-126delTT	28-36	18
hSOD1-G127X	35	36

Table was modified from Joyce, *et al.* (2011)

ND indicates the survival time was not described.
[a] The SOD1-A4V mutation only produces motor neuron disease when co-expressed with the human wild-type SOD1.
[b] Artificial mutations that prevent copper from binding the enzyme.
[c] Mouse transgene.
[d] Age of onset and survival vary depending upon the copy number of the gene, with increased copy number leading to earlier onset and shorter survival.
[e] Artificial mutation that truncates the protein.

Since the discovery of ALS-associated mutations in TDP43, several TDP43 mouse models of ALS have been developed. Most of these models overexpress the human wild-type TDP43 gene, however the human A315T mutation has been successfully inserted into transgenic mice. These models also make use of different promoters which allow the transgene to be expressed in specific cell types or brain regions, as well as throughout the body (Joyce et al 2011). The phenotype expressed by these models varies depending upon the promoter and expression level of the protein. It is important to note that TDP43 aggregation seen in human patients is not always exhibited by TDP43 transgenic mice. Since this is a relatively new area of research, there is still work to be done to produce better TDP43 mouse models of the disease.

Many of the same human gene mutations used in mouse models have been utilized in rat models of ALS. Both the H46R and G93A human SOD1 mutations have been successfully inserted into rats. These SOD1 transgenic rat models exhibit an ALS-like phenotype similar to their mouse counterparts, upon overexpression of these mutant forms of protein. Rat models expressing both the wild type TDP43 and a mutatant form containing the M337V mutation have also been developed (Zhou et al 2010). Expression of wild type TDP43 does not lead to a disease phenotype in rats however the expression of the M337V mutation produces an ALS-like phenotype exhibiting lower motor neuron loss and gliosis, but does not mimic the TDP43 aggregation seen in human patients much like the TDP43 transgenic mouse model.

The popularity of rodents as models of human disease stems from the fact that they are evolutionarily closely related and their overall development parallels that of humans. Genetically, mouse chromosomes are organized in a similar fashion to those of humans, with genes displayed in similar patterns across the genome. In addition, mice and rats can be inbred to create a homogeneous genetic background which is beneficial when studying the expression of a transgene (Gama Sosa et al 2012). The technology used to insert genes into mice has been translated for use in rats, but is much less available for use in rats, which is probably the

reason for the greater variety in mouse models of disease. These genetic manipulations have been expanded to include knocking down genes, and transgenic animals can be crossed with other strains of animals that are missing certain genes to study the effects of the removal of a protein on disease. Mice and rats are small, easy to care for and breed, live in an environment similar to humans that can be tightly controlled in a lab setting, and can be easily used to study the effects of drugs. Unlike invertebrate and fish models of disease, rodents can be administered drugs in the same manner as humans (i.e., orally, subcutaneously, intravenously, etc.) which is beneficial when conducting pharmacological studies that examine the route of administration, absorption, excretion, and things of that nature. Rats are much larger than mice and have a greater capacity for learning in behavioral tasks, which is beneficial when drugs need to be inserted directly into the brain or when examining the effects of a disease or treatment on behavior. With respect to neurodegenerative disorders, the organization of the rodent CNS is similar to that of humans, with the expression astrocytes and other cell types involved in creating the blood-brain barrier and the blood-spinal cord barrier, which is vital when studying treatments that need to cross these barriers in order to effectively treat diseases. Mice and rats also exhibit immune function similar to that of humans and these disease models often display some of the same neuroinflammatory processes that are commonly observed in patients.

Although transgenic rodents make good models of human diseases due to their similarities with humans, they are probably not the best models for ALS. In mouse models of ALS that develop severe paralysis, such as the SOD1 G93A mouse, the paralysis only occurs in the rear limbs and is primarily a lower motor neuron disease. Although humans develop lower motor neuron symptoms, they also show significant upper motor neuron degeneration, and mouse models do not which is a major disadvantage to studying these animals. ALS rat models that overexpress mutant forms of SOD1 may be better models than their mouse counterparts as

they develop symptoms that are closer to those observed in human patients. Rats overexpressing the G93A mutation have an aggressive disease and can exhibit symptoms in hind limbs or forelimbs (Joyce et al 2011; Nagai et al 2001), whereas mice expressing this mutation show only hind limb paralysis. Both mouse and rat models of ALS show some of the pathological hallmarks that human patients exhibit, such as protein aggregation and activation of microglia and astrocytes, but they may also show artifacts resulting from the expression of the transgene itself which may not translate to human studies.

1.4 Purpose of the Study

ALS is a devastating neurodegenerative disease in which motor neurons are selectively killed. The prognosis of the disease is typically poor and once a positive diagnosis is made, patients typically only have a few years of life left. Due to the lack of treatment options for the disease patient quality of life tends to be poor, as patients not only become paralyzed, but they may lose the ability to speak and even breathe on their own. Since motor neurons cannot divide to replace cells that have died, the best treatment options would be those that can prevent motor neuron death. In order to achieve this, the disease would have to be detected early on, prior to significant cell death. This would require patients seeking treatment at the earliest signs of symptoms, as well as reliable biological markers of the disease and better methods of detection.

ALS research has advanced significantly in the past few decades, with the discovery of a wide range of molecular mechanisms providing several potential therapeutic targets of the disease. A constantly expanding variety of animal models of the disease has aided in the discovery of drugs that may slow ALS progression, however many drugs that have shown to be beneficial in animal models of ALS have failed to show the same level of efficacy in human trials (Beghi et al 2007). This may, in part, be due to the fact that there has been incomplete

metabolic profiling of animal models of the disease and overexpression of mutant ALS-associated proteins may actually lead to systematic metabolic defects in these models. In addition, many studies using animal models, as well as human patients, fail to separate male and female data and may miss potential gender differences in the disease itself, as well as gender differences related to treatments. Several studies have implicated a neuroprotective effect of estrogen in spinal cord injury (Chaovipoch et al 2006; Kachadroka et al 2010) and ALS (Choi et al 2008; Groeneveld et al 2004) and hormones have been shown to effect inflammatory processes (Karpuzoglu & Ahmed 2006; Lang 2004; Salem 2004; Straub 2007), which can impact disease progression. Metabolic differences have also been observed between men and women. Women have been shown to have lower resting metabolic rates than men (Arciero et al 1993) and a variety of studies have suggested that there are gender differences in energy utilization that may be modulated by hormones (Wismann & Willoughby 2006). These basic gender differences in metabolism have implications for gender differences in xenobiotic metabolism. In rats gender-specific differences have been observed in certain cytochrome P450s, enzymes important in drug metabolism (Kato & Yamazoe 1992), and human studies have shown that women recover from general anesthesia faster than men (Bajaj et al 2007). These observations suggest that gender should be considered when studying the general progression of a disease, as well as the response to drug treatments for a disease, in both animal and human studies in order to determine differences in underlying mechanisms and the best therapeutic intervention for the patient.

The purpose of this study was to understand the gender-specific effects of treating transgenic mice overexpressing the human SOD1 protein containing the G93A mutation with L-methionine sulfoximine (MSO), an irreversible inhibitor of glutamine synthetase (GS). Initial studies using this drug in ALS mice showed that it extends the lifespan of these animals and targets glutamate excitotoxicity, lowering levels of glutamine and glutamate in specific brain

regions (Ghoddoussi et al 2010). My studies have expanded on these experiments by looking at gender differences in survival of ALS mice treated with MSO and the impact of sex hormones on the disease progression and treatment efficacy. These experiments, discussed in Chapter 2, show that MSO extends the lifespan of these animals in a gender-specific fashion, having a greater effect on females than males. In addition, sex hormones play a role in MSO's ability to extend lifespan, as gonadectomy removes the response to MSO in both males and females.

The second portion of this study examines MSO's effect on amino acid and nitrogen metabolism in SOD1 G93A mice. The goal of these experiments was to characterize basic metabolism in untreated wild-type and ALS mice, as well as in mice treated with MSO, and to understand the effects of mutant transgene expression and MSO treatment on amino acid and nitrogen metabolism accounting for gender. Enzymatic assays and analysis of plasma metabolite levels were performed to monitor metabolic changes between genders, as well as genotypes. These experiments, discussed in Chapter 3, show that there are a variety of metabolic differences between males and females, some of which are specific to transgenic animals. MSO treatment significantly lowers brain and spinal cord glutamine synthetase activity and shows no differences in activity levels between genders or genotypes, suggesting that its gender-specific effects on survival are probably not due to its effect on GS. MSO treatment and SOD1 expression, however, do not have an effect on other enzymes involved in nitrogen metabolism, specifically glutaminase and carbamoyl phosphate synthetase one (CPSI). Interestingly, CPSI activity is higher in females than males providing evidence supporting underlying gender differences in nitrogen metabolism. SOD1 mice show some oddities in their metabolic profiles, such as a cysteine deficiency, suggesting that overexpression of the transgene itself may have an impact on overall metabolic processes.

CHAPTER 2

THE GENDER-SPECIFIC EFFECT OF MSO ON SURVIVAL

2.1 Introduction

2.1.1 Glutamine Synthetase

Glutamine synthetase (GS) is an extremely important enzyme that is expressed in a variety of organisms, from bacteria to mammals. It is a major enzyme involved in the metabolism of nitrogen found in all extant organisms and the genes encoding GS have been suggested to be some of the oldest functioning genes in existence (Kumada et al 1993). There are three different classes of glutamine synthetases: (1) Class I glutamine synthetases (GSI) which are expressed by prokaryotes, (2) Class II glutamine synthetases (GSII) which are expressed by eukaryotes, plants, and certain bacteria (particularly bacteria belonging to the Rhizobiaceae, Frakiaceae, and the Streptomycetaceae families), and (3) Class III glutamine synthetases (GSIII) which have only been found in bacteria colonizing the gastrointestinal tracts of animals, specifically *Bacteroides fragilis* and *Butyrivibrio fibrisolvens* (Brown et al 1994). The structure of glutamine synthetase varies and can be an octamer, decamer, or a dodecamer, depending upon the organism in which it is expressed (Eisenberg et al 2000; Krajewski et al 2008; Liaw & Eisenberg 1994).

Class II glutamine synthetases are the only class expressed by eukaryotes. The structures of Class II glutamine synthetases varies, but have been found to be octomeric in at least one species of plant (*Phaseolus vulgaris*) (Llorca et al 2006) and decameric in maize (Unno et al 2006) and some mammals (canines and humans) (Krajewski et al 2008). The decameric form of GS is made up of two rings, each of which is composed of five monomers, which lie back-to-back forming the barrel-shaped enzyme. At the interface of each monomer

there is an active site and the active sites of the pentameric rings are slightly offset, producing a decamer that contains a total of 10 active sites (Krajewski et al 2008).

GS is responsible for converting glutamate into glutamine, catalyzing the reaction Glutamate + NH_4^+ + ATP ⟷ Glutamine + ADP + P_i in the presence of magnesium or manganese. The crystal structure of human GS was determined with the enzyme bound to magnesium, ADP, and phosphate, and with the enzyme bound to magnesium, ADP, and an irreversible inhibitor of GS, methionine sulfoximine. The structures show that there are three magnesium ions present in each active site and suggest that a single molecule of each reactant – glutamate, ATP, and ammonia – can enter an active site to produce glutamine (Krajewski et al 2008). As a result, the decamer has the potential to produce 10 molecules of glutamine, one from each active site. The conversion of glutamate to glutamine is believed to take place in two steps, the first of which involves the enzyme binding to glutamate and ATP, forming the enzyme-bound intermediate, γ-glutamyl phosphate. During the second step, which requires the presence of ADP in the active site, ammonium is covalently bound to the activated glutamate intermediate to form glutamine and phosphate and ADP are released (Krishnaswamy et al 1962; Liaw & Eisenberg 1994; Meister 1985).

GS can be found in the cytosol or the mitochondria, depending upon the organism and the tissue in which it is expressed. In vertebrate neural tissue GS is expressed primarily in astrocytes where it is found in the cytosol (Kennedy et al 1974; Linser & Moscona 1983; Smith & Campbell 1983; Smith et al 1987). However, liver GS can be found in the cytosol or the mitochondria, depending upon the method of ammonia detoxification utilized by the organism. In organisms such as birds, reptiles and sharks, that utilize uricotelic or ureosmotic methods to remove excess nitrogen, liver GS is found in the mitochondria (Campbell et al 1987; Smith & Campbell 1983; 1987; Smith et al 1987). In higher vertebrates that utilize ureotelic methods to remove excess nitrogen, like mammals, GS is cytosolic in liver (Smith & Campbell 1988; Wu

1963). In mammalian liver GS is primarily found in pericentral hepatocytes, a small population of cells that surround the venules of the liver (Haussinger 1987).

Glutamine synthetase is expressed throughout the body and the concentration of GS in a cell, as well as enzyme activity, vary depending upon the cell type (van Straaten et al 2006). Glutamine is found in high concentrations in the body and is considered a non-essential amino acid, as it can be produced by GS and taken up from the diet (Nelson & Cox 2008). As a result, cells can utilize GS either to produce glutamine or to remove the potentially toxic substances, glutamate and ammonia. Lower levels of GS are expressed in cells utilizing the enzyme for glutamine production, while high levels of GS are found in cells that function primarily to remove ammonia and glutamate (Lie-Venema et al 1998; van Straaten et al 2006). Organs expressing high levels of GS, typically express it in a subset of cells (Lie-Venema et al 1998; van Straaten et al 2006). This is seen in the brain and liver where GS is restricted to certain cell types – astrocytes in the brain and pericentral hepatocytes in the liver. In organs that express low levels of GS, such as adipocytes and myocytes, the enzyme appears to be expressed throughout the organ (Lie-Venema et al 1998; van Straaten et al 2006). Mammalian GS has not been as well characterized as bacterial forms of the enzyme, which can be regulated by a variety of post-translational modifications. As a result, the regulation of mammalian GS is not fully understood, but it appears to occur at the level of translation, with protein stability playing a role in regulation (van Straaten et al 2006). GS is susceptible to both reactive oxygen and nitrogen species and has been found to be reversibly inhibited by nitration of tyrosine residues, however this modification may be more important under conditions where cells are exposed to high levels of oxidative stress (Gorg et al 2007).

GS is a central enzyme in nitrogen metabolism in a wide variety of organisms. It is the only enzyme capable of producing glutamine, the most abundant amino acid in the body, which acts as a carrier of ammonia in the bloodstream and as a non-toxic form of glutamate in the

nervous system. As mentioned in Chapter 1, GS is an important enzyme in the central nervous system, where it acts as the primary player in the recycling of the neurotransmitter glutamate. In the liver, GS produces glutamine that donates ammonia to CPSI for the production of urea and the excretion of excess nitrogen. Glutamine is also important for protein production and can act as a fuel for a variety of cell types.

2.1.2 L-Methionine Sulfoximine

In the early twentieth century nitrogen trichloride (also called agene) was used to age and bleach flour that was used for animal and human consumption. During this time it was noticed that there was a problem with dogs developing a nervous disorder (referred to as running fits), which was later determined to be caused by the consumption of foods containing flour that had been treated with nitrogen trichloride (Mellanby 1946). Despite this finding, studies conducted on a variety of animals showed that there appeared to be species-specific sensitivity to foods that had been treated with agene, and humans, along with monkeys and rats, did not show any sensitivity to consumption of these substances (Newell et al 1949a; Newell et al 1949b). Shortly after this discovery, it was determined that treating flour with agene lead to the production of a toxic factor which could be isolated (Bentley et al 1949; Campbell et al 1951; Reiner et al 1950). Around this same time, this toxic factor was also synthesized and identified as methionine sulfoximine (Bentley et al 1950; Misani & Reiner 1950).

Methionine sulfoximine (MSO) is a modified form of methionine where the sulfur atom is bound to an oxygen atom and an imine group, in addition to the methyl group. Figure 2.1.1 (A and B) shows the structural similarities between methionine and methionine sulfoximine. Several studies conducted in the 1950s attempted to identify targets of MSO and in 1952, glutamine synthetase was identified as its primary target (Pace & McDermott 1952). It has also been shown to inhibit alanine aminotransferase (De Robertis et al 1967) and stimulate ornithine

decarboxylase activity (Di Giacomo et al 1997). MSO is also structurally similar to buthionine sulfoximine (BSO) (Figure 2.1.1C), which acts as an inhibitor of γ-glutamylcysteine synthetase, the first and rate-limiting step in the production of glutathione. While BSO does not inhibit GS, MSO has been shown to inhibit γ-glutamylcysteine synthetase (Richman et al 1973).

Figure 2.1.2.1 Chemical structure of MSO and analogous compounds.

MSO (**A**) is a modified form of the amino acid methionine (**B**) with an oxygen atom and an imine group attached to the sulfur atom. BSO (**C**), an inhibitor of γ-glutamylcysteine synthetase, is structurally similar to MSO with the sulfur atom attached to a butyl group in place of the methyl group.

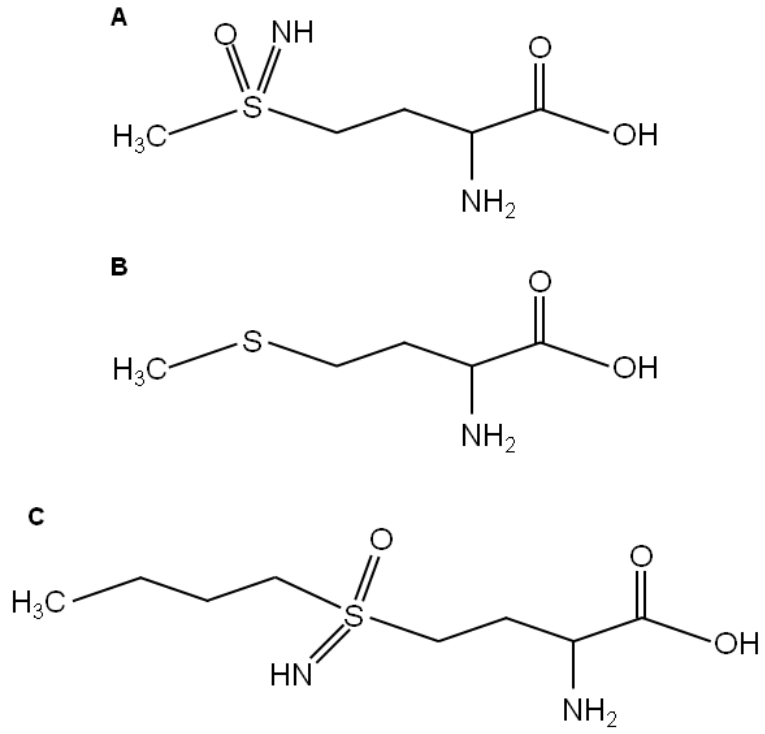

Despite the identification of other enzymatic targets of MSO, the vast majority of research conducted on this compound has focused on its ability to inhibit glutamine synthetase. Initial studies conducted to determine the mechanism by which MSO inhibits GS suggested that the compound competitively inhibited the enzyme, as the addition of glutamate seemed to prevent inhibition by MSO (Sellinger & Weiler 1963). These studies lead to the idea that MSO behaved as a glutamate analog, binding the enzyme in the portion of the active site normally occupied by glutamate. Further studies showed that inhibition of GS by MSO was more complex, as it required ATP and once the enzyme was inhibited, glutamate was no longer capable of reversing inhibition suggesting that MSO irreversibly inhibited GS. These studies also showed that MSO was phosphorylated by the enzyme, producing a new compound (methionine sulfoximine phosphate) that interacted tightly with GS but could be removed by denaturing the enzyme (Rao & Meister 1972; Ronzio & Meister 1968; Rowe et al 1969). Methionine sulfoximine phosphate is produced when MSO and ATP bind the enzyme and GS phosphorylates MSO. The phosoporylated product and ADP are left behind, stuck in the active site rendering the enzyme inactive (Krajewski et al 2008; Rao & Meister 1972; Ronzio & Meister 1968; Rowe et al 1969). It is important to note that MSO contains two chiral centers, one at the α-carbon and a second at the sulfur atom, and therefore has four potential isomers. Only one of these isomers, L-methionine-S-sulfoximine, has been shown to bind to GS and become phosphorylated leading to enzymatic inhibition (Manning et al 1969) and has also been linked to the convulsant properties of MSO (Rowe & Meister 1970).

The only way that GS can overcome inhibition by MSO is through degradation and production of new protein. In studies where rats were given a single i.p. injection of a subconvulsive dose of MSO, it was shown that different tissues respond differently to the drug. Liver GS shows maximal inhibition four hours after MSO administration, while brain GS shows maximal inhibition 24 hours after administration. In addition, the return to normal enzymatic

activity levels varies between tissues (Lamar 1968). Similar studies conducted on mice agree with the results obtained from rats and show that liver GS has a higher turnover rate, as activity levels return to normal within 30-60 days of MSO administration, while brain GS levels are only 75% of normal at 90 days after MSO administration (Rao & Meister 1972). Maximal formation of methionine sulfoximine phosphate, the product that inhibits GS, occurs about 5 hours after MSO injection in both the brain and the liver. However, it is more rapidly removed from the liver than the brain and complete removal corresponds to the return to normal enzymatic activity level (Rao & Meister 1972).

Despite its ability to cause convulsions in certain species, MSO has shown to have some beneficial effects in certain disease models and has been a useful tool in understanding the importance of glutamine metabolism. In diseases which elevate ammonia levels in the body, such as acute liver failure, brain GS attempts to lower ammonia levels by incorporating it into glutamine which builds up in astrocytes and disrupts the osmotic balance leading to astrocyte swelling. MSO treatment of cell culture and rat models of this disease, decreases glutamine production by inhibiting GS and reduces astrocyte swelling (Norenberg & Bender 1994; Willard-Mack et al 1996). In a mouse model of acute liver failure, pretreatment with MSO has been shown to significantly increase survival and lower levels of several cytokines, including the pro-inflammatory cytokine TNF-α (Jambekar et al 2011). Treatment of ALS mice with MSO has also been shown to extend lifespan and target excitotoxicity by lowering levels of glutamine and glutamate in certain brain regions (Ghoddoussi et al 2010). It is not entirely clear if all of the beneficial effects of MSO are due to glutamine synthetase inhibition, as there are other potential targets of the drug that have not been well characterized. Human studies examining the effects of consuming agenized flour, did not show that consumption of foods containing MSO had any negative effects on people (Newell et al 1949a; Newell et al 1949b). As a result, more work

needs to be done to fully understand how MSO exerts its beneficial effects and if it has any therapeutic potential.

2.1.3 Effect of Gender on Lifespan, Disease Progression, and the Response to Methionine Sulfoximine

Amyotrophic lateral sclerosis (ALS) is a progressive neurodegenerative disorder characterized by the death of motor neurons running through ventral roots and corticospinal tracts of the spinal cord through the brainstem and primary motor cortex. The death of these motor neurons gives rise to symptoms such as involuntary muscle spasms, muscle weakness and atrophy, and eventually leads to paralysis. Patients typically die within 2-5 years due to pulmonary complications and respiratory failure (Wijesekera & Leigh 2009).

ALS has been subdivided into two categories: (1) Sporadic ALS, the most common type of the disease, which appears to have no genetic component, and (2) Familial ALS, which is hereditary and accounts for only 5-10% of all cases (Wijesekera & Leigh 2009). The familial form of the disease tends to be autosomal dominant and has been linked to a variety of gene mutations, including the genes for TAR-DNA binding protein (TDP-43), and superoxide dismutase 1 (SOD1) (Wijesekera & Leigh 2009), the later mutation is commonly exploited in transgenic mouse models of the disease. Despite the discovery of several inheritable mutations involved in ALS, the underlying cause of motor neuron death remains unclear.

One mutation in particular, the SOD1 G93A mutation, has been transferred to a transgenic mouse (Gurney et al 1994) to create the primary animal model for characterizing this disease and for testing the effects of various drugs. This mouse lives approximately 120-130 days before the disease progresses to the point where the mouse must be euthanized. In a previous study we showed that methionine sulfoximine (MSO), a well-characterized inhibitor of glutamine synthetase, can extend the lifespan of the SOD1 G93A mouse by 8% when given i.p.

injections of 20 mg/kg three times a week (Ghoddoussi et al 2010). This lifespan extension, comparable to that seen with many other drugs tested on this mouse, was accompanied by changes in brain metabolites which support the conclusion that there is an interruption in the glutamine-glutamate cycle in the CNS, resulting in a decrease in both glutamine and glutamate and supporting the idea that the therapeutic effects are a consequence of a reduction in excitotoxicity.

We have continued these studies to test both the effect of dosage (since this mechanism-based inhibitor has very long-lasting effects on glutamine synthetase) and the gender-specificity of this drug, since ALS and other neurodegenerative diseases display gender specificity – affecting one gender more than the other. We also tested the role of sex hormones in both disease progression and the response to MSO treatment by measuring survival, disease progression, and response to MSO of ovariectomized female mice and castrated male mice. The results of those experiments demonstrate the involvement of sex hormones in both disease progression and the response of these mice to MSO treatment.

2.2 Materials and Methods

Animal Handling. Breeding pairs of the SOD1 mouse – B6JL (G93A) – were purchased from Jackson Laboratories and offspring containing the human SOD1 G93A mutation were identified by PCR of tail DNA, using primers described for this strain by Jackson Laboratories (jax.org). All animal experiments were approved by the Animal Investigation Committee of Wayne State University.

Methionine sulfoximine (MSO), obtained from Sigma Chemical Company (catalogue no. 5379) was dissolved in 0.9% saline and administered intraperitoneally (i.p.) at a dose of 20 mg/kg.

Mice were injected with MSO or saline once per week starting at 50 (+/- 2) days of age until they were euthanized. Mice were observed daily by the supervising veterinarians and laboratory-animal staff and were euthanized when either 1) they lost 20% of their maximum body weight, 2) they were unable to right themselves when put on their back or side, or 3) if, in the opinion of the supervising veterinarians, the mice were in distress or unable to obtain adequate food and water.

Hang-time Analysis. Mice were placed on a steel wire grid which was then inverted and placed over a plastic bin approximately 13 inches deep, with paper towels at the bottom to cushion the fall. The hang-time for each mouse was recorded as the time before the mouse released the grid and fell or at 120 seconds if the mouse did not fall before then. Mice were tested twice/week, starting at 50 days of age.

Animal Surgeries. All surgeries were performed between 30 and 40 days of age, before the animals had reached sexual maturity. Mice were anesthetized with i.p. injections of 0.4-0.75 mg/g body weight Avertin. A stock solution of Avertin was prepared by dissolving 25g of 2-2-2-tribromoethanol (Sigma) in 15.5 mL of tert-amyl alcohol (Sigma). This was then diluted to a 20 mg/mL working solution by adding 0.5 mL of the stock Avertin to 39.5 mL of PBS and filtering through a sterile 45 µm filter. Both the stock solution and the working solution were kept in foil-wrapped containers and the working solution was stored at 4°C when not in use.

Ovariectomies were performed by first shaving the lower backs of female mice and then sterilizing the area with Betadine and isopropanol. An incision was made in the middle of the lower back running parallel to the spinal cord. The skin was gently pulled away from the muscle and the first ovary was located. A very small incision was then made just below the kidney and the periovarian fat pad was gently pulled out of the body, bringing the ovary with it. Being careful not to crush the ovary, mosquito forceps were used to crush the fallopian tube and cranial-most portion of the uterine horn. The ovary was then removed by cutting above the

crushed area and the uterine horn was returned to the abdominal cavity. This was then repeated on the other side. Once both ovaries were removed, the skin incision was closed with wound clips.

Castrations were performed by first forcing the testicles to descend by applying light pressure to the abdominal region and pushing towards the tail. The testicles were then shaved and the area was sterilized with Betadine and isopropanol. An incision was made in the scrotum between the testicles. A second incision was then made in the tunica of the first testicle and the testis, vas deferens, and the fat pad were gently pulled out of the body. The blood vessels supporting the testis were cauterized and the testis was removed by cutting just below the site of cauterization. This was repeated on the other side and the skin incision was closed with wound clips.

Statistics and Data Analysis. The survival studies were analyzed by both parametric (Student's t test) and nonparametric (Kaplan-Meier) methods. Student's t test significance values, p, are always two-tailed. Means are notated as x(y), where x is the mean and y is its standard error. Unless noted, *p* values are from the t test. Kaplan-Meier analysis supplemented the t test by allowing the comparison of the survival curves (e.g., log rank statistic). The use of both types of analyses was possible because the certainty of death by the disease meant that no animals needed to be censored, although two mice died very early from causes unrelated to ALS and were removed from the study. Effect size was determined by calculating Cohen's *d* with the use of pooled standard deviations (Cohen 1988; Rosnow & Rosenthal 1996), and Cox regression was used to obtain the hazard ratio as an additional measure of effect size. The interpretation of *d* given in the text is according to Cohen's explanation. The 'hang-time' analysis used the same statistical tools as the survival studies with the terminal event in the 'time to event' Kaplan-Meier procedure being the inability to hang onto the grid.

2.3 Results

A weekly injection of MSO increases survival of the SOD1 G93A mouse. We previously showed that mice injected with 20 mg/kg MSO had their survival extended by approximately 8% (Ghoddoussi et al 2010). Since MSO is a mechanism-based inhibitor of glutamine synthetase, a single treatment lowers GS levels for an extended period of time, as animals have to synthesize more enzyme to overcome the inhibition – up to a week or more in rats and mice (Lamar 1968; Rao & Meister 1972). A single weekly injection should therefore be just as effective as multiple injections. Figure 2.3.1 shows the Kaplan-Meier survival curves for SOD1 G93A mice treated with a weekly i.p. injection of either saline or MSO (20 mg/kg), starting at 50 (+/- 2) days of age and illustrates that this dosing-schedule improves the survival of ALS mice (p=0.001, log rank test). A single weekly injection extends the mean lifespan from 128 (1) to 136 (2) days, where the value in parenthesis is the standard error of the mean.

Figure 2.3.1 Kaplan-Meier survival curves for MSO's effect on the lifespan of SOD1 G93A mice.

Animals were treated once a week with i.p. injections of either saline (diamonds) or 20 mg/kg MSO (squares). Mice treated with MSO (136 (2) days, *n*=50) lived significantly longer than saline-treated mice (128 (1) days, *n*=50), *p*<0.001, two-tailed, *d*=0.7.

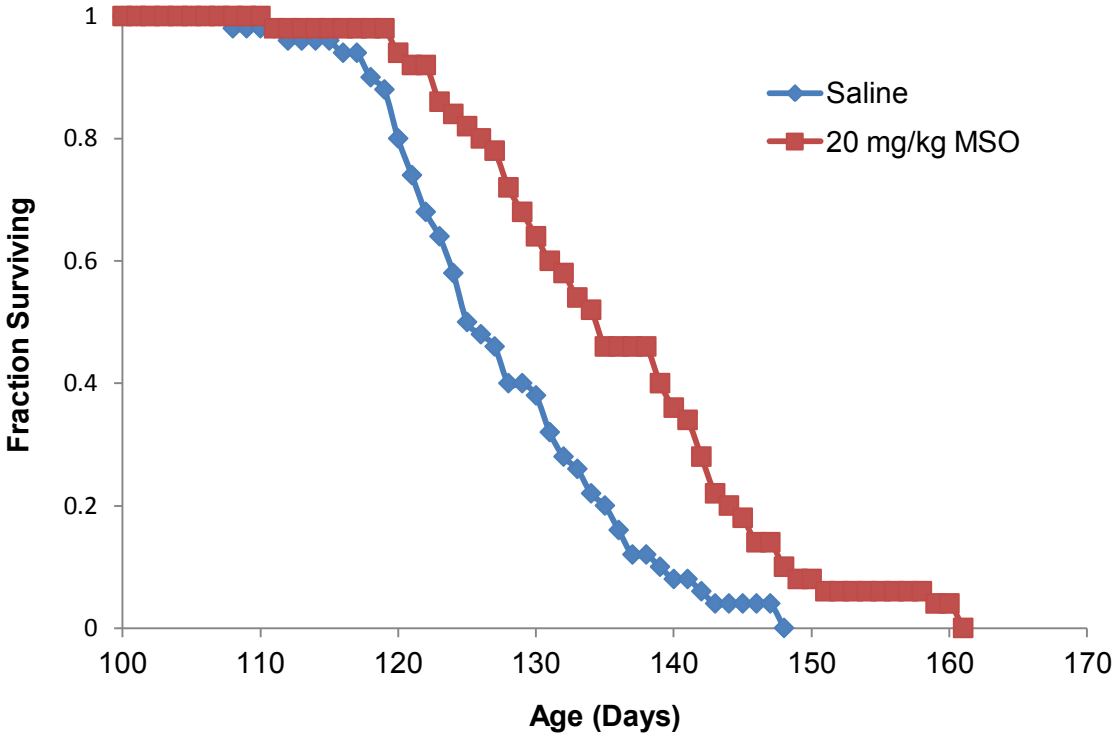

The increase in survival in MSO-treated SOD1 G93A mice depends on gender. A complete summary of the statistics for gender-dependent and treatment-dependent survival analyses is shown in Table 2.3.1. Cox regression analysis of the entire data set showed that gender and treatment (saline vs. MSO), were significantly affecting survival, with bootstrapped significance values of 0.008 and 0.001 respectively. Castration or overiectomization were also significant at 0.006 and 0.04 respectively. When we further analyzed the results by gender, MSO significantly extended the mean lifespan of both males and females, although females were more responsive. The mean lifespan of females is extended from 130 (2) to 140 (2) days (p=0.001, d=1.0), while the mean lifespan of males is extended from 125(2) to 132(2) days (p=0.02, d=0.6) (Table 2.3.1 and Figure 2.3.2). The effect sizes (d) indicate a greater effect on females. The conclusion that the therapeutic effects of this drug on lifespan are greater on females than on males is also supported by further analysis of survival data of MSO-treated animals. When comparing the mean lifespan of males and females treated with MSO, we see that females live significantly longer than males (140 (2) days and 132 (2) days respectively, p=0.004, d=0.8). Kaplan-Meier survival analysis of saline-treated males compared to that of saline-treated females were not significantly different (p=0.09, log rank test), but the same analysis of the survival curves of MSO-treated males and females showed that MSO-treated females lived significantly longer than MSO-treated males (p=0.004, log rank test).

Table 2.3.1 Summary of survival comparisons and associated statistical values.

Category	Comparison	*n*	mean (SEM)	*p* (t test)	*p* (log rank)
All Intact	Saline	50	128 (1)		
Mice	MSO	50	136 (2)	0.001	0.0001
Intact	Saline	25	130 (2)		
Females	MSO	24	140 (2)	0.001	0.0004
Intact	Saline	25	125 (2)		
Males	MSO	26	132 (2)	0.02	0.02
OVR	Saline	9	129 (2)		
Females	MSO	9	130 (3)	0.8	0.4
CSTR	Saline	11	128 (3)		
Males	MSO	11	130 (4)	0.6	0.4
Saline-treated	Intact	25	130 (2)		
females	OVR	9	129 (2)	0.7	0.6
Saline-treated	Intact	25	125 (2)		
males	CSTR	11	128 (3)	0.4	0.4
MSO-treated	Intact	24	140 (2)		
females	OVR	9	130 (3)	0.01	0.004
MSO-treated	Intact	26	132 (2)		
males	CSTR	11	130 (4)	0.5	0.9
Intact	Females	25	130 (2)		
Saline-treated	Males	25	125 (2)	0.06	0.09
Intact	Females	24	140 (2)		
MSO-treated	Males	26	132 (2)	0.004	0.004
Neutered	Females	9	129 (2)		
Saline-treated	Males	11	128 (3)	0.8	0.9
Neutered	Females	9	130 (3)		
MSO-treated	Males	11	130 (4)	0.9	0.6

Category = mice evaluated; Comparison = gender, treatment, or surgery group compared; *n* = the number of animals/group; Mean (SEM) = average age (standard error of the mean); *p* (t test) = *p* value determined by a bootstrapped t test with 1000 samples; *p* (log rank) = *p* value determined using Kaplan-Meier; OVR = ovariectomized; CSTR = castrated.

Figure 2.3.2 Kaplan-Meier survival curves of MSO's effect on the longevity of each gender.

The data shown in Figure 2.3.1 was separated by gender and replotted. **A.** The mean age of survival for females treated with MSO (140 (2) days, *n*=24) was significantly higher than that of saline-treated females (130 (2) days, *n*=25), *p*=0.001, two-tailed, *d*=1.0. **B.** The mean lifespan of male mice treated with MSO (132 (2) days, *n*=26) was also found to be significantly higher than that of saline-treated males (125 (2) days, *n*=25), *p*=0.02, two-tailed, *d*=0.6. Diamonds represent saline-treated animals and squares represent animals treated with MSO.

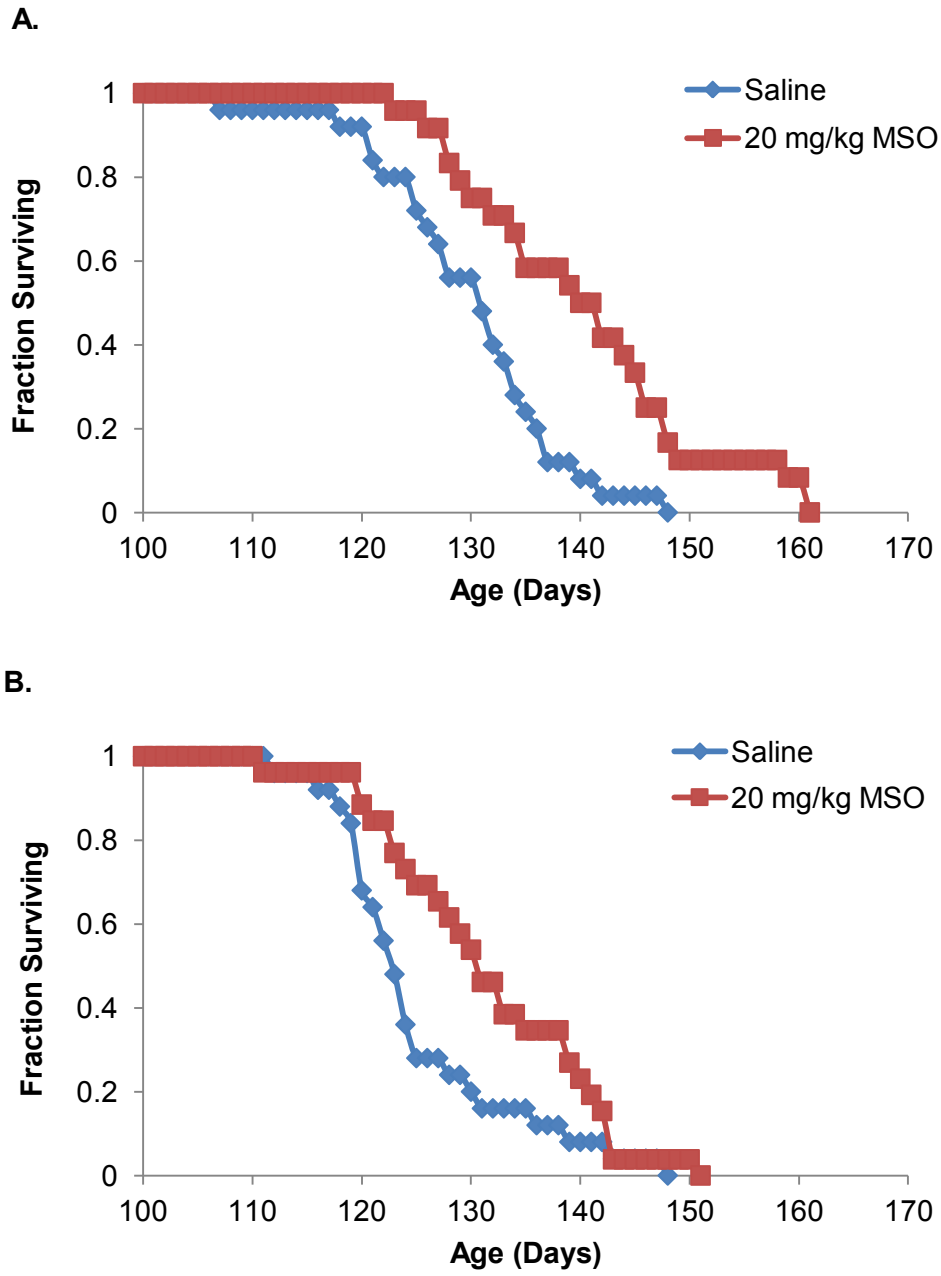

Tests of neuromuscular function. We conducted an analysis of neuromuscular function, a hang-time analysis (see Materials and Methods), by measuring how long mice could hang on to an inverted wire grid before losing their grip and falling. The results of this test were analyzed in two ways. First, we plotted the average hang-time (in seconds, 120 maximum) for each population versus age, as shown in Figure 2.3.3 for female and male mice. For female mice, MSO improves hang-time over the interval from 114 to 123 days of age ($p<0.05$ for the points indicated in Figure 2.3.3). For male mice, treatment makes no significant difference in neuromuscular function. We then carried out a Kaplan-Meier analysis of these same data, using a hang-time of zero as the terminal event. This approach allows us to analyze the effects of gender and drug treatment on the disease progression. Additionally, a hang-time of zero is a more objective measure of a disease endpoint than determining if a mouse has met our criteria for euthanasia. The analysis, shown in Figure 2.3.4, demonstrates that MSO extends the time to the complete loss of hang-time competence for females (123 (2) to 132 (2) days, p=0.0008 log rank test) and thus delays disease progression in the later stages of the disease. It also confirms that this drug, a specific inhibitor of glutamine synthetase, exerts its effects in a gender-specific manner. This analysis shows that the drug might benefit males – mostly in the later stages of the disease – in addition to females, but it clearly benefits females to a greater extent. A complete summary of the gender-dependence and treatment-dependence of the Kaplan-Meier hang-time competence analyses are shown in Table 2.3.2.

Figure 2.3.3 Hang-time data for female mice and male mice treated with saline and 20 mg/kg MSO.

Each of the four groups consisted of 17 mice except for the MSO-treated females, which consisted of 15 mice. Each point represents the average hang-time of at least 15 mice measured at that age +/- 2 days. In the curves for female mice **(A)** , we have calculated the significance for the points where the curves diverge using a t-test, and the resultant *p* values are listed above the three points on the graphs where MSO treatment produces a significant difference. The curves for male mice **(B)** show no significant differences in hang-time. Curves were truncated shortly after the mice started dying when how we treated dead mice in this analysis began to significantly affect the statistics.

A.

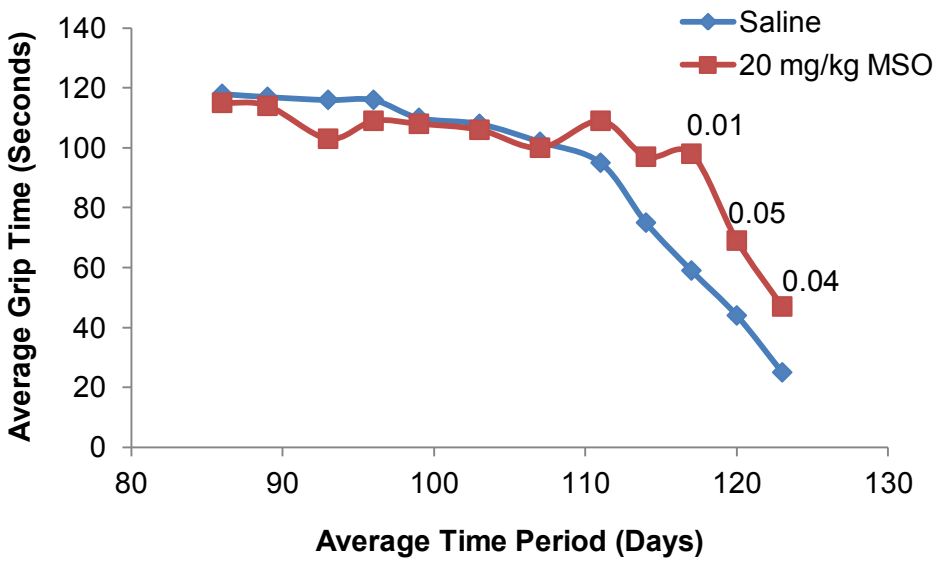

B.

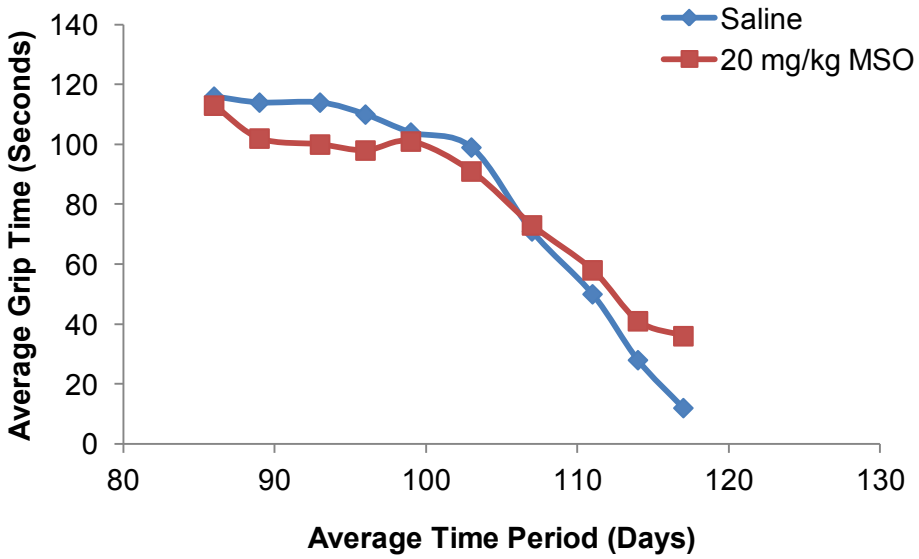

Figure 2.3.4 Kaplan-Meier hang-time competence curves using zero hang-time (complete inability to hang on to a wire grid) as the terminal event.

A. The average age at which hang-time competence was lost in females was improved significantly with MSO treatment (132 (2) days, *n*=15) when compared to that of saline-treated females (123 (2) days, *n*=17), *p*=0.0004, two-tailed, *d*=1.4. **B.** In male mice, the average age at which hang-time competence was lost was not significantly improved by MSO treatment (122 (2) days, *n*=17) when compared to saline treatment (118 (1) day, *n*=17), *p*=0.09, two-tailed, *d*=0.6. Diamonds represent saline-treated animals and squares represent animals treated with MSO.

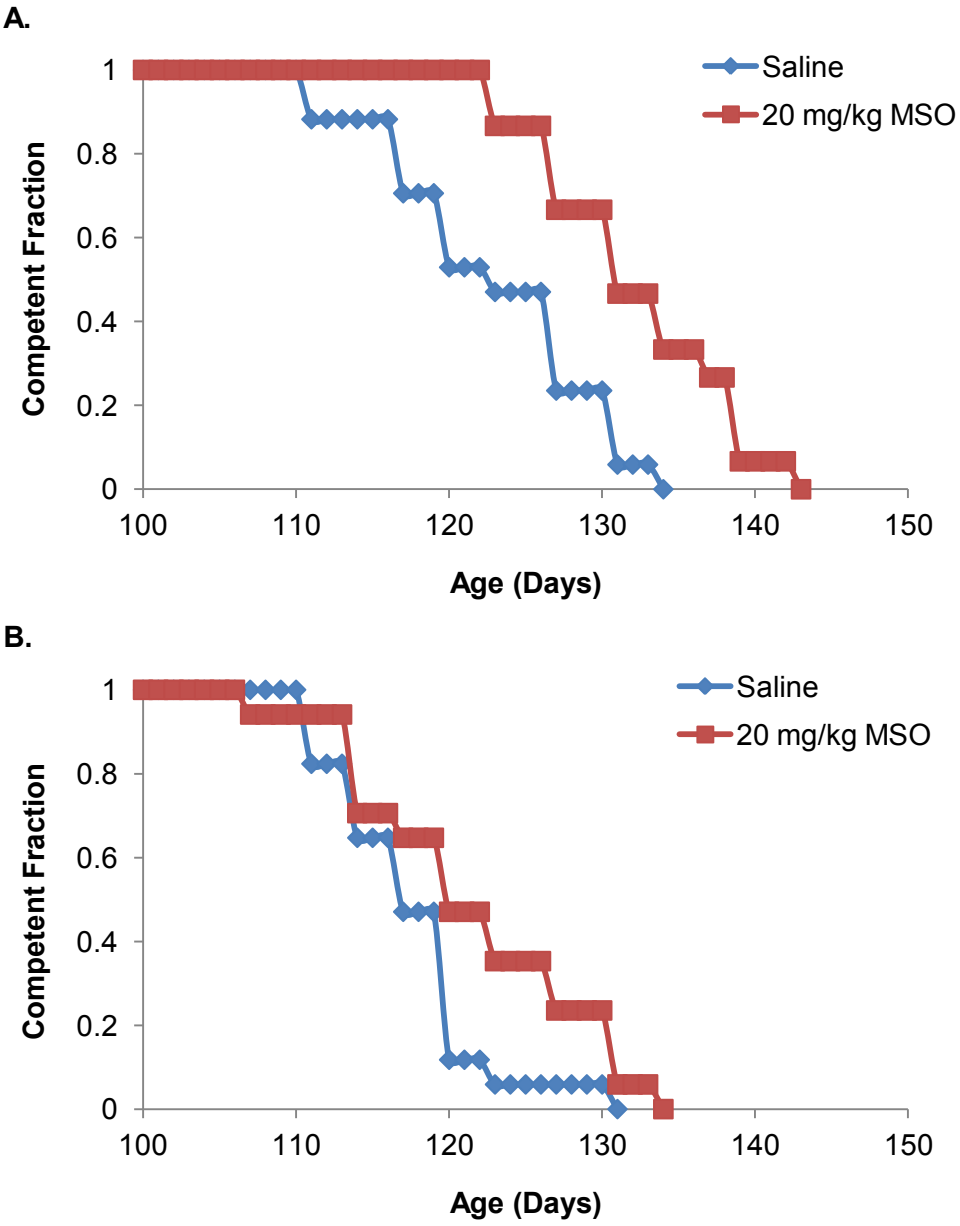

Table 2.3.2 Summary of hang-time competence comparisons and associated statistical values.

Category	Comparison	*n*	mean (SEM)	*p* (t test)	*p* (log rank)
All Intact	Saline	34	120 (1)		
Mice	MSO	32	127 (2)	0.002	0.0007
Intact	Saline	17	123 (2)		
Females	MSO	15	132 (2)	0.0004	0.0008
Intact	Saline	17	118 (1)		
Males	MSO	17	122 (2)	0.09	0.06
OVR	Saline	9	124 (2)		
Females	MSO	9	124 (3)	0.9	0.9
CSTR	Saline	11	123 (2)		
Males	MSO	11	126 (3)	0.4	0.3
Saline-treated	Intact	17	123 (2)		
females	OVR	9	124 (2)	0.7	0.6
Saline-treated	Intact	17	118 (1)		
males	CSTR	11	123 (2)	0.03	0.02
MSO-treated	Intact	15	132 (2)		
females	OVR	9	124 (3)	0.009	0.01
MSO-treated	Intact	17	122 (2)		
males	CSTR	11	126 (3)	0.2	0.07
Intact	Females	17	123 (2)		
Saline-treated	Males	17	118 (1)	0.02	0.02
Intact	Females	15	132 (2)		
MSO-treated	Males	17	122 (2)	0.0002	0.0004
Neutered	Females	9	124 (2)		
Saline-treated	Males	11	123 (2)	0.8	0.9
Neutered	Females	9	124 (3)		
MSO-treated	Males	11	126 (3)	0.6	0.2

Category = mice evaluated; Comparison = gender, treatment, or surgery group compared; *n* = the number of animals/group; Mean (SEM) = average age (standard error of the mean); *p* (t test) = *p* value determined by the t test using bootstrapped samples of 1000; *p* (log rank) = *p* value determined using the log rank test for Kaplan-Meier, time to event; OVR = ovariectomized; CSTR = castrated.

Effects of castration and ovariectomization on survival and grip strength. Given the strong gender effect of MSO treatment, we conducted the same analyses of survival and hang-time on neutered mice – ovariectomized females and castrated males – to determine if female sex hormones were beneficial in the response to MSO, or if male sex hormones were detrimental to that response. The Kaplan-Meier survival analysis shown in Figure 2.3.5A demonstrates that MSO does not extend the lifespan of ovariectomized females (p=0.4, log rank test), and the results of the Kaplan Meier hang-time competence analysis, shown in Figure 2.3.6A, indicate that MSO does not slow neuromuscular deterioration (p=0.9, log rank test). Therefore, removing female sex hormones eliminates the beneficial effects of MSO on female mice.

Castrating the male mice tested the role of male sex hormones on disease progression in both the absence (saline) and presence of MSO. Figure 2.3.5B shows the results of the Kaplan-Meier survival analysis and illustrates that MSO does not significantly affect castrated mouse survival (p=0.4, log rank test). Nor does MSO treatment have a significant effect on the time to the complete loss of hang-time competence in castrated mice (p=0.3 log rank test, Figure 2.3.6B and Table 2.3.2). So neutering mice eliminated the beneficial effects of MSO on survival of both male and female mice, and eliminated the beneficial effects of MSO on disease progression, as measured by grip in females.

Figure 2.3.5 Kaplan-Meier survival curves of MSO's effect on longevity in the absence of sex hormones.

Ovariectomized female and castrated male SOD1 G93A mice were treated once a week with i.p. injections of either saline (diamonds) or 20 mg/kg MSO (squares). **A.** The average lifespan of ovariectomized female mice treated with MSO (130 (3) days, *n*=9) was similar to that of saline-treated ovariectomized females (129 (2) days, *n*=9). In the absence of estrogens, MSO no longer had an effect on the longevity of female mice, *p*=0.8. **B.** In castrated male mice, MSO does not have an effect on the average lifespan (130 (4) days, *n*=11) compared to saline treatment (128 (3) days, *n*=11), *p*=0.6.

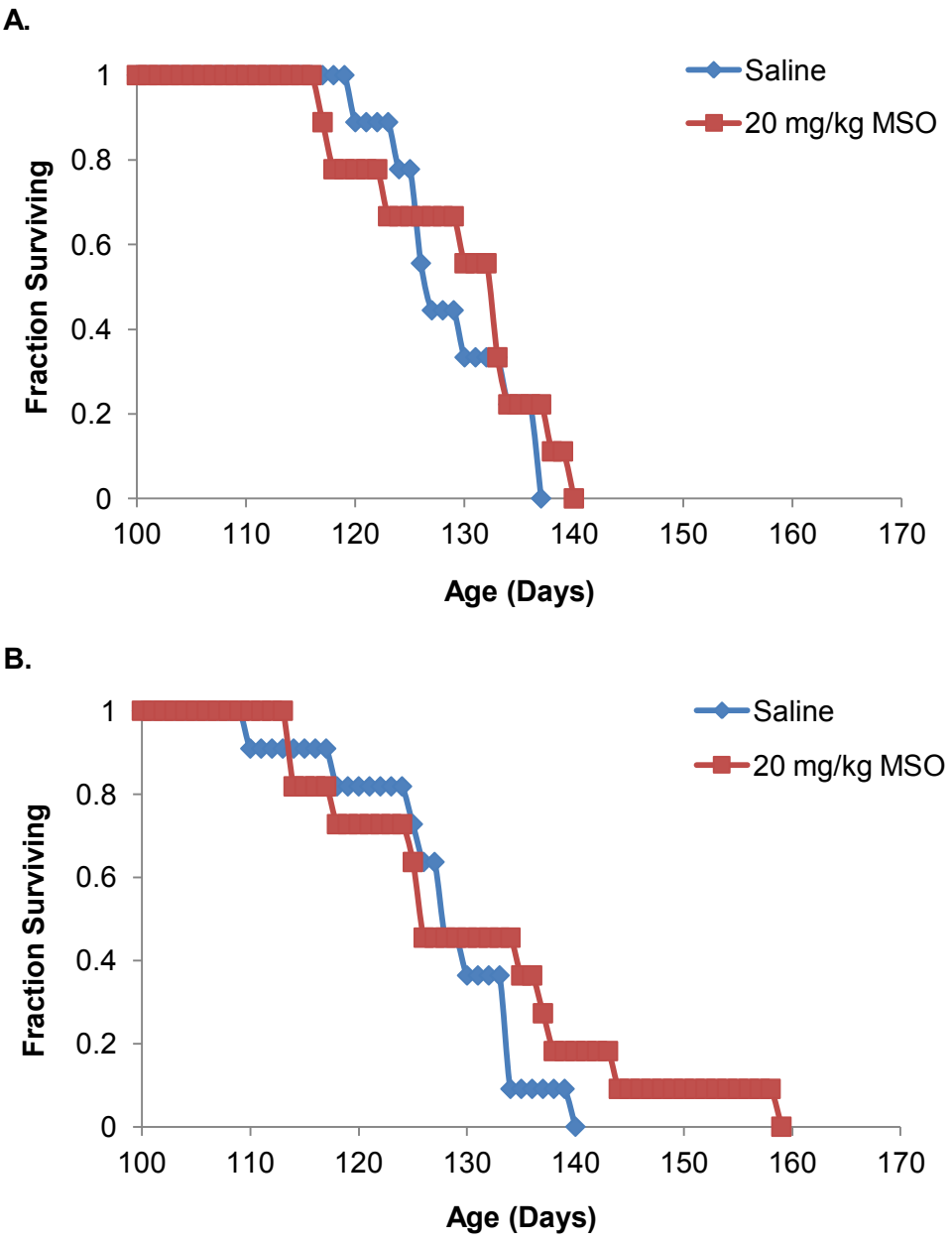

Figure 2.3.6 Kaplan-Meier hang-time competence curves (using zero hang-time as the terminal event) for gonadectomized mice.

A. There is no difference in the average age at which hang-time competence was lost between ovariectomized females treated with MSO and saline (124 (3) days and 124 (2) days respectively, *n*=9 for each treatment group), *p*=0.8. **B.** MSO treatment did not increase the average age at which hang-time competence was lost in castrated males (126 (3) days and 123 (2) days respectively, *n*=11 for each treatment group), *p*=0.4. Diamonds represent saline-treated animals and squares represent animals treated with MSO.

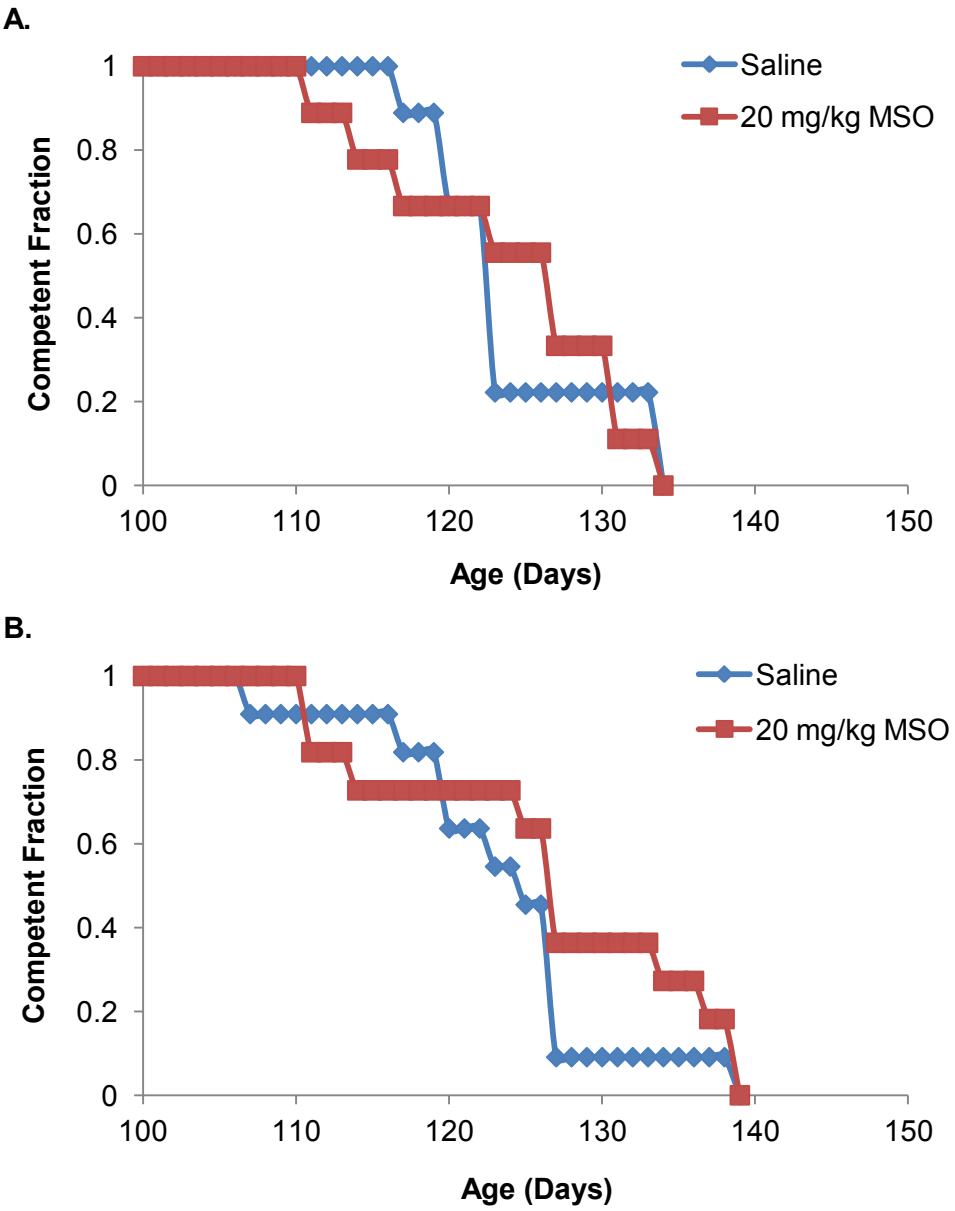

Interestingly, these studies showed that castration alone had a significant effect on the hang-time competence of the male mice. Figure 2.3.7 shows a normal Kaplan-Meier analysis of the lifespan of saline-treated gonadectomized versus non-gonadectomized males and females. There was no significant difference in the survival curves due to gonadectomization for either gender (p=0.4 for females and p=0.4 for males as determined by the log rank test). However, Figure 2.3.8 and Table 2.3.2 show the Kaplan-Meier analysis of hang-time, using zero grip time as the terminal event, and reveal that castration alone produces significant improvement in saline-treated male mice (p=0.02, log rank test), but ovariectomization has no effect on hang-time competence of female mice (p=0.6, log rank test). These results suggest that removal of male sex-hormones has a beneficial effect on neuromuscular function of male SOD1 G93A mice.

Figure 2.3.7 Kaplan-Meier survival plots comparing the longevity of saline-treated mice with intact gonads to those that have undergone gonadectomy.

Diamonds represent saline-treated animals with intact gonads and squares represent gonadectomized saline-treated animals. **A.** Saline-treated females with intact ovaries (130 (2) days, *n*=25) do not live significantly longer than ovariectomized females treated with saline (129 (2) days, *n*=9), *p*=0.7, two-tailed, *d*=0.1. **B.** Saline-treated males with intact testes (125 (2) days, *n*=25) do not live significantly longer than castrated males treated with saline (128 (3) days, *n*=11), *p*=0.4, two-tailed, *d*=0.3.

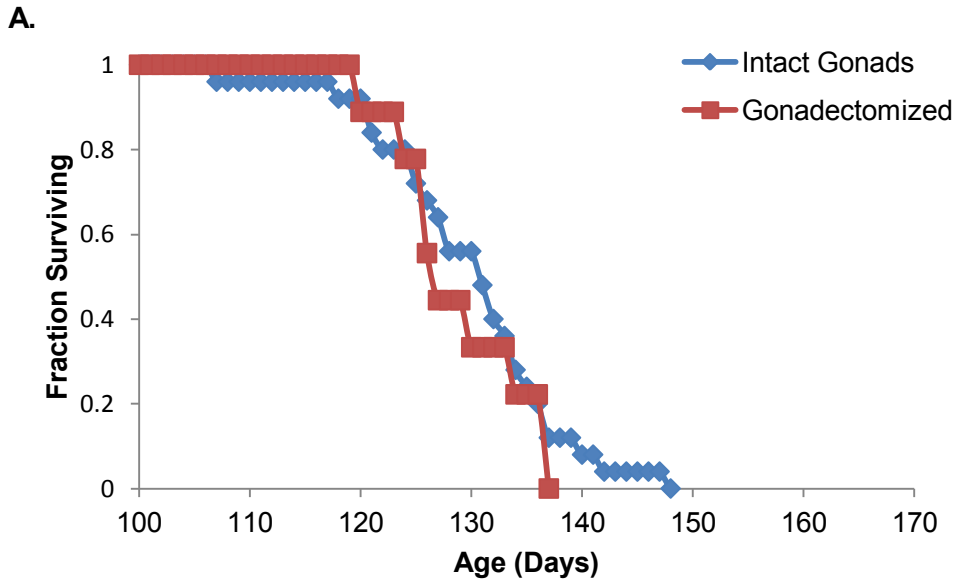

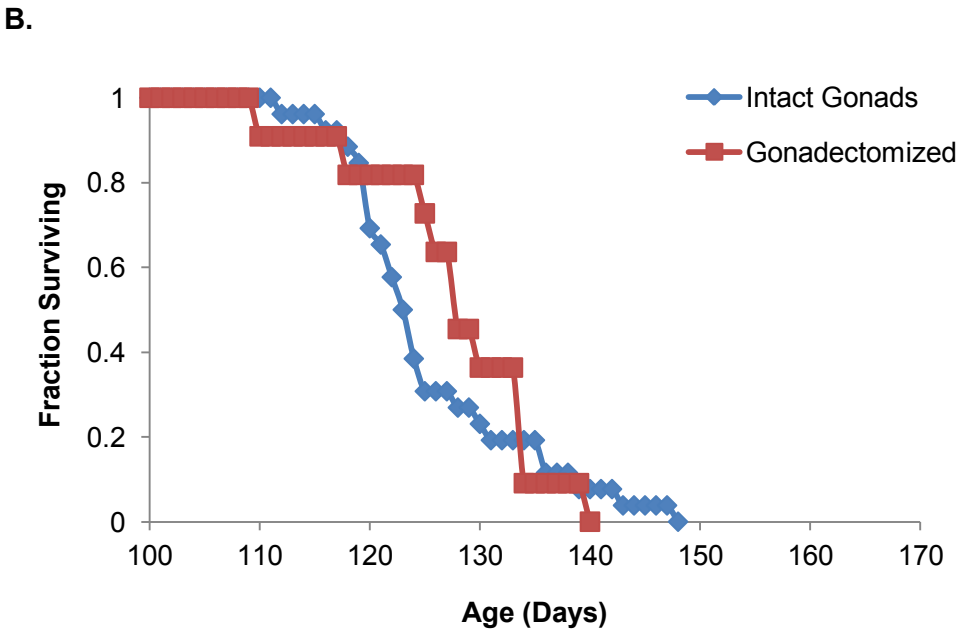

Figure 2.3.8 Kaplan-Meier hang-time competence plots comparing saline-treated mice with intact gonads to those that have undergone gonadectomy.

Diamonds represent animals with intact gonads and squares represent gonadectomized animals. **A.** For saline-treated female mice, there is no difference in the average age at which hang-time competence was lost between females with intact ovaries (123 (2) days, *n*=17) and ovariectomized females (124 (2) days, *n*=9), *p*=0.7, two-tailed, *d*=0.1. **B.** Castration of male mice significantly increases the average age at which hang-time competence was lost in saline-treated males (123 (2) days, *n*=11 for castrated males, compared to 118 (1) day, *n*=17 for males with intact gonads), *p*=0.03, two-tailed, *d*=0.9.

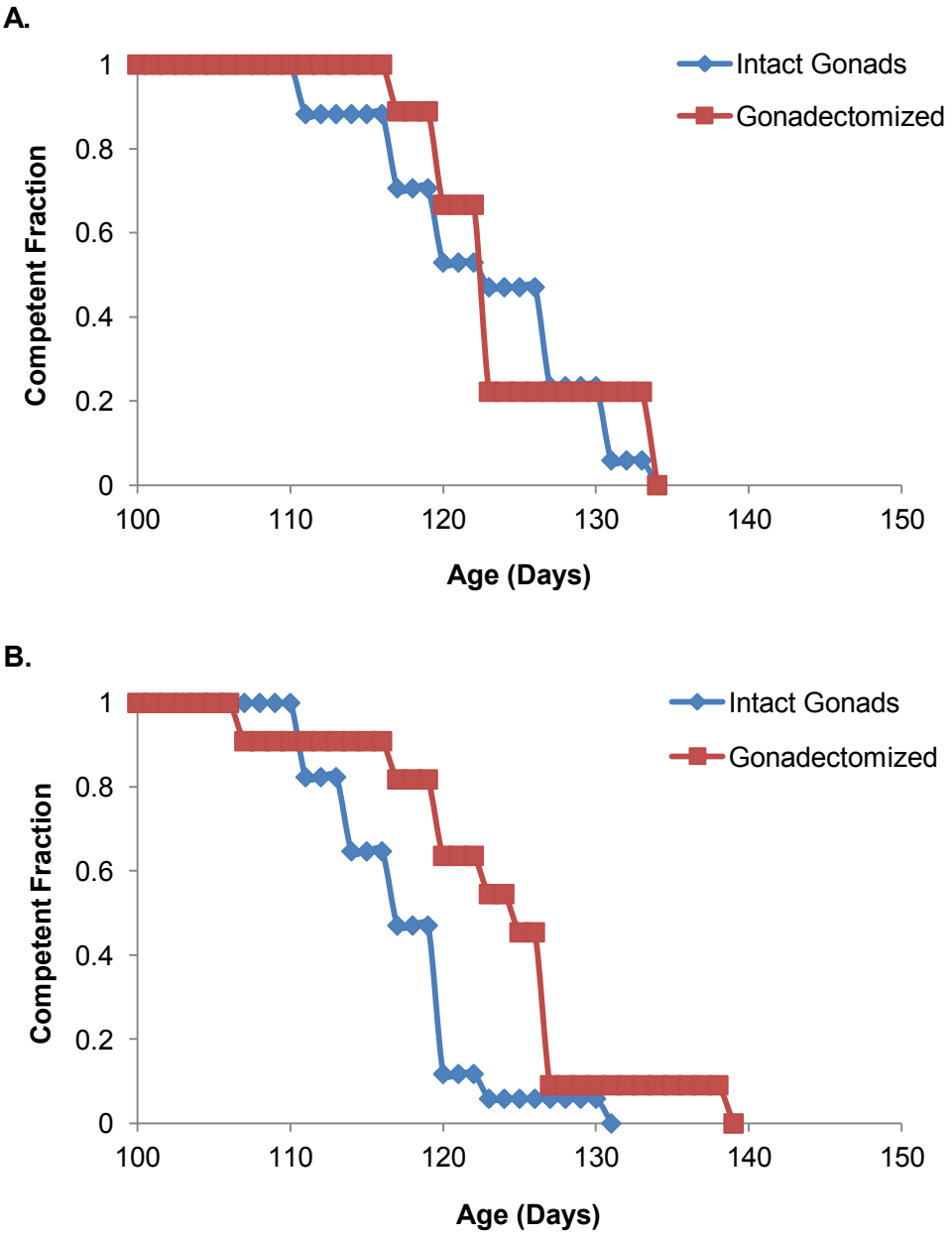

2.4 Discussion

We have previously shown that MSO, a potent inhibitor of glutamine synthetase, both extends the lifespan of SOD1 G93A mice and alters the levels of several neurochemicals - notably glutamine, glutamate, and GABA - in different brain regions (Ghoddoussi et al 2010). Those studies used the published dosage of 20 mg/kg MSO (Blin et al 2002), injected three times per week. In this report we expanded those experiments in three ways: 1) by increasing the total number of mice tested, 2) by using a grip assay monitoring neuromuscular function to provide an alternative to death for measuring the effects of the drug, and 3) by examining gender-dependence of the response to MSO and, in particular, the involvement of male and female sex hormones in disease progression through ovariectomy and castration of SOD1 G93A mice.

Our first survival study consisted of 30 mice – half treated with saline and half treated with MSO three times per week (Ghoddoussi et al 2010). The current study consisted of 100 mice – half treated with saline and half treated with MSO once a week. Since MSO is a mechanism-based inhibitor of glutamine synthetase, inhibition can only be overcome by synthesizing more of the enzyme. Hence, recovery of full brain GS activity takes a long time – up to several weeks (Lamar 1968; Rao & Meister 1972). If the action of the drug on these mice involves inhibition of glutamine synthetase, the reduced dosage should have the same effects as the higher dosage. We found that in fact the reduced dosing schedule produced essentially the same extension of lifespan in the SOD1 G93A mouse model for ALS, despite the reduction in frequency of administration, providing additional support for MSO having a significant effect on disease progression and again indicating that the therapeutic target is glutamine synthetase.

In order to reduce the uncertainties involved in applying criteria for euthanasia, we conducted grip (hang-time) assays to monitor neuromuscular function and then carried out a Kaplan-Meier analysis using the time the mice were unable to grip (hang-time of zero; i.e. total

failure of tested muscle strength) as the terminal event, instead of death. This measurement is more objective and provides an additional check on disease progression. While euthanasia criteria were applied in a blinded manner the decision was made by the veterinary staff, introducing a small measure of subjectivity to the survival analysis.

This Kaplan-Meier hang-time competence analysis also supported the conclusion that MSO is acting in a gender-specific fashion. In the actual survival analysis, the drug appears to be working better on females than on males, although the extension of lifespan is significant for both. While the log rank test for differences in survival due to MSO treatment resulted in a much smaller *p* value for females (0.0004) than for males (0.02), this does not mean that the MSO affected females more strongly. Calculating effect sizes (*d*) according to Cohen (Cohen 1988), the effect size for females (1.0) is larger than that for males (0.6). This corresponds to 36% of the females improving with MSO treatment, as compared to 26% of the males. Calculating hazard ratios by Cox regression, females reduced their risk of death on MSO by 65%; while males reduced their risk of death by 46%, again indicating that MSO has a larger effect on female survival. In the hang-time analysis, the effect of drug treatment did not reach significance for males (p=0.06, log rank test) while it did for females (p=0.0008). More importantly, the 95% confidence intervals for the hazard ratio for males, in contrast to that for females, included a hazard ratio of 1.0, indicating that MSO does not necessarily improve neuromuscular function.

Both ovariectomizing females and castrating males eliminated the beneficial response of mice to MSO treatment, demonstrating that the therapeutic effects of this drug involve enzymes or pathways whose activities are influenced by estrogen or testosterone, or some other sex hormone. Whether the hormone-dependent effects are on glutamine synthetase itself, or on some aspect of metabolism that is influenced by both glutamine synthetase and sex hormones, was not tested in these studies. We have assayed brain glutamine synthetase activity in this

mouse model, as previously described (Ghoddoussi et al 2010) and found no significant gender differences in either treated or untreated mice. Finally, the results from castrated male mice show that male sex hormones facilitate disease progression, since castration delayed progression in the hang-time analysis even though it did not ultimately affect lifespan. Testosterone or another hormone therefore acts on some process that accelerates neurodegeneration. Ovariectomizing females, however, affected only the response to MSO but neither lifespan nor disease progression as measured by the hang-time assay. The hormone-responsive target affected by MSO treatment is therefore probably some pathway or protein that can ameliorate disease progression when MSO is present, but which is not otherwise a significant component of the disease process. In fact, comparing our various measurements on ovariectomized females and castrated males revealed no significant differences between these groups (Tables 1 and 2). The fact that the differences between males and females arise only in animals with intact gonads is another indication that sex hormones play a significant role in disease progression – male hormones exacerbate the disease, and both male and female hormones influence some aspect of metabolism or cell biology that can respond beneficially to treatment with MSO.

In humans, the age of onset of ALS is between 50 and 60 years of age for both the sporadic and familial forms (Bruijn et al 2004), which are clinically indistinguishable from one another. ALS has a slight male prevalence with a male to female ratio of 3:2 (Pasinelli & Brown 2006; Wijesekera & Leigh 2009). In large studies examining both sporadic and familial cases of ALS, the overall incidence and prevalence of the disease are greater in mean than women (McCombe & Henderson 2010). Although gender does not seem to have an effect on survival, most of the ALS patients that fall within the younger age groups in these studies are men. Interestingly, the male to female ratio decreases with increasing age and approaches 1:1 after 60 years of age (Haverkamp et al 1995), suggesting sex hormones may play a role in the

disease. Gender differences in clinical features of the disease have also been noted, but are difficult to explain (McCombe & Henderson 2010). Some potential explanations for these differences are biological differences between males and females - including gender differences in the overall immune response and the central nervous system and its ability to repair damage, possibly due to protective effects of certain hormones, and gender differences in exposure to certain toxins.

Mouse models of ALS also reflect several gender differences in the disease. Survival data from SOD1 G93A transgenic mice shows that females have a slightly longer lifespan than males. The average lifespan of female transgenic mice is between 130 and 135 days, whereas the average male lifespan is between 125 and 130 days (Choi et al 2008; Heiman-Patterson et al 2005). Male mice typically show an earlier onset of the disease than females (Heiman-Patterson et al 2005), which is consistent with data collected from ALS patients. Studies looking at gender differences in the extension reflex and rotarod performance of these animals provide evidence suggesting the disease progresses more slowly in female mice (Choi et al 2008). In contrast to our results, those studies showed that ovariectomizing these mice leads to accelerated disease progression (Choi et al 2008) and a decrease in the average lifespan. This decrease in lifespan was shown to be reversed with 17β-estradiol treatment (Choi et al 2008; Groeneveld et al 2004), further supporting the idea that estrogen plays a protective role in female ALS mice. Our studies, however, show no protection by female sex hormones in the absence of MSO, but suggest that male sex hormones facilitate the disease progression.

Data from both human and animal studies show that there are biological differences between males and females that can influence the progression of diseases like ALS. If sex hormones can alter the progression of a disease, then they should be able to influence the effectiveness of treatment, as is seen in these studies. Using the SOD1 G93A mouse model for ALS, Teng et al. showed that a β2-adrenoceptor agonist, clenbuterol, exhibited a gender-

specific effect (Teng et al 2006). Clenbuterol was able to help prevent weight loss, delay motor symptoms, and extend the median survival, and seemed to exert a protective effect on neurons in female, but not male, mice (Teng et al 2006). It has also been shown that in the SOD1 mouse, ROS production is increased in male spinal cords but not females, and that males and females had different responses to treatment with GCSF (Naumenko et al 2011). Gender-specific differences in both neurological parameters and electrophysiological changes have also been observed in the SOD1 mouse (Alves et al 2011).

There has been little biochemical characterization of the overall metabolic profile of the SOD1 G93A mouse model for ALS, much less for information on the gender-specific differences in metabolites and metabolic enzymes. The fact that an inhibitor directed at a central enzyme of nitrogen metabolism can delay disease progression and extend lifespan in a gender-specific manner suggests that this disease may involve a metabolic defect that responds to sex hormones, either directly or indirectly. Such gender-specific differences must therefore be identified and accounted for in the development of therapies to treat ALS. We are currently trying to identify metabolic differences between wild-type and SOD1 G93A mice in order to determine how treatment with MSO might influence those differences, in an effort to identify targets for other such “metabolic” therapies.

CHAPTER 3

BIOCHEMICAL EFFECTS OF MSO TREATMENT ON ALS MICE

3.1 Introduction

3.1.1 Amino Acid Metabolism

Amino acids are the basic building blocks of proteins within the body and can be classified in a variety of ways – based on charge of the R-group, architecture, the body's ability to synthesize them, or based on their degradative end products and the metabolic cycle they are then shuttled into. There are 20 common amino acids and a variety of uncommon amino acids that are derived from them. Of the 20 common amino acids, humans are capable of producing 11 of them, while the other 9 must be obtained through the diet (Nelson & Cox 2008). Histidine, isoleucine, leucine, lysine, methionine, phenylalanine, threonine, tryptophan, and valine must be provided in the diet and are therefore considered to be essential amino acids. The body has pathways that can produce alanine, asparagine, aspartate, glutamate, and serine and as a result, these amino acids are considered to be nonessential. Arginine, cysteine, glutamine, glycine, proline, and tyrosine can also be produced by the body, but are required during development and some disease conditions and are therefore classified as conditionally essential amino acids (Nelson & Cox 2008).

Amino acids are ultimately broken down into seven potential end products which converge at the citric acid cycle, where their carbon skeletons can be completely oxidized to carbon dioxide and water or go on to produce glucose or ketone bodies. Those amino acids that are broken down to produce acetoacetyl-CoA (leucine, lysine, phenylalanine, tryptophan, and tyrosine) and acetyl-CoA (isoleucine, leucine, threonine, and tryptophan) are considered to be ketogenic because they can ultimately go on to produce ketone bodies. Those amino acids that are converted to glutamate (glutamine, arginine, histidine, and proline) or broken down into

succinyl-CoA (isoleucine, methionine, threonine, and valine), fumarate (phenylalanine and tyrosine), oxaloacetate (asparagine and aspartate), or pyruvate (alanine, cysteine, glycine, serine, threonine, and tryptophan) are considered to be glucogenic amino acids because their carbon skeletons can be used for the production of glucose (Nelson & Cox 2008). Tryptophan, tyrosine, isoleucine, phenylalanine, and threonine are both glucogenic and ketogenic. Figure 3.1.1.1 shows the structures of the common amino acids, organized by the charge of the R-group.

Figure 3.1.1.1 The common amino acids.

The 20 common amino acids contain a variety of R-groups that can be positively or negatively charged, polar (hydrophilic), nonpolar (hydrophobic), or aromatic. Those amino acids in red are glucogenic, those in blue are ketogenic, and those in purple have the ability to be either ketogenic or glucogenic. Essential amino acids are labeled with asterisks (*) and conditionally essential amino acids are labeled with a cross (†).

Polar, Uncharged Amino Acids

Serine

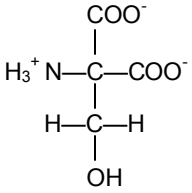

Threonine*

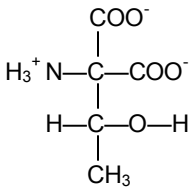

Cysteine*

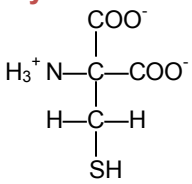

Asparagine

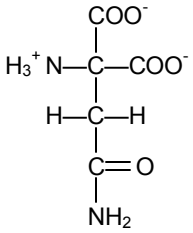

Glutamine†

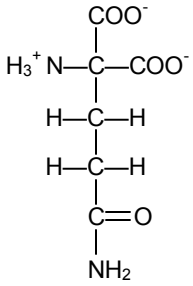

Nonpolar, Aliphatic Amino Acids

Glycine†

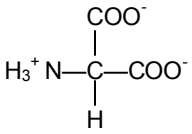

Alanine

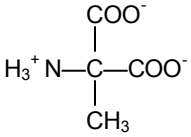

Proline†

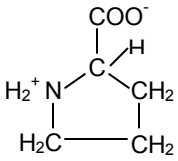

Valine*

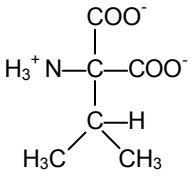

Leucine*

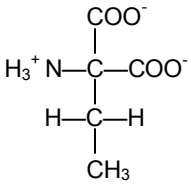

Isoleucine*

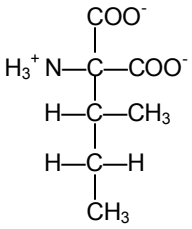

Methionine*

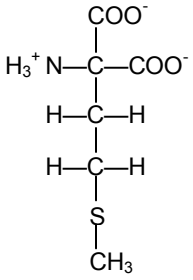

Aromatic Amino Acids

Phenylalanine*

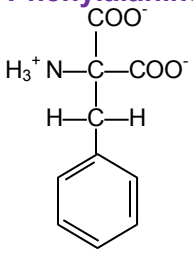

Tyrosine†

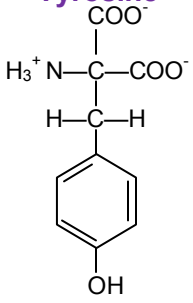

Tryptophan*

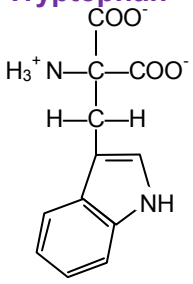

Positively Charged Amino Acids

Lysine*

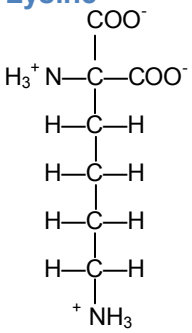

Arginine†

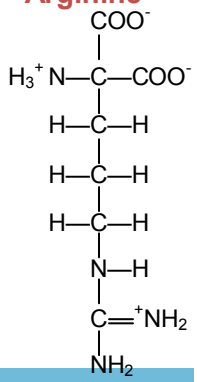

Histidine*

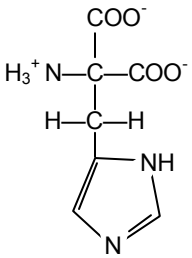

Negatively Charged Amino Acids

Aspartate

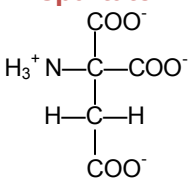

Glutamate

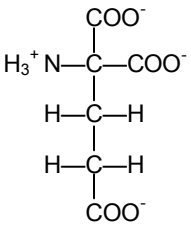

Protein obtained through the diet is denatured and broken down by the stomach and passed to the small intestine where it is further broken down and absorbed. Absorption occurs through enterocytes, which line the small intestine and colon. Microvilli on the surface of enterocytes increase the surface area available for the absorption of nutrients and the glycocalyx coating the inside of the gastrointestinal tract contains a variety of enzymes to aid in further protein breakdown (Purves et al 2001). Individual amino acids and small peptide fragments can be taken up by enterocytes (Adibi et al 1967) through a variety of amino acid transport systems, some of which depend upon the sodium gradient within the gut for transport (Broer 2008). The anatomy of the small intestine is such that it contains millions of projections (called villi) extending into the lumen, each of which contains venules and arterioles lining the center through which blood circulates (Tortora & Grabowski 1996). One mechanism believed to be important in the uptake of amino acids by the intestine is the γ-glutamyl cycle, which utilizes intracellular glutathione to help bring amino acids into the cell (Cornell & Meister 1976; Meister et al 1979; Orlowski & Meister 1970). Figure 3.1.1.2 shows the γ-glutamyl cycle, which brings amino acids into the cell by first attaching them to glutathione via γ-glytamyl transpeptidase and then releasing them inside the cell and replenishing glutathione. Peptides taken up by enterocytes lining the villi in the lumen are broken down within the cell and transported into the blood stream through the basolateral membrane (Broer 2008). Once in the bloodstream, amino acids are circulated to organs and taken up through transport systems similar to those utilized in the small intestine (Broer 2008). The brain, which contains barriers preventing the entry of many substances, also expresses a variety of amino acid transport systems (Smith 2000) to bring in precursors of neurotransmitters and neuropeptides.

Figure 3.1.1.2 The γ-glutamyl cycle of amino acid uptake.

1) γ-glutamyl transpeptidase (γ-GT) within the membrane transfers the γ-glutamyl moiety of glutathione to the amino acid, bringing it into the cell as γ-glutamyl amino acid (γ-Gaa). 2a) γ-glytamyl cyclotransferase (γ-GCT) cleaves the amino acid, releasing it in the cytosol, and producing 5-oxoproline (5-OP). 2b) The cysteinyl-glycine (Cys-Gly) produced by γ-GT in the first step of the cycle is cleaved by peptidase into glycine and cysteine. 3) 5-oxoprolinase converts 5-OP into glutamate. 4) γ-glutamylcysteine ligase (γ-GCL) begins to replenish glutathione by attaching cysteine to the carboxylate group of glutamate to produce γ-glutamyl cysteine (γ-GC). 5) Glutathione synthetase replenishes glutathione (GSH) by attaching glycine to γ-GC.

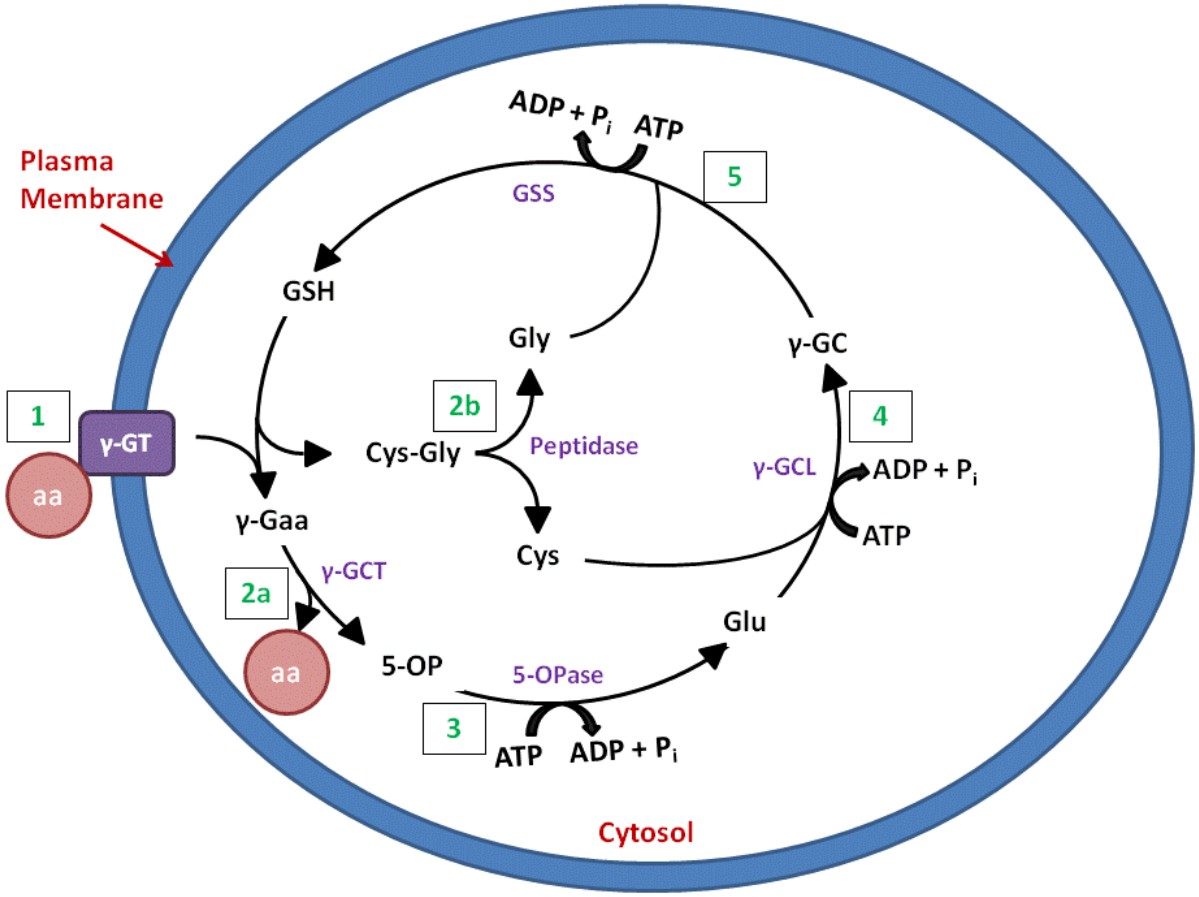

3.1.2 L-Glutamine and Nitrogen Metabolism

L-Glutamine is the most abundant amino acid in the body, with plasma levels ranging from 500 to 700 μM in humans (Rennie et al 1981). Glutamine obtained from the diet is absorbed by enterocytes in the intestine, which utilize glutamine as a source of energy and probably use most of what they absorb, resulting in very small amounts of dietary glutamine released into the bloodstream (Windmueller & Spaeth 1974). Glutamine is in high demand in the body since most tissues utilize glutamine for a variety of cellular processes. However, this is not a problem for most mammalian tissues, since they express glutamine synthetase (Krebs 1935) and can therefore produce glutamine from glutamate. In addition, skeletal muscle has the largest glutamine store in the body and has the ability to release it into circulation to maintain plasma glutamine levels (Newsholme 1994; Newsholme & Parry-Billings 1990), ensuring its availability for all tissues.

Glutamine is probably the most important amino acid in the body due to the wide variety of roles it can play. One of its most important roles is to detoxify ammonia and transport it through the bloodstream (Bulus et al 1989) to the liver for urea production. Glutamine can act as an ammonia donor for carbamoyl phosphate synthetase I (CPSI) (Nelson & Cox 2008), the first enzyme in the urea cycle, and it can be converted to glutamate by mitochondrial glutaminase, which can also donate ammonia to CPSI. Figure 3.1.2.1 shows the role of glutamine and glutamate in the urea cycle. CPSI acts as the first and rate limiting enzyme in the urea cycle, catalyzing the reaction between bicarbonate, ammonia and two molecules of ATP to produce carbamoyl phosphate. This carbamoyl phosphate is then used in the second step in the cycle, catalyzed by ornithine transcarbamoylase, where the phosphate group is released and it is combined with ornithine producing citrulline. The citrulline is then transported to the cytosol where it undergoes a reaction with ATP, catalyzed by arginosuccinate synthetase, forming an intermediate that then reacts with aspartate (produced within the mitochondria)

yielding arginosuccinate. Arginosuccinate lyase then removes fumarate from arginosuccinate to produce arginine, which is converted to urea and ornithine through the ureohydrolase arginase. The ornithine produced in this last step is then taken back up by the mitochondria for another round of the cycle (Berg et al 2007; Nelson & Cox 2008).

Figure 3.1.2.1 The urea cycle.

The urea cycle starts in the mitochondrial matrix. Amino acids enter the urea cycle as glutamate which can be taken up by mitochondria, or produced within the mitochondrial matrix from glutamine via glutaminase. The carbon atom in urea comes from bicarbonate that is incorporated into carbamoyl phosphate, while one of the amino groups is donated by external amino acids and the other is donated by aspartate produced within the mitochondria via aspartate aminotransferase.

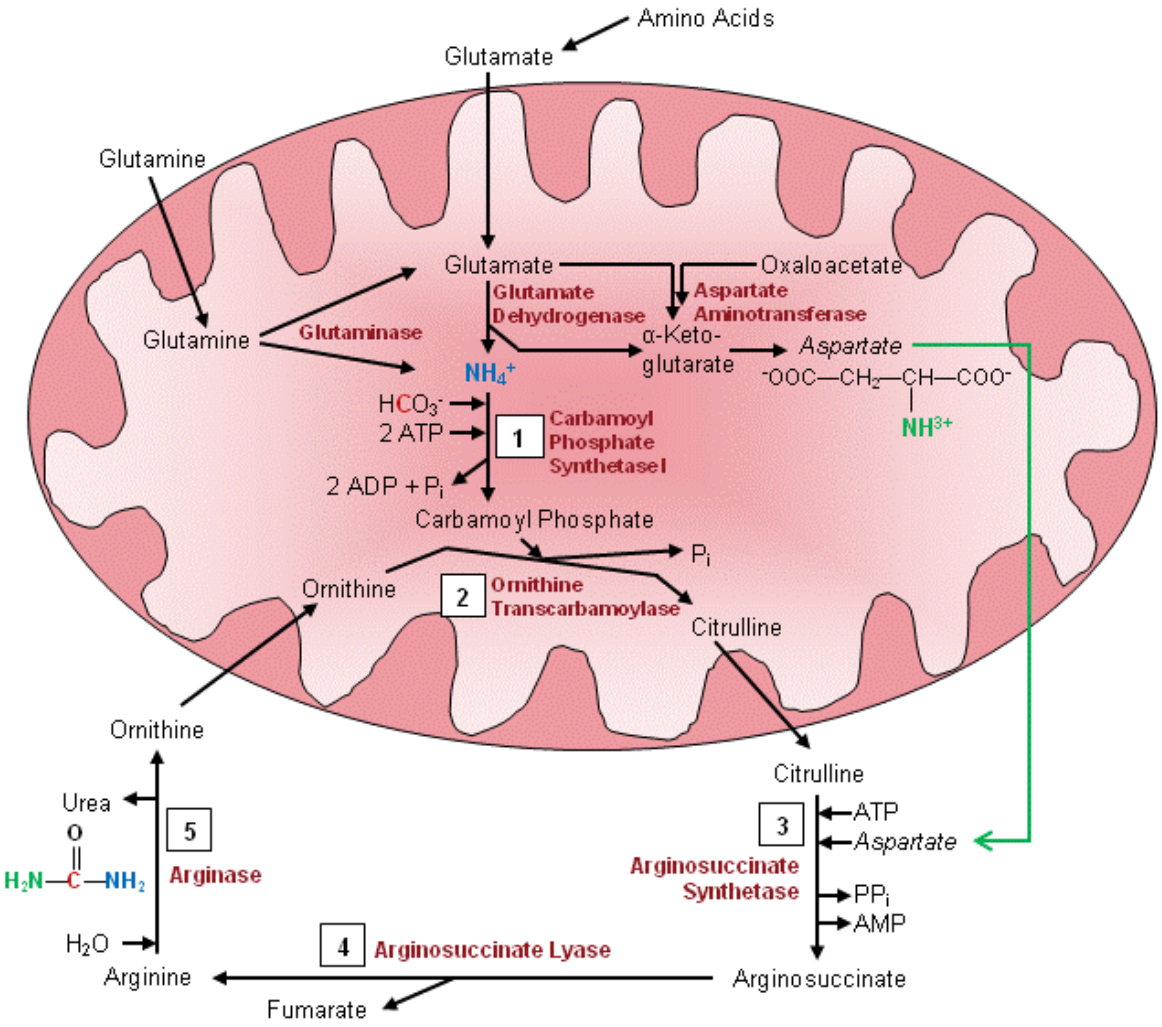

Glutamine has many other roles within the body, besides acting as a source of ammonia. The kidneys utilize glutamine to maintain acid-base homeostasis (Newsholme et al 2003) and in the brain glutamine acts as a nontoxic form of glutamate and ammonia (Nestler et al 2001). Glutamine also acts as a source of metabolic intermediates for a variety of cells (Newsholme et al 2003). Enterocytes consume glutamine as a source of energy, but other cells, such as colonocytes, fibroblasts, tumor cells, and proliferating immune cells, also utilize glutamine at high rates (Askanazi et al 1980; Kovacevic & McGivan 1983; Koyama et al 1998). Glutamine acts as a nitrogen donor for the production of nucleotides and can be incorporated into proteins (Nelson & Cox 2008), which makes it especially important for proliferating cells. Mononuclear cells lack the ability to synthesize glutamine (Ardawi & Newsholme 1983; Rohde et al 1996) and must rely on glutamine circulating in the bloodstream. Lymphocyte proliferation upon stimulation is dependent upon the presence of glutamine in cell culture systems and the ability of stimulated lymphocytes to produce cytokines is dependent upon the extracellular concentration of glutamine (Ardawi & Newsholme 1982; 1983; Crawford & Cohen 1985; Rohde et al 1996; Wallace & Keast 1992). In addition, the phagocytotic ability of peritoneal macrophages isolated from mice has been shown to be dependent upon glutamine (Parry-Billings et al 1990; Wallace & Keast 1992).

3.1.3 The Effects of Gender and MSO Treatment on Nitrogen Metabolism in SOD1 G93A Mice

The first disease-associated mutations in the gene encoding superoxide dismutase 1 (SOD1) were discovered in 1993 and linked with the familial form of the ALS (Rosen et al 1993), which accounts for only 5-10% of all cases of the disease. Mutations in SOD1 account for approximately 20% of familial cases, and a much smaller percentage of overall cases of ALS. Over 100 mutations in SOD1 have been characterized and associated with the disease, but the exact mechanism by which these mutations lead to disease is unknown. Mutations in SOD1

have also been implicated in sporadic ALS and recent research suggests that the normal wild-type form of SOD1 may play a role in the disease, through transcriptional and posttranslational modifications of the protein (Milani et al 2011).

Superoxide dismutases are a group of enzymes that scavenge superoxide free radical anions, converting them to hydrogen peroxide and molecular oxygen (McCord & Fridovich 1969). There are three isoforms of superoxide dismutase ubiquitously expressed by mammalian cells: 1) SOD1, a homodimeric copper/zinc-binding form of the enzyme found in the cytosol (Fridovich 1974); 2) SOD2, a tetromeric manganese-binding form of the enzyme found within the mitochondria (Abe & Okazaki 1987); and 3) SOD3, a tetromeric copper/zinc-binding form of the enzyme found outside of cells (Zelko et al 2002). These three isoforms of the enzyme help to protect cells against oxidative damage that can occur as a result of oxidative phosphorylation (Zelko et al 2002). All of the ALS-related SOD mutations have been isolated to the SOD1 isoform and most of these mutations allow the enzyme to retain its normal superoxide scavenging activity. Disease associated mutations in SOD1 are believed to exert their deleterious effects through a toxic gain of function, however most of these mutations have not been well characterized and the exact functions gained through the various mutations are unknown.

These toxic functions gained by mutant SOD1 proteins can vary, depending upon the mutation, and can have a tremendous impact on metabolic processes within the cell. Mutant SOD1 protein can undergo conformational changes which can result in new, potentially detrimental, protein-protein interactions. Several studies have shown that mutant SOD1 proteins have novel binding partners and can disrupt normal cellular functions. Motor neuron cultures expressing mutant SOD1 protein have been used in immunoprecipitation studies that showed that SOD1 with the G93A mutation interacts with cytosolic malate dehydrogenase, part of the malate-aspartate shuttle involved in maintaining the NADH/NAD+ balance in brain

mitochondria (Mali & Zisapels 2008). Mutant SOD1 protein has also been shown to interact with the anti-apoptotic protein Bcl-2 (Pasinelli et al 2004). When bound to Bcl-2, mutant SOD1 induces a conformational change in the protein, resulting in the exposure of a toxic domain that has been found to be deleterious to cells in the spinal cords of mice and humans (Pedrini et al 2010). Mutant SOD1 protein with the G93A mutation has been shown to interact with TDP-43 in cell culture and animal models (Higashi et al 2010) and with cytosolic and mitochondrial lysyl-tRNA synthetase, an enzyme required for the translation of protein, resulting in decreased mitochondrial protein synthesis and overall morphological changes in mitochondria (Kawamata et al 2008). In addition, mutant SOD1 protein can form detergent insoluble aggregates with the heat shock proteins HSP70, HSP40, and αB-cyrstallin in cells isolated from transgenic mice (Shinder et al 2001).

Interactions between mutant SOD1 proteins and mitochondrial proteins, such as lysyl-tRNA synthetase, indicate that the normally cytosolic protein ends up in the mitochondria where it can encounter different proteins. Since mitochondria are vital to producing energy within the cell, mutant SOD1 entering the organelle where it could potentially come into contact with integral energy producing proteins might have a major impact on energy production. In transgenic mouse models of ALS, expression of the mutant SOD1 protein has been shown to lead to morphological abnormalities, such as vacuolization occurring within the intermembrane space, in spinal cord mitochondria (Higgins et al 2003). It has also been shown to be selectively recruited to mitochondria in cells of the spinal cord in areas affected by the disease (Liu et al 2004). Although most of these studies have focused on spinal cord tissue, studies of mitochondrial function have shown that mitochondrial respiration is decreased not only in mitochondria isolated from brain and spinal cord, but liver as well (Mattiazzi et al 2002). Liver tissue from ALS patients shows morphological changes in mitochondria and rough ER, and records from these patients suggest that they also suffered from mild liver dysfunction (Nakano

et al 1987). Transgenic mouse models of ALS also show global metabolic deficits and a high energy diet has been shown to extend the average lifespan (Dupuis et al 2004). These data combined with data from human patients suggests that dysfunctional liver metabolism may play a role in ALS.

Since ALS is classified as a neurodegenerative disorder most research conducted on ALS patients and animal models focuses on the central nervous system. Motor neurons are the primary target of degeneration and several cellular processes undergo alterations during the disease, all of which can lead to cell death. However, in human and animal models where mutated genes are considered to be the cause of the disease, these mutated proteins are typically expressed throughout the body. ALS is almost always age-related so the effects of expressing mutant proteins builds up over time and leads to cell death in motor neurons, but can affect other cell types which often go ignored because problems in these cells do not cause paralysis. The following experiments were designed to test the hypothesis that transgenic mice overexpressing the human form of SOD1 containing the G93A mutation have defective nitrogen metabolism, specifically alterations in the urea cycle. To test this hypothesis, we examined the activity of nitrogen-metabolizing enzymes in the brain (glutamine synthetase and glutaminase, which are also important to the glutamate-glutamine cycle) and examined the levels of several plasma metabolites, including ammonia. Preliminary analysis of plasma metabolite levels suggested that nitrogen metabolism may be affected in these animals, so we followed up the plasma metabolite studies with assays of carbamoyl phosphate synthetase I and glutamine synthetase in the liver. These assays were carried out in both wild-type and SOD1 G93A-expressing mice.

Since our previous studies showed that treating SOD1 G93A mice with an irreversible inhibitor of glutamine synthetase, MSO, significantly extends the lifespan and improves neuromuscular function in these mice in a gender-specific fashion (with females benefiting more

than males), we treated a group of mice with MSO and examined both the effects of MSO and gender on nitrogen metabolism. The results of our experiments show that expression of the transgene does not affect glutamine synthetase activity, but MSO treatment significantly lowers GS activity in both genders and genotypes, suggesting that MSO's gender-specific effects are not through its action on GS. We found that there are gender-specific differences in plasma metabolite profiles in nontransgenice mice and metabolic profiles of these mice change with age, providing evidence for gender-specific and age-related changes in general metabolism. We also found that presymptomatic mice have several deficits in plasma metabolites indicative of underlying metabolic defects. These plasma metabolite deficits are gender-specific, with males and females showing different metabolic profiles, and change with age suggesting that, at least early in the disease, compensatory mechanisms can "normalize" metabolism to some extent. MSO treatment significantly alters the metabolic profile of SOD1 mice, while doing little to that of wild-type mice, and has the ability to alter metabolites in a gender-specific manner. Taken together, these data suggest that global metabolic defects play a role in the pathogenesis of ALS in this mouse model and that gender is also a significant factor in the disease.

3.2 Materials and Methods

Animal Breeding and Care. All animal experiments were approved by Wayne State University's Animal Investigation Committee. SOD1 breeding mice were obtained from Jackson Laboratories. Female C57BL/6*SJL mice were crossed with B6SJL males overexpressing the human SOD1 transgene containing the G93A mutation (SOD1 G93A). Offspring were genotyped by performing PCR on DNA isolated from tail clippings using primers recommended by Jackson Laboratories for this strain of transgenic mice (jax.org). Animals were assigned to one of five groups – a 50, 70, or 110 day time point, or a surgery group which consisted of SOD1 females.

Experimental Groups. The 50 day group consisted of untreated wild-type and SOD1 mice from which liver, central nervous system tissue and plasma were collected at 50 ± 2 days of age. The 70 day group consisted of wild-type and SOD1 mice that were given weekly i.p. injections of saline or 20 mg/kg body weight MSO (prepared in 0.9% saline; Sigma Chemical Company, no. 5379) starting at 50 ± 2 days of age and were euthanized at 70 ± 2 days of age. The 110 day group consisted of wild-type and SOD1 mice that were given weekly i.p. injections of saline or 20 mg/kg body weight MSO starting at 50 ± 2 days of age and were euthanized at 110 ± 2 days of age. The 70 and 110 day mice were given their final injection within three days of euthanasia. Central nervous system tissue, liver, and plasma were collected from 50 and 70 day animals while only CNS tissue and plasma were collected from 110 day animals.

Plasma and Tissue Collection. A stock solution of Avertin was prepared by dissolving 25 g of 2-2-2-tribromoethanol (Sigma Chemical Company) in 15.5 mL of tert-amyl alcohol (Sigma Chemical Company). This solution was then used to prepare a working solution of 20 mg/mL by dissolving 0.5 mL of the stock solution in 39.5 mL of PBS.

Mice were anesthetized with an i.p. injection of Avertin (0.4-0.75 mg/g body weight) and blood was collected via cardiac puncture. Blood was placed in BD Microtainer tubes containing

lithium heparin and centrifuged at 13,000 rpm for 3 minutes in a Sorvall Biofuge pico desktop centrifuge to obtain plasma. For the 50 and 70 day groups, 100 µL aliquots of plasma were taken for plasma ammonia analysis and the remaining plasma was immediately frozen on dry ice for later use. For the 110 day group, plasma was frozen on dry ice immediately. All tissue samples were placed in centrifuge tubes and immediately frozen on dry ice and thawed prior to homogenization.

Plasma Ammonia Determination. Plasma ammonia levels were determined using an ion-exchange resin and the Berthelot indophenol reaction as described by Brusilow (Brusilow 1991). A 100 µL aliquot was taken immediately after obtaining the plasma and added to a microfuge tube containing 200 µL of deionized water and 50 µL of prepared ion-exchange resin (BioRad AG 50W-X4 Resin, 100-200 Mesh hydrogen form). The procedure was carried out according to Brusilow (1991) and absorbance values were read at 630 nm. Ammonia levels were determined by comparing sample absorbances to those of an ammonium sulfate standard curve and values were expressed as µmoles of ammonia per liter of plasma.

Plasma Metabolite Analysis. Plasma samples that were not used for ammonia determination were immediately frozen on dry ice and transported to the Biochemical Genetics Laboratory in the Detroit Medical Center where Dr. Robert Grier processed and analyzed them for a variety of metabolites using HPLC.

Glutamine Synthetase Activity Assays. Brain and spinal cord preparation for GS activity were carried out according to Alton Meister's Methods in Enzymology protocol (Meister 1985). Liver sample preparation was carried out using a modified version of Pierson's protocol for preparation of samples for CPSI activity assays (Pierson 1980). GS activity was determined using a modified version of Meister's protocol.

Whole mouse brains and spinal cords were thawed and homogenized by hand using a glass and Teflon Dounce homogenizer in 1-2mL of homogenizing buffer (150 mM KCl, 5 mM 2-

mercaptoethanol, 1 mM EDTA, 1 mM PMSF, and protease inhibitor cocktail (Sigma, P8340), pH 7.2). Brain and spinal cord homogenates were centrifuged for five minutes at 5000 rpm in a Sorvall RC 5B Plus centrifuge (SS-34 rotor) cooled to 4°C. Liver samples were prepared by homogenizing 100 mg of liver in 2mL of buffer containing 50 mM triethanolamine, 10 mM ATP, 15 mM magnesium acetate, and 1 mM dithiothreitol, pH 8, using 4-5 strokes in a motorized glass and Teflon Dounce homogenizer set to a speed of six. Liver homogenates were centrifuged in a Sorvall Ultracentrifuge (OTD65B; Beckman TY 65 rotor) cooled to 4°C at 37,000 x g for 15 minutes. After centrifugation, 1 mL of the supernatant was added to 10 µL protease inhibitor cocktail (Sigma, P8340) and 10 µL of 100 mM PMSF. Protein concentrations for brain, spinal cord, and liver samples were determined using the Coomassie Plus Protein Assay (Thermoscientific).

Enzyme activity was determined by following the reaction in which GS catalyzes the conversion of L-glutamine to L-γ-glutamyl hydroxamate in the presence of hydroxylamine, ADP, arsenate, and Mn^{2+}:

$$\text{L-Glutamine} + NH_2OH \xrightarrow{ADP,\ Mn^{2+},\ As_i} \text{L-}\gamma\text{-Glutamyl Hydroxamate} + NH_3.$$

This reaction was carried out by adding 100 µg of protein from sample homogenates to 0.5 mL of GS reaction buffer (100 mM imidazole, 0.2 mM $MnCl_2$, 62.5 mM hydroxylamine, 10 mM sodium arsenate, 0.4 mM ATP, and 100 mM L-glutamine, pH 7.4) and incubating in a 37°C water bath. After 10 minutes the reaction was quenched with 0.5 mL stop solution consisting of 370 mM $FeCl_3$, 670 mM HCl, and 200 mM trichloroacetic acid. Samples were centrifuged for three minutes at 15,000rpm in a Sorvall Microspin 24S desktop centrifuge and absorbances were read at 535 nm.

GS activity assays were performed on 5-9 animals per treatment group for each gender at every time point. Absorbance values were converted to micromoles of product formed by

comparing them to an L-γ-glutamyl hydroxamate standard curve and specific activities were determined accordingly.

Glutaminase Activity Assays. Glutaminase activity assays were carried out on the same brain homogenates used for GS activity assays. Brain glutaminase activity was determined by monitoring the production of ammonia using a modified version of Sigma's protocol for the enzymatic assay of glutaminase from *E. coli*. Test tubes containing 0.9 mL of glutaminase reaction buffer (100 mM sodium phosphate, and 20 mM L-glutamine, pH 8.0) were equilibrated to 37°C in a water bath and 100 µL of brain homogenate was added. The reaction was allowed to proceed for 15 minutes at 37°C before being quenched with 9 mL of cold deionized water on ice. A 100 µL aliquot from the quenched reaction mixture was added to a tube containing 200 µL of deionized water and 50 µL of the prepared ion-exchange resin used for determining ammonia levels. The ammonia assay was then carried out from this point to determine the amount of ammonia produced during the reaction.

Several controls were run to eliminate any color development due to ammonia contamination of water, glutamine hydrolysis, and protein breakdown within samples. Controls in which the reaction was immediately quenched on ice following the addition of homogenate were run for each sample to determine any background from protein breakdown within the sample itself. A hot blank (containing reaction buffer and no protein) was assayed to determine any background due to glutamine hydrolysis. A corresponding cold blank (containing reaction buffer and no protein), which was quenched immediately on ice, was also assayed to determine any background from ammonia contamination of the deionized water.

Ammonia produced during the reaction was quantified by reading absorbances of samples at 630 nm and comparing them to absorbance values from an ammonium sulfate standard curve. Glutaminase activity assays were performed on 5-8 brain samples per treatment group for each gender at every time point.

Carbamoyl Phosphate Synthase I Activity Assays. Sample preparation and carbamoyl phosphate synthetase I enzymatic activity assays were carried out according to a modified version of a protocol by Pierson (Pierson 1980). A 100 mg sample of mouse liver was homogenized in 2 mL of buffer containing 50 mM triethanolamine, 10 mM ATP, 15 mM magnesium acetate, and 1 mM dithiothreitol with a final pH of 8.0. Four to five strokes of a motor-driven glass and Teflon Dounce homogenizer were used to homogenize samples, which were then centrifuged at 37,000 x g for 15 minutes in a 4°C Sorvall Ultracentrifuge (OTD65B, TY65 rotor). A 0.5 mL aliquot of the resulting supernatant was desalted by running it over a Sephadex G-25 spin column (GE Healthcare PD MiniTrap G-25; 28-9180-07), according to the manufacturer's specifications. Protein concentrations were determined by using the Coomassie Plus Protein Assay (Thermoscientific).

Enzyme activity was determined by adding 5 µL of desalted liver homogenate to 200 µL of CPSI reaction buffer (50 mM NH_4HCO_3, 50 mM triethanolamine, 10 mM magnesium acetate, 5 mM ATP, 5 mM N-acetyl-L-glutamic acid, and 1 mM dithiothreitol, pH 8.0) and incubating at 37°C for 10 minutes. The carbamoyl phosphate produced during the reaction was then chemically converted to hydroxyurea by adding 10 µL of 2 M hydroxylamine, pH 7.0, and incubating for 10 minutes at 95°C. To quantify the hydroxyurea, 800 µL of chromogenic reagent was added and samples were incubated for another 15 minutes at 95°C. Samples were cooled to room temperature and absorbances were measured at 458 nm.

The chromogenic reagent was prepared fresh just prior to use (during the last 5 minutes of the first 95°C incubation) and consisted of equal volumes of Solutions A and B. Solution A was made by dissolving 0.85 g antipyrine in 40% (v/v) H_2SO_4. Solution B was prepared by dissolving 0.625 g of 2, 3-butanedione monoxime in 100 mL of 5% (v/v) acetic acid in a brown bottle.

The concentration of hydroxyurea was determined by use of a carbamoyl phosphate standard curve. The standard curve was prepared by adding known amounts of carbamoyl phosphate to 200 µL of CPSI reaction buffer (without ATP, N-acetyl-L-glutamic acid, and dithiothreitol), converting the carbamoyl phosphate to hydroxyurea by the addition of 10 µL of 2 M hydroxylamine, and measuring the absorbance at 458 nm. The carbamoyl phosphate standard curve was linear up to 100 nmoles and the equation of the line of regression was used to calculate the amount of carbamoyl phosphate produced. Specific activities were calculated accordingly. CPSI activity assays were performed on 10 animals per treatment group for each gender at the 70 day time point.

Statistical Analysis of Data. Data were organized by gender and genotype and each data set was subjected to a Grubb's test using an online calculator (http://www.graphpad.com/quickcalcs/Grubbs1.cfm). Data points which failed Grubb's test with an α value of 0.01, extreme outliers, were dropped from the analysis. Two male wild-type mice were dropped from the spinal cord GS analysis (one from the 50 day group and one from the 70 day saline-treated group), two 110 day old saline-treated wild-type mice were dropped from both the brain and spinal cord GS analysis (one female and one male), one 110 day old MSO-treated female wild-type mouse was dropped from the brain glutaminase analysis, two male wild-type mice were dropped from the plasma ammonia analysis (one 50 day old and one saline-treated 70 day old mouse), and one 70 day old MSO-treated female wild-type mouse was dropped from the liver GS analysis. Animals that were suspected of having received the wrong treatment were also dropped from the analysis. Once outliers were detected and removed, data files were analyzed using SPSS. An analysis of variance (ANOVA) was used to analyze data from all enzyme activity assays and plasma ammonia data. A multivariate analysis of variance (MANOVA) was used to analyze plasma metabolite data. Plasma metabolites that were below

the detection limit were entered as zero and the MANOVA was carried out. Student's t test was used to double check ANOVA and MANOVA *p* values.

3.3 Results

3.3.1 Glutamine Synthetase Activity in the CNS

Glutamine synthetase is a cytosolic enzyme expressed primarily in astrocytes in the central nervous system. MSO is an irreversible inhibitor of glutamine synthetase and a single subconvulsive dose has been shown to inhibit brain glutamine synthetase activity in mice for several weeks, with the enzyme regaining 75% of control activity after 90 days (Rao & Meister 1972). Survival studies in which SOD1 G93A mice were given a single i.p. injection of 20 mg/kg MSO once per week showed that this dosing schedule had a positive impact on survival, extending lifespan by about 10% (see Chapter 2). As a result we measured the specific activity of the enzyme in central nervous system tissue (brain and spinal cord) to monitor changes that may occur with age as the disease progresses. Brain and spinal cord samples were homogenized and assayed for glutamine synthetase activity (see Materials and Methods) at three time points. Treatment was started at 50 ± 2 days of age and treated animals were euthanized at 70 ± 2 and 110 ± 2 days of age. Animals in the 50 day group were not exposed to i.p. injections and were euthanized at 50 ± 2 days of age. The 50 day time point provided a baseline level of glutamine synthetase activity at the time treatment was started, while the 70 day time point provided presymptomatic GS activity after four i.p. injections of saline. The 110 day time-point provided end-stage GS activity levels after long-term treatment.

End-stage mice expressing the SOD1 G93A transgene have lower glutamine synthetase activity. Figure 3.3.1.1 shows the specific activity of brain glutamine synthetase in untreated 50 day old animals (A) and saline-treated 70 and 110 day old animals (B and C respectively). There is no difference in GS activity between wild-type and SOD1 untreated presymptomatic

mice (Figure 3.3.1.1A). At 70 days of age, GS activity remains the same and continues to show no difference between wild-type and SOD1 saline-treated mice (Figure 3.3.1.1B). However, at 110 days of age, GS activity is significantly reduced in both wild-type and SOD1 mice treated with saline when compared to 70 day old saline-treated animals, with $p<0.001$ for both groups. Figure 3.3.1.1C shows that in the 110 day age group, saline-treated SOD1 mice have significantly lower GS activity (890 ± 70 nmoles/min/mg protein) than their wild-type counterparts (1130 ± 20 nmoles/min/mg protein), $p<0.001$.

Figure 3.3.1.1 Brain glutamine synthetase activity in wild-type and SOD1 mice.

The specific activity of GS was measured in brain homogenates from 50, 70, and 110 day old wild-type (WT) and SOD1 mice. Data are presented as the average specific activity with error bars representing the S.E.M. Green bars indicate the enzyme activity of wild-type mice while purple bars indicate the activity of SOD1 mice. **A.** Average specific activity of brain GS in 50 day old untreated wild-type and SOD1 mice (n=16 mice/group). **B.** Average specific activity of brain GS in 70 day old saline-treated wild-type and SOD1 mice (n=18 wild-type and n=16 SOD1 mice). (C) Average specific activity of brain GS in 110 day old saline-treated wild-type and SOD1 mice (n=15 wild-type and n=13 SOD1 mice; ** indicates $p<0.01$).

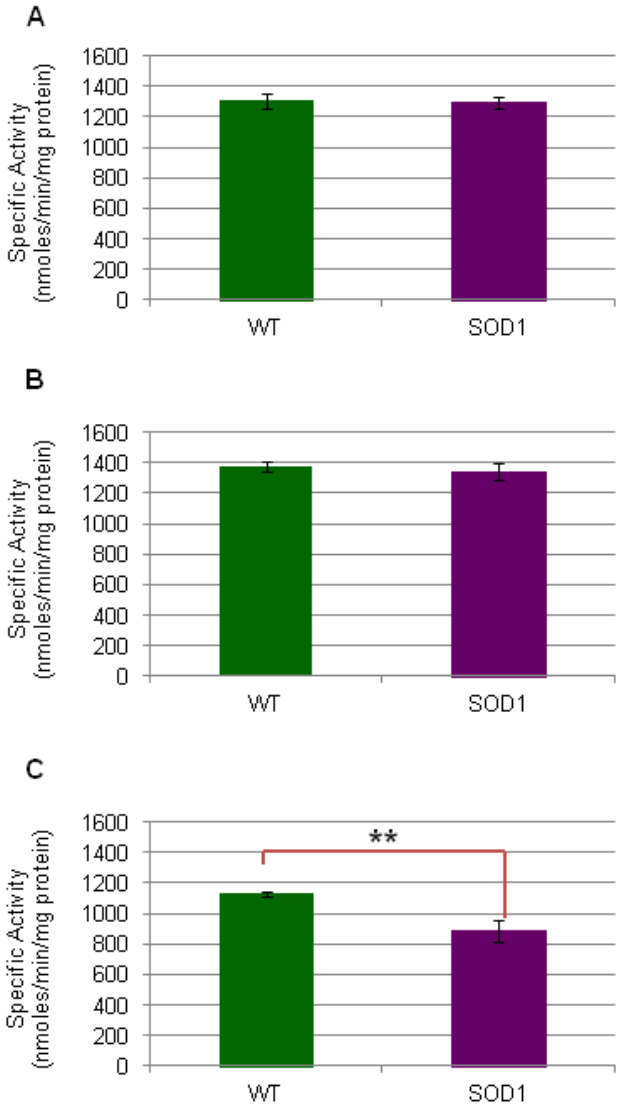

Since the majority of neurodegeneration occurs within the spinal cord of SOD1 G93A mice, we also looked at GS activity in whole spinal cord homogenates to examine changes with age and disease progression. Spinal cord samples were extracted from the same animals that brain samples were taken from; however one wild-type spinal cord sample from the 50 day group was determined to be an outlier and subsequently dropped from the analysis. The specific activity of spinal cord GS is significantly lower (approximately 40-50% lower) than that of brain GS in both wild-type and SOD1 mice, with $p<0.001$. Figure 3.3.1.2 shows the specific activity of GS from spinal cord homogenates of 50 day old untreated mice, as well as 70 and 110 day old saline-treated mice. At 50 days of age, the specific activity of spinal cord GS is similar in wild-type and SOD1 mice (Figure 3.3.1.2A). There is no change in GS activity in 70 day old saline-treated mice and the specific activity of GS of SOD1 mice remains the same as that of wild-type mice (Figure 3.3.1.2B). Overall, the spinal cord GS activity follows the same trend as that of brain GS activity and by 110 days of age, the average specific activity significantly decreases in both SOD1 and wild-type mice when compared to their 70 day old counterparts, with $p<0.001$ for SOD1 mice and $p<0.01$ for wild-type mice. As with brain GS activity, saline-treated SOD1 mice show significantly lower spinal cord GS activity (450 ± 50 nmoles/min/mg protein) than wild-type mice (630 ± 30 nmoles/min/mg protein) at 110 days of age, $p<0.01$ (Figure 3.3.1.2C).

Figure 3.3.1.2 Spinal cord glutamine synthetase activity in wild-type and SOD1 mice.

The specific activity of GS was measured in spinal cord homogenates from 50, 70, and 110 day old wild-type (WT) and SOD1 mice. Data are presented as the average specific activity with error bars representing the S.E.M. Green bars indicate the enzyme activity of wild-type mice while purple bars indicate the activity of SOD1 mice. **A.** Average specific activity of spinal cord GS in 50 day old untreated wild-type and SOD1 mice (n=15 WT and n=16 SOD1 mice). **B.** Average specific activity of spinal cord GS in 70 day old saline-treated wild-type and SOD1 mice (n=18 wild-type and n=16 SOD1 mice). **C.** Average specific activity of spinal cord GS in 110 day old saline-treated wild-type and SOD1 mice (n=15 wild-type and n=13 SOD1 mice; ** indicates $p<0.01$).

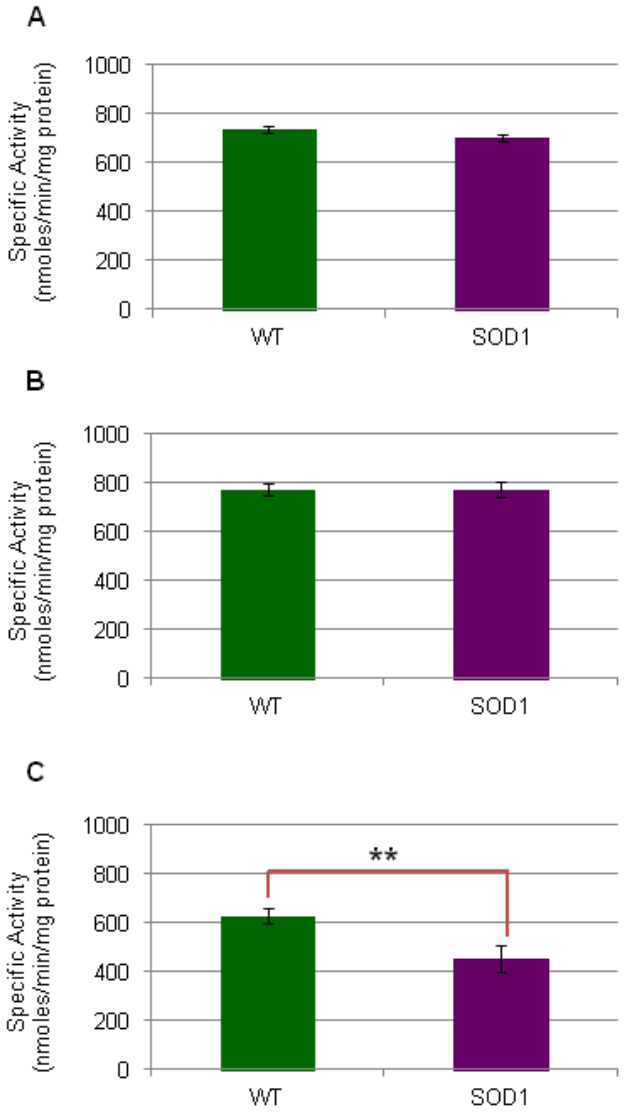

End-stage male and female SOD1 mice show lower levels of brain and spinal cord GS activity. Glutamine synthetase activity data were further broken down by gender and genotype to examine the effects of gender on enzyme activity. Figure 3.3.1.3 shows the average specific activity of brain glutamine synthetase broken down by gender and genotype. Untreated male and female wild-type and SOD1 mice all have similar levels of brain GS activity (Figure 3.3.1.3A). Saline-treated animals in the 70 day age group show levels of brain GS activity similar to that of untreated 50 day mice, with no gender or genotype differences (Figure 3.3.1.3B). In saline-treated male and female mice of both genders, the specific activity of brain GS significantly decreases between 70 and 110 days of age, $p<0.01$. Male and female SOD1 mice experience a greater decrease in GS activity than their wild-type counterparts. This age group shows that saline-treated wild-type males and females have similar levels of brain GS activity (Figure 3.3.1.3C). Both 110 day old male and female SOD1 mice, have lower levels of GS activity than their wild-type counterparts, with SOD1 males showing significantly lower brain GS (760 ± 80 nmoles/min/mg protein) activity than wild-type males (1110 ± 30 nmoles/min/mg protein), $p<0.001$.

Figure 3.3.1.3 Brain glutamine synthetase activity broken down by gender and genotype.

Data are presented as the average specific activity with error bars representing the S.E.M. Green bars indicate the enzyme activity of wild-type mice while purple bars indicate the activity of SOD1 mice. **A.** Average specific activity of brain GS in 50 day old untreated male and female wild-type and SOD1 mice (n=8 mice/group). **B.** Average specific activity of brain GS in 70 day old saline-treated male and female wild-type and SOD1 mice (n=9 wild-type mice/group and n=8 SOD1 mice/group). **C.** Average specific activity of brain GS in 110 day old saline-treated male and female wild-type and SOD1 mice (n(F,WT)=7, n(M, WT)=8, n(F, SOD1)=8, n(M, SOD1)=5; ** indicates $p<0.01$).

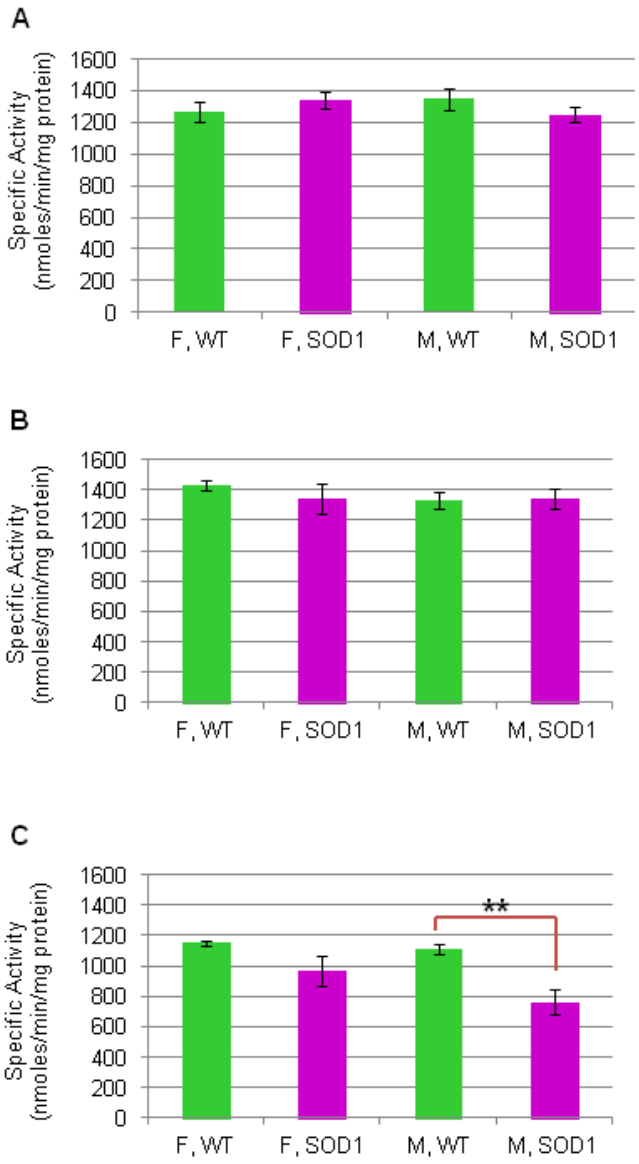

When spinal cord GS activity data are broken down by gender and genotype, enzyme activity in spinal cord homogenates is significantly lower than that of brain homogenates. Figure 3.3.1.4 shows the specific activity of spinal cord GS broken down by gender and genotype. In 50 day old untreated mice, enzyme activity is approximately the same across all groups (Figure 3.3.1.4A). Saline-treated male and female wild-type and SOD1 mice in the 70 day group, have spinal cord GS activity similar to that of untreated 50 day old animals, with no gender or genotype differences in enzyme activity (Figure 3.3.1.4B). Between 70 and 110 days of age, the specific activity of GS in spinal cord significantly decreases, with female SOD1 mice showing the greatest decrease in activity. Like with brain GS activity, spinal cord GS activity is lower in both male and female saline-treated SOD1 mice than wild-type mice (Figure 3.3.1.4C). Saline-treated female SOD1 mice show significantly lower GS activity (410 ± 50 nmoles/min/mg protein) than their wild-type counterparts (650 ± 60 nmoles/min/mg protein), $p<0.01$.

Figure 3.3.1.4 Spinal cord glutamine synthetase activity broken down by gender and genotype.

Data are presented as the average specific activity with error bars representing the S.E.M. Green bars indicate the enzyme activity of wild-type mice while purple bars indicate the activity of SOD1 mice. **A.** Average specific activity of spinal cord GS in 50 day old untreated male and female wild-type and SOD1 mice (n=8 mice/group, except for male, wild-type where n=7). **B.** Average specific activity of spinal cord GS in 70 day old saline-treated male and female wild-type and SOD1 mice (n=9 wild-type mice/group and n=8 SOD1 mice/group). **C.** Average specific activity of spinal cord GS in 110 day old saline-treated male and female wild-type and SOD1 mice (n(F,WT)=7, n(M, WT)=8, n(F, SOD1)=8, n(M, SOD1)=5; ** indicates $p<0.01$).

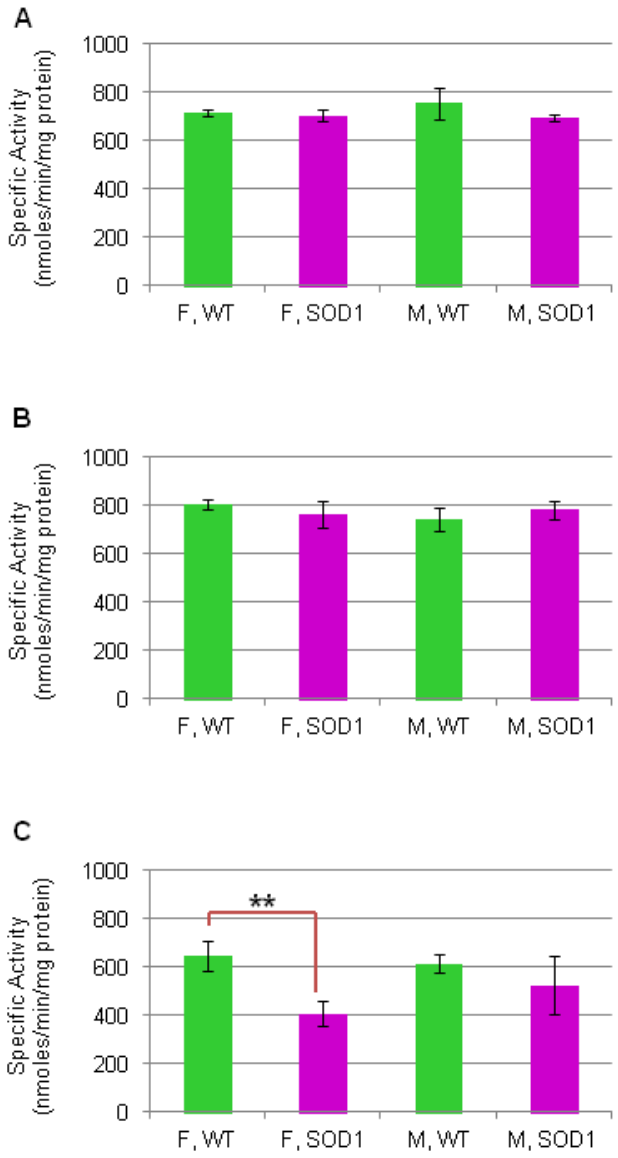

A weekly i.p. injection of 20 mg/kg MSO lowers brain and spinal cord glutamine synthetase activity. To examine the effects of MSO treatment on brain and spinal cord glutamine synthetase activity, we first grouped the data by genotype to determine if MSO treatment affected SOD1 animals differently than wild-type animals. Figure 3.3.1.5 shows the effects of MSO treatment on brain GS activity in 70 and 110 day old mice. In 70 day old wild-type and SOD1 mice, a single weekly injection significantly inhibits brain GS activity by approximately 90% (Figure 3.3.1.5A). Glutamine synthetase activity in wild-type mice is significantly reduced from 1380 ± 30 nmoles/min/mg protein (saline-treated mice) to 170 ± 20 nmoles/min/mg protein with MSO treatment (p<0.001), while brain GS activity of SOD1 mice is reduced from 1340 ± 60 nmoles/min/mg protein (saline-treated mice) to 150 ± 10 nmoles/min/mg protein with MSO treatment (p<0.001). As previously mentioned, brain glutamine synthetase activity in saline-treated mice is significantly lower in 110 day old mice than in 70 day old mice in both genotypes. This trend, however, is not reflected in MSO-treated mice. MSO treatment inhibits brain GS to the same extent in 110 day old mice, by approximately 90% (Figure 3.3.1.5B). Glutamine synthetase activity in 110 day old wild-type mice is significantly reduced from 1130 ± 20 nmoles/min/mg protein (saline treatment) to 140 ± 10 nmoles/min/mg protein with MSO treatment (p<0.001), while enzyme activity of SOD1 mice is reduced from 890 ± 70 nmoles/min/mg protein (saline treatment) to 120 ± 10 nmoles/min/mg protein with MSO treatment (p<0.001).

Figure 3.3.1.5 Brain glutamine synthetase activity in saline and MSO-treated mice.

Wild-type and SOD1 mice were treated with a single weekly i.p. injection of MSO and brain GS activity was measured at different time points. Data are presented as the average specific activity with error bars representing the S.E.M. Blue bars indicate the enzyme activity of wild-type and SOD1 mice treated with saline, while red bars indicate the activity of wild-type and SOD1 mice treated with MSO. **A.** MSO treatment significantly lowers the specific activity of brain GS in both wild-type and SOD1 mice at 70 days of age (n=18 wild-type mice/treatment, n (SOD, Saline) =16, and n (SOD, MSO) =17). **B.** MSO treatment lowers the specific activity of brain GS in 110 day old mice (n (WT, Saline) =15, n (WT, MSO) =18, n (SOD, Saline) =13, and n (SOD, MSO) =15). *** indicates that values are significant with $p<0.001$.

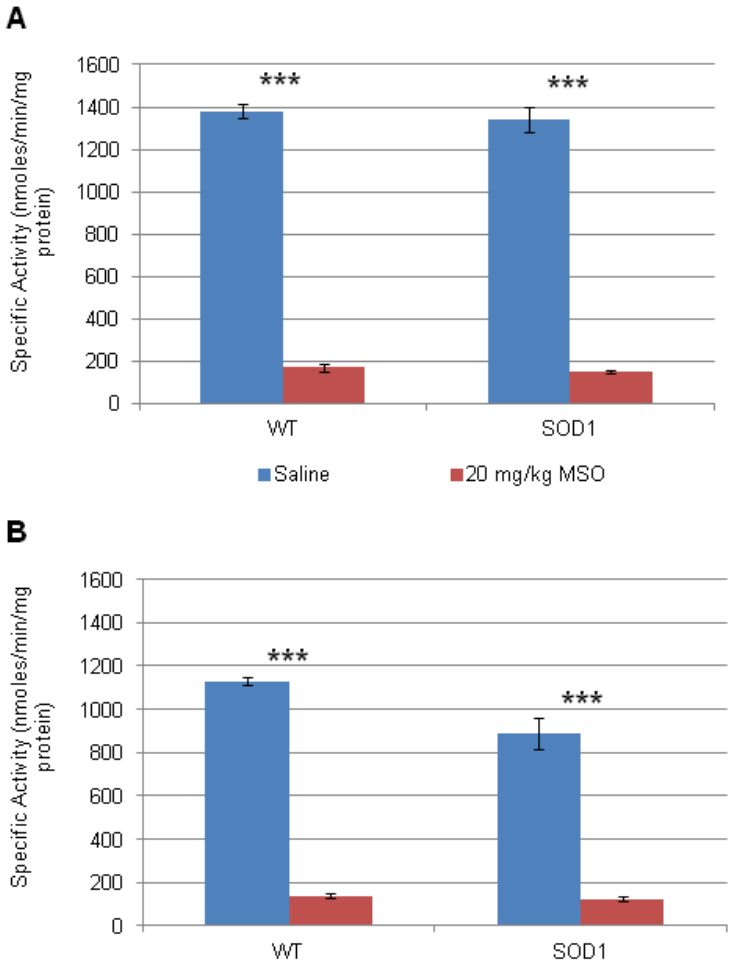

Figure 3.3.1.6 compares the specific activity of spinal cord glutamine synthetase of mice treated with saline to that of MSO-treated mice. Like brain GS activity, spinal cord GS activity is inhibited by 90% with a single weekly injection of MSO in wild-type and SOD1 70 day old mice (Figure 3.3.1.6A). Enzyme activity in the spinal cord of 70 day old saline-treated SOD1 mice (770 ± 30 nmoles/min/mg of protein) is significantly lower than that of brain GS (1340 ± 60 nmoles/min/mg protein), and MSO further decreases spinal cord GS activity (50 ± 5 nmoles/min/mg protein). Saline-treated wild-type mice from this age group show a similar pattern of enzyme activity, with significantly higher GS activity in brain than spinal cord and a corresponding decrease in activity with MSO treatment, which does not differ significantly from SOD1 mice. There is no difference in the enzyme activity of MSO-treated mice between 70 and 110 days of age, unlike what was seen in saline-treated animals. Like with 70 day wild-type and SOD1 mice, we see a 90% reduction in the average specific activity of GS isolated from spinal cord with MSO treatment (Figure 3.3.1.6B). MSO treatment reduces spinal cord GS activity in 110 day old SOD1 mice from 450 ± 50 nmoles/min/mg protein (saline treatment) to 40 ± 5 nmoles/min/mg protein (p<0.001), while spinal cord GS activity in wild-type mice is reduced from 630 ± 30 nmoles/min/mg protein to 50 ± 5 nmoles/min/mg protein (p<0.001). As seen with saline-treated mice, brain GS activity is significantly higher than spinal cord GS activity with MSO treatment for both age groups, with p<0.001.

Figure 3.3.1.6 Spinal cord glutamine synthetase activity in saline and MSO-treated mice.

Wild-type and SOD1 mice were treated with a single weekly i.p. injection of MSO and brain GS activity was measured at different time points. Data are presented as the average specific activity with error bars representing the S.E.M. Blue bars indicate the enzyme activity of wild-type and SOD1 mice treated with saline, while red bars indicate the activity of wild-type and SOD1 mice treated with MSO. **A.** MSO treatment significantly lowers the specific activity of spinal cord GS in both wild-type and SOD1 mice at 70 days of age (n (WT, Saline) =18, n (WT, MSO) =17, n (SOD, Saline) =16, and n (SOD, MSO) =17). **B.** MSO treatment lowers the specific activity of spinal cord GS in 110 day old mice (n (WT, Saline) =15, n (WT, MSO) =18, n (SOD, Saline) =13, and n (SOD, MSO) =15). *** indicates that values are significant with $p<0.001$.

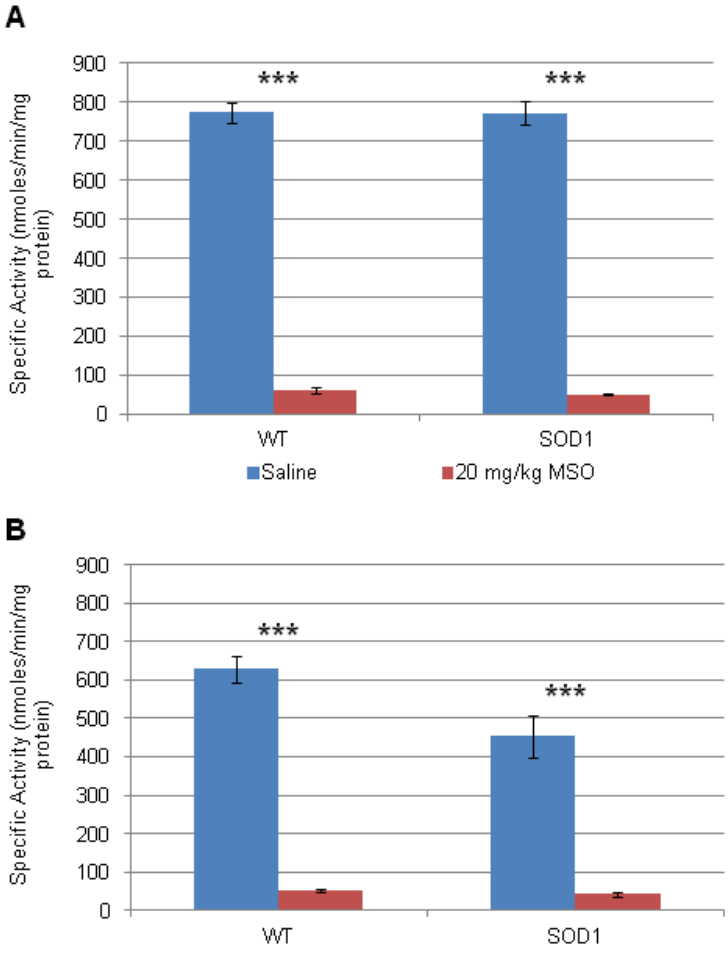

MSO treatment does not inhibit brain and spinal cord glutamine synthetase activity in a gender-specific fashion. To examine whether or not MSO inhibits the activity of GS in the central nervous system in a gender-specific manner, both brain and spinal cord GS activity data were broken down by gender and genotype. Figure 3.3.1.7 shows brain GS activity broken down by gender and genotype and compares the activity of saline and MSO-treated mice. The specific activity of brain glutamine synthetase is inhibited by approximately 90% in male and female wild-type and SOD1 mice at 70 days of age, with no significant gender or genotype differences in enzyme activity (Figure 3.3.1.7A). Although we see a slight decrease in the specific activity of brain GS in MSO-treated male and female wild-type and SOD1 mice between 70 and 110 days, this difference is not considered significant like that of saline-treated animals. Overall, MSO significantly reduces brain GS activity in 110 day old male and female wild-type and SOD1 mice to the same extent as 70 day old mice with no significant gender or genotype differences (Figure 3.3.1.7B).

Figure 3.3.1.7 Brain glutamine synthetase specific activity broken down by gender and genotype.

Data are presented as the average specific activity with error bars representing the S.E.M. Blue bars indicate the enzyme activity of male and female wild-type and SOD1 mice treated with saline, while red bars indicate the activity of male and female wild-type and SOD1 mice treated with MSO. **A.** The specific activity of brain glutamine synthetase is significantly decreased by MSO treatment in 70 day old male and female wild-type and SOD1 mice (n=8 male and 8 female WT mice/group, n=8 female SOD1 mice/group, n(M, SOD1, Saline)=8, and n(M, SOD1, MSO)=9). **B.** The specific activity of brain glutamine synthetase is significantly decreased by MSO treatment in 110-day old male and female wild-type and SOD1 mice (n=5-9 mice/group). *** indicates that values are significant with $p<0.001$.

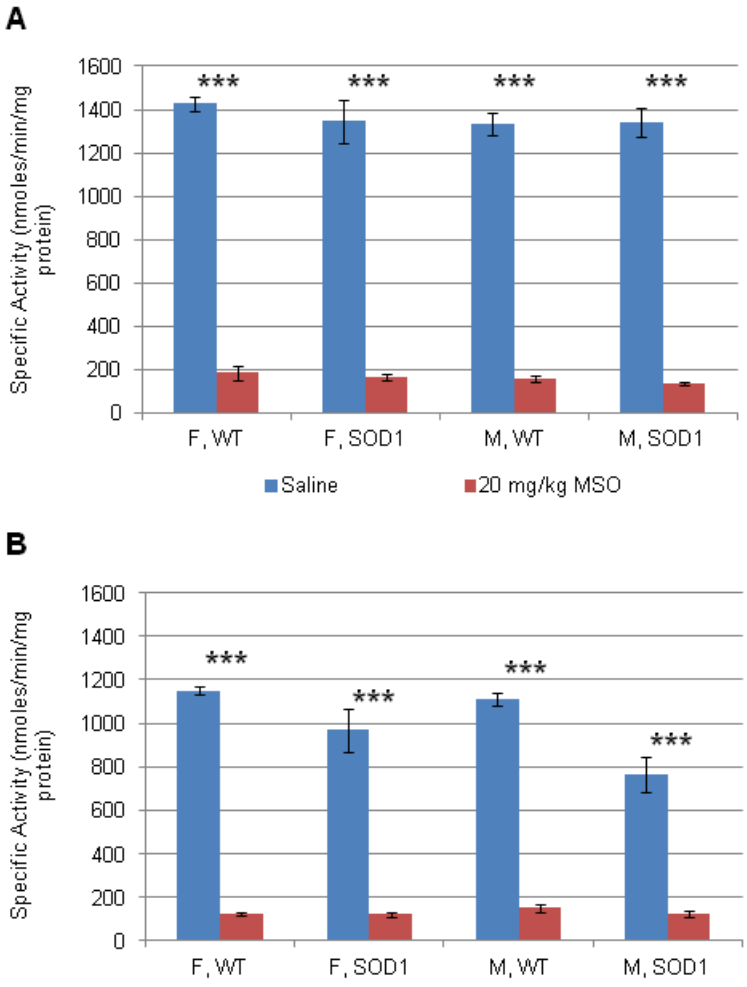

Figure 3.3.1.8 shows spinal cord glutamine synthetase activity broken down by gender and genotype and compares that of saline to MSO-treated mice. In MSO-treated animals the specific activity of brain GS is significantly higher than that of spinal cord GS in male and female wild-type and SOD1 mice, with $p<0.001$ for all groups. Like with brain GS activity, spinal cord enzyme activity is significantly reduced by approximately 90% in male and female wild-type and SOD1 mice at 70 (Figure 3.3.1.8A) and 110 (Figure 3.3.1.8B) days of age. While there are no gender or genotype differences in enzyme activity of 70 day old mice, there is a decrease in GS activity in saline-treated male and female SOD1 mice compared to their wild-type counterparts at 110 days of age, but this difference is not reflected in MSO-treated animals in this age group.

Figure 3.3.1.8 Spinal cord glutamine synthetase activity broken down by gender and genotype.

Data are presented as the average specific activity with error bars representing the S.E.M. Blue bars indicate the enzyme activity of male and female wild-type and SOD1 mice treated with saline, while red bars indicate the activity of male and female wild-type and SOD1 mice treated with MSO. **A.** The specific activity of spinal cord glutamine synthetase is significantly decreased by MSO treatment in 70 day old male and female wild-type and SOD1 mice (n=8-9 mice/group). **B.** The specific activity of spinal cord glutamine synthetase is significantly decreased by MSO treatment in 110-day old male and female wild-type and SOD1 mice (n=5-9 mice/group). *** indicates that values are significant with $p<0.001$.

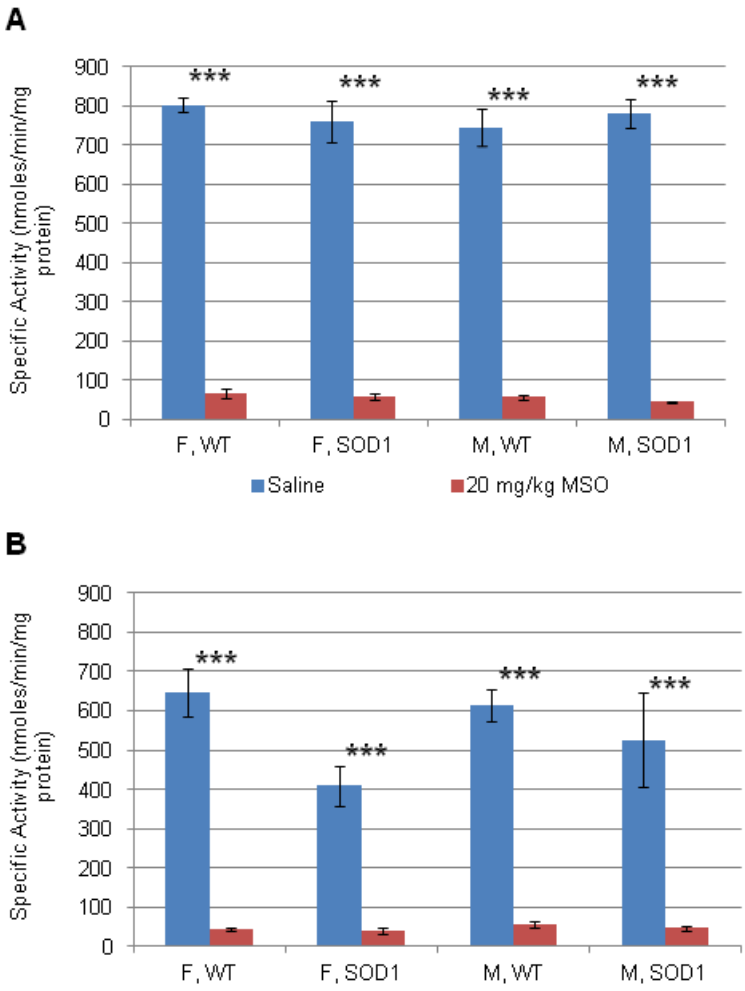

In general, we see that brain and spinal cord glutamine synthetase activity is about the same in presymptomatic wild-type and SOD1 mice - 50 day old untreated and 70 day old saline-treated mice. Changes in GS activity occur between 70 and 110 days of age, when both brain and spinal cord GS activity of saline-treated wild-type and SOD1 mice decrease significantly. This decrease in activity is greater in SOD1 mice and probably begins around the time of symptom onset, approximately 90 days of age. The specific activity of brain glutamine synthetase in untreated and saline-treated control mice is approximately 40-50% higher than that of spinal cord GS for all age groups. When the data are broken down by gender and genotype, there are no significant differences in either brain or spinal cord GS activity observed in presymptomatic mice. We continue to see a decrease in activity between 70 and 110 day old saline-treated mice, but it is independent of gender and genotype. In the 110 day age group, both male and female saline-treated SOD1 mice show lower levels of brain and spinal cord GS activity. Male SOD1 mice show significantly lower brain GS activity when compared to wild-type male mice, while female SOD1 mice show significantly lower spinal cord GS activity when compared to their wild-type counterparts. A single weekly injection of MSO (20 mg/kg body weight) significantly reduces both brain and spinal cord activity by about 90%. Prolonged treatment (110 days – about 10 injections) inhibits enzyme activity to the same extent as short-term treatment (70 days – about 4 injections), and results in no gender or genotype differences in brain or spinal cord GS activity.

3.3.2 Glutaminase Activity in the Brain

We have shown that treating ALS mice with MSO at a dose of 20 mg/kg three times a week, not only increases the lifespan of these animals, but also lowers levels of some neurochemicals (glutamine, glutamate, and GABA) and increases levels of the antioxidant tripeptide glutathione in specific regions of the brain (Ghoddoussi et al 2010). Survival studies,

explained in Chapter 2, show that reducing the dosing schedule of MSO to 20 mg/kg administered once a week has the same effect on the survival of SOD1 G93A mice. The results of the brain and spinal cord glutamine synthetase assays show that MSO treatment reduces enzyme activity by 90% in all animals. One would expect that this inhibition of glutamine synthetase would lower levels glutamine while simultaneously increasing levels of glutamate, because this excitotoxic amino acid would no longer be able to be converted to glutamine. The aforementioned results indicate that this is not the case and that MSO somehow lowers levels of glutamate, along with glutamine. In an effort to better understand how MSO lowers glutamate levels in the brain, we examined the activity of brain glutaminase, the neuronal enzyme responsible for converting glutamine back into glutamate. Using a modified version of Sigma's protocol for assaying the enzymatic activity of glutaminase purified from E. coli, we were able to monitor the specific activity of glutaminase from mouse brain homogenates by measuring the production of ammonia.

The specific activity of brain glutaminase is not affected by the overexpression of mutant SOD1 protein. The specific activity of brain glutaminase was measured using the same mouse brain homogenates that were assayed for glutamine synthetase activity. Enzyme activity was measured in untreated 50 day old animals, as well as saline and MSO-treated 70 and 110 day old animals. Figure 3.3.2.1 shows the average specific activity of brain glutaminase from wild-type and SOD1 mice. At 50 days of age, untreated wild-type and SOD1 mice have similar levels of glutaminase activity in the brain (Figure 3.3.2.1A). At 70 days of age, saline-treated wild-type mice show a slight decrease in glutaminase activity while SOD1 mice show no change (Figure 3.3.2.1B). Glutaminase activity increases slightly by 110 days of age in both wild-type and SOD1 saline-treated mice, but this change is not significant (Figure 3.3.2.1C).

Figure 3.3.2.1 Specific activity of brain glutaminase in wild-type and SOD1 mice.

Data are presented as the average specific activity bars with error bars representing the S.E.M. Green bars represent data from wild-type mice while purple bars represent data from SOD1 mice. **A.** In untreated 50 day old mice there is no difference in specific activity of brain glutaminase in wild-type and SOD1 mice (n=15 SOD1 and n=16 WT mice). **B.** The activity of brain glutaminase does not change in 70 day old wild-type and SOD1 mice (n=16 mice/group). **C.** By 110 days of age, the average specific activity of glutaminase seems to increase in both wild-type and SOD1 mice, however this change is not significant (n=13 SOD1 and n=15 WT mice).

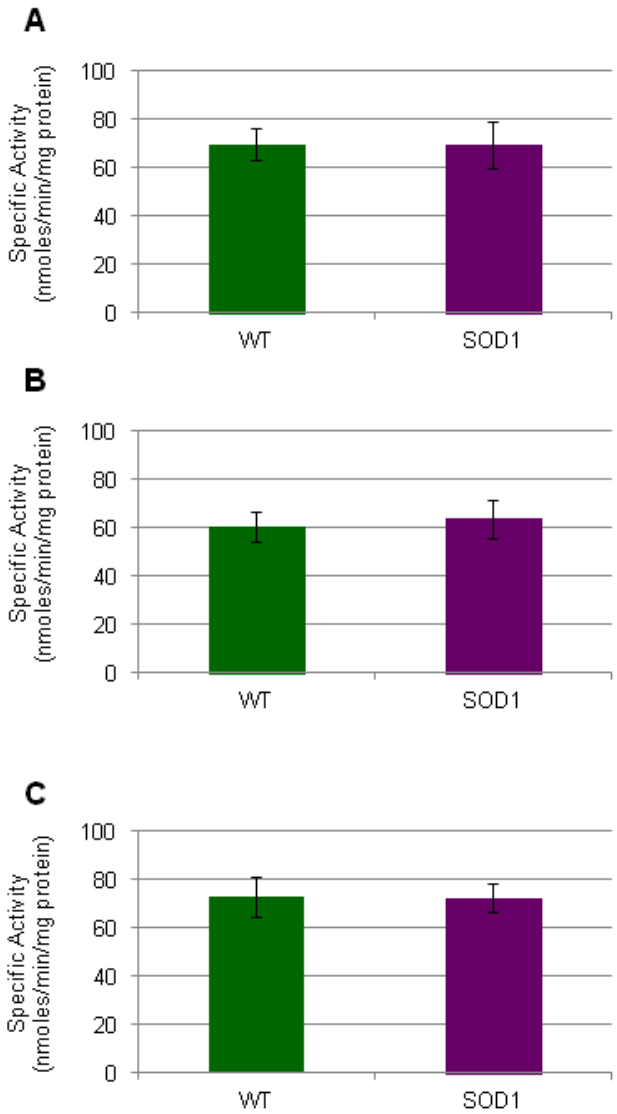

There are no gender differences in the specific activity of brain glutaminase. To examine gender differences in brain glutaminase activity, the data were broken down by gender and genotype. Figure 3.3.2.2 shows the average specific activity of brain glutaminase of untreated 50 day old animals and saline-treated 70 and 110 day old animals broken down by gender and genotype. There are no significant gender differences in the enzyme activity of untreated 50 day old animals (Figure 3.3.2.2A). In 70 day old saline-treated mice, it appears as though there may be a gender difference in brain glutaminase activity, with females showing lower activity than males (Figure 3.3.2.2B). Saline-treated male SOD1 mice in this age group have significantly higher brain glutaminase activity (88 ± 12 nmoles/min/mg protein) than female SOD1 mice (56 ± 7 nmoles/min/mg protein), with $p<0.05$, however the difference between male and female wild-type mice is not considered significant. Between 70 and 110 days of age, the average specific activity of glutaminase appears to increase in female mice and decrease in male mice of both genotypes. However, this difference is only significant for wild-type females where glutaminase activity increases from 52 ± 8 nmoles/min/mg protein at 70 days of age to 87 ± 11 nmoles/min/mg protein at 110 days of age ($p<0.05$). In 110 day old saline-treated mice (Figure 3.3.2.2C), there again appears to be a gender difference in enzyme activity with females now having higher glutaminase activity than males, however this was not found to be significant.

Figure 3.3.2.2 Brain glutaminase activity broken down by gender and genotype.

Data are presented as the average specific activity bars with error bars representing the S.E.M. Green bars represent data from wild-type mice while purple bars represent data from SOD1 mice. **A.** When glutaminase activity data are broken down by gender and genotype, there are no clear gender differences in 50 day old untreated mice (n=8 mice/group except for the female SOD1 group which contains 7 mice). **B.** In 70 day old saline-treated mice, females appear to have lower brain glutaminase than males (n=8 mice/group; * indicates values are significant with $p<0.05$). **C.** Female saline-treated mice appear to have higher glutaminase activity than male saline-treated mice at 110 days of age (n=5-8 mice/group).

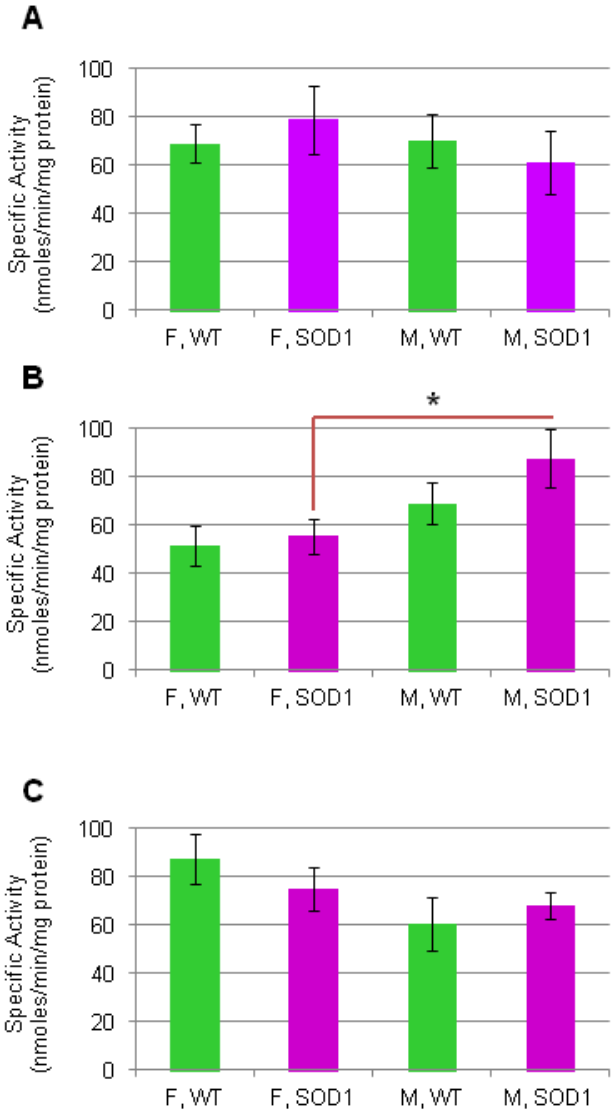

MSO treatment does not impact glutaminase activity in the brain. Figure 3.3.2.3 compares the average specific activity of brain glutaminase in saline-treated wild-type and SOD1 mice to that of MSO-treated wild-type and SOD1 mice. MSO treatment does not have an effect on glutaminase activity in the brains of 70 day old mice (Figure 3.3.2.3A). The average specific activities of glutaminase from MSO-treated wild-type and SOD1 mice are similar to that of saline-treated mice. In 110 day old mice, brain glutaminase activity is elevated in saline and MSO-treated wild-type and SOD1 mice compared to 70 day old mice, but this increase in activity is not significant. In the 110 day age group brain homogenates of both genotypes show higher glutaminase activity with MSO treatment (Figure 3.3.2.3B), however this increase is not significant.

Figure 3.3.2.3 The effects of MSO treatment on glutaminase activity.

Data are presented as the average specific activity with error bars representing the S.E.M. Blue bars represent data from saline-treated wild-type and SOD1 mice and red bars represent data from mice treated once a week with 20 mg/kg MSO. **A.** The average specific activity of glutaminase from 70 day old saline-treated wild-type and SOD1 mice compared to that of MSO-treated mice (n=16 mice/group). **B.** The average specific activity of glutaminase from 110 day old saline-treated wild-type and SOD1 mice compared to that of MSO-treated mice (n=13-19 animals/group).

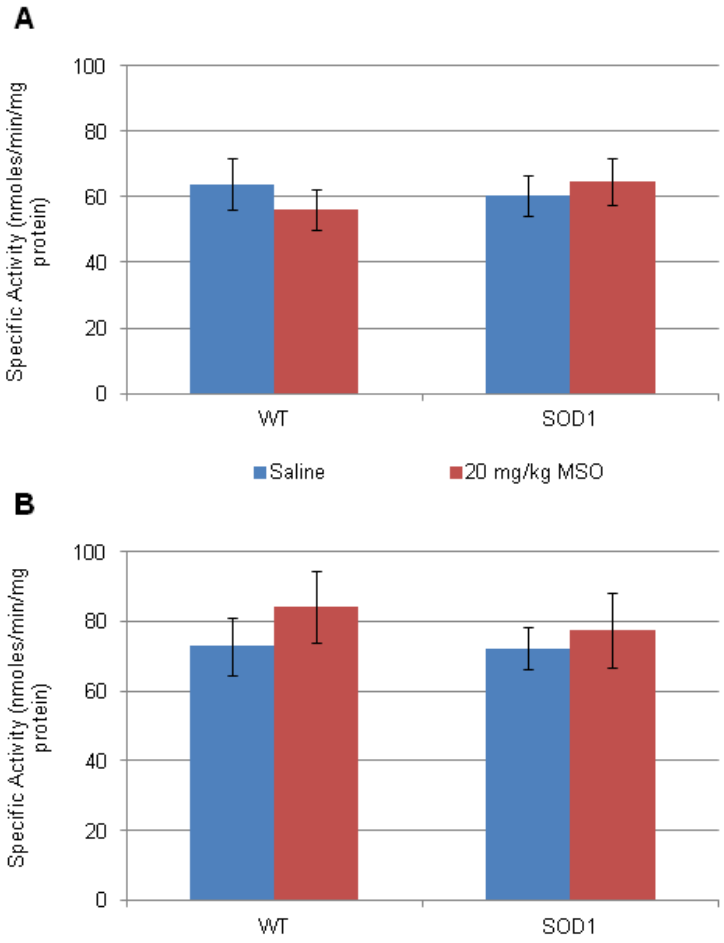

There are no significant gender differences in glutaminase activity with MSO treatment. Glutaminase activity data were further broken down by gender and genotype to determine if MSO treatment affects glutaminase activity in a gender-specific fashion. Figure 3.3.2.4 compares saline and MSO-treated mice by gender and genotype. Based on these data, the effects of MSO on glutaminase activity of male and female wild-type and SOD1 mice are unclear. In Figure 3.3.2.4A, it appears as though MSO may be elevating enzyme activity in females while reducing it in males in 70 day old mice, however none of these changes were considered statistically significant. The results of glutaminase activity assays performed on 110 day old mice treated with saline and MSO are equally confusing. In this age group, it appears as though MSO may be elevating glutaminase activity in male SOD1 and female wild-type mice, lowering activity in male wild-type mice, and having no effect on female SOD1 mice (Figure 3.3.2.4B). Like with the 70 day age group, these changes in enzyme activity with MSO treatment were not found to be significant.

Figure 3.3.2.4 Brain glutaminase activity of saline and MSO-treated mice broken down by gender and genotype.

Data are presented as the average specific activity with error bars representing the S.E.M. Blue bars represent data from saline-treated wild-type and SOD1 mice and red bars represent data from mice treated once a week with 20 mg/kg MSO. **A.** The average specific activity of glutaminase from 70 day old saline-treated wild-type and SOD1 mice compared to that of MSO-treated mice broken down by gender and genotype (n=8 mice/group). **B.** The average specific activity of glutaminase from 110 day old saline-treated wild-type and SOD1 mice compared to that of MSO-treated mice broken down by gender and genotype (n=5-9 animals/group).

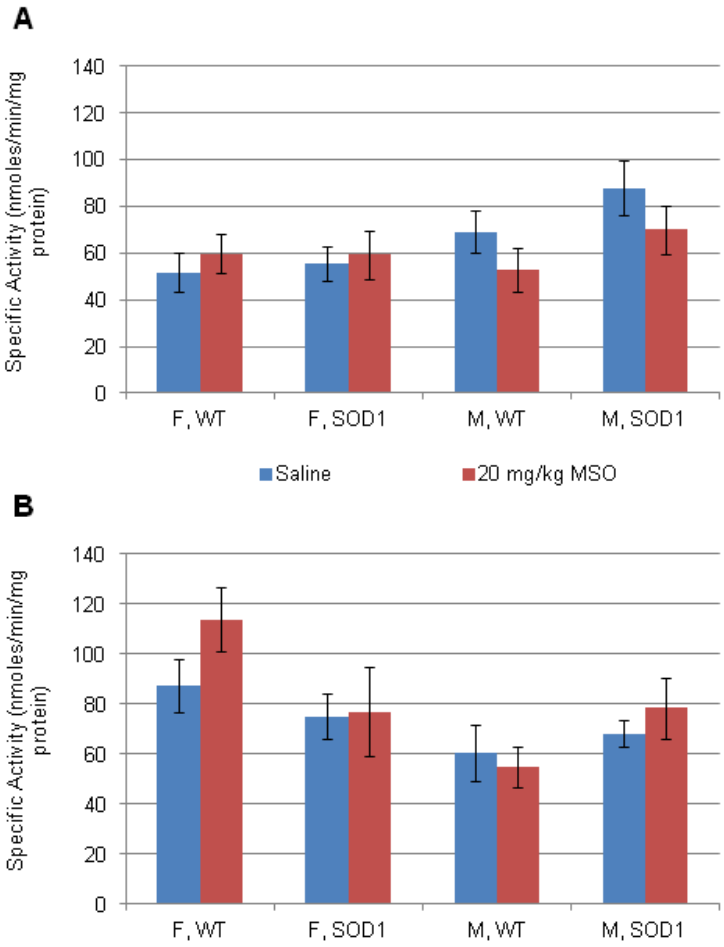

Overall, the results of the glutaminase activity assays show no differences in enzyme activity. We see no differences in activity levels of wild-type and SOD1 mice at all time points, and enzyme activity doesn't appear to change with age. When the data are broken down by gender and genotype, there are no significant gender differences in glutaminase activity in untreated 50 day old mice. It appears as though gender differences in activity begin to emerge at 70 days of age, with females exhibiting lower levels of brain glutaminase activity than males, but only SOD1 mice show a significant gender difference in enzyme activity. By 110 days of age, there seems to be a reversal in activity levels, with males now exhibiting lower glutaminase activity than females, but these differences were not significant. MSO treatment does not have a clear effect on glutaminase activity and it has not been determined to interact directly with the enzyme. If MSO has an effect on glutaminase it may be region-specific or indirect, possibly through altering levels of reactants, such as glutamate.

3.3.3 Plasma Metabolite Analysis

Glutamine synthetase is the only enzyme capable of producing glutamine and is expressed in varying concentrations throughout the body (van Straaten et al 2006). Glutamine is the most abundant free amino acid in the body (Brosnan 2003) and acts as an ammonia carrier in the bloodstream. It is considered to be a nonessential amino acid and can be taken up from the diet, and as a result the primary role of GS in certain organs is not to produce glutamine but to detoxify glutamate and ammonia. We have previously shown that MSO lowers levels of glutamate, glutamine, and GABA in certain brain regions (Ghoddoussi et al 2010), but GS is expressed throughout the body and widespread inhibition of the enzyme by MSO could potentially alter these chemicals in other areas.

Glutamine plays several roles in the body. It donates nitrogen for the production of purines and ammonia to CPSI for the production of carbamoyl phosphate, leading to the

production of arginine which then continues on to form urea (in the liver) and nitric oxide (through nitric oxide synthases in a variety of tissues) (Newsholme et al 2003). Glutamine is also involved in protein synthesis and acts as a precursor in the production of glutamate (Nelson & Cox 2008; Newsholme et al 2003). Glutamate, which in most cells is the immediate product of glutamine metabolism, can act as a precursor for GABA and n-acetyl glutamate (an allosteric activator of CPSI), and indirectly acts as a precursor for glucose through α-ketoglutarate and its flow into the Citric Acid Cycle (Newsholme et al 2003). Glutamate is also involved in protein synthesis and is one of three amino acids that make up the antioxidant glutathione. Altering glutamine levels through the use of MSO has the potential to affect several aspects of metabolism throughout the body. We decided to examine a variety of amino acids, and other metabolites including ammonia, in the plasma of presymptomatic mice to 1) understand the effects that the overexpression of the mutant SOD1 protein has on nitrogen metabolism and 2) monitor the effects of MSO treatment on nitrogen metabolism.

Young untreated SOD1 mice have elevated levels of plasma ammonia. Plasma ammonia levels were examined in 50 day old untreated wild-type and SOD1 mice, as well as saline-treated 70 day old animals. Figure 3.3.3.1 shows the results of the plasma ammonia analysis. In 50 day old untreated mice, plasma ammonia levels are significantly higher in SOD1 animals (78 ± 7 μmoles/L plasma) when compared to wild-type mice of the same age (52 ± 5 μmoles/L plasma), with $p<0.01$ (Figure 3.3.3.1A). Between 50 and 70 days of age, plasma ammonia levels drop and both 70 day old wild-type and SOD1 mice treated with saline have significantly lower levels of ammonia detected in their plasma when compared to untreated 50 day old animals ($p<0.001$). By 70 days of age, plasma ammonia levels have evened out and no longer differ between wild-type and SOD1 mice (Figure 3.3.3.1B).

Figure 3.3.3.1 Plasma ammonia concentrations in wild-type and SOD1 mice.

Plasma ammonia levels are expressed as the average concentration of ammonia in μmoles/L of plasma with error bars representing the S.E.M. Green bars indicate plasma ammonia levels in wild-type mice, while purple bars indicate that of SOD1 mice. **A.** The average concentration of ammonia in 50 day old, untreated wild-type and SOD1 mice (n=31 mice/group; ** indicates that values differ significantly with $p<0.01$). **B.** The average concentration of ammonia in 70 day old wild-type and SOD1 mice treated with saline (n=24 mice/group).

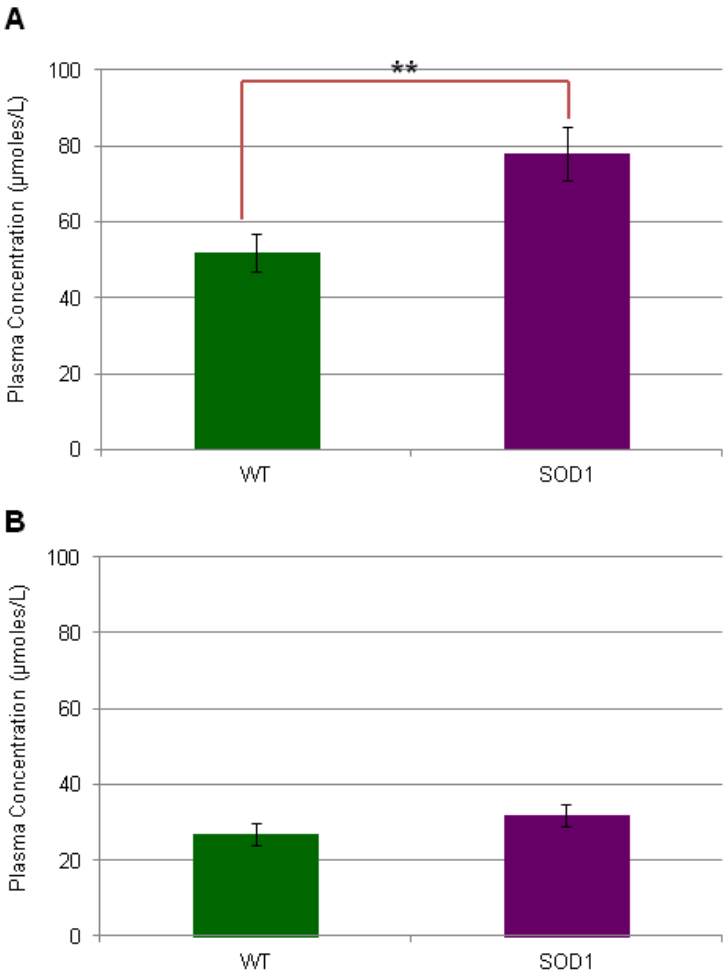

Plasma ammonia levels in SOD1 mice show no gender-specific differences. Figure 3.3.3.2 shows the plasma ammonia data broken down by gender and genotype. In 50 day old untreated mice, both female and male SOD1 mice have higher levels of ammonia in their plasma. Female SOD1 mice were found to have significantly higher levels of ammonia (83 ± 11 μmoles/L plasma) than wild-type females (56 ± 5 μmoles/L plasma), with $p<0.05$, while males were not found to differ significantly (Figure 3.3.3.2A). There are no significant differences in the levels of plasma ammonia between males and females of the same genotype. Between 50 and 70 days of age, plasma ammonia levels drop in all groups analyzed. There is a much larger decrease in plasma ammonia levels of SOD1 males and females than in wild-type males and females, but the overall decrease is significant for all groups ($p<0.01$). Interestingly, by 70 days of age, plasma ammonia in saline-treated SOD1 male and female mice resemble that of male and female wild-type mice, with no significant differences between genders (Figure 3.3.3.2B).

Figure 3.3.3.2 Plasma ammonia concentrations broken down by gender and genotype.

Plasma ammonia levels are expressed as the average concentration of ammonia in μmoles/L of plasma with error bars representing the S.E.M. Green bars indicate plasma ammonia levels in wild-type male and female mice, while purple bars indicate that of SOD1 male and female mice. **A.** Plasma ammonia levels are higher in both male and female SOD1 mice in 50 day old untreated mice (n=16 female mice/group and n=15 male mice/group; * indicates that values differ significantly with $p<0.05$). **B.** Plasma ammonia levels in 70 day old saline-treated mice broken down by gender and genotype (n=12 mice/group).

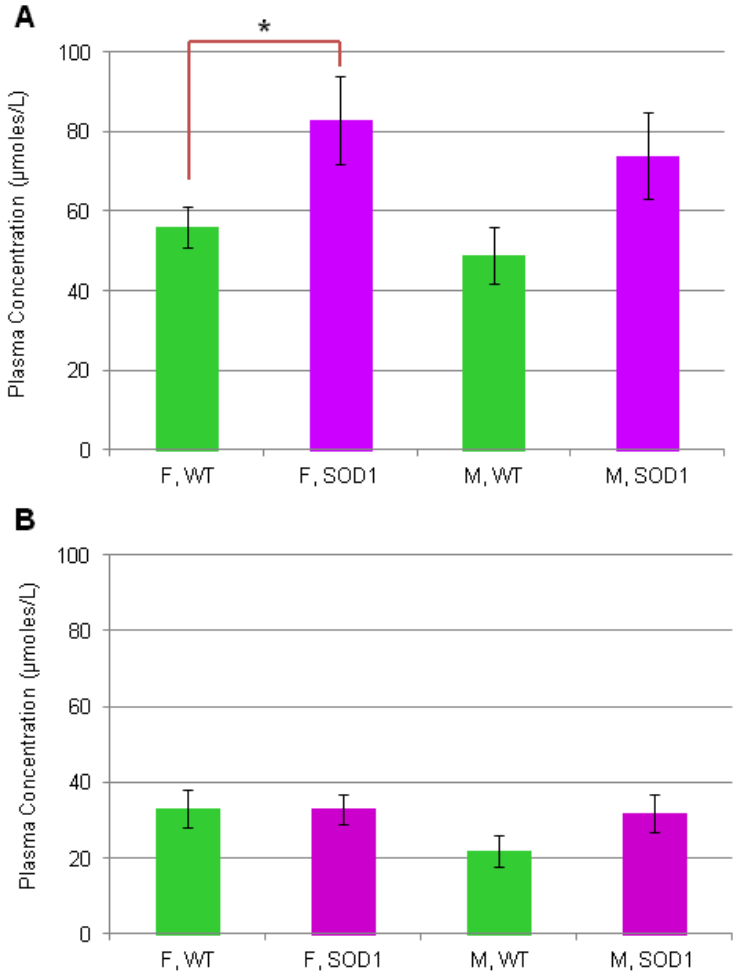

A single weekly injection of MSO elevates plasma ammonia levels in wild-type and SOD1 mice. Animals were given an i.p. injection of saline or 20 mg/kg MSO starting at 50 ± 2 days of age and continued to receive a weekly injection until euthanized at 70 ± 2 days of age. Plasma was taken and immediately assayed for ammonia content and the results are presented in Figure 3.3.3.3. In both wild-type and SOD1 mice, treatment with MSO significantly increases plasma ammonia levels with $p<0.01$ (Figure 3.3.3.3A). These data were further broken down by gender and genotype to determine if MSO has a gender-specific effect on plasma ammonia levels. MSO treatment significantly increases plasma ammonia levels in all groups with $p<0.05$, except male SOD1 mice where the elevation in plasma ammonia was not found to be significant (Figure 3.3.3.3B). Male wild-type mice have the lowest levels of plasma ammonia of all groups examined, when treated with both saline and MSO. Male wild-type mice treated with MSO have significantly lower levels of plasma ammonia (34 ± 2 μmoles/L plasma) when compared with both female wild-type mice treated with MSO (48 ± 4 μmoles/L plasma; $p<0.01$) and male SOD1 mice treated with MSO (50 ± 7 μmoles/L plasma; $p<0.05$).

Figure 3.3.3.3 The effects of MSO treatment on plasma ammonia levels.

Plasma ammonia levels are expressed as the average concentration of ammonia in μmoles/L of plasma with error bars representing the S.E.M. Blue bars indicate plasma ammonia levels in wild-type and SOD1 mice treated with saline, while red bars indicate that of wild-type and SOD1 mice treated with MSO. **A.** The effects of MSO treatment on plasma ammonia levels in 70 day old wild-type and SOD1 mice (n=24 mice/group; ** indicates that values differ significantly with $p<0.01$). **B.** The effects of MSO treatment on plasma ammonia levels in 70 day old male and female wild-type and SOD1 mice (n=12 mice/group; * indicates that values differ significantly with $p<0.05$).

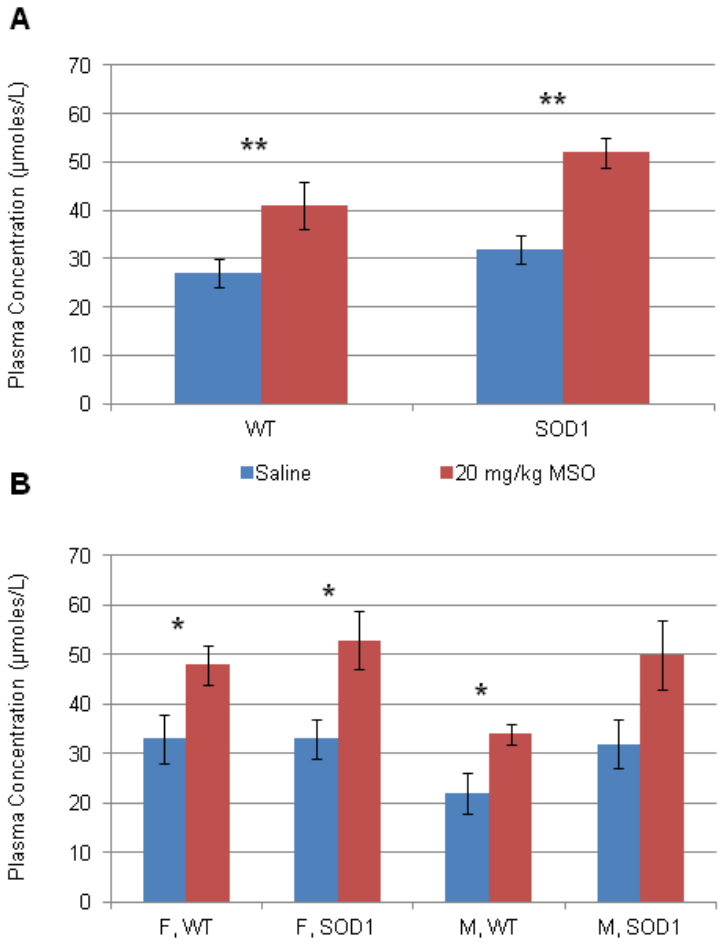

Several glucogenic amino acids are significantly lower in presymptomatic SOD1 mice when compared to wild-type mice. Mouse plasma samples were obtained by anesthetizing mice and drawing blood directly from the heart, which was immediately centrifuged in plasma separator tubes. If needed, a portion of the plasma was used for ammonia determination and the rest was immediately frozen on dry ice and then placed at -80°C until analyzed for metabolite content. Plasma samples were taken from 50 day old untreated mice as well as 70 day old saline and MSO-treated mice of both genotypes. In 50 day old, untreated animals several plasma metabolites were found to differ significantly between wild-type and SOD1 G93A mice. The top of Table 3.3.3.1 compares the concentrations (expressed in μmoles/L with the standard error of the mean in parentheses) of several plasma metabolites analyzed in SOD1 mice (n=13) and compares them to those of wild-type control animals (n=19) of the same age. A multivariate analysis of variance (MANOVA) was used to compare plasma metabolite concentrations and the *p* values obtained are listed in the right-most column of the table. Phosphoserine, phosphoethanolamine, urea, and citrulline are all significantly lower in SOD1 plasma compared to wild-type plasma. Lysine, a ketogenic amino acid that can be converted into acetoacetyl-CoA and eventually ketone bodies, is significantly lower in SOD1 plasma. In addition, aspartate, cystine, methionine, and arginine, all of which are glucogenic amino acids and can be converted to glucose and glycogen, are also significantly lower in the plasma of SOD1 animals at 50 days of age. Asparagine and glutamine, which are also glucogenic amino acids, are elevated in SOD1 plasma when compared to that of wild-type animals. Of the metabolites that differ between SOD1 and wild-type mice, glutamine, methionine and lysine are essential, while cystine and arginine are considered to be conditionally essential amino acids. Interestingly, cystine was detectable in all wild-type plasma samples but could only be detected in one SOD1 sample.

Table 3.3.3.1 Plasma metabolite differences between 50 day old untreated and 70 day old saline-treated SOD1 and wild-type mice.

Age	Metabolite	WT	SOD1	*p* (MANOVA)
50 Days	**Phser**	14.43 (0.84)	6.76 (1.24)	0.000009
	Pea	11.55 (1.27)	5.57 (2.00)	0.01
	Urea	9866.08 (358.87)	8088.85 (696.89)	0.02
	Asp	18.03 (1.51)	11.32 (0.87)	0.002
	Asn	38.98 (2.09)	47.83 (4.03)	0.04
	Gln†	560.08 (13.21)	676.66 (37.19)	0.002
	Citr	109.36 (4.91)	87.14 (5.46)	0.006
	Cys†	27.91 (2.40)	0.36 (0.36)	0.000000
	Met*	87.38 (5.84)	65.47 (7.01)	0.02
	Lys*	319.96 (12.69)	273.63 (16.00)	0.03
	Arg†	122.45 (8.41)	86.84 (7.51)	0.006
70 Days (Saline)	**Pea**	6.11 (1.74)	1.12 (0.61)	0.008
	Asp	13.06 (1.38)	9.15 (0.35)	0.007
	Sarc	9.33 (5.38)	32.38 (5.12)	0.005
	Ala	720.05 (52.53)	593.61 (32.61)	0.045
	Cys†	13.34 (5.45)	0.00 (0.00)	0.02
	Pro†	116.87 (10.32)	75.54 (11.55)	0.01

Amino acid levels are expressed as the mean (S.E.M.) in μmoles/L.
Amino acids highlighted in red are glucogenic and can be converted to glucose and glycogen.
Amino acids highlighted in blue are ketogenic and can be converted to acetoacetyl-CoA and/or acetyl-CoA.
* indicates essential amino acids.
† indicates conditionally essential amino acids.
n (WT, 50 days) = 19
n (SOD1, 50 days) = 13
n (WT, 70 days) = 12
n (SOD1, 70 days) = 14

When we examine plasma metabolite changes in 70 day old SOD1 and wild-type mice treated with saline we see a strikingly different profile. There are fewer metabolite differences between saline-treated SOD1 and wild-type mice at 70 days of age and the metabolites that differ significantly between the two groups are different from what we see in 50 day old untreated mice. The bottom of Table 3.3.3.1 shows the amino acids that differ significantly between 70 day old saline-treated SOD1 and wild-type mice, as well as the *p* values obtained from the MANOVA. As with 50 day old untreated mice, phosphoethanolamine, aspartate, and cystine levels were all found to be significantly lower in saline-treated SOD1 mice when compared to saline-treated wild-type mice. Cystine levels were found to follow a similar pattern in 70 day old animals, with levels being undetectable in all SOD1 plasma analyzed. Alanine and proline levels were also found to be significantly lower in saline-treated SOD1 animals, while sarcosine (N-methylglycine) levels were found to be elevated in SOD1 plasma. Of these metabolites, aspartate, alanine, cystine, and proline are all glucogenic and both cystine and proline are considered to be conditionally essential amino acids. We also no longer see significant differences in plasma urea or glutamine levels in SOD1 mice at 70 days of age.

Many metabolites vary between genotypes within the same gender. When we break the data from Table 3.3.3.1 down and look at genotype differences in plasma metabolites within each gender, we see that male and female SOD1 mice, when compared to their wild-type counterparts, have different plasma metabolite profiles. Table 3.3.3.2 shows the data broken down by gender, comparing wild-type mice to SOD1 mice. Female SOD1 mice in the 50 day age group show a variety of differences in plasma metabolites, some of these differences are the same seen in Table 3.3.3.1, while other differences are specific to females and are not detected when gender is not accounted for. For example, lower levels of plasma phosphoserine, citrulline, cystine, methionine, lysine, and arginine, and higher levels of glutamine, seen in female SOD1 mice agree with plasma metabolite differences seen between

wild-type and SOD1 mice when gender is not accounted for. However, when we examine genotype differences in plasma metabolites of female mice, we now detect significant differences in threonine and ornithine, both of which are significantly lower in plasma from SOD1 females (Table 3.3.3.2). When we look at 50 day old male mice a similar pattern is observed, where several of the plasma metabolite differences agree with those seen in Table 3.3.3.1 and new male-specific differences become apparent. Lower levels of plasma phosphoserine, phosphoethanolamine, urea, aspartate, and cystine, and higher levels of asparagine and glutamine, detected in male SOD1 mice when compared to male wild-type mice agree with differences seen when gender is not accounted for. However, focusing on genotype differences in plasma metabolites from male mice shows that there are several metabolite differences that are specific to males. Male SOD1 mice show significantly higher plasma levels of alanine, tyrosine, phenylalanine, and proline, which are not seen in females.

Several of the plasma metabolite differences between 50 day old wild-type and SOD1 mice are not considered to be gender-specific. Decreased levels of phosphoserine and cystine, and elevated levels of glutamine are seen in both male and female SOD1 mice when the data are broken down by gender. It is also interesting to point out that several of the differences seen in 50 day old SOD1 mice in Table 3.3.3.1 are accounted for by only one gender. Lower levels of methionine, lysine, and arginine are specific to females, while male specific changes include alterations in levels of phosphoethanolamine, urea, aspartate, and asparagine.

Table 3.3.3.2 Plasma metabolite profiles of 50 and 70 day old mice broken down by gender.

Age & Gender	Metabolite	WT	SOD1	*p* (MANOVA)
50 day Females	Phser	14.45 (1.47)	8.66 (1.54)	0.02
	Thr*	203.07 (10.99)	131.50 (16.26)	0.002
	Gln†	568.60 (16.63)	709.78 (74.95)	0.04
	Citr	119.86 (8.34)	72.97 (7.40)	0.002
	Cys†	23.32 (3.73)	0.77 (0.77)	0.0003
	Met*	97.44 (10.56)	47.63 (6.17)	0.003
	Orn	99.00 (8.66)	53.06 (8.53)	0.003
	Lys*	356.96 (17.17)	255.59 (24.42)	0.004
	Arg†	138.40 (13.63)	76.58 (11.60)	0.007
50 day Males	Phser	14.40 (0.96)	5.13 (1.75)	0.0002
	Pea	11.02 (2.28)	2.37 (1.82)	0.01
	Urea	10907.49 (366.39)	8117.83 (1287.87)	0.03
	Asp	20.73 (1.76)	11.20 (1.15)	0.001
	Asn	35.65 (2.21)	53.62 (4.98)	0.002
	Gln†	552.41 (20.69)	648.27 (28.90)	0.01
	Ala	532.65 (19.38)	754.24 (26.03)	0.000004
	Cys†	32.04 (2.58)	0.00 (0.00)	0.000000
	Tyr†	65.22 (3.55)	81.65 (5.26)	0.02
	Phe*	58.07 (2.25)	68.15 (3.43)	0.02
	Pro†	84.78 (4.10)	129.72 (11.49)	0.0008
70 day Females	Pea	11.21 (1.40)	1.61 (1.06)	0.0002
	Sarc	8.90 (5.65)	37.80 (4.86)	0.002
70 day Males	Gly†	325.48 (13.66)	281.24 (5.40)	0.009
	Ala	673.60 (28.49)	521.33 (43.07)	0.02

Amino acid levels are expressed as the mean (S.E.M.) in μmoles/L.
Amino acids highlighted in red are glucogenic, those in blue are ketogenic, and purple indicates amino acids that can be both ketogenic and glucogenic.
* indicates essential amino acids and † indicates conditionally essential amino acids.
n (WT, F, 50 days) = 9 n (WT, M, 50 days) = 10
n (SOD1, F, 50 days) = 6 n (SOD1, M, 50 days) = 7
n (WT, F, 70 days) = 6 n (WT, M, 70 days) = 6
n (SOD1, F, 70 days) = 7 n (SOD1, M, 70 days) = 7

When we look at genotype differences between 70 day old female and male mice, we see that there are far fewer metabolite differences than with 50 day old mice. The bottom of Table 3.3.3.2 shows the differences between 70 day old saline-treated wild-type and SOD1 female and male mice. Some of the genotype differences seen in Table 3.3.3.1, when the data were examined by genotype only, disappear when gender is accounted for, while the other differences appear to be gender-specific. When we look at 70 day old females treated with saline, we see that SOD1 females have significantly lower levels of phosphoethanolamine, with elevated sarcosine, which agrees with the genotype differences seen in Table 3.3.3.1. These alterations in phosphoethanolamine and sarcosine are specific to females, as males show no significant changes in levels of these metabolites. When we look at 70 day old males treated with saline, we see that SOD1 males show decreased plasma levels of glycine and alanine, which are not shared with females but are seen when gender is not accounted for (Table 3.3.3.1). Significant differences in aspartate and proline, observed between wild-type and SOD1 mice (Table 3.3.3.1) are no longer seen when gender is accounted for. Differences in cystine levels do not reach significance when gender is accounted for, but continue to be undetectable in 70 day old saline-treated SOD1 male and female mice.

Several plasma metabolites differ between males and females of the same genotype. When the plasma metabolite data are broken down by genotype and analyzed for gender differences, 50 day old wild-type mice show more gender differences than SOD1 mice. Table 3.3.3.3 shows the plasma metabolites that differ significantly between 50 day old female and male wild-type and SOD1 mice, as well as differences between saline-treated 70 day old females and males. Nine plasma metabolites differ between 50 day old female and male mice – urea, threonine, serine, alanine, citrulline, tyrosine, lysine, histidine, and tryptophan. Of these metabolites, only urea is significantly higher in male wild-type mice. Male wild-type mice show significantly lower levels of the other eight plasma metabolites. This is much different than what

is observed in SOD1 mice. First, there are fewer plasma metabolites that differ between male and female SOD1 mice. The overall plasma metabolite profile of these animals is different than that of wild-type mice. Only two of the significantly different metabolites in SOD1 mice – threonine and citrulline – overlap with the metabolites that differ in wild-type mice. All of the differences seen between SOD1 females and males occur because males have significantly higher levels than females, whereas the differences in wild-type animals are due to males having significantly lower levels than females. SOD1 males have significantly higher levels of threonine than SOD1 females, but their levels of threonine are closer to those of wild-type females, which have higher threonine levels than wild-type males. We also see that levels of citrulline in SOD1 male mice, which are significantly higher than those of SOD1 females, are similar to citrulline levels in wild-type male mice.

Table 3.3.3.3 Gender differences in plasma metabolites of wild-type and SOD1 mice.

Age & Genotype	Metabolite	Female	Male	*p* (MANOVA)
50 day WT	Urea	8708.96 (354.88)	10907.49 (366.39)	0.0005
	Thr*	203.07 (11.00)	163.34 (9.19)	0.01
	Ser	163.93 (7.19)	138.98 (4.92)	0.01
	Ala	627.88 (40.72)	532.65 (19.39)	0.04
	Citr	119.86 (8.34)	99.90 (3.88)	0.04
	Tyr†	79.45 (5.61)	65.22 (3.55)	0.04
	Lys*	356.96 (17.17)	286.65 (10.76)	0.02
	His*	73.38 (2.87)	66.08 (2.76)	0.03
	Trp*	76.56 (3.39)	43.50 (7.64)	0.001
50 day SOD1	Thr*	131.50 (16.26)	187.67 (12.48)	0.02
	Citr	72.97 (7.40)	99.29 (4.30)	0.009
	Met*	47.63 (6.17)	80.77 (8.41)	0.01
	Orn	53.06 (8.53)	88.90 (11.71)	0.04
	Pro†	77.27 (10.86)	129.72 (11.49)	0.007
70 day WT	Taur	374.83 (20.66)	281.63 (21.25)	0.01
	Pea	11.21 (1.40)	1.02 (1.02)	0.0002
	Gln*	638.99 (34.74)	531.61 (29.86)	0.04
	1-Mhis	15.07 (1.41)	10.09 (1.22)	0.02
	His*	81.79 (3.31)	67.63 (2.41)	0.006
	Trp*	76.07 (7.38)	50.16 (4.57)	0.01
70 day SOD1	Urea	9447.01 (548.05)	11606.02 (354.13)	0.006
	Gln†	646.85 (25.91)	540.98 (29.63)	0.02
	Ala	665.88 (31.81)	521.33 (43.07)	0.02
	Phe*	71.48 (2.11)	61.65 (2.94)	0.02
	Lys*	318.41 (17.80)	242.03 (26.80)	0.04
	His*	81.73 (6.61)	64.16 (2.34)	0.03

Amino acid levels are expressed as the mean (S.E.M.) in μmoles/L and n values are the same as those of Table 3.3.3.2. * indicates essential amino acids and † indicates conditionally essential amino acids. Amino acids highlighted in red are glucogenic, those in blue are ketogenic, and purple indicates amino acids that can be both ketogenic and glucogenic.

When the data from 70 day old saline-treated mice are broken down by genotype and examined for gender differences, we see a different plasma metabolite profile than what was observed in 50 day old mice, with new metabolite differences appearing. The bottom portion of Table 3.3.3.3 lists the plasma metabolites found to differ significantly between male and female 70 day old mice treated with saline. When we compare male and female wild-type mice treated with saline, significant gender differences in six plasma metabolites are observed. Male wild-type mice in this age group have significantly lower plasma levels of taurine, phosphoethanolamine, glutamine, 1-methylhistidine, histidine, and tryptophan. Of these differences, only two are shared with 50 day old wild-type mice – histidine and tryptophan – which are also lower in male wild-type mice compared to females. When we compare metabolite levels in plasma from male and female SOD1 mice treated with saline there is very little overlap with the profile of wild-type males and females. In both wild-type and SOD1 mice glutamine and histidine levels are found to be significantly higher in females when compared to males. The other plasma metabolites that show gender differences in SOD1 mice at this age – urea, alanine, phenylalanine, and lysine – are lower in males than females, with the exception of urea which is elevated in male SOD1 mice. The 50 and 70 day age groups show no similarities with respect to gender differences in plasma metabolite levels.

MSO treatment significantly lowers plasma glutamine levels, increases plasma cystine levels, and alters the profile of several other plasma metabolites in SOD1 mice. The plasma metabolite profile of SOD1 mice treated with MSO shows several changes in the levels of a variety of chemicals. We examined plasma metabolite levels in 14 mice treated with saline and 16 mice treated with MSO and Figure 3.3.3.4 shows the plasma metabolites that are altered with MSO treatment in these SOD1 mice. Phosphoethanolamine, AAAA (α-aminoadipic acid, an intermediate in lysine metabolism), and ornithine levels increase, while sarcosine levels decrease in MSO-treated SOD1 mice compared to their saline-treated counterparts. The levels

of several glucogenic amino acids are altered with MSO treatment. Asparagine, alanine, arginine, and cystine levels increase significantly with MSO treatment, while glutamine levels decrease significantly with treatment. Interestingly, cystine, which is undetectable in saline-treated SOD1 mice, becomes detectable with MSO treatment. Lysine, an essential ketogenic amino acid, also increases significantly in SOD1 mice with MSO treatment. We also compared the plasma metabolite profile of wild-type mice treated with saline to that of MSO-treated wild-type mice and only found one amino acid to change with treatment. Lysine levels in wild-type mice increase significantly from 290.03 ± 18.13 to 352.86 ± 17.99 μmoles/L, with p=0.02. This is similar to the increase in plasma lysine levels seen in SOD1 mice with MSO treatment.

Table 3.3.3.4 The effects of MSO treatment on plasma metabolite levels of SOD1 mice.

Metabolite	SOD1 Saline	SOD1 MSO	*p* (MANOVA)
Pea	1.12 (0.61)	4.68 (1.16)	0.01
Asn	42.92 (2.77)	56.49 (4.05)	0.01
Gln†	593.91 (23.94)	449.48 (29.23)	0.0008
Sarc	32.38 (5.12)	18.30 (3.36)	0.03
AAAA	10.63 (1.37)	17.60 (1.69)	0.004
Ala	593.61 (32.61)	743.30 (35.23)	0.005
Cys†	0.00 (0.00)	5.29 (2.10)	0.03
Orn	73.53 (5.88)	99.46 (7.98)	0.02
Lys*	280.22 (18.74)	358.42 (24.71)	0.02
Arg†	100.60 (7.59)	137.16 (10.36)	0.01

Amino acid levels are expressed as the mean (S.E.M.) in μmoles/L.
Amino acids highlighted in red are glucogenic and can be converted to glucose and glycogen.
Amino acids highlighted in blue are ketogenic and can be converted to acetoacetyl-CoA and/or acetyl-CoA.
* indicates essential amino acids.
† indicates conditionally essential amino acids.
n (Saline) = 14
n (MSO) = 16

There are several gender-specific changes in plasma metabolites of 70 day old mice with MSO treatment. When the plasma metabolite data are further broken down by gender and genotype and examined for changes with MSO treatment, the plasma concentrations of several metabolites are altered in a gender-specific fashion. Table 3.3.3.5 lists the metabolites that change significantly with MSO treatment, as well as their concentrations in saline and MSO-treated animals. When we compare the concentrations of plasma metabolites of saline-treated wild-type female mice to those of MSO-treated wild-type female mice, there are no significant changes with MSO treatment. However, when we look at treatment-related changes in plasma metabolites of female SOD1 mice we see that glutamine and sarcosine levels are significantly lower, while arginine levels are significantly higher, in MSO-treated mice. This corresponds to the overall changes that were seen when in plasma metabolite levels were examined only by genotype (Table 3.3.3.4). We see a greater number of plasma metabolites change with MSO treatment in male wild-type mice. Male wild-type mice treated with MSO have significantly higher levels of phosphoserine, phosphoethanolamine, glutamate, ornithine, and lysine in their plasma than their saline-treated counterparts. Fewer plasma metabolite changes are seen in male SOD1 mice that have been treated with MSO. As with wild-type males, plasma levels of phosphoethanolamine increase with MSO treatment in SOD1 males. This is the only similarity between wild-type and SOD1 male mice. SOD1 males also show significantly increased levels of AAAA, alanine, and tryptophan in their plasma with MSO treatment, which are not seen in wild-type males.

Table 3.3.3.5 Gender-specific changes in plasma metabolites with MSO treatment.

Gender Genotype	Metabolite	Saline	MSO	*p* (MANOVA)
Female WT	No changes with MSO treatment			
Female SOD1	Gln†	646.85 (25.91)	465.34 (45.07)	0.005
	Sarc	37.80 (4.86)	20.18 (4.86)	0.02
	Arg†	114.79 (8.33)	152.43 (13.55)	0.04
Male WT	Phser	6.53 (1.14)	13.50 (2.05)	0.01
	Pea	1.02 (1.02)	9.02 (3.10)	0.03
	Glu	8.34 (3.75)	28.75 (5.84)	0.01
	Orn	70.73 (10.78)	101.92 (6.61)	0.04
	Lys*	262.49 (8.92)	323.20 (21.19)	0.02
Male SOD1	Pea	0.63 (0.63)	5.72 (1.71)	0.02
	AAAA	10.10 (0.84)	16.76 (2.33)	0.02
	Ala	521.33 (43.07)	710.40 (53.65)	0.02
	Trp*	42.58 (7.40)	66.02 (4.31)	0.01

Amino acid levels are expressed as the mean (S.E.M.) in μmoles/L.
Amino acids highlighted in red are glucogenic and can be converted to glucose and glycogen.
Amino acids highlighted in blue are ketogenic and can be converted to acetoacetyl-CoA and/or acetyl-CoA.
Amino acids highlighted in purple can be ketogenic or glucogenic.
* indicates essential amino acids.
† indicates conditionally essential amino acids.
n (F, WT, Saline) = 6
n (F, WT, MSO) = 6
n (F, SOD1, Saline) = 7
n (F, SOD1, MSO) = 8
n (M, WT, Saline) = 6
n (M, WT, MSO) = 5
n (M, SOD1, Saline) = 7
n (M, SOD1, MSO) = 8

To summarize the results of the plasma metabolite analysis, we see that there are a variety of differences in SOD1 mice when compared to wild-type mice, some of which are gender-specific. We see that 50 day old untreated SOD1 mice have significantly higher levels of plasma ammonia than wild-type mice, but the overall level of ammonia in both groups declines with age and these genotype differences disappear in 70 day old saline-treated mice. We also see that when plasma ammonia data are broken down by gender and genotype, both female and male SOD1 mice have higher plasma ammonia levels, but the differences between wild-type and SOD1 females reached significance, while those between males did not. The same trend is seen in 70 day data broken down by gender and genotype, where overall plasma ammonia levels decrease in all groups and show no significant gender or genotype differences. MSO treatment significantly increases plasma ammonia levels in both wild-type and SOD1 mice, and no gender differences are seen with treatment.

With respect to plasma metabolites, 50 day old untreated animals show many more genotype differences in metabolites than 70 day old saline-treated mice and several of these differences in plasma metabolite levels between wild-type and SOD1 mice show gender-specificity when data are broken down by both genotype and gender. For example, significantly lower levels of methionine, lysine, and arginine are only seen in 50 day old female SOD1 (when compared to female wild-type) mice and significant differences in levels of phosphoethanolamine, urea, aspartate, and asparagine are only seen when 50 day old male SOD1 and wild-type mice are compared. When gender is taken into account, genotype differences in metabolites from 50 day old mice that are not seen when gender is ignored become apparent. For example, when 50 day old wild-type and SOD1 mice are grouped according to gender and examined for genotype differences females show differences in ornithine and threonine, while males show differences in alanine, tyrosine, phenylalanine, and proline, which are not observed when animals are simply grouped by genotype. Gender

specific differences in plasma metabolites continue to be seen in 70 day old saline-treated mice, but there are fewer than what was observed in 50 day old mice. MSO treatment alters a variety of metabolite levels in SOD1 mice, however only lysine levels are altered in wild-type mice. When treatment data are broken down by gender and genotype, there are a variety of metabolite changes observed but no changes occur in female wild-type mice.

3.3.4 Nitrogen Metabolism in the Liver

Preliminary analysis of plasma metabolite data suggested that several amino acids, particularly those involved in urea production, were significantly different in SOD1 mice when compared to wild-type animals. In mammals urea production occurs primarily in the liver (and to some extent in the kidney) through the urea cycle, which consists of five reactions that function to remove ammonia from the body. The first two reactions occur in the mitochondria, the first of which is catalyzed by carbamoyl phosphate synthetase one (CPSI) and is the rate limiting step of the urea cycle. The mutant SOD1 protein is ubiquitously expressed in the SOD1 G93A mouse model of ALS and the protein has been shown to associate with mitochondria isolated from spinal cord (Liu et al 2004) and aggregate in brain mitochondria (Vijayvergiya et al 2005) of these animals. In addition, mice expressing mutant SOD1 protein have been found to have overall defects energy homeostasis (Dupuis et al 2004) and liver samples collected from ALS patients exhibit hepatic ultrastructural changes and abnormal mitochondria, suggestive of liver dysfunction (Nakano et al 1987). As a result, it seems reasonable to believe that the SOD1 mutation could potentially interact with liver mitochondria in such a way as to impair the urea cycle. We decided to assay CPSI activity to see if SOD1 mice exhibit changes in enzyme activity prior to symptom onset. We also examined the impact of gender and MSO treatment on CPSI activity.

The specific activity of CPSI does not differ between wild-type and SOD1 mice. Figure 3.3.4.1 compares the specific activity of CPSI in wild-type mice to that of SOD1 mice. In 50 day old untreated mice, both wild-type and SOD1 animals have about the same level of CPSI activity, approximately 150 nmoles/min/mg protein (Figure 3.3.4.1A). At 70 days of age, CPSI activity increases significantly in both wild-type ($p<0.001$) and SOD1 ($p<0.05$) mice treated with saline (Figure 3.3.4.1B). It also appears as though SOD1 mice may have lower CPSI activity than wild-type mice at this age; however this difference did not reach significance.

Figure 3.3.4.1 Specific activity of liver CPSI in wild-type and SOD1 mice.

The data are presented as the average specific activity of CPSI with error bars representing the S.E.M. Green bars indicate data from wild-type mice, while purple bars indicate data from SOD1 mice. **A.** The specific activity of CPSI in 50 day old wild-type and SOD1 mice (n=20 mice/group). **B.** The specific activity of CPSI in saline-treated 70 day old wild-type and SOD1 mice (n=20 mice/group).

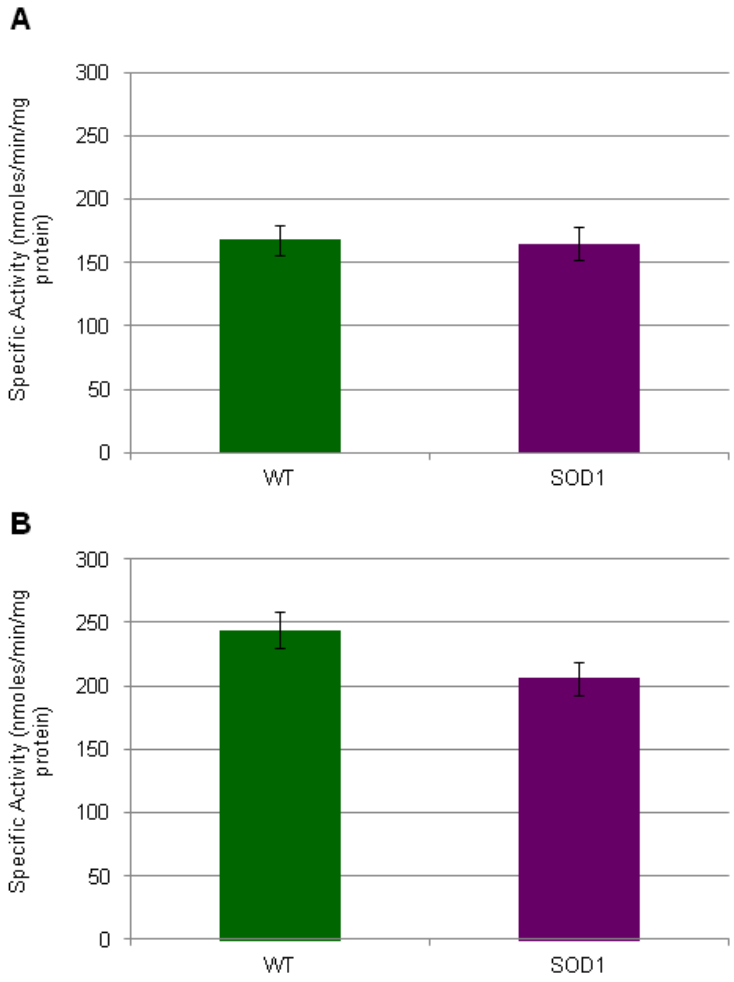

Female mice have higher CPSI activity levels than males, regardless of genotype. When the CPSI activity data are broken down by gender and genotype there is a clear difference between males and females. Figure 3.3.4.2 shows the results of the CPSI activity assays broken down by gender and genotype. In 50 day old untreated wild-type and SOD1 female mice, the average CPSI activity is around 200 nmoles/min/mg protein, almost twice the activity of CPSI in wild-type and SOD1 males (Figure 3.3.4.2A). In 70 day old saline-treated mice, CPSI activity is elevated across all groups when compared to 50 day old untreated animals ($p<0.05$). The gender difference in the specific activity of CPSI remains apparent in 70 day old mice (Figure 3.3.4.2B). Saline-treated female wild-type mice show significantly higher CPSI activity (280 ± 20 nmoles/min/mg protein) than their male counterparts (210 ± 10 nmoles/min/mg protein), with $p<0.05$. Saline-treated SOD1 female mice also show significantly higher CPSI activity (250 ± 10 nmoles/min/mg protein) than their male counterparts (160 ± 10 nmoles/min/mg protein), with $p<0.001$. It is also interesting to point out that in the 70 day age group, saline-treated SOD1 males have significantly lower CPSI activity levels than saline-treated wild-type males ($p<0.01$), but this difference is not observed when female SOD1 and wild-type mice are compared.

Figure 3.3.4.2 Specific activity of liver CPSI broken down by gender and genotype.

The data are presented as the average specific activity of CPSI with error bars representing the S.E.M. Green bars indicate data from male and female wild-type mice, while purple bars indicate data from male and female SOD1 mice. **A.** Specific activity of CPSI from 50 day old untreated mice (n=10 mice/group; *** indicate values are significant with $p<0.001$). **B.** Specific activity of CPSI from 70 day old mice treated with saline (n=10 mice/group; *, **, and *** indicate values are significant with $p<0.05$, 0.01, and 0.001 respectively).

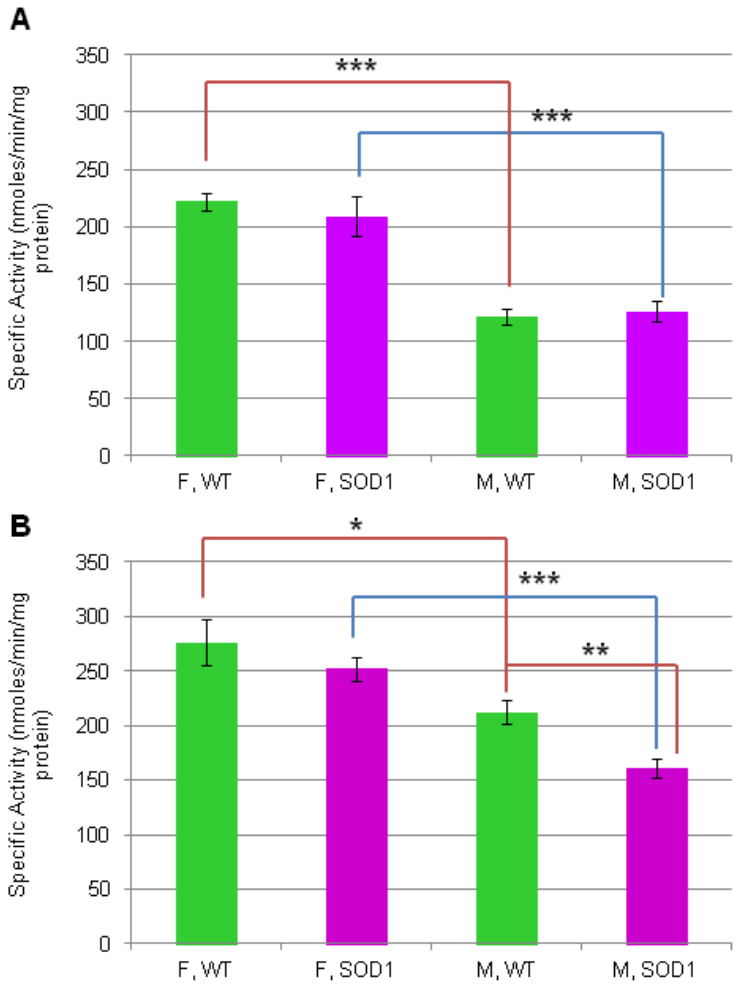

MSO treatment does not affect CPSI activity levels in wild-type or SOD1 mice. Figure 3.3.4.3 shows the effect of MSO treatment on CPSI activity. When the data are grouped by genotype, 70 day old wild-type animals treated with saline have CPSI activity levels similar to those of wild-type animals treated with MSO and the same holds true for SOD1 mice (Figure 3.3.4.3A). SOD1 mice in this age group have slightly lower, but not significant, CPSI activity levels than wild-type mice for both treatment groups. When the data are broken down by gender and genotype (Figure 3.3.4.3B), we see that MSO-treated wild-type females have slightly higher, but not significant, CPSI activity than saline-treated wild-type females. However, female SOD1 mice and male wild-type and SOD1 mice all show slightly lower, but not significant, levels of CPSI activity when treated with MSO.

Figure 3.3.4.3 The effects of MSO treatment on CPSI activity in presymptomatic wild-type and SOD1 mice.

The data are presented as the average specific activity of CPSI with error bars representing the S.E.M. Blue bars indicate data from both wild-type and SOD1 mice treated with saline while red bars indicate data from wild-type and SOD1 mice treated with MSO. **A.** In 70 day old mice, MSO treatment has no effect on CPSI activity in wild-type or SOD1 mice (n=20 mice/group). **B.** When the data depicted in **A** are broken down by gender and genotype, MSO treatment still has no effect on CPSI activity in 70 day old animals (n=10 mice/group).

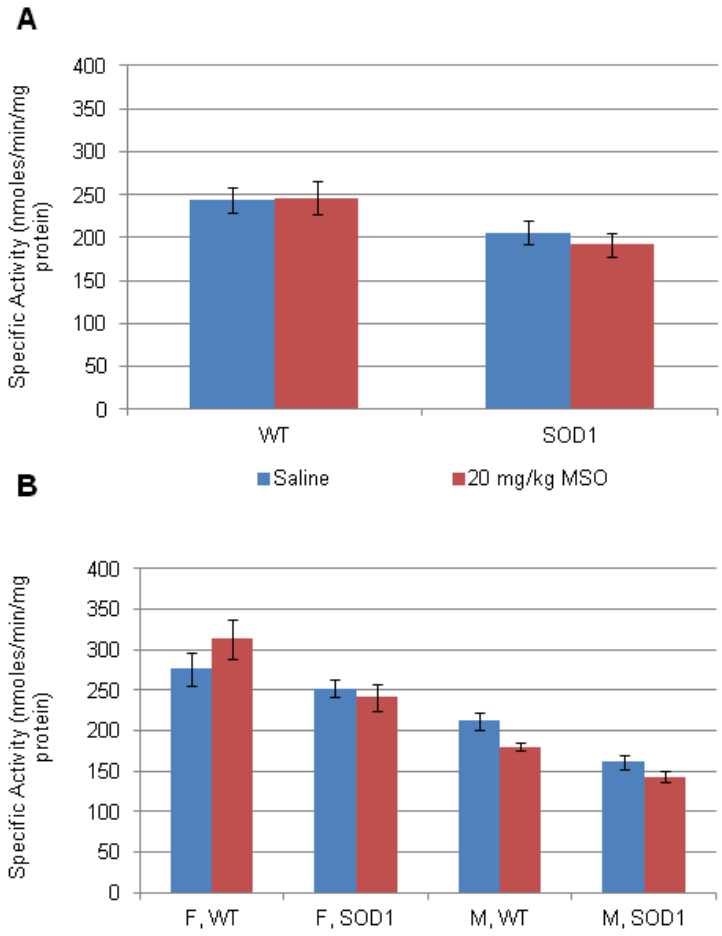

In summary, we see no significant differences in CPSI activity between wild-type and SOD1 mice at 50 or 70 days of age. However, we do see that CPSI activity is significantly elevated in 70 day old saline-treated mice of both genotypes when compared to 50 day old animals. When CPSI activity data are further broken down by gender and genotype, we see that there is a clear gender difference in 50 day old mice, in which female mice of both genotypes have significantly higher CPSI activity levels than their male counterparts. We continue to see significantly elevated CPSI activity in all groups of mice at 70 days of age. While we still see a gender difference in this age group (females continue to having significantly higher CPSI activity than males), we also start to see changes in CPSI activity in male SOD1 mice, which have the lowest activity level of all the groups examined. MSO treatment shows no effect on CPSI activity in wild-type and SOD1 mice of both genders.

After analyzing CPSI activity levels in the liver of wild-type and SOD1 mice, we assayed glutamine synthetase activity levels in the same mice. In mammals, CPSI and GS protein expression are compartmentalized within different cell types. In the mammalian liver CPSI is broadly expressed in most hepatocytes, while glutamine synthetase expression is restricted to only a small number of cells which do not express CPSI, specifically those surrounding the terminal hepatic venules where GS is found in the cytosol (Smith & Campbell 1988). Glutamine synthetase is also cytosolic in the brain, however it is much more widely expressed within astrocytes which can make up about 50% of the volume in certain regions (Squire et al 2008). As previously mentioned, a single dose of MSO has been shown to inhibit glutamine synthetase activity in the brain for an extended period of time, with brain GS regaining 75% of control activity after 90 days. This same study also showed that a single subconvulsive dose of MSO had slightly different effects on the liver. Maximal inhibition of glutamine synthetase in mouse liver was obtained within one hour of injection with MSO and the enzyme regained 70% of control activity within 4 days of injection (Rao & Meister 1972). In an effort to continue the

characterization of glutamine metabolism in ALS mice, as well as to examine potential metabolic effects of the overexpression of mutant SOD1 protein in liver, we assayed the specific activity of liver glutamine synthetase in both wild-type and SOD1 mice and looked at the effects of MSO treatment on enzyme activity.

The SOD1 G93A mutation does not affect the specific activity of glutamine synthetase in liver homogenates of presymptomatic mice. All animals assigned to these experiments were given a final injection of MSO within 24 hours prior to euthanasia. When liver samples were processed, a portion of the supernatant from each liver homogenate was desalted for CPSI enzyme activity assays, while the remainder was set aside for liver GS activity assays. The activity assays were performed in the same manner as those conducted on brain and spinal cord GS, differing only in sample preparation. The results of liver GS activity assays can be seen in Figure 3.3.4.4. In 50 day old untreated mice, there is no difference in the specific activity of GS between wild-type and SOD1 mice (Figure 3.3.4.4A). The specific activity of liver GS in wild-type mice appears to increase slightly by 70 days of age, while that of SOD1 mice remains the same as that of 50 day old mice. In 70 day old saline-treated mice, liver GS activity appears to be slightly lower in SOD1 mice than wild-type mice (Figure 3.3.4.4B), but this difference was not found to be significant.

Figure 3.3.4.4 Specific activity of liver glutamine synthetase in wild-type and SOD1 mice.

The data are presented as the average specific activity of GS with error bars representing the S.E.M. Green bars indicate data from wild-type mice, while purple bars indicate data from SOD1 mice. **A.** The specific activity of liver GS in untreated, 50 day old wild-type and SOD1 mice (n=20 mice/group). **B.** The specific activity of liver GS in saline-treated, 70 day old wild-type and SOD1 mice (n=20 mice/group).

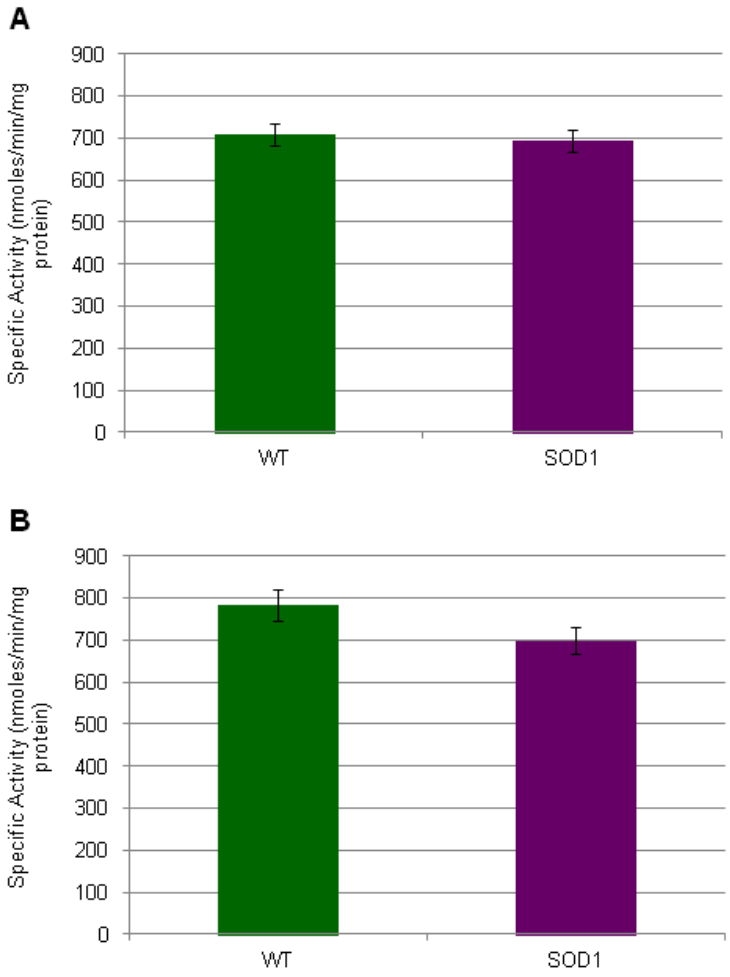

Male SOD1 mice treated with saline have significantly lower liver GS activity than female SOD1 and male wild-type mice. Figure 3.3.4.5 shows the specific activity of liver GS broken down by gender and genotype. Untreated 50 day old mice have about the same level of GS activity across genders and genotypes (Figure 3.3.4.5A). In 70 day old mice treated with saline, we see that the specific activity of liver GS is higher in female mice when compared to male mice of both genotypes (Figure 3.3.4.5B). However, this difference is only significant when comparing female SOD1 mice to male SOD1 mice treated with saline. Saline-treated female SOD1 mice have significantly higher liver GS activity (810 ± 30 nmoles/min/mg protein) than male SOD1 mice (580 ± 30 nmoles/min/mg protein), with $p<0.001$. Saline-treated male SOD1 mice also have significantly lower GS activity than their wild-type counterparts (580 ± 30 nmoles/min/mg protein compared to 740 ± 50 nmoles/min/mg protein), with $p<0.05$.

Figure 3.3.4.5 Specific activity of liver GS broken down by gender and genotype.

The data are presented as the average specific activity of GS with error bars representing the S.E.M. Green bars indicate data from male and female wild-type mice, while purple bars indicate data from male and female SOD1 mice. **A.** Specific activity of liver GS from 50 day old untreated mice (n=10 mice/group). **B.** Specific activity of liver GS from 70 day old mice treated with saline (n=10 mice/group; * and *** indicate values are significant with $p<0.05$ and 0.001 respectively).

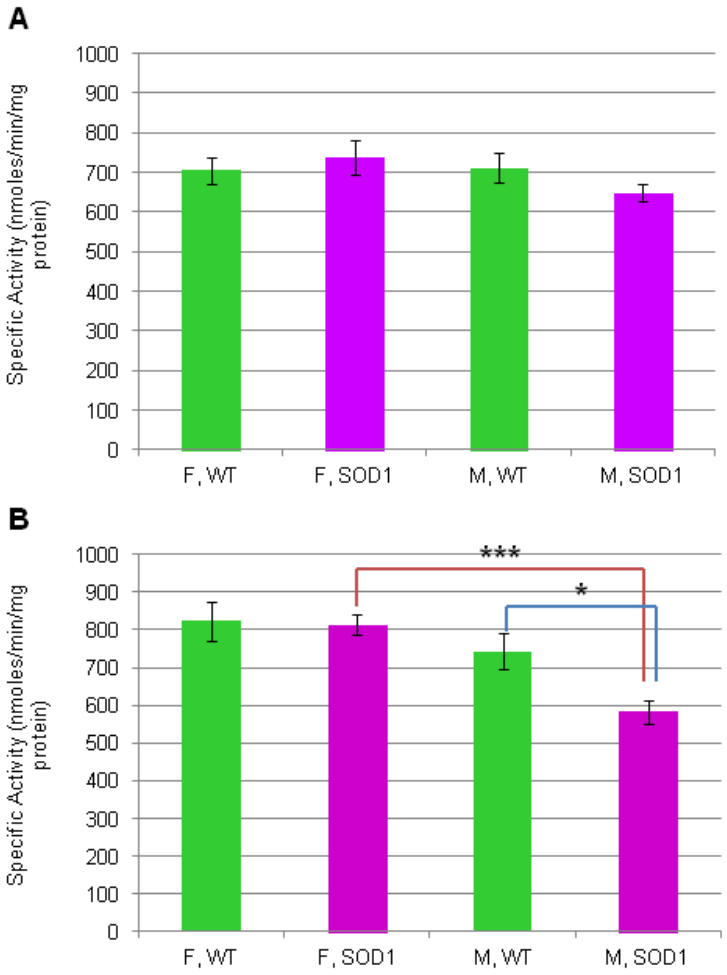

MSO treatment significantly lowers liver glutamine synthetase activity. Figure 3.3.4.6 shows the effects of MSO treatment on the specific activity of liver glutamine synthetase. Much like with brain and spinal cord GS activity, a single weekly injection of 20 mg/kg MSO lowers liver glutamine synthetase activity; however the extent of inhibition varies slightly. Whereas with brain and spinal cord, in which MSO treatment lowered GS activity by about 90% in both genotypes, we see that liver GS activity at 70 days of age is inhibited by almost 90% in wild-type mice, but in SOD1 mice GS activity is only inhibited by approximately 70% (Figure 3.3.4.6A). SOD1 mice treated with MSO have significantly higher liver GS activity (200 ± 35 nmoles/min/mg protein) than wild-type mice treated with MSO (110 ± 10 nmoles/min/mg protein), $p<0.05$. When these data are broken down by gender and genotype, we see that liver GS activity is significantly lowered in all groups ($p<0.001$). However, GS activity is clearly altered in SOD1 male mice compared to wild-type male and SOD1 female mice (Figure 3.3.4.6B). While MSO treatment lowers GS activity by approximately 85% in male and female wild-type mice, as well as female SOD1 mice, it only lowers GS activity in male SOD1 mice by approximately 55%. When compared to wild-type male mice treated with MSO (95 ± 10 nmoles/min/mg protein), male MSO-treated SOD1 mice have significantly higher liver GS activity (260 ± 50 nmoles/min/mg protein), with $p<0.05$. While female SOD1 mice treated with MSO have lower GS activity than their male counterparts, this difference was not found to be significant. Interestingly, female wild-type mice treated with MSO were found to have significantly higher GS activity (120 ± 30 nmoles/min/mg protein) than their male counterparts (95 ± 10 nmoles/min/mg protein), with $p<0.05$.

Figure 3.3.4.6 The effects of MSO treatment on liver GS activity in presymptomatic wild-type and SOD1 mice.

The data are presented as the average specific activity of GS with error bars representing the S.E.M. Blue bars indicate data from both wild-type and SOD1 mice treated with saline while red bars indicate data from wild-type and SOD1 mice treated with MSO. **A.** MSO treatment significantly lowers liver GS activity in 70 day old wild-type and SOD1 mice (n=20 mice/group, except for WT mice treated with MSO where n=19 mice/group). **B.** When the data are further broken down by gender and genotype, MSO inhibits GS activity by approximately 90% in all groups, except male SOD mice where GS activity is only inhibited by 55% (n=10 mice/group, except for female WT mice treated with MSO where n=9 mice/group; *** indicates that values differ significantly with $p<0.001$).

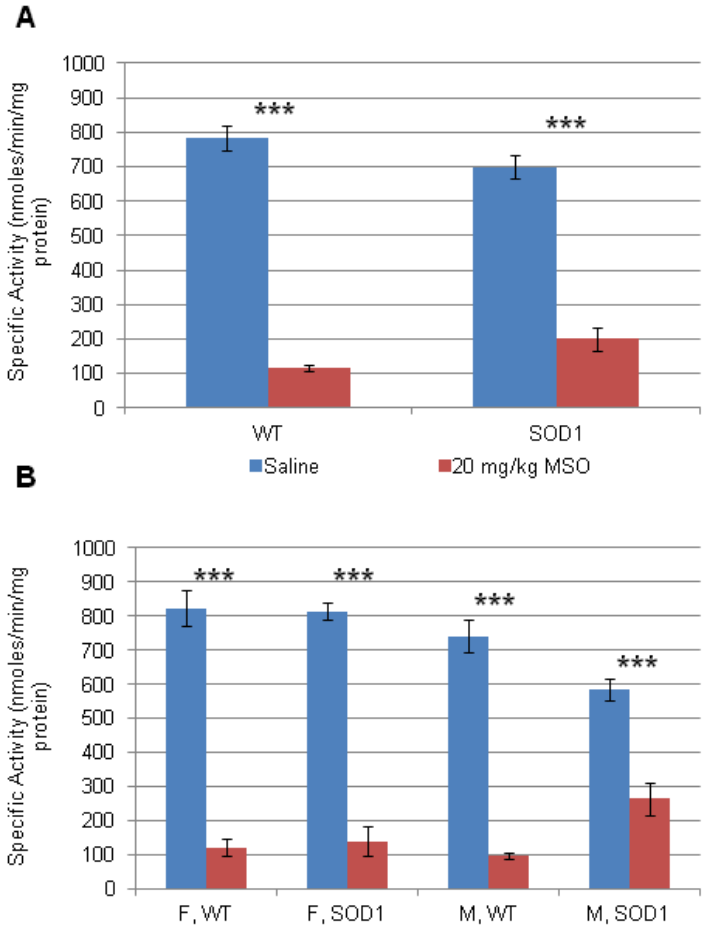

In summary, we see that there are no significant differences in liver glutamine synthetase activity between wild-type and SOD1 mice at 50 days of age. The specific activity of liver GS is slightly, but not significantly, lower in SOD1 mice treated with saline at 70 days of age when compared to saline-treated wild-type mice. When the data are further broken down by gender and genotype, we see no significant gender differences at 50 days of age. However, much like with CPSI activity, we begin to see differences emerging in male SOD1 mice at 70 days of age. Liver GS activity in saline-treated male SOD1 mice decreases at 70 days of age and is significantly lower than that of female SOD1 mice, as well as wild-type male mice, treated with saline. A similar pattern is seen with the CPSI activity in these animals, but is not reflected in the activities of brain or spinal cord GS in animals of the same age. MSO treatment significantly lowers liver glutamine synthetase activity in both wild-type and SOD1 mice, but has a much greater impact on GS activity in wild-type mice where activity is decreased by almost 90%. MSO treatment impacts liver GS activity in male and female wild-type mice and female SOD1 mice similarly, but it does not inhibit liver GS activity in male SOD1 mice to the same extent. Whereas females of both genotypes and male wild-type mice show between 83 and 85% liver GS inhibition with MSO treatment, male SOD1 mice show only 55% inhibition.

3.3.5 The Effects of Ovariectomization on Enzyme Activity and Plasma Metabolites

In an effort to understand how the removal of sex hormones impacts ammonia and amino acid metabolism, we performed glutamine synthetase assays on liver and brain extracts, glutaminase assays on brain extracts, ammonia and metabolite analyses on plasma, and CPSI activity assays on liver extracts isolated from 70 day old female SOD1 mice that had treated with weekly i.p. injections of saline starting at 50 days of age. We focused on female mice because survival experiments and grip assays showed that females benefit more from MSO treatment than males. Obtaining a metabolic profile from these SOD1 female mice might help in

understanding how ammonia and amino acid metabolism change when female sex hormones are removed, and possibly pinpoint a metabolic pathway that may be responsive to these hormones as well as MSO treatment. For these experiments, female SOD1 mice were ovariectomized between 30 and 40 days of age, prior to reaching sexual maturity and subsequent exposure to sex hormones. Intraperitoneal injections of saline were administered once a week starting at 50 ± 2 days of age and mice were euthanized at 70 ± 2 days of age. Metabolic profiles of these mice were compared to those obtained from SOD1 females treated with saline that had not undergone ovariectomy to understand how metabolism was affected by removal of sex hormones.

Ovariectomized SOD1 females have altered glutamine metabolism when compared to SOD1 females with intact ovaries. Table 3.3.5.1 compares the activity levels of enzymes involved in glutamine and ammonia metabolism from 70 day old female SOD1 mice that had their ovaries removed to those from female SOD1 mice with intact ovaries. As shown in Chapter 2, SOD1 females that have undergone ovariectomy no longer respond to MSO treatment and those treated with saline show no change in lifespan. When compared to normal SOD1 females treated with saline, 70 day old ovariectomized SOD1 females have significantly lower levels of brain glutamine synthetase activity and elevated brain glutaminase activity. These mice also exhibit significantly lower levels of liver glutamine synthetase activity. The average specific activity of CPSI from ovariectomized female SOD1 mice is lower than that of females with intact ovaries, but this difference did not reach significance.

Table 3.3.5.1 The effects of ovariectomization on enzyme activity in SOD1 females.

Enzyme Assay	SOD1 Specific Activity	OVR SOD1 Specific Activity	*p* (ANOVA)
Brain GS	1345 (97)	1099 (29)	0.04
Brain Glutaminase	56 (7)	99 (8)	0.002
Liver GS	814 (26)	695 (21)	0.003
Liver CPSI	252 (11)	213 (14)	0.05

Enzyme activities are expressed as average specific activity (S.E.M.) in nmoles/minute/mg protein. OVR indicates ovariectomized females.
n (OVR, SOD1) = 7-10
n (SOD1) = 8-12

Ovariectomized female SOD1 mice treated with saline exhibit a different plasma metabolite profile than non-ovariectomized female SOD1 mice. Table 3.3.5.2 lists the plasma metabolites that differ significantly between 70 day old ovariectomized and non-ovariectomized female SOD1 mice treated with saline. Ovariectomized female mice have slightly higher levels of plasma ammonia than non-ovariectomized female mice however this difference did not reach significance. We do see that there are significant differences in several other plasma metabolites in SOD1 females that have had their ovaries removed. Aspartate, proline, and AAAA levels are elevated in plasma from ovariectomized SOD1 females, while threonine, serine, sarcosine, lysine, and histidine are all significantly lower in ovariectomized SOD1 females. It is interesting to note that SOD1 females treated with saline show elevated levels of plasma sarcosine when compared to their wild-type counterparts (Table 3.3.3.2) and that MSO treatment lowers plasma sarcosine levels in these mice (Table 3.3.3.5), but ovariectomized female SOD1 mice have undetectable levels of sarcosine in their plasma.

Table 3.3.5.2 The effects of ovariectomization on plasma metabolite levels in SOD1 female mice.

Metabolite	SOD1	OVR SOD1	*p* (MANOVA)
NH_3	33 (4)	41 (4)	0.2
Asp	9.15 (0.60)	13.51 (4.57)	0.04
Thr*	189.55 (11.37)	153.59 (10.79)	0.04
Ser	151.72 (6.30)	120.88 (5.90)	0.003
Sarc	37.80 (4.86)	0.00 (0.00)	0.000000
AAAA	11.17 (2.71)	19.59 (1.41)	0.009
Lys*	318.41 (17.80)	249.69 (16.0)	0.01
His*	81.73 (6.61)	62.77 (2.81)	0.009
Pro†	70.32 (19.24)	113.06 (6.48)	0.03

Amino acid levels are expressed as the mean (S.E.M.) in μmoles/L with OVR indicating ovariectomized female mice.
Amino acids highlighted in red are glucogenic and can be converted to glucose and glycogen.
Amino acids highlighted in blue are ketogenic and can be converted to acetoacetyl-CoA and/or acetyl-CoA, while those in purple can be glucogenic or ketogenic.
* indicates essential amino acids.
† indicates conditionally essential amino acids.
n (OVR SOD1) = 11
n (SOD1) = 7

In general, we see a variety of changes take place in SOD1 females upon ovariectomy. The specific activity of glutamine synthetase from both brain and liver is significantly lower, while the specific activity of brain glutaminase is significantly higher, in ovariectomized female SOD1 mice treated with saline. In addition, the specific activity of liver CPSI is slightly lower in these mice. Plasma ammonia levels are not significantly different from those of female SOD1 mice with intact ovaries; however we do see several plasma metabolite differences in ovariectomized female mice. Threonine, serine, sarcosine, lysine, and histidine levels in the plasma are all significantly lower in ovariectomized female SOD1 mice compared to non-ovariectomized female SOD1 mice, while aspartate, proline, and AAAA levels are significantly elevated. Sarcosine is particularly interesting because it is elevated in SOD1 female mice with intact ovaries and MSO treatment significantly lowers plasma levels of this metabolite. In ovariectomized females, sarcosine is undetectable in all of the mice tested.

3.4 Discussion

3.4.1 Glutamine Synthetase Activity in the CNS

The results obtained from glutamine synthetase activity assays performed on wild-type and SOD1 brain and spinal cord homogenates show that there are no genotype-specific differences in GS activity in presymptomatic mice. Untreated, 50 day old mice have brain and spinal cord GS activity levels similar to those of saline-treated 70 day old mice, and all age groups show that brain homogenates have higher levels of GS activity than spinal cord homogenates. This is probably due to a greater density of astrocytes, the primary GS-expressing cell type, in the brain than spinal cord. However, GS activity levels begin to decrease after symptom onset in 110 day old saline-treated mice and SOD1 mice show significantly lower GS activity levels in brain and spinal cord extracts. Studies conducted on ALS mice show that GS expression does not change over the course of the disease and that

enzyme activity is elevated in the lumbar spinal cords of end stage mice (120-150 days of age) (Fray et al 2001). The results obtained from the current study show that GS activity in the whole spinal cord of SOD1 mice is lower than that of wild-type mice. Studies performed on rat primary astrocyte cultures have shown that the cytokine, TNFα, (which has been implicated in ALS (Hensley et al 2003)) can reduce GS expression and inhibit glutamate-induced activation of the enzyme (Zou et al 2010). In mouse models of ALS, TNFα mRNA expression has been shown to increase until the terminal stages of the disease (Elliott 2001) and it is possible that the decrease in GS activity seen in 110 day old saline-treated SOD1 mice may be due to gradually increasing levels of TNFα production over the course of the disease. However, cytokine levels would have to be measured at the same time intervals at which GS activity levels were examined in order to correlate the decrease in GS activity levels to TNFα production.

When gender differences in GS activity levels were examined, presymptomatic mice (50 day untreated and 70 day old saline-treated animals) showed similar levels of GS activity in males and females. However, symptomatic 110 day old saline-treated mice, which showed an overall decrease in GS activity, also showed some gender-specific changes in GS activity. Male SOD1 mice show significantly lower levels of brain GS activity, while female SOD1 mice show significantly lower levels of spinal cord GS activity. Since studies conducted in other laboratories suggested that GS protein levels do not change over the course of the disease in ALS mice (Fray et al 2001), GS expression was not examined. Microarray analysis of estradiol treated mice showed that astrocyte-specific genes, including GS, are increased compared to vehicle-treated controls (Mong & Blutstein 2006). Studies conducted on female rats and mice show that female hormones increase GS expression in specific brain regions (arcuate nucleus, ventromedial nucleus, amygdala, and hippocampus), but these studies did not examine enzyme activity levels (Blutstein et al 2009; Blutstein et al 2006). These results suggest that there could be region-specific differences in GS activity in female ALS mice, but since whole tissue

homogenates (brain and spinal cord) were used to assay enzyme activity, these potential differences were not observed. It is possible that female hormones that lead to increased levels of GS protein expression in certain brain regions, may also lead to a corresponding increases in enzyme activity, leading to the normalized levels of whole brain GS activity observed in SOD1 females. Low serum levels of free testosterone have been implicated in human ALS (Militello et al 2002) and dihydrotestosterone treatment of ALS mice has been shown to increase lifespan and ameliorate motor neuron and muscle degeneration that occurs during the disease (Yoo & Ko 2012). However, studies on the developing rat brain showed that testosterone did not have an impact on GS activity (Patel et al 1983). These studies also showed that female hormones did not affect GS activity in the developing rat brain, suggesting that hormones may play a greater role in the fully developed brain, but no studies examining the effects of testosterone on GS activity could be found. Since ALS targets a subset of neurons, whole brain and spinal cord homogenates may not be the best samples to use in order to examine enzyme activity. In order to better understand potential gender-specific alterations in GS activity levels, enzyme activity and expression levels should be examined in a region-specific manner.

Treatment with a single weekly i.p. injection of 20 mg/kg MSO showed that enzyme activity was significantly decreased by approximately 90% in both brain and spinal cord homogenates from SOD1 mice and their wild-type counterparts. This observation was consistent across age groups and 110 day old mice treated with MSO show the same levels of inhibition as 70 day old mice treated with MSO. When examined for gender-specific changes in GS activity with MSO treatment, male and female (wild-type and SOD1) mice show consistent levels of GS activity. These results suggest that the gender-specific effects of MSO treatment on survival of these mice observed in Chapter 2 are probably not entirely due to MSO's ability to inhibit glutamine synthetase, but may be due to some other effect of the drug.

3.4.2 Glutaminase Activity in the Brain

The results obtained from the brain glutaminase activity assays show that there are no significant differences in enzyme activity between wild-type and SOD1 mice. There are also no clear gender-specific differences in glutaminase activity. Saline-treated male SOD1 mice at 70 days of age show significantly increased glutaminase activity levels when compared to female SOD1 mice of the same age, but these differences are not observed in 50 day old mice or postsymptomatic 110 day old mice. By 110 days of age, glutaminase activity in male SOD1 mice has decreased to levels similar to that of female SOD1 mice. In addition, MSO treatment does not have an impact on glutaminase activity in wild-type or SOD1 mice and there are no gender-specific differences in enzyme activity with treatment. Studies showing that estradiol increases levels of GS protein levels in the female rat arcuate nucleus also show that glutaminase protein levels increase with estradiol treatment (Blutstein et al 2009), but did not examine enzyme activity levels. The results of these experiments do not show any increase in activity in female mice. The lack of an effect of transgene expression as well as a treatment effect on glutaminase activity suggests that glutaminase activity is not affected by mutant SOD1 protein and glutaminase does not play a role in MSO's ability to prolong lifespan in this mouse model.

3.4.3 Plasma Metabolite Analysis

3.4.3.1 Plasma Ammonia Levels

The assays measuring plasma ammonia levels show that untreated 50 day old SOD1 mice have elevated levels of plasma ammonia, suggesting that expression of the mutant transgene alters ammonia metabolism in this mouse model. When gender differences were examined, both male and female 50 day old untreated SOD1 mice show elevated average

plasma ammonia levels but only female ammonia levels reached significance. This elevation in plasma ammonia disappears in 70 day old mice, as saline-treated SOD1 mice have levels of ammonia similar to those of wild-type mice at this age. Plasma ammonia levels in 70 day old saline-treated wild-type and SOD1 mice are also significantly lower than the levels seen in 50 day untreated mice, suggesting that elevations in ammonia in young animals may have something to do with development as mice are just reaching sexual maturity at the 50 day time point. Gender differences in plasma ammonia levels at 50 days of age also disappear in saline-treated 70 day old animals and all genders show similar levels of plasma ammonia.

MSO treatment significantly increases plasma ammonia levels in both wild-type and SOD1 animals. When broken down by gender the same trend is observed in all groups examined, including male wild-type mice which have lower levels of plasma ammonia than any other group, with and without MSO treatment. Elevations in plasma ammonia with MSO treatment were expected since the drug irreversibly inhibits the incorporation of ammonia into glutamine, and therefore prevents it from being transported to the liver as glutamine for proper removal.

3.4.1.2 Plasma Metabolites in 50 Day Untreated Mice

The plasma metabolite profile of 50 day old untreated animals shows that several metabolites differ between wild-type and SOD1 mice. Most of these metabolite differences are due to SOD1 animals having significantly lower levels of various metabolites than wild-type mice. Several of the metabolites that are significantly lower in SOD1 mice are associated with the urea cycle, specifically urea, aspartate, citrulline, and arginine. The fact that urea is significantly lower in plasma collected from 50 day untreated SOD1 mice corresponds to the observation that ammonia levels in these animals are elevated and suggests that ammonia is not being incorporated into urea, implying an underlying defect in the urea cycle. Plasma

glutamine, a precursor of both ammonia and glutamate, is elevated in these mice and could indicate an increase in glutamine uptake from the diet, as glutamine synthetase activity was not elevated in these animals. It is interesting to note that the average plasma levels of glutamate and ornithine, which are also involved in the urea cycle, are also slightly lower in SOD1 mice, but these levels do not reach significance (see Appendix A).

In addition to urea cycle intermediates, several other plasma metabolites are altered in SOD1 mice. Phosphoserine, phosphoethanolamine, cystine, methionine, and lysine are all significantly lower in plasma from SOD1 mice when compared to their wild-type counterparts, while asparagine levels are elevated. Six of the metabolites that are significantly altered (aspartate, asparagine, cystine, methionine, and arginine) are glucogenic amino acids that can be used as a carbon source to produce glucose. Since most of these metabolites are significantly lower in the plasma of SOD1 mice, this could suggest changes in the rate of gluconeogenesis in this model. Hindlimb suspension loading is a common technique used in rats to simulate the weightlessness experienced during space flights (Morey-Holton & Globus 2002). This method induces muscular atrophy, as rats are positioned in such a way that their hindlimbs no longer support their body weight, and recent research has shown that the rate of gluconeogenesis in these rats is elevated in a time-dependent manner (Bederman et al 2012). It is possible that SOD1 mice experience an increase in gluconeogenesis associated with muscle atrophy, leading to an overall reduction in the levels of certain glucogenic amino acids in the plasma. These animals may experience insulin resistance or some other problem utilizing glucose obtained from the diet and may resort to using amino acids as fuel. Both insulin resistance and biomarkers suggestive of insulin resistance have been observed in ALS patients (Gonzalez de Aguilar et al 2005; Pradat et al 2010). ALS mice have been shown to have a significantly lower body mass than their wild-type littermates, decreased plasma levels of leptin and insulin, and increased plasma levels of corticosterone suggestive of global metabolic

defects (Dupuis et al 2004). Data obtained from human ALS studies suggests that hypermetabolism may occur in patients, as a low body-mass is typically observed in patients suffering from the disease (Desport et al 1999; Vaisman et al 2009) and worsens with progression (Desport et al 2000; Kasarskis et al 1996; Wijesekera & Leigh 2009). In addition to low body-mass, ALS patients also show increased levels of energy expenditure (Desport et al 2001; Desport et al 2005; Funalot et al 2009) further supporting the idea of impaired metabolism as a factor in ALS.

One interesting finding from these studies is that SOD1 mice appear to have a cysteine deficiency, as cystine levels were undetectable in all but one 50 day old SOD1 plasma sample. These results have serious implications for oxidative damage during the disease due to impaired glutathione synthesis, as cysteine is one of the three amino acids that make up the antioxidant tripeptide. Oxidative damage has been implicated in the progression of ALS and mutant SOD1 mice deficient in a subunit of γ-glutamylcysteine ligase (the first enzyme in glutathione synthesis catalyzing the condensation of cysteine and glutamate) show a 55% reduction in average lifespan (Vargas et al 2011). Cell culture models of the disease show that motor neurons expressing mutant SOD1 protein under standard culture conditions have significantly lower glutathione levels than those expressing wild-type SOD1 protein (D'Alessandro et al 2011). It is possible that SOD1 mice have decreased glutathione levels due to a lack of cysteine, which could exacerbate oxidative damage in sensitive neuronal cells. Decreased levels of glutathione in SOD1 mice could further exacerbate amino acid uptake by inhibiting the γ-glutamyl cycle, which has been shown to play a role in amino acid uptake in cells of the intestine (Cornell & Meister 1976). Follow up experiments to determine if the undetectable levels of cystine in the plasma of SOD1 mice correlate with decreased levels of glutathione and altered amino acid uptake must be performed.

When plasma metabolite data from 50 day old untreated mice is further broken down and analyzed based on gender, a different plasma metabolite profile emerges. Plasma glutamine levels remain elevated in both male and female SOD1 mice when compared to their wild-type counterparts, but only female SOD1 mice show significantly lower citrulline, arginine, and ornithine levels. Male SOD1 mice, however, show significantly lower plasma levels of aspartate and urea. These gender-specific differences in plasma levels of urea cycle intermediates suggest that the expression of the transgene alters the urea cycle differently depending upon gender. Cysteine levels, which are decreased in SOD1 mice, continue to be significantly lower in these animals when gender is accounted for.

When plasma metabolite data from 50 day old mice are grouped by genotype and gender differences are examined, there are several significant differences between males and females of both genotypes. Wild-type animals show a wider range of gender differences in plasma metabolites, with males showing significantly lower levels of several metabolites when compared to females. These data suggests that there are basic gender differences in metabolism in nontransgenic mice. SOD1 mice, however, show fewer gender differences in plasma metabolites and males show significantly higher levels of the metabolites that differ. It is interesting to note that those metabolites that show gender differences in both wild-type and SOD1 mice tend to be increased in wild-type females but decreased in SOD1 females. For example, threonine levels are significantly higher in female wild-type mice compared to male wild-type mice but are significantly lower in SOD1 female mice. The levels of threonine in male mice of both genotypes are similar, suggesting that the changes observed are due to an overall decrease in female SOD1 mice. A similar pattern is seen in citrulline levels, which are similar in male mice of both genotypes, but lower in female SOD1 mice. Women have been shown to have a lower resting metabolic rate than men (Arciero et al 1993), and as a result one might expect to see slightly higher levels of metabolites in the plasma of female animals compared to

males. However, in this SOD1 mouse model of ALS female mice show lower levels of certain metabolites, that do not differ between male wild-type and SOD1 mice, suggesting higher rates of utilization or impaired uptake of these substances. A list of all average plasma metabolite levels and *p* values and all of the comparisons made of 50 day old untreated mice can be found in Appendix A.

3.4.1.3 Plasma Metabolites in 70 Day Saline-treated Mice

Plasma metabolite levels from 70 day old saline-treated mice were examined to see how metabolite profiles from older mice compared to those obtained from young, untreated mice and to understand how wild-type and SOD1 mice differ. When comparing 70 day old saline-treated wild-type and SOD1 mice, there are fewer differences in plasma metabolites than what was observed in 50 day old mice. Phosphoethanolamine, aspartate, and cystine levels, which are significantly lower in 50 day old SOD1 mice, continue to be low in 70 day old saline-treated SOD1 mice. Cystine is completely undetectable in the plasma of 70 day old SOD1 mice and may indicate that cysteine is not being properly absorbed from the diet, or that it is being utilized faster than it can be absorbed by these mice.

Plasma levels of alanine and proline, which were not significantly different in 50 day old SOD1 mice, are significantly lower and sarcosine (n-methylglycine) levels are significantly higher in SOD1 plasma. High levels of plasma glutamine and alterations in urea cycle intermediates observed in 50 day old untreated mice are no longer seen in 70 day old saline-treated mice and may indicate the existence of compensatory mechanisms that normalize metabolism in these animals. Alanine, however, can act as a carrier of the carbon skeleton of pyruvate and of ammonia from muscle to the liver (Nelson & Cox 2008) and lower levels of alanine in the plasma of SOD1 mice may be an early sign of alterations in muscle metabolism prior to significant atrophy. Sarcosine, which is an intermediate in glycine metabolism, is

significantly higher in SOD1 plasma, with levels exceeding three times that found in wild-type mice. Sarcosine dehydrogenase is a tetrahydrofolate-binding enzyme responsible for the production of glycine from sarcosine found in the matrix of liver mitochondria (Eschenbrenner & Jorns 1999). Defects in this enzyme cause sarcosinemia and are associated with elevated levels of sarcosine in the blood (Eschenbrenner & Jorns 1999). In the CNS sarcosine acts as a natural agonist of glycine transporter 1 which increases the effect of glycine on NMDA receptors and has been shown to have beneficial effects in patients suffering from schizophrenia when added to antipsychotic treatments for the disorder (Tsai et al 2004). There are a variety of factors that may play a role in elevating sarcosine levels in SOD1 mouse plasma. These mice may have a defect in sarcosine dehydrogenase activity due to the expression of mutant SOD1 protein expression or due to a deficiency in folate. Folate deficiencies have been shown to lead to increased levels of sarcosine in humans (Allen et al 1993) and treatment of SOD1 mice with folate has been shown to delay the onset and progression of the disease (Zhang et al 2008).

When plasma metabolites were grouped by gender and compared based on genotype, a different profile is seen in male and female mice, much like with 50 day old mice. Alterations in phosphoethanolamine and sarcosine are specific to female SOD1 mice, while decreases in glycine and alanine levels are specific to male SOD1 mice. Phosphoethanolamine is used to make sphingomyelins, glycolipids involved in the production of membranes (Nelson & Cox 2008). Low levels of phosphoethanolamine in plasma may lead to problems in producing cell membrane material in female SOD1 mice. Male SOD1 mice show low levels of glycine, which acts as a coagonist of NMDA receptors during glutamatergic signaling, and may impair excitatory synaptic signaling. Although it was not determined to be statistically significant by the MANOVA, cystine levels continue to be undetectable in plasma from both male and female SOD1 mice and may contribute to reduced glutathione levels and oxidative damage in ALS mice.

When plasma metabolite data are broken down by genotype and males and females are compared, several gender differences in plasma metabolites can be observed in both wild-type and SOD1 mice. Glutamine and histidine levels are similar in wild-type and SOD1 mice, with females showing significantly higher plasma levels of glutamine. In SOD1 mice, urea levels are significantly higher in male mice, while females show significantly higher levels of all other plasma metabolites. Much like with 50 day old untreated mice, 70 day old saline-treated mice show gender differences in metabolism. However, the alterations in urea cycle intermediates are completely absent, with the exception of urea itself which is elevated in male SOD1 mice. Plasma levels of ammonia in these mice show no gender differences and are actually much lower than what is observed in 50 day old animals. These results suggest that between 50 and 70 days of age, compensatory mechanisms normalize nitrogen metabolism in SOD1 mice. A list of all average plasma metabolite levels and *p* values and all of the comparisons made of 70 day old saline-treated mice can be found in Appendix A.

3.4.1.4 Plasma Metabolites in 70 Day MSO-treated Mice

Wild-type and SOD1 mice began a weekly treatment with either saline or MSO at approximately 50 days of age and plasma was taken at approximately 70 ± 2 days of age, resulting in animals receiving a total of 4 injections. Plasma metabolite levels were grouped by genotype and treatment effects were examined. Wild-type mice show only one significant metabolite alteration with MSO treatment and that is in lysine levels, which increase significantly. This effect is also observed in SOD1 mice treated with MSO. SOD1 mice, however, have similar plasma lysine levels to wild-type mice with and without treatment and this effect of MSO is probably not significant to the disease. SOD1 mice show several other changes in plasma metabolite levels with MSO treatment, despite this one similarity. MSO treatment significantly increases the levels of a variety of metabolites including

phosphoethanolamine, alanine, cystine, ornithine, and arginine. Increased levels of phosphoethanolamine and cystine in the plasma may allow these substances to be more available for use in making membranes and glutathione respectively. It is important to note that previous studies have shown that MSO increases glutathione levels in certain brain regions (Ghoddoussi et al 2010), and this may be due to its ability to increase cysteine levels in the plasma. Although the plasma metabolite profile of saline-treated mice did not suggest urea cycle defects, MSO treatment increases levels of ornithine and arginine, two urea cycle intermediates, and also significantly elevates plasma ammonia levels. Glutamine levels, which were not found to differ in saline-treated SOD1 and wild-type mice, are significantly decreased by MSO treatment in SOD1 mice. Since MSO inhibits the enzyme responsible for the production of glutamine, GS, it is not surprising to see a significant decrease in glutamine levels in mice treated with MSO. Lower levels of glutamine may impair the immune response and reduce neuroinflammation in ALS mice by starving immune cells of glutamine. Alanine levels, which were found to be significantly lower in saline-treated SOD1 mice, are increased with MSO treatment and may indicate a normalization of the alanine-glucose cycle.

When 70 day plasma metabolite data are broken down by gender and analyzed by treatment, a variety of metabolite changes appear to be gender-specific. Female wild-type mice show no significant alterations in plasma metabolite levels with MSO treatment, while female SOD1 mice show decreases in plasma glutamine and sarcosine and increases in plasma arginine levels. All plasma metabolites that are altered with MSO treatment in male wild-type mice increase upon treatment. A similar pattern is observed in male SOD1 mice, but the metabolites that increase differ from those that increase in wild-type males. Although it is not clear how all of these treatment-related changes in plasma metabolites impact the disease, it is a start to understanding how MSO treatment extends the lifespan of ALS mice. Since many of these metabolites show gender-specific alterations and MSO treatment alters plasma

metabolites in a gender-specific fashion, it is possible that sex hormones may modulate metabolic pathways affected by the drug therefore producing gender-specific effects in survival and neuromuscular function.

Human and animal studies of circulating metabolite levels associated with ALS have been conducted however these studies have not been done in a consistent manner and have produced widely conflicting data. Cerebrospinal fluid (CSF), which circulates through the CNS, may provide more information about metabolite changes due to neuroinflammation and neurodegeneration in diseases of the CNS. CSF is difficult to obtain from animals and studies of CSF from ALS patients have not provided the best data, as often times controls used in these studies are patients with neurological disorders due to the difficulty of obtaining CSF from healthy controls (Blin et al 1994; Iijima et al 1978; Patten et al 1978). As a result, better information can be obtained from blood samples, which are easier to obtain from healthy controls. However, many of the studies analyzing plasma or serum also use samples from controls with other diseases. In a study which detected elevated levels of ornithine in the serum of ALS patients, some of the controls used suffered from neuropathy and multiple sclerosis (Patten et al 1978), diseases which are believed to have underlying mechanisms similar to those thought to play a role in ALS. In another study in which plasma samples were examined, patients were not clearly classified as having ALS (Iijima et al 1978) and may have had other motor neuron diseases. In addition to issues with experimental design many studies of ALS patients include both genders, which are matched in control groups, but fail to examine gender differences in the disease. As a result, most biochemical data collected on ALS patients comes from ambiguous groups composed of both males and females and underlying gender differences remain unclear.

The data presented here show that there are clear differences in plasma metabolites in presymptomatic SOD1 mice when compared to their wild-type counterparts, suggesting that

early metabolic defects (in 50 day old mice) play a role in, or are related to neurodegeneration in this mouse model. Some of the differences seen in plasma metabolites are gender-specific and only appear when comparing wild-type and SOD1 mice by gender, suggesting that expression of the transgene alters metabolism differently in male and female mice. In addition, there are several metabolites that differ between male and female SOD1 mice, providing further evidence of gender-specific metabolic effects of mutant SOD1 expression. There are also age-related changes in plasma metabolites that indicate there may be some ability to compensate for metabolic defects, at least in presymptomatic mice. In order to fully understand metabolic abnormalities associated with the disease, these experiments should also be performed in mice at the time of symptom onset, as well as in postsymptomatic animals. MSO's ability to reverse some of the changes in plasma metabolites in a gender-specific manner further supports the idea that metabolic defects are involved in the disease progression and that gender is also an important factor in the disease.

Several studies conducted with ALS patients provide evidence of metabolic defects in the human disease, but it is unknown as to whether these defects are a direct result of the disease itself or are present prior to development of the disease. Most studies conducted on animal models of ALS focus on the central nervous system and there are only a few studies available in which metabolism has been the primary focus. However, those studies that have focused on metabolism in mouse models of ALS support the idea of metabolic defects playing a role in the disease. It is important to note that gender is typically not discussed in studies of ALS patients and mice, even though both genders have been studied. Most articles published make note that patients and mice have been age and gender-matched, but data are not broken down by gender resulting in a missing piece in the puzzle.

3.4.1.5 Nitrogen Metabolism in the Liver

Carbamoyl phosphate synthetase I (CPSI) activity was measured in desalted liver homogenates from both wild-type and SOD1 mice. At 50 days of age, CPSI activity in SOD1 mice does not differ significantly from that of wild-type mice, even though plasma metabolite analysis shows that SOD1 mice have slightly lower levels of plasma urea and significantly higher levels of plasma ammonia. CPSI is the rate-limiting enzyme in the urea cycle, but the decrease in plasma levels of urea cycle intermediates and the finding that CPSI activity is not affected by the SOD1 transgene suggests that there may be a problem with one of the other enzymes in the cycle. Decreased citrulline levels could indicate a problem with ornithine transcarbamoylase, while decreased levels of arginine could indicate a decrease in activity of arginosuccinate synthetase or arginosuccinate lyase. Although it was not determined to be significant, ornithine levels are also slightly lower in these mice and could be an indicator of decreased arginase activity.

When liver CPSI activity data are broken down by gender, 50 day old untreated females of both genotypes have significantly higher activity levels than males. These results suggest that in 50 day old mice, gender is a more important factor in determining CPSI activity than transgene expression. Since CPSI is the rate-determining enzyme in the urea cycle, low activity is expected to correlate with low levels of urea and elevated levels of other intermediates that are not being consumed in the cycle but this trend is not observed in these mice. Only wild-type mice show a gender difference in plasma urea levels, with males having higher urea levels than females. In addition, wild-type females show elevated levels of citrulline compared to males which would not be expected if the overall rate of the cycle is comparable to that of CPSI which is high in females. SOD1 females, however, show decreased levels of ornithine and citrulline compared to their male counterparts which would correlate with a higher rate of the urea cycle.

More work needs to be done to fully characterize potential urea cycle defects and the role of gender in neurodegeneration in this mouse model.

CPSI activity levels are significantly increased in 70 day old saline-treated mice compared to 50 day old untreated mice of both genotypes, suggesting age-related changes in activity occur. This corresponds to an overall decrease in plasma ammonia levels that are seen in both wild-type and SOD1 mice treated with saline at 70 days of age. Mice in this age group also no longer show significant alterations in plasma metabolites associated with the urea cycle. Males of both genotypes continue to show significantly lower levels of CPSI activity in 70 day old saline-treated mice; however it is at this point that SOD1 males start to show alterations in CPSI activity. Saline-treated 70 day old male SOD1 mice not only have lower activity than female SOD1 mice, but also show significantly lower CPSI activity than their wild-type counterparts. The changes in plasma metabolite levels in 70 day old saline-treated male SOD1 mice do not correlate well with the changes in CPSI activity. In order to better understand if these changes are disease-related, CPSI activity levels at later time points in postsymptomatic or end stage animals should be examined.

It is possible that CPSI activity differences result from gender differences in allosteric regulation of the enzyme. N-acetyl-L glutamate is an allosteric activator of the enzyme (Nelson & Cox 2008) but a consistent amount of this activator was added to the reaction mixture and should not cause gender-specific differences in activity levels, suggesting the presence of another regulator of the enzyme. Purine nucleotides, ornithine, and increased levels of ammonia have been found to activate CPSI, while pyrimidine nucleotides and decreased ATP levels have been found to inhibit the enzyme (Meister 1989). It could be that other gender-specific cycles that feed into the urea cycle are affected. MSO treatment has no effect on CPSI activity levels, despite its ability to significantly increase plasma ammonia, ornithine, and arginine levels. In addition, CPSI activity in the presence of MSO is unaffected by gender and

expression of the transgene. MSO's ability to extend the lifespan may be through its effects on plasma metabolite levels, but it does not affect the urea cycle.

Liver glutamine synthetase activity levels were examined using the same samples that were used to assay CPSI activity. The results of these assays in 50 day old untreated mice are similar to those of brain GS activity, showing no differences between wild-type and SOD1 mice. When broken down by gender, GS activity remains at about the same level across gender and genotype. In 70 day old saline-treated mice, there are still no differences in GS activity between wild-type and SOD1 mice, however there appear to be changes in GS activity in SOD1 male mice. When the data are broken down by gender, male SOD1 mice show significantly lower activity than female SOD1 mice and male wild-type mice, similar to the results of CPSI activity assays in these mice. This suggests that nitrogen metabolism in the liver of male SOD1 mice may start to decline prior to symptom onset. MSO treatment significantly decreases GS activity in both wild-type and SOD1 mice and continues to significantly decrease GS activity when these groups are further broken down by gender. However, MSO does not inhibit GS in male SOD1 mice to the same extent as the rest of the groups. MSO inhibits liver GS activity by about 85% in all groups, except male SOD1 mice where it only inhibits GS activity by about 55%. This further supports the idea that liver metabolism undergoes changes in presymptomatic male SOD1 mice and may partially explain why male SOD1 mice have a shorter lifespan than female SOD1 mice, as well as MSO's reduced effect on increasing lifespan and neuromuscular function in these mice.

Since ALS is a neurodegenerative disease and motor neurons are the primary target, most research conducted in animal and human studies revolves around the central nervous system. As a result, there are few studies that actually focus on global metabolism in animal models of the disease. In studying transgenic animal models of disease, especially those that ubiquitously express (or overexpress) a transgene throughout the body, it is important to not

only study the major organ(s) affected but to also study organs outside of the target system. This allows researchers to better understand the disease model and potential effects that can occur in other organs upon expression of a transgene. It also provides researchers with the ability to understand shortcomings of the model that may confound the results of studies conducted on therapeutic interventions, as expression of transgenes that alter metabolism may also impact the pharmacology of a drug. This being said, it is also important to consider gender in these studies as sex hormones have the ability to alter the expression of a wide range of genes and may also impact drug metabolism.

3.4.1.6 The Effects of Ovariectomization on Enzyme Activity and Plasma Metabolites

As shown in Chapter 2, removal of sex hormones in female mice through ovariectomy, removes the MSO effect on survival. Ovariectomized SOD1 female mice treated with saline have significantly lower levels of brain GS activity with a corresponding increase in brain glutaminase activity. In addition to these changes in the CNS, ovariectomized SOD1 females also exhibit significantly lower levels of liver glutamine synthetase activity and lower CPSI activity levels. These results suggest that estrogen has the ability to influence nitrogen metabolism and that removing the ovaries, and subsequently estrogen, lowers activities of several enzymes involved in nitrogen metabolism.

In addition to showing altered activity levels of enzymes involved in nitrogen metabolism, ovariectomized female mice treated with saline have a different metabolic profile than their normal female counterparts. Although the results are not considered to be significant, plasma ammonia levels in ovariectomized SOD1 females are lower than those in SOD1 females with intact ovaries. There are also no significant alterations in urea cycle intermediates in ovariectomized females in this age, which agrees with results obtained from other 70 day old SOD1 mice. It is interesting to note that sarcosine levels, which are significantly increased in

SOD1 females with intact ovaries and are lowered with MSO treatment, are completely undetectable in ovariectomized mice. This suggests that changes in sarcosine levels in female SOD1 mice may be part of the disease process and enzymes involved in sarcosine production and breakdown should be examined in order to better understand its role in disease.

3.5 Future Experiments

The results of these biochemical studies show that the expression of the SOD1 transgene impacts plasma metabolite levels in this mouse model, but does not have much of an impact on the nitrogen handling enzymes examined. Young presymptomatic SOD1 mice appear to have defects in nitrogen metabolism that are no longer observed in 70 day old mice, suggesting that there are age related changes in metabolism of these mice. Gender also plays a role in altering plasma metabolites and estrogen impacts nitrogen metabolizing enzymes as well as plasma metabolites. It is not clear how MSO's impact on plasma metabolites and glutamine synthetase activity lead to an increase in lifespan in SOD1 mice, but estrogen appears to facilitate its ability to extend the lifespan and suggests that MSO impacts estrogen-sensitive pathways.

GS and glutaminase data from older postsymptomatic mice aid in our understanding of defective glutamine metabolism and treatment effects in this disease model, showing that brain and spinal cord GS activity levels begin to decline later in the disease. While glutaminase activity does not seem to be important, gender-specific age-related decreases in GS activity may be important. Males show decreased activity in brain, while females show decreased activity in spinal cord and these results may be important in explaining why females are able to maintain grip strength with MSO treatment. Presymptomatic male SOD1 mice also show slight alterations in liver GS (and CPSI) activity that may indicate the beginning of disease associated metabolic perturbations. MSO is able to decrease the glutamine-glutamate cycle, leading to

decreased glutamine and glutamate levels in specific brain regions (Ghoddoussi et al 2010), and may further decrease levels of these chemicals in the spinal cords of female mice and allow them to maintain neuromuscular connections. NMR examination of gender differences in spinal cord chemicals must be done to understand if this may be part of MSO's gender-specificity.

While we have data from the CNS of wild-type and SOD1 mice profiling the course of the disease and treatment, we do not have liver enzyme and plasma metabolite data from older mice and are missing part of the story. Since there are age-related changes in plasma ammonia and other metabolites, as well as CPSI activity and liver GS activity in SOD1 males, these metabolite levels and enzyme activities could further change as the disease progresses. For this reason, plasma metabolite profiles and liver enzyme activities should be examined in these animals at later time points. It is possible that male metabolism declines faster than that of females and plays a role in MSO's gender-specific effects on survival. In addition, obtaining these data from MSO-treated mice would provide more information about long-term effects of treatment. Since muscle has been targeted as a major source of glutamine and undergoes atrophy as the disease progresses, further studies should consider potential defects in muscle metabolism as well.

Most of the research on MSO has focused on its ability to inhibit glutamine synthetase, but other targets of the drug have been identified, such as alanine aminotransferase (Pace & McDermott 1952), ornithine decarboxylase (Di Giacomo et al 1997), and γ-glutamylcysteine synthetase (Richman et al 1973). In order to understand exactly how this drug works in ALS mice, these targets should be further characterized. Further characterization of γ-glutamylcysteine synthetase is particularly important, as MSO has been shown to inhibit this enzyme which catalyzes the first step in glutathione synthesis (Richman et al 1973) and our early data shows that MSO treatment increases glutathione levels in specific brain regions (Ghoddoussi et al 2010). Increasing glutathione levels in ALS is important to prevent oxidative

damage, but this conflicting data about MSO's ability to inhibit glutathione synthesis warrants further examination.

MSO has been found to alter cytokine levels in a mouse model of acute liver failure (Jambekar et al 2011) and since some immune cells have been shown to lack GS (Ardawi & Newsholme 1983; Rohde et al 1996), there may be other potential targets of MSO that have yet to be identified. Since neuroinflammation has been implicated to play a significant role in the progression of ALS and peripheral immune cells (which require glutamine) have been found to infiltrate the CNS, these cell types should be characterized to understand how MSO affects the immune response in these mice. Basic gender differences in general immune responses have been characterized and MSO's impact on these cells may explain its gender-specific effects in ALS mice.

There is a need to continue ALS research to better understand how motor neurons are selectively killed, identify biomarkers of the disease for early detection, and to discover better treatments capable of improving the quality of life of patients. These studies have shown that MSO has the ability to extend the lifespan and alter plasma metabolites in the most common mouse model of ALS in a gender-specific manner. Most research on MSO revolves around its ability to inhibit GS, but it is apparent that its effects in the SOD1 G93A mouse model may extend beyond its inhibitory effects on GS to other potential targets. In order to make the most of MSO as a tool for elucidating mechanisms of ALS and other diseases, these other targets must be identified and better characterized.

APPENDIX A

50 DAY PLASMA METABOLITE COMPARISONS

Table A-1: List of all mean 50 day mouse plasma metabolite values grouped by genotype and the corresponding *p* values obtained from the MANOVA.

	WT		SOD1		
Metabolite	**Mean**	**SEM**	**Mean**	**SEM**	***p* (MANOVA)**
Phser	14.43	0.84	6.76	1.24	.000009
Taur	464.48	33.18	429.15	36.75	.488474
Pea	11.55	1.27	5.57	2.00	.012771
Urea	9866.08	358.87	8088.85	696.89	.019385
Asp	18.03	1.51	11.32	0.87	.001851
Thr	182.68	8.27	161.74	12.57	.156457
Ser	150.80	5.09	140.31	7.29	.232226
Asn	38.98	2.09	47.83	4.03	.041775
Glu	35.32	4.40	26.26	2.56	.125255
Gln	560.08	13.21	676.66	37.19	.002029
Sarc	11.91	4.42	11.81	5.27	.988485
AAAA	25.83	3.16	21.44	3.73	.378244
Gly	298.53	7.31	285.10	12.89	.338465
Ala	577.76	23.95	672.69	66.76	.136491
Citr	109.36	4.91	87.14	5.46	.005742
Val	247.16	7.71	237.57	22.61	.648060
Cys	27.91	2.39	0.36	0.36	.000000
Met	87.38	5.84	65.47	7.01	.022942
Ile	87.20	3.50	94.00	5.91	.300051
Leu	144.72	5.12	153.71	11.28	.426790
Tyr	71.96	3.57	72.78	5.19	.893887
Phe	60.28	1.63	64.96	3.13	.158838
Orn	92.02	6.90	72.35	8.80	.085838
Lys	319.96	12.69	273.63	16.00	.029437
1-Mhis	11.18	1.16	11.65	1.17	.787789
His	70.48	2.22	62.56	3.61	.057402
Trp	59.16	5.74	53.49	9.04	.581522
Arg	122.45	8.41	86.84	7.51	.005630
Hypro	14.10	3.45	23.98	3.68	.065295
Pro	89.27	3.96	105.51	10.73	.116248

Amino acid levels are expressed as μmoles/L plasma.

Table A-2: List of all mean 50 day female plasma metabolite values grouped by genotype and the corresponding *p* values obtained from the MANOVA.

	WT Female		SOD1 Female		
Metabolite	**Mean**	**SEM**	**Mean**	**SEM**	***p* (MANOVA)**
Phser	14.45	1.47	8.66	1.54	.020751
Taur	420.15	21.83	479.74	66.56	.337043
Pea	12.14	1.07	9.30	3.32	.356879
Urea	8,708.96	354.88	8,055.03	450.50	.271216
Asp	15.04	2.19	11.45	1.42	.245272
Thr	203.07	10.99	131.50	16.26	.002222
Ser	163.93	7.19	135.88	13.60	.067672
Asn	42.67	3.37	41.08	5.71	.802155
Glu	30.56	3.83	26.12	5.18	.493090
Gln	568.60	16.63	709.78	74.95	.044414
Sarc	16.02	7.16	11.19	7.43	.659119
AAAA	23.28	4.64	19.01	6.10	.581708
Gly	290.37	12.12	258.21	22.06	.188813
Ala	627.88	40.72	577.55	137.36	.684298
Citr	119.86	8.34	72.97	7.40	.001715
Val	247.54	12.37	214.08	18.73	.142795
Cys	23.32	3.73	0.77	0.77	.000329
Met	97.45	10.56	47.63	6.17	.003493
Ile	94.29	5.54	89.33	8.10	.608021
Leu	152.39	8.36	151.51	14.46	.955598
Tyr	79.45	5.61	62.43	7.85	.092612
Phe	62.73	2.19	61.23	5.40	.773206
Orn	99.00	8.66	53.06	8.53	.003171
Lys	356.96	17.17	255.59	24.42	.003866
1-Mhis	11.30	1.50	12.05	2.15	.771866
His	75.38	2.87	66.22	6.47	.168983
Trp	76.56	3.39	62.68	13.67	.257627
Arg	138.40	13.63	76.58	11.60	.006908
Hypro	9.57	4.81	18.79	6.91	.278058
Pro	94.27	6.91	77.27	10.86	.187351

Amino acid levels are expressed as μmoles/L plasma.

Table A-3: List of all mean 50 day male plasma metabolite values grouped by genotype and the corresponding *p* values obtained from the MANOVA.

	WT Male		SOD1 Male		
Metabolite	**Mean**	**SEM**	**Mean**	**SEM**	***p* (MANOVA)**
Phser	14.40	0.96	5.13	1.75	.000158
Taur	504.37	58.56	385.80	34.25	.140181
Pea	11.02	2.28	2.37	1.82	.014574
Urea	10907.49	366.39	8117.83	1287.87	.028406
Asp	20.73	1.76	11.20	1.15	.000977
Thr	164.34	9.19	187.67	12.48	.143889
Ser	138.98	4.92	144.10	7.75	.566131
Asn	35.65	2.21	53.62	4.98	.002285
Glu	39.61	7.59	26.38	2.28	.177657
Gln	552.41	20.70	648.27	28.90	.014115
Sarc	8.21	5.47	12.33	7.97	.664111
AAAA	28.13	4.42	23.51	4.85	.499483
Gly	305.88	8.56	308.14	8.79	.860338
Ala	532.65	19.39	754.24	26.03	.000004
Citr	99.90	3.88	99.29	4.30	.919093
Val	246.82	10.17	257.71	38.76	.754715
Cys	32.04	2.58	0.00	0.00	.000000
Met	78.31	4.62	80.77	8.41	.786531
Ile	80.82	3.51	98.01	8.78	.058409
Leu	137.81	5.72	155.59	17.94	.293354
Tyr	65.22	3.55	81.65	5.26	.016576
Phe	58.07	2.25	68.15	3.44	.021428
Orn	85.73	10.57	88.89	11.71	.846077
Lys	286.65	10.76	289.10	20.95	.911321
1-Mhis	11.08	1.82	11.30	1.31	.929296
His	66.08	2.76	59.43	3.85	.169528
Trp	43.50	7.64	45.61	12.15	.879071
Arg	108.09	8.47	95.65	9.25	.344685
Hypro	18.17	4.78	28.43	2.98	.122502
Pro	84.78	4.10	129.72	11.49	.000764

Amino acid levels are expressed as μmoles/L plasma.

Table A-4: List of all mean 50 day wild-type mouse plasma metabolite values grouped by gender and the corresponding *p* values obtained from the MANOVA.

	WT Female		WT Male		
Metabolite	**Mean**	**SEM**	**Mean**	**SEM**	***p* (MANOVA)**
Phser	14.45	1.47	14.40	0.96	.977777
Taur	420.15	21.83	504.37	58.56	.214180
Pea	12.14	1.07	11.02	2.28	.671958
Urea	8708.96	354.88	10907.49	366.39	.000496
Asp	15.04	2.19	20.73	1.76	.056956
Thr	203.07	10.99	164.34	9.19	.014481
Ser	163.93	7.19	138.98	4.92	.009668
Asn	42.67	3.37	35.65	2.21	.093654
Glu	30.56	3.83	39.61	7.59	.318440
Gln	568.60	16.63	552.41	20.70	.555787
Sarc	16.02	7.16	8.21	5.47	.392743
AAAA	23.28	4.64	28.13	4.42	.459507
Gly	290.37	12.12	305.88	8.56	.302800
Ala	627.88	40.72	532.65	19.39	.043338
Citr	119.86	8.34	99.90	3.88	.038316
Val	247.54	12.37	246.82	10.17	.963949
Cys	23.32	3.73	32.04	2.58	.067127
Met	97.45	10.56	78.31	4.62	.103217
Ile	94.29	5.54	80.82	3.51	.051072
Leu	152.39	8.36	137.81	5.72	.161014
Tyr	79.45	5.61	65.22	3.55	.042666
Phe	62.73	2.19	58.07	2.25	.157474
Orn	99.00	8.66	85.73	10.57	.351418
Lys	356.96	17.17	286.65	10.76	.002484
1-Mhis	11.30	1.50	11.08	1.82	.929766
His	75.38	2.87	66.08	2.76	.032326
Trp	76.56	3.39	43.50	7.64	.001420
Arg	138.40	13.63	108.09	8.47	.070387
Hypro	9.57	4.81	18.17	4.78	.223317
Pro	94.27	6.91	84.78	4.10	.242627

Amino acid levels are expressed as μmoles/L plasma.

Table A-5: List of all mean 50 day SOD1 mouse plasma metabolite values grouped by gender and the corresponding *p* values obtained from the MANOVA.

	SOD1 Female		SOD1 Male		
Metabolite	**Mean**	**SEM**	**Mean**	**SEM**	***p* (MANOVA)**
Phser	8.66	1.54	5.13	1.75	.165966
Taur	479.74	66.56	385.80	34.25	.216216
Pea	9.30	3.32	2.37	1.82	.082722
Urea	8055.03	450.50	8117.83	1287.87	.966461
Asp	11.45	1.42	11.20	1.15	.891300
Thr	131.50	16.26	187.67	12.48	.017791
Ser	135.88	13.60	144.10	7.75	.596319
Asn	41.08	5.71	53.62	4.98	.124567
Glu	26.12	5.18	26.38	2.28	.961401
Gln	709.78	74.95	648.27	28.90	.433670
Sarc	11.19	7.43	12.33	7.97	.919352
AAAA	19.01	6.10	23.51	4.85	.570300
Gly	258.21	22.06	308.14	8.79	.047675
Ala	577.55	137.36	754.24	26.03	.199172
Citr	72.97	7.40	99.29	4.30	.008607
Val	214.08	18.73	257.71	38.76	.358363
Cys	0.77	0.77	0.00	0.00	.299690
Met	47.63	6.17	80.77	8.41	.010443
Ile	89.33	8.10	98.01	8.78	.488275
Leu	151.51	14.46	155.59	17.94	.865850
Tyr	62.43	7.85	81.65	5.26	.060810
Phe	61.23	5.40	68.15	3.44	.288759
Orn	53.06	8.53	88.89	11.71	.035433
Lys	255.59	24.42	289.10	20.95	.316951
1-Mhis	12.05	2.15	11.30	1.31	.765144
His	66.22	6.47	59.43	3.85	.370413
Trp	62.68	13.67	45.61	12.15	.369072
Arg	76.58	11.60	95.65	9.25	.219672
Hypro	18.79	6.91	28.43	2.98	.203275
Pro	77.27	10.86	129.72	11.49	.007326

Amino acid levels are expressed as μmoles/L plasma.

APPENDIX B

70 DAY SALINE TREATMENT PLASMA METABOLITE COMPARISONS

Table B-1: List of all mean 70 day saline-treated mouse plasma metabolite values grouped by genotype and the corresponding *p* values obtained from the MANOVA.

	WT		SOD1		
Metabolite	**Mean**	**SEM**	**Mean**	**SEM**	***p* (MANOVA)**
Phser	9.61	2.69	6.09	0.97	.203497
Taur	328.23	19.93	320.02	26.23	.810515
Pea	6.11	1.74	1.12	0.61	.008322
Urea	10638.12	460.47	10526.52	433.47	.861584
Asp	13.06	1.38	9.15	0.35	.006977
Thr	200.01	16.49	183.01	7.90	.339951
Ser	162.33	10.15	144.39	5.37	.116629
Asn	50.48	5.41	42.92	2.77	.206180
Glu	14.89	3.65	10.31	3.19	.352352
Gln	585.30	27.18	593.91	23.94	.813428
Sarc	9.33	5.38	32.38	5.12	.004920
AAAA	14.70	2.83	10.63	1.37	.188492
Gly	314.52	11.57	282.61	19.13	.183576
Ala	720.05	52.53	593.61	32.61	.045629
Citr	91.99	6.94	80.81	3.63	.150177
Val	311.94	24.77	266.01	16.11	.123330
Cys	13.34	5.45	0.00	0.00	.013968
Met	98.30	12.32	82.12	6.89	.245710
Ile	109.92	9.01	97.40	5.14	.222863
Leu	186.02	15.46	163.87	8.36	.202357
Tyr	81.54	5.93	73.24	5.06	.293833
Phe	73.09	4.88	66.56	2.21	.213174
Orn	87.76	11.50	73.53	5.88	.261826
Lys	290.03	18.13	280.22	18.74	.712566
1-Mhis	12.58	1.16	10.91	1.35	.366192
His	74.71	2.89	72.94	4.16	.738541
Trp	63.11	5.69	57.25	8.15	.573419
Arg	108.90	8.30	100.60	7.59	.467178
Hypro	25.60	6.92	21.00	4.25	.564548
Pro	116.87	10.32	75.54	11.55	.014711

Amino acid levels are expressed as μmoles/L plasma.

Table B-2: List of all mean 70 day saline-treated female plasma metabolite values grouped by genotype and the corresponding *p* values obtained from the MANOVA.

	WT Female		SOD1 Female		
Metabolite	**Mean**	**SEM**	**Mean**	**SEM**	***p* (MANOVA)**
Phser	12.69	5.17	5.51	1.32	.176331
Taur	374.83	20.66	348.69	37.23	.570488
Pea	11.21	1.40	1.61	1.06	.000168
Urea	10150.32	674.15	9447.01	548.05	.430534
Asp	13.26	2.35	9.15	0.60	.095743
Thr	204.22	30.26	189.55	11.37	.639083
Ser	173.98	18.82	151.72	6.30	.256377
Asn	56.77	9.42	47.09	3.20	.321511
Glu	21.43	5.23	9.55	3.73	.085281
Gln	638.99	34.74	646.85	25.91	.856985
Sarc	8.90	5.65	37.80	4.86	.002455
AAAA	16.12	5.42	11.17	2.71	.410276
Gly	303.57	18.83	283.98	39.44	.679888
Ala	766.50	102.31	665.88	31.81	.336704
Citr	94.21	13.68	84.35	5.54	.494238
Val	334.47	41.53	256.47	18.31	.097265
Cys	12.43	7.87	0.00	0.00	.113579
Met	109.82	18.49	85.19	12.46	.280868
Ile	123.89	14.72	102.74	5.14	.176130
Leu	210.02	25.28	170.36	9.44	.146637
Tyr	84.11	10.23	82.94	6.18	.921283
Phe	79.47	8.04	71.48	2.11	.323679
Orn	104.78	18.71	74.15	7.35	.134400
Lys	317.58	32.62	318.41	17.80	.981690
1-Mhis	15.07	1.41	12.13	1.58	.198615
His	81.79	3.31	81.73	6.61	.994224
Trp	76.07	7.38	71.92	12.69	.792300
Arg	119.42	14.41	114.79	8.33	.777886
Hypro	18.35	8.31	13.98	5.14	.653207
Pro	121.12	20.34	70.32	19.24	.097402

Amino acid levels are expressed as μmoles/L plasma.

Table B-3: List of all mean 70 day saline-treated male plasma metabolite values grouped by genotype and the corresponding *p* values obtained from the MANOVA.

	WT Male		SOD1 Male		
Metabolite	**Mean**	**SEM**	**Mean**	**SEM**	***p* (MANOVA)**
Phser	6.53	1.14	6.66	1.50	.950618
Taur	281.63	21.25	291.36	36.36	.829347
Pea	1.02	1.02	0.63	0.63	.742623
Urea	11125.92	619.10	11606.02	354.13	.499072
Asp	12.86	1.68	9.14	0.41	.040910
Thr	195.79	16.55	176.47	11.26	.343616
Ser	150.69	6.72	137.06	8.20	.234856
Asn	44.20	4.91	38.76	4.14	.411383
Glu	8.34	3.75	11.07	5.48	.699702
Gln	531.61	29.86	540.98	29.63	.828905
Sarc	9.77	9.77	26.97	8.95	.220481
AAAA	13.29	2.27	10.10	0.84	.189239
Gly	325.48	13.66	281.24	5.40	.008551
Ala	673.60	28.49	521.33	43.07	.016112
Citr	89.76	4.80	77.27	4.71	.091535
Val	289.40	27.79	275.55	27.55	.731536
Cys	14.25	8.28	0.00	0.00	.087854
Met	86.78	16.53	79.05	6.87	.656922
Ile	95.95	7.91	92.07	8.86	.753571
Leu	162.02	13.50	157.39	14.14	.818810
Tyr	78.98	6.87	63.54	6.43	.129326
Phe	66.70	4.90	61.65	2.94	.379318
Orn	70.73	10.78	72.91	9.78	.883197
Lys	262.49	8.92	242.03	26.80	.513198
1-Mhis	10.09	1.22	9.68	2.23	.880259
His	67.63	2.41	64.16	2.34	.324544
Trp	50.16	4.57	42.58	7.40	.421331
Arg	98.38	7.17	86.41	10.63	.387605
Hypro	32.85	10.99	28.02	5.96	.694851
Pro	112.63	6.91	80.76	14.11	.081212

Amino acid levels are expressed as μmoles/L plasma.

Table B-4: List of all mean 70 day saline-treated wild-type mouse plasma metabolite values grouped by gender and the corresponding *p* values obtained from the MANOVA.

	WT Female		WT Male		
Metabolite	**Mean**	**SEM**	**Mean**	**SEM**	***p* (MANOVA)**
Phser	12.69	5.17	6.53	1.14	.272281
Taur	374.83	20.66	281.63	21.25	.010420
Pea	11.21	1.40	1.02	1.02	.000153
Urea	10150.32	674.15	11125.92	619.10	.311531
Asp	13.26	2.35	12.86	1.68	.892935
Thr	204.22	30.26	195.79	16.55	.811674
Ser	173.98	18.82	150.69	6.72	.270784
Asn	56.77	9.42	44.20	4.91	.263843
Glu	21.43	5.23	8.34	3.75	.069329
Gln	638.99	34.74	531.61	29.86	.041048
Sarc	8.90	5.65	9.77	9.77	.939669
AAAA	16.12	5.42	13.29	2.27	.640832
Gly	303.57	18.83	325.48	13.66	.368476
Ala	766.50	102.31	673.60	28.49	.402286
Citr	94.21	13.68	89.76	4.80	.765163
Val	334.47	41.53	289.40	27.79	.388342
Cys	12.43	7.87	14.25	8.28	.876291
Met	109.82	18.49	86.78	16.53	.374679
Ile	123.89	14.72	95.95	7.91	.125514
Leu	210.02	25.28	162.02	13.50	.124917
Tyr	84.11	10.23	78.98	6.87	.686404
Phe	79.47	8.04	66.70	4.90	.205039
Orn	104.78	18.71	70.73	10.78	.145856
Lys	317.58	32.62	262.49	8.92	.134341
1-Mhis	15.07	1.41	10.09	1.22	.023584
His	81.79	3.31	67.63	2.41	.006124
Trp	76.07	7.38	50.16	4.57	.013659
Arg	119.42	14.41	98.38	7.17	.220204
Hypro	18.35	8.31	32.85	10.99	.317249
Pro	121.12	20.34	112.63	6.91	.700712

Amino acid levels are expressed as μmoles/L plasma.

Table B-5: List of all mean 70 day saline-treated SOD1 mouse plasma metabolite values grouped by gender and the corresponding *p* values obtained from the MANOVA.

	SOD1 Female		SOD1 Male		
Metabolite	**Mean**	**SEM**	**Mean**	**SEM**	***p* (MANOVA)**
Phser	5.51	1.32	6.66	1.50	.578220
Taur	348.69	37.23	291.36	36.36	.292147
Pea	1.61	1.06	0.63	0.63	.442753
Urea	9447.01	548.05	11606.02	354.13	.006238
Asp	9.15	0.60	9.14	0.41	.988134
Thr	189.55	11.37	176.47	11.26	.429462
Ser	151.72	6.30	137.06	8.20	.181758
Asn	47.09	3.20	38.76	4.14	.136933
Glu	9.55	3.73	11.07	5.48	.822609
Gln	646.85	25.91	540.98	29.63	.019677
Sarc	37.80	4.86	26.97	8.95	.308812
AAAA	11.17	2.71	10.10	0.84	.714570
Gly	283.98	39.44	281.24	5.40	.946299
Ala	665.88	31.81	521.33	43.07	.019310
Citr	84.35	5.54	77.27	4.71	.349278
Val	256.47	18.31	275.55	27.55	.574656
Cys	0.00	0.00	0.00	0.00	
Met	85.19	12.46	79.05	6.87	.673958
Ile	102.74	5.14	92.07	8.86	.318172
Leu	170.36	9.44	157.39	14.14	.460239
Tyr	82.94	6.18	63.54	6.43	.050202
Phe	71.48	2.11	61.65	2.94	.018749
Orn	74.15	7.35	72.91	9.78	.921026
Lys	318.41	17.80	242.03	26.80	.035161
1-Mhis	12.13	1.58	9.68	2.23	.387300
His	81.73	6.61	64.16	2.34	.027537
Trp	71.92	12.69	42.58	7.40	.068969
Arg	114.79	8.33	86.41	10.63	.057390
Hypro	13.98	5.14	28.02	5.96	.099441
Pro	70.32	19.24	80.76	14.11	.669325

Amino acid levels are expressed as μmoles/L plasma.

APPENDIX C

70 DAY PLASMA MSO-TREATED METABOLITE COMPARISONS

Table C-1: List of all mean 70 day wild-type mouse plasma metabolite values grouped by treatment and the corresponding *p* values obtained from the MANOVA.

	WT Saline		WT MSO		
Metabolite	**Mean**	**SEM**	**Mean**	**SEM**	***p* (MANOVA)**
Phser	9.61	2.69	11.43	1.57	.574738
Taur	328.23	19.93	395.99	41.42	.144739
Pea	6.11	1.74	9.12	1.82	.246880
Urea	10638.12	460.47	9146.05	582.81	.055629
Asp	13.06	1.38	14.83	1.13	.337382
Thr	200.01	16.49	218.26	13.05	.400963
Ser	162.33	10.15	176.67	11.16	.351772
Asn	50.48	5.41	53.13	4.00	.701964
Glu	14.89	3.65	18.79	4.19	.487941
Gln	585.30	27.18	557.24	39.21	.557242
Sarc	9.33	5.38	10.23	5.42	.907711
AAAA	14.70	2.83	16.05	2.77	.739149
Gly	314.52	11.57	301.65	19.93	.574421
Ala	720.05	52.53	844.44	70.01	.165522
Citr	91.99	6.94	96.57	4.91	.601330
Val	311.94	24.77	285.58	15.05	.384131
Cys	13.34	5.45	26.66	5.34	.096435
Met	98.30	12.32	96.64	8.00	.913104
Ile	109.92	9.01	107.41	5.43	.817321
Leu	186.02	15.46	177.73	8.50	.651767
Tyr	81.54	5.93	89.45	6.28	.369783
Phe	73.09	4.88	72.20	2.75	.879171
Orn	87.76	11.50	86.27	7.31	.916251
Lys	290.03	18.13	352.86	17.99	.022960
1-Mhis	12.58	1.16	10.83	1.51	.364649
His	74.71	2.89	77.23	4.06	.613876
Trp	63.11	5.69	50.43	8.38	.217336
Arg	108.90	8.30	112.78	7.57	.735051
Hypro	25.60	6.92	22.87	4.05	.742757
Pro	116.87	10.32	117.75	9.54	.951244

Amino acid levels are expressed as μmoles/L plasma.

Table C-2: List of all mean 70 day SOD1 mouse plasma metabolite values grouped by treatment and the corresponding *p* values obtained from the MANOVA.

	SOD1 Saline		SOD1 MSO		
Metabolite	**Mean**	**SEM**	**Mean**	**SEM**	***p* (MANOVA)**
Phser	6.09	0.97	7.09	1.58	.603230
Taur	320.02	26.23	356.80	17.70	.244954
Pea	1.12	0.61	4.68	1.16	.014200
Urea	10526.52	433.47	9882.69	432.57	.304200
Asp	9.15	0.35	10.40	0.80	.184506
Thr	183.01	7.90	209.75	13.59	.112417
Ser	144.39	5.37	153.77	7.17	.315400
Asn	42.92	2.77	56.49	4.05	.011917
Glu	10.31	3.19	17.95	3.40	.115627
Gln	593.91	23.94	449.48	29.23	.000808
Sarc	32.38	5.12	18.30	3.36	.025673
AAAA	10.63	1.37	17.60	1.69	.003925
Gly	282.61	19.13	275.32	10.37	.731411
Ala	593.61	32.61	743.30	35.23	.004517
Citr	80.81	3.63	89.36	4.95	.185241
Val	266.01	16.11	302.59	19.68	.168868
Cys	0.00	0.00	5.29	2.10	.025781
Met	82.12	6.89	96.24	6.69	.153442
Ile	97.40	5.14	105.77	4.69	.238197
Leu	163.87	8.36	180.33	7.42	.150689
Tyr	73.24	5.06	80.91	5.05	.294171
Phe	66.56	2.21	70.29	2.72	.305675
Orn	73.53	5.88	99.46	7.98	.016463
Lys	280.22	18.74	358.42	24.71	.020121
1-Mhis	10.91	1.35	9.47	0.75	.344738
His	72.94	4.16	73.37	2.40	.927951
Trp	57.25	8.15	70.90	6.15	.185516
Arg	100.60	7.59	137.16	10.36	.009664
Hypro	21.00	4.25	17.40	3.77	.529625
Pro	75.54	11.55	96.70	11.63	.209456

Amino acid levels are expressed as μmoles/L plasma.

Table C-3: List of all mean 70 day female wild-type mouse plasma metabolite values grouped by treatment and the corresponding *p* values obtained from the MANOVA.

	Female Saline		Female MSO		
Metabolite	**Mean**	**SEM**	**Mean**	**SEM**	***p* (MANOVA)**
Phser	12.69	5.17	9.70	2.22	.607096
Taur	374.83	20.66	341.62	18.91	.262994
Pea	11.21	1.40	9.19	2.39	.483439
Urea	10150.32	674.15	8484.25	918.68	.174415
Asp	13.26	2.35	13.28	1.72	.994428
Thr	204.22	30.26	219.89	24.17	.694414
Ser	173.98	18.82	185.62	17.78	.662636
Asn	56.77	9.42	55.01	6.65	.881851
Glu	21.43	5.23	10.49	3.35	.108579
Gln	638.99	34.74	587.33	68.26	.515227
Sarc	8.90	5.65	12.24	8.08	.741493
AAAA	16.12	5.42	14.28	3.45	.781273
Gly	303.57	18.83	267.03	26.05	.282248
Ala	766.50	102.31	888.13	100.72	.416684
Citr	94.21	13.68	104.92	7.38	.506795
Val	334.47	41.53	262.41	18.10	.142788
Cys	12.43	7.87	26.71	8.24	.238523
Met	109.82	18.49	92.11	14.14	.464140
Ile	123.89	14.72	106.26	6.78	.302071
Leu	210.02	25.28	169.97	11.29	.178631
Tyr	84.11	10.23	89.77	10.82	.711799
Phe	79.47	8.04	71.71	3.69	.400919
Orn	104.78	18.71	73.23	9.60	.164447
Lys	317.58	32.62	377.58	24.88	.174306
1-Mhis	15.07	1.41	12.52	2.43	.385520
His	81.79	3.31	83.07	2.54	.764741
Trp	76.07	7.38	67.40	4.96	.352589
Arg	119.42	14.41	117.80	9.74	.927223
Hypro	18.35	8.31	19.72	4.55	.887539
Pro	121.12	20.34	104.63	11.38	.495285

Amino acid levels are expressed as μmoles/L plasma.

Table C-4: List of all mean 70 day female SOD1 mouse plasma metabolite values grouped by treatment and the corresponding *p* values obtained from the MANOVA.

	Female Saline		Female MSO		
Metabolite	**Mean**	**SEM**	**Mean**	**SEM**	***p* (MANOVA)**
Phser	5.51	1.32	6.27	1.49	.714939
Taur	348.69	37.23	382.35	31.45	.498940
Pea	1.61	1.06	3.63	1.59	.321242
Urea	9447.01	548.05	9802.29	421.67	.611157
Asp	9.15	0.60	9.03	0.61	.887741
Thr	189.55	11.37	221.53	21.19	.225054
Ser	151.72	6.30	165.77	10.15	.276701
Asn	47.09	3.20	61.10	6.39	.083888
Glu	9.55	3.73	13.13	5.43	.606145
Gln	646.85	25.91	465.34	45.07	.005159
Sarc	37.80	4.86	20.18	4.86	.024089
AAAA	11.17	2.71	18.44	2.57	.073518
Gly	283.98	39.44	260.09	11.90	.549262
Ala	665.88	31.81	776.21	46.18	.078419
Citr	84.35	5.54	96.07	6.90	.216917
Val	256.47	18.31	286.92	19.70	.282501
Cys	0.00	0.00	3.61	2.89	.265627
Met	85.19	12.46	100.11	9.14	.343749
Ile	102.74	5.14	110.23	6.19	.376756
Leu	170.36	9.44	180.04	9.99	.497543
Tyr	82.94	6.18	83.05	5.94	.990105
Phe	71.48	2.11	73.67	3.47	.611836
Orn	74.15	7.35	101.76	11.42	.071060
Lys	318.41	17.80	400.52	36.11	.073514
1-Mhis	12.13	1.58	11.37	0.83	.664781
His	81.73	6.61	79.65	2.64	.762944
Trp	71.92	12.69	75.79	11.68	.826045
Arg	114.79	8.33	152.43	13.55	.039927
Hypro	13.98	5.14	11.44	4.56	.717204
Pro	70.32	19.24	81.94	20.17	.685982

Amino acid levels are expressed as μmoles/L plasma.

Table C-5: List of all mean 70 day male wild-type mouse plasma metabolite values grouped by treatment and the corresponding *p* values obtained from the MANOVA.

	Male Saline		Male MSO		
Metabolite	**Mean**	**SEM**	**Mean**	**SEM**	***p* (MANOVA)**
Phser	6.53	1.14	13.50	2.05	.012415
Taur	281.63	21.25	461.24	83.37	.048706
Pea	1.02	1.02	9.02	3.10	.026201
Urea	11125.92	619.10	9940.21	559.60	.196810
Asp	12.86	1.68	16.70	1.03	.098440
Thr	195.79	16.55	216.30	7.62	.321409
Ser	150.69	6.72	165.93	12.59	.290549
Asn	44.20	4.91	50.88	4.43	.347640
Glu	8.34	3.75	28.75	5.84	.013997
Gln	531.61	29.86	521.15	29.52	.810698
Sarc	9.77	9.77	7.82	7.82	.883291
AAAA	13.29	2.27	18.16	4.73	.351081
Gly	325.48	13.66	343.19	19.40	.463303
Ala	673.60	28.49	792.01	102.36	.256051
Citr	89.76	4.80	86.56	2.18	.585681
Val	289.40	27.79	313.39	20.01	.517898
Cys	14.25	8.28	26.60	7.41	.304452
Met	86.78	16.53	102.09	6.17	.443573
Ile	95.95	7.91	108.78	9.60	.324728
Leu	162.02	13.50	187.05	12.91	.218733
Tyr	78.98	6.87	89.07	6.39	.318011
Phe	66.70	4.90	72.80	4.58	.394486
Orn	70.73	10.78	101.92	6.61	.044017
Lys	262.49	8.92	323.20	21.19	.020005
1-Mhis	10.09	1.22	8.80	1.36	.497626
His	67.63	2.41	70.22	7.64	.734478
Trp	50.16	4.57	30.05	12.61	.140806
Arg	98.38	7.17	106.75	12.49	.558197
Hypro	32.85	10.99	26.64	7.27	.663518
Pro	112.63	6.91	133.49	13.89	.188968

Amino acid levels are expressed as μmoles/L plasma.

Table C-6: List of all mean 70 day male SOD1 mouse plasma metabolite values grouped by treatment and the corresponding *p* values obtained from the MANOVA.

	Male Saline		Male MSO		
Metabolite	**Mean**	**SEM**	**Mean**	**SEM**	***p* (MANOVA)**
Phser	6.66	1.50	7.92	2.87	.715006
Taur	291.36	36.36	331.25	12.93	.295047
Pea	0.63	0.63	5.72	1.70	.019937
Urea	11606.02	354.13	9963.08	788.85	.093929
Asp	9.14	0.41	11.77	1.36	.105537
Thr	176.47	11.26	197.97	17.38	.333528
Ser	137.06	8.20	141.76	8.73	.703881
Asn	38.76	4.14	51.89	4.82	.062755
Glu	11.07	5.48	22.76	3.66	.092641
Gln	540.98	29.63	433.62	39.49	.053598
Sarc	26.97	8.95	16.41	4.87	.302371
AAAA	10.10	0.84	16.76	2.33	.024692
Gly	281.24	5.40	290.55	15.89	.609440
Ala	521.33	43.07	710.40	53.65	.018407
Citr	77.27	4.71	82.64	6.67	.533401
Val	275.55	27.55	318.25	34.68	.362182
Cys	0.00	0.00	6.96	3.11	.057373
Met	79.05	6.87	92.37	10.19	.312487
Ile	92.07	8.86	101.32	7.09	.424863
Leu	157.39	14.14	180.63	11.67	.223170
Tyr	63.54	6.43	78.77	8.52	.186732
Phe	61.65	2.94	66.91	4.05	.324974
Orn	72.91	9.78	97.17	11.88	.145803
Lys	242.03	26.80	316.32	28.40	.081930
1-Mhis	9.68	2.23	7.56	0.84	.365141
His	64.16	2.34	67.09	2.52	.414048
Trp	42.58	7.40	66.02	4.31	.014299
Arg	86.41	10.63	121.90	14.48	.076323
Hypro	28.02	5.96	23.35	5.47	.572899
Pro	80.76	14.11	111.47	10.51	.099526

Amino acid levels are expressed as μmoles/L plasma.

APPENDIX D

THE EFFECTS OF OVARIECTOMIZATION ON PLASMA METABOLITES

Table D-1: List of all mean 70 day saline-treated female plasma metabolite values grouped by intact or removed gonads and the corresponding *p* values obtained from the MANOVA.

	Intact Females		OVR Females		
Metabolite	**Mean**	**SEM**	**Mean**	**SEM**	***p* (MANOVA)**
Phser	5.51	1.32	2.96	0.69	.076841
Taur	348.69	37.23	270.76	16.02	.034264
Pea	1.61	1.06	1.39	0.71	.974615
Urea	9447.01	548.05	8408.40	366.88	.121846
Asp	9.15	0.60	4.57	1.67	.035407
Thr	189.55	11.37	153.59	10.79	.056491
Ser	151.72	6.30	120.88	5.90	.003138
Asn	47.09	3.20	43.81	3.17	.525487
Glu	9.55	3.73	14.23	0.97	.184986
Gln	646.85	25.91	630.12	19.32	.429163
Sarc	37.80	4.86	0.00	0.00	.000000
AAAA	11.17	2.71	19.59	1.41	.006611
Gly	283.98	39.44	253.01	8.86	.375726
Ala	665.88	31.81	569.99	40.38	.119981
Citr	84.35	5.54	96.22	6.29	.189837
Val	256.47	18.31	224.09	17.66	.231240
Cys	0.00	0.00	0.00	0.00	
Met	85.19	12.46	64.71	5.39	.171933
Ile	102.74	5.14	99.05	8.44	.701062
Leu	170.36	9.44	152.26	9.79	.176260
Tyr	82.94	6.18	85.56	6.33	.729931
Phe	71.48	2.11	69.30	3.51	.730354
Orn	74.15	7.35	65.25	4.66	.292058
Lys	318.41	17.80	249.69	16.00	.014590
1-Mhis	12.13	1.58	11.94	1.21	.950118
His	81.73	6.61	62.77	2.81	.013492
Trp	71.92	12.69	69.96	4.13	.861269
Arg	114.79	8.33	101.39	6.38	.230145
Hypro	13.98	5.14	8.90	2.57	.376231
Pro	70.32	19.24	113.06	6.48	.017115

Amino acid levels are expressed as μmoles/L plasma.

REFERENCES

Abbott N. 2002. Astrocyte-endothelial interactions and blood-brain barrier permeability. *J Anat* 200:527

Abe Y, Okazaki T. 1987. Purification and properties of the manganese superoxide dismutase from the liver of bullfrog, Rana catesbeiana. *Arch Biochem Biophys* 253:241-8

Adibi SA, Gray SJ, Menden E. 1967. The kinetics of amino acid absorption and alteration of plasma composition of free amino acids after intestinal perfusion of amino acid mixtures. *Am J Clin Nutr* 20:24-33

Al-Chalabi A, Andersen PM, Chioza B, Shaw C, Sham PC, et al. 1998. Recessive amyotrophic lateral sclerosis families with the D90A SOD1 mutation share a common founder: evidence for a linked protective factor. *Hum Mol Genet* 7:2045-50

Al-Chalabi A, Andersen PM, Nilsson P, Chioza B, Andersson JL, et al. 1999. Deletions of the heavy neurofilament subunit tail in amyotrophic lateral sclerosis. *Hum Mol Genet* 8:157-64

Alberts B, Johnson A, Lewis J, Raff M, Roberts K, Walter P. 2002. *Molecular Biology of the Cell*. New York, NY: Garland Science

Allen RH, Stabler SP, Lindenbaum J. 1993. Serum betaine, N,N-dimethylglycine and N-methylglycine levels in patients with cobalamin and folate deficiency and related inborn errors of metabolism. *Metabolism* 42:1448-60

Alonso A, Logroscino G, Jick SS, Hernan MA. 2009. Incidence and lifetime risk of motor neuron disease in the United Kingdom: a population-based study. *Eur J Neurol* 16:745-51

Alves CJ, de Santana LP, dos Santos AJ, de Oliveira GP, Duobles T, et al. 2011. Early motor and electrophysiological changes in transgenic mouse model of amyotrophic lateral sclerosis and gender differences on clinical outcome. *Brain Res* 1394:90-104

Aman P, Panagopoulos I, Lassen C, Fioretos T, Mencinger M, et al. 1996. Expression patterns of the human sarcoma-associated genes FUS and EWS and the genomic structure of FUS. *Genomics* 37:1-8

Amoresano A, Di Costanzo A, Leo G, Di Cunto F, La Mantia G, et al. 2010. Identification of DeltaNp63alpha protein interactions by mass spectrometry. *J Proteome Res* 9:2042-8

Andersen PM. 2006. Amyotrophic lateral sclerosis associated with mutations in the CuZn superoxide dismutase gene. *Curr Neurol Neurosci Rep* 6:37-46

Andersen PM, Forsgren L, Binzer M, Nilsson P, Ala-Hurula V, et al. 1996. Autosomal recessive adult-onset amyotrophic lateral sclerosis associated with homozygosity for Asp90Ala CuZn-superoxide dismutase mutation. A clinical and genealogical study of 36 patients. *Brain* 119 (Pt 4):1153-72

Andersson MK, Stahlberg A, Arvidsson Y, Olofsson A, Semb H, et al. 2008. The multifunctional FUS, EWS and TAF15 proto-oncoproteins show cell type-specific expression patterns and involvement in cell spreading and stress response. *BMC Cell Biol* 9:37

Annunziata P, Volpi N. 1985. High levels of C3c in the cerebrospinal fluid from amyotrophic lateral sclerosis patients. *Acta Neurol Scand* 72:61-4

Arai T, Hasegawa M, Akiyama H, Ikeda K, Nonaka T, et al. 2006. TDP-43 is a component of ubiquitin-positive tau-negative inclusions in frontotemporal lobar degeneration and amyotrophic lateral sclerosis. *Biochem Biophys Res Commun* 351:602-11

Arciero PJ, Goran MI, Poehlman ET. 1993. Resting metabolic rate is lower in women than in men. *J Appl Physiol* 75:2514-20

Ardawi MS, Newsholme EA. 1982. Maximum activities of some enzymes of glycolysis, the tricarboxylic acid cycle and ketone-body and glutamine utilization pathways in lymphocytes of the rat. *Biochem J* 208:743-8

Ardawi MS, Newsholme EA. 1983. Glutamine metabolism in lymphocytes of the rat. *Biochem J* 212:835-42

Aronica E, Gorter JA, Ijlst-Keizers H, Rozemuller AJ, Yankaya B, et al. 2003. Expression and functional role of mGluR3 and mGluR5 in human astrocytes and glioma cells: opposite regulation of glutamate transporter proteins. *Eur J Neurosci* 17:2106-18

Ash PE, Zhang YJ, Roberts CM, Saldi T, Hutter H, et al. 2010. Neurotoxic effects of TDP-43 overexpression in C. elegans. *Hum Mol Genet* 19:3206-18

Askanazi J, Furst P, Michelsen CB, Elwyn DH, Vinnars E, et al. 1980. Muscle and plasma amino acids after injury: hypocaloric glucose vs. amino acid infusion. *Ann Surg* 191:465-72

Atkin JD, Farg MA, Walker AK, McLean C, Tomas D, Horne MK. 2008. Endoplasmic reticulum stress and induction of the unfolded protein response in human sporadic amyotrophic lateral sclerosis. *Neurobiol Dis* 30:400-7

Awano T, Johnson GS, Wade CM, Katz ML, Johnson GC, et al. 2009. Genome-wide association analysis reveals a SOD1 mutation in canine degenerative myelopathy that resembles amyotrophic lateral sclerosis. *Proc Natl Acad Sci U S A* 106:2794-9

Ayala YM, De Conti L, Avendano-Vazquez SE, Dhir A, Romano M, et al. 2011. TDP-43 regulates its mRNA levels through a negative feedback loop. *EMBO J* 30:277-88

Ayala YM, Pantano S, D'Ambrogio A, Buratti E, Brindisi A, et al. 2005. Human, Drosophila, and C.elegans TDP43: nucleic acid binding properties and splicing regulatory function. *J Mol Biol* 348:575-88

Ayala YM, Zago P, D'Ambrogio A, Xu YF, Petrucelli L, et al. 2008. Structural determinants of the cellular localization and shuttling of TDP-43. *J Cell Sci* 121:3778-85

Baechtold H, Kuroda M, Sok J, Ron D, Lopez BS, Akhmedov AT. 1999. Human 75-kDa DNA-pairing protein is identical to the pro-oncoprotein TLS/FUS and is able to promote D-loop formation. *J Biol Chem* 274:34337-42

Bajaj P, Raiger LK, Jain SD, Kumar S. 2007. Women emerge from general anesthesia faster than men. *Middle East J Anesthesiol* 19:173-83

Banack SA, Murch SJ. 2009. Multiple neurotoxic items in the Chamorro diet link BMAA with ALS/PDC. *Amyotroph Lateral Scler* 10 Suppl 2:34-40

Barbeito L, Cheramy A, Godeheu G, Desce JM, Glowinski J. 1990. Glutamate Receptors of a Quisqualate-Kainate Subtype are Involved in the Presynaptic Regulation of Dopamine Release in the Cat Caudate Nucleus in vivo. *Eur J Neurosci* 2:304-11

Baron P, Bussini S, Cardin V, Corbo M, Conti G, et al. 2005. Production of monocyte chemoattractant protein-1 in amyotrophic lateral sclerosis. *Muscle Nerve* 32:541-4

Bastow EL, Gourlay CW, Tuite MF. 2011. Using yeast models to probe the molecular basis of amyotrophic lateral sclerosis. *Biochem Soc Trans* 39:1482-7

Bederman I, Chandramouli V, Sandlers Y, Henderson L, Cabrera ME. 2012. Time-course of hepatic gluconeogenesis during hindlimb suspension unloading. *Exp Physiol*

Beers DR, Henkel JS, Zhao W, Wang J, Appel SH. 2008. CD4+ T cells support glial neuroprotection, slow disease progression, and modify glial morphology in an animal model of inherited ALS. *Proc Natl Acad Sci U S A* 105:15558-63

Beghi E, Mennini T, Bendotti C, Bigini P, Logroscino G, et al. 2007. The heterogeneity of amyotrophic lateral sclerosis: a possible explanation of treatment failure. *Curr Med Chem* 14:3185-200

Belzil VV, Valdmanis PN, Dion PA, Daoud H, Kabashi E, et al. 2009. Mutations in FUS cause FALS and SALS in French and French Canadian populations. *Neurology* 73:1176-9

Benavides J, Camelin JC, Mitrani N, Flamand F, Uzan A, et al. 1985. 2-Amino-6-trifluoromethoxy benzothiazole, a possible antagonist of excitatory amino acid neurotransmission--II. Biochemical properties. *Neuropharmacology* 24:1085-92

Bendotti C, Atzori C, Piva R, Tortarolo M, Strong MJ, et al. 2004. Activated p38MAPK is a novel component of the intracellular inclusions found in human amyotrophic lateral sclerosis and mutant SOD1 transgenic mice. *J Neuropathol Exp Neurol* 63:113-9

Bendotti C, Calvaresi N, Chiveri L, Prelle A, Moggio M, et al. 2001. Early vacuolization and mitochondrial damage in motor neurons of FALS mice are not associated with apoptosis or with changes in cytochrome oxidase histochemical reactivity. *J Neurol Sci* 191:25-33

Bentley HR, Mc DE, et al. 1949. Action of nitrogen trichloride (agene) on proteins; isolation of crystalline toxic factor. *Nature* 164:438

Bentley HR, Mc DE, Moran T, Pace J, Whitehead JK. 1950. Action of nitrogen trichloride on certain proteins. I. Isolation and identification of the toxic factor. *Proc R Soc Lond B Biol Sci* 137:402-17

Berg JM, Tymoczko JL, Stryer L. 2007. *Biochemistry*. New York, NY: W. H. Freeman and Company

Biechele TL, Camp ND, Fass DM, Kulikauskas RM, Robin NC, et al. 2010. Chemical-genetic screen identifies riluzole as an enhancer of Wnt/beta-catenin signaling in melanoma. *Chem Biol* 17:1177-82

Binazzi A, Belli S, Uccelli R, Desiato MT, Talamanca IF, et al. 2009. An exploratory case-control study on spinal and bulbar forms of amyotrophic lateral sclerosis in the province of Rome. *Amyotroph Lateral Scler* 10:361-9

Blin M, Crusio WE, Hevor T, Cloix JF. 2002. Chronic inhibition of glutamine synthetase is not associated with impairment of learning and memory in mice. *Brain Res Bull* 57:11-5

Blin O, Samuel D, Nieoullon A, Serratice G. 1994. Changes in CSF amino acid concentrations during the evolution of amyotrophic lateral sclerosis. *J Neurol Neurosurg Psychiatry* 57:119-20

Blutstein T, Baab PJ, Zielke HR, Mong JA. 2009. Hormonal modulation of amino acid neurotransmitter metabolism in the arcuate nucleus of the adult female rat: a novel action of estradiol. *Endocrinology* 150:3237-44

Blutstein T, Devidze N, Choleris E, Jasnow AM, Pfaff DW, Mong JA. 2006. Oestradiol up-regulates glutamine synthetase mRNA and protein expression in the hypothalamus and hippocampus: implications for a role of hormonally responsive glia in amino acid neurotransmission. *J Neuroendocrinol* 18:692-702

Boillee S, Vande Velde C, Cleveland DW. 2006. ALS: a disease of motor neurons and their nonneuronal neighbors. *Neuron* 52:39-59

Bonini NM, Fortini ME. 2003. Human neurodegenerative disease modeling using Drosophila. *Annu Rev Neurosci* 26:627-56

Borchelt DR, Wong PC, Becher MW, Pardo CA, Lee MK, et al. 1998. Axonal transport of mutant superoxide dismutase 1 and focal axonal abnormalities in the proximal axons of transgenic mice. *Neurobiol Dis* 5:27-35

Bose JK, Huang CC, Shen CK. 2011. Regulation of autophagy by neuropathological protein TDP-43. *J Biol Chem* 286:44441-8

Boston-Howes W, Gibb SL, Williams EO, Pasinelli P, Brown RH, Jr., Trotti D. 2006. Caspase-3 cleaves and inactivates the glutamate transporter EAAT2. *J Biol Chem* 281:14076-84

Bowling AC, Schulz JB, Brown RH, Jr., Beal MF. 1993. Superoxide dismutase activity, oxidative damage, and mitochondrial energy metabolism in familial and sporadic amyotrophic lateral sclerosis. *J Neurochem* 61:2322-5

Bristol LA, Rothstein JD. 1996. Glutamate transporter gene expression in amyotrophic lateral sclerosis motor cortex. *Ann Neurol* 39:676-9

Broer S. 2008. Amino acid transport across mammalian intestinal and renal epithelia. *Physiol Rev* 88:249-86

Brooks BR. 1994. El Escorial World Federation of Neurology criteria for the diagnosis of amyotrophic lateral sclerosis. Subcommittee on Motor Neuron Diseases/Amyotrophic Lateral Sclerosis of the World Federation of Neurology Research Group on Neuromuscular Diseases and the El Escorial "Clinical limits of amyotrophic lateral sclerosis" workshop contributors. *J Neurol Sci* 124 Suppl:96-107

Brosnan JT. 2003. Interorgan amino acid transport and its regulation. *J Nutr* 133:2068S-72S

Brotherton TE, Li Y, Cooper D, Gearing M, Julien JP, et al. 2012. Localization of a toxic form of superoxide dismutase 1 protein to pathologically affected tissues in familial ALS. *Proc Natl Acad Sci U S A*

Brown JR, Masuchi Y, Robb FT, Doolittle WF. 1994. Evolutionary relationships of bacterial and archaeal glutamine synthetase genes. *J Mol Evol* 38:566-76

Browne SE, Yang L, DiMauro JP, Fuller SW, Licata SC, Beal MF. 2006. Bioenergetic abnormalities in discrete cerebral motor pathways presage spinal cord pathology in the G93A SOD1 mouse model of ALS. *Neurobiol Dis* 22:599-610

Bruijn LI, Miller TM, Cleveland DW. 2004. Unraveling the mechanisms involved in motor neuron degeneration in ALS. *Annu Rev Neurosci* 27:723-49

Brusilow SW. 1991. *Determination of urine orotate and orotidine and plasma ammonium*. New York: Wiley-Liss. 3 pp.

Bulus N, Cersosimo E, Ghishan F, Abumrad NN. 1989. Physiologic importance of glutamine. *Metabolism* 38:1-5

Buratti E, Baralle FE. 2008. Multiple roles of TDP-43 in gene expression, splicing regulation, and human disease. *Front Biosci* 13:867-78

Buratti E, De Conti L, Stuani C, Romano M, Baralle M, Baralle F. 2010. Nuclear factor TDP-43 can affect selected microRNA levels. *FEBS J* 277:2268-81

Buratti E, Dork T, Zuccato E, Pagani F, Romano M, Baralle FE. 2001. Nuclear factor TDP-43 and SR proteins promote in vitro and in vivo CFTR exon 9 skipping. *EMBO J* 20:1774-84

Cairns NJ, Neumann M, Bigio EH, Holm IE, Troost D, et al. 2007. TDP-43 in familial and sporadic frontotemporal lobar degeneration with ubiquitin inclusions. *Am J Pathol* 171:227-40

Calvio C, Neubauer G, Mann M, Lamond AI. 1995. Identification of hnRNP P2 as TLS/FUS using electrospray mass spectrometry. *RNA* 1:724-33

Campbell JW, Vorhaben JE, Smith DD, Jr. 1987. Uricoteley:its nature and origin during the evolution of tetrapod vertebrates. *J Exp Zool* 243:349-63

Campbell PN, Work TS, Mellanby E. 1951. The isolation of a toxic substance from agenized wheat flour. *Biochem J* 48:106-13

Cassina P, Cassina A, Pehar M, Castellanos R, Gandelman M, et al. 2008. Mitochondrial dysfunction in SOD1G93A-bearing astrocytes promotes motor neuron degeneration: prevention by mitochondrial-targeted antioxidants. *J Neurosci* 28:4115-22

Cassina P, Pehar M, Vargas MR, Castellanos R, Barbeito AG, et al. 2005. Astrocyte activation by fibroblast growth factor-1 and motor neuron apoptosis: implications for amyotrophic lateral sclerosis. *J Neurochem* 93:38-46

Chance PF, Rabin BA, Ryan SG, Ding Y, Scavina M, et al. 1998. Linkage of the gene for an autosomal dominant form of juvenile amyotrophic lateral sclerosis to chromosome 9q34. *Am J Hum Genet* 62:633-40

Chaovipoch P, Jelks KA, Gerhold LM, West EJ, Chongthammakun S, Floyd CL. 2006. 17beta-estradiol is protective in spinal cord injury in post- and pre-menopausal rats. *J Neurotrauma* 23:830-52

Chapman AM, Silkwood-Sherer D. 2000. *Fundamentals of Neuroanatomy: An Introduction to the Structure and Function of the Nervous System*. Grand Rapids, MI: C & S Works

Chen H, Richard M, Sandler DP, Umbach DM, Kamel F. 2007. Head injury and amyotrophic lateral sclerosis. *Am J Epidemiol* 166:810-6

Chen Y, Guan Y, Zhang Z, Liu H, Wang S, et al. 2012. Wnt signaling pathway is involved in the pathogenesis of amyotrophic lateral sclerosis in adult transgenic mice. *Neurol Res* 34:390-9

Cheng RK, Jesuthasan S, Penney TB. 2011. Time for zebrafish. *Front Integr Neurosci* 5:40

Cheramy A, Barbeito L, Godeheu G, Glowinski J. 1992. Riluzole inhibits the release of glutamate in the caudate nucleus of the cat in vivo. *Neurosci Lett* 147:209-12

Cheroni C, Marino M, Tortarolo M, Veglianese P, De Biasi S, et al. 2009. Functional alterations of the ubiquitin-proteasome system in motor neurons of a mouse model of familial amyotrophic lateral sclerosis. *Hum Mol Genet* 18:82-96

Chio A, Benzi G, Dossena M, Mutani R, Mora G. 2005. Severely increased risk of amyotrophic lateral sclerosis among Italian professional football players. *Brain* 128:472-6

Chiu IM, Chen A, Zheng Y, Kosaras B, Tsiftsoglou SA, et al. 2008. T lymphocytes potentiate endogenous neuroprotective inflammation in a mouse model of ALS. *Proc Natl Acad Sci U S A* 105:17913-8

Choi CI, Lee YD, Gwag BJ, Cho SI, Kim SS, Suh-Kim H. 2008. Effects of estrogen on lifespan and motor functions in female hSOD1 G93A transgenic mice. *J Neurol Sci* 268:40-7

Cohen J. 1988. *Statistical power analysis for the behavioral sciences* Hillsdale, N.J.: Lawrence Earlbaum Associates

Cooper JR, Bloom FE, Roth RH, eds. 2003. *The Biochemical Basis of Neuropharmacology*. New York, NY: Oxford University Press

Corbo M, Hays AP. 1992. Peripherin and neurofilament protein coexist in spinal spheroids of motor neuron disease. *J Neuropathol Exp Neurol* 51:531-7

Cornell JS, Meister A. 1976. Glutathione and gamma-glutamyl cycle enzymes in crypt and villus tip cells of rat jejunal mucosa. *Proc Natl Acad Sci U S A* 73:420-2

Corrado L, Carlomagno Y, Falasco L, Mellone S, Godi M, et al. 2011. A novel peripherin gene (PRPH) mutation identified in one sporadic amyotrophic lateral sclerosis patient. *Neurobiol Aging* 32:552 e1-6

Corrado L, Del Bo R, Castellotti B, Ratti A, Cereda C, et al. 2010. Mutations of FUS gene in sporadic amyotrophic lateral sclerosis. *J Med Genet* 47:190-4

Costantini F, Lacy E. 1981. Introduction of a rabbit beta-globin gene into the mouse germ line. *Nature* 294:92-4

Crawford J, Cohen HJ. 1985. The essential role of L-glutamine in lymphocyte differentiation in vitro. *J Cell Physiol* 124:275-82

Cronin S, Greenway MJ, Prehn JH, Hardiman O. 2007. Paraoxonase promoter and intronic variants modify risk of sporadic amyotrophic lateral sclerosis. *J Neurol Neurosurg Psychiatry* 78:984-6

Crozat A, Aman P, Mandahl N, Ron D. 1993. Fusion of CHOP to a novel RNA-binding protein in human myxoid liposarcoma. *Nature* 363:640-4

Curti D, Malaspina A, Facchetti G, Camana C, Mazzini L, et al. 1996. Amyotrophic lateral sclerosis: oxidative energy metabolism and calcium homeostasis in peripheral blood lymphocytes. *Neurology* 47:1060-4

D'Alessandro G, Calcagno E, Tartari S, Rizzardini M, Invernizzi RW, Cantoni L. 2011. Glutamate and glutathione interplay in a motor neuronal model of amyotrophic lateral sclerosis reveals altered energy metabolism. *Neurobiol Dis* 43:346-55

D'Ambrogio A, Buratti E, Stuani C, Guarnaccia C, Romano M, et al. 2009. Functional mapping of the interaction between TDP-43 and hnRNP A2 in vivo. *Nucleic Acids Res* 37:4116-26

De Robertis E, Sellinger OZ, Rodriguez de L, Alberici M, Zieher LM. 1967. Nerve endings in methionine sulphoximine convulsant rats, a neurochemical and ultrastructural study. *J Neurochem* 14:81-9

De Vos KJ, Grierson AJ, Ackerley S, Miller CC. 2008. Role of axonal transport in neurodegenerative diseases. *Annu Rev Neurosci* 31:151-73

Debono MW, Le Guern J, Canton T, Doble A, Pradier L. 1993. Inhibition by riluzole of electrophysiological responses mediated by rat kainate and NMDA receptors expressed in Xenopus oocytes. *Eur J Pharmacol* 235:283-9

Deng HX, Hentati A, Tainer JA, Iqbal Z, Cayabyab A, et al. 1993. Amyotrophic lateral sclerosis and structural defects in Cu,Zn superoxide dismutase. *Science* 261:1047-51

Deng HX, Shi Y, Furukawa Y, Zhai H, Fu R, et al. 2006. Conversion to the amyotrophic lateral sclerosis phenotype is associated with intermolecular linked insoluble aggregates of SOD1 in mitochondria. *Proc Natl Acad Sci U S A* 103:7142-7

Desport JC, Preux PM, Magy L, Boirie Y, Vallat JM, et al. 2001. Factors correlated with hypermetabolism in patients with amyotrophic lateral sclerosis. *Am J Clin Nutr* 74:328-34

Desport JC, Preux PM, Truong CT, Courat L, Vallat JM, Couratier P. 2000. Nutritional assessment and survival in ALS patients. *Amyotroph Lateral Scler Other Motor Neuron Disord* 1:91-6

Desport JC, Preux PM, Truong TC, Vallat JM, Sautereau D, Couratier P. 1999. Nutritional status is a prognostic factor for survival in ALS patients. *Neurology* 53:1059-63

Desport JC, Torny F, Lacoste M, Preux PM, Couratier P. 2005. Hypermetabolism in ALS: correlations with clinical and paraclinical parameters. *Neurodegener Dis* 2:202-7

Devos D, Moreau C, Lassalle P, Perez T, De Seze J, et al. 2004. Low levels of the vascular endothelial growth factor in CSF from early ALS patients. *Neurology* 62:2127-9

Di Giacomo C, Sorrenti V, Acquaviva R, Campisi A, Vanella G, et al. 1997. Ornithine decarboxylase activity in cerebral post-ischemic reperfusion damage: effect of methionine sulfoximine. *Neurochem Res* 22:1145-50

Di Noto L, Whitson LJ, Cao X, Hart PJ, Levine RL. 2005. Proteasomal degradation of mutant superoxide dismutases linked to amyotrophic lateral sclerosis. *J Biol Chem* 280:39907-13

Dibaj P, Steffens H, Zschuntzsch J, Nadrigny F, Schomburg ED, et al. 2011. In Vivo imaging reveals distinct inflammatory activity of CNS microglia versus PNS macrophages in a mouse model for ALS. *PLoS One* 6:e17910

Dong Y, Benveniste EN. 2001. Immune function of astrocytes. *Glia* 36:180-90

Dupuis L, Oudart H, Rene F, Gonzalez de Aguilar JL, Loeffler JP. 2004. Evidence for defective energy homeostasis in amyotrophic lateral sclerosis: benefit of a high-energy diet in a transgenic mouse model. *Proc Natl Acad Sci U S A* 101:11159-64

Eisenberg D, Gill HS, Pfluegl GM, Rotstein SH. 2000. Structure-function relationships of glutamine synthetases. *Biochim Biophys Acta* 1477:122-45

Elliott JL. 2001. Cytokine upregulation in a murine model of familial amyotrophic lateral sclerosis. *Brain Res Mol Brain Res* 95:172-8

Engelhardt B, Coisne C. 2011. Fluids and barriers of the CNS establish immune privilege by confining immune surveillance to a two-walled castle moat surrounding the CNS castle. *Fluids Barriers CNS* 8:4

Engelhardt JI, Soos J, Obal I, Vigh L, Siklos L. 2005. Subcellular localization of IgG from the sera of ALS patients in the nervous system. *Acta Neurol Scand* 112:126-33

Epstein CJ, Avraham KB, Lovett M, Smith S, Elroy-Stein O, et al. 1987. Transgenic mice with increased Cu/Zn-superoxide dismutase activity: animal model of dosage effects in Down syndrome. *Proc Natl Acad Sci U S A* 84:8044-8

Eschenbrenner M, Jorns MS. 1999. Cloning and mapping of the cDNA for human sarcosine dehydrogenase, a flavoenzyme defective in patients with sarcosinemia. *Genomics* 59:300-8

Fang F, Quinlan P, Ye W, Barber MK, Umbach DM, et al. 2009. Workplace exposures and the risk of amyotrophic lateral sclerosis. *Environ Health Perspect* 117:1387-92

Fields RD, Stevens-Graham B. 2002. New insights into neuron-glia communication. *Science* 298:556-62

Figlewicz DA, Krizus A, Martinoli MG, Meininger V, Dib M, et al. 1994. Variants of the heavy neurofilament subunit are associated with the development of amyotrophic lateral sclerosis. *Hum Mol Genet* 3:1757-61

Forsberg K, Andersen PM, Marklund SL, Brannstrom T. 2011. Glial nuclear aggregates of superoxide dismutase-1 are regularly present in patients with amyotrophic lateral sclerosis. *Acta Neuropathol* 121:623-34

Fray AE, Dempster S, Williams RE, Cookson MR, Shaw PJ. 2001. Glutamine synthetase activity and expression are not affected by the development of motor neuronopathy in the G93A SOD-1/ALS mouse. *Brain Res Mol Brain Res* 94:131-6

Fray AE, Ince PG, Banner SJ, Milton ID, Usher PA, et al. 1998. The expression of the glial glutamate transporter protein EAAT2 in motor neuron disease: an immunohistochemical study. *Eur J Neurosci* 10:2481-9

Fridovich I. 1974. Superoxide dismutases. *Adv Enzymol Relat Areas Mol Biol* 41:35-97

Frutiger K, Lukas TJ, Gorrie G, Ajroud-Driss S, Siddique T. 2008. Gender difference in levels of Cu/Zn superoxide dismutase (SOD1) in cerebrospinal fluid of patients with amyotrophic lateral sclerosis. *Amyotroph Lateral Scler* 9:184-7

Fujii R, Okabe S, Urushido T, Inoue K, Yoshimura A, et al. 2005. The RNA binding protein TLS is translocated to dendritic spines by mGluR5 activation and regulates spine morphology. *Curr Biol* 15:587-93

Fujii R, Takumi T. 2005. TLS facilitates transport of mRNA encoding an actin-stabilizing protein to dendritic spines. *J Cell Sci* 118:5755-65

Fukada K, Nagano S, Satoh M, Tohyama C, Nakanishi T, et al. 2001. Stabilization of mutant Cu/Zn superoxide dismutase (SOD1) protein by coexpressed wild SOD1 protein accelerates the disease progression in familial amyotrophic lateral sclerosis mice. *Eur J Neurosci* 14:2032-6

Funalot B, Desport JC, Sturtz F, Camu W, Couratier P. 2009. High metabolic level in patients with familial amyotrophic lateral sclerosis. *Amyotroph Lateral Scler* 10:113-7

Funfschilling U, Supplie LM, Mahad D, Boretius S, Saab AS, et al. 2012. Glycolytic oligodendrocytes maintain myelin and long-term axonal integrity. *Nature* 485:517-21

Furukawa Y, O'Halloran TV. 2005. Amyotrophic lateral sclerosis mutations have the greatest destabilizing effect on the apo- and reduced form of SOD1, leading to unfolding and oxidative aggregation. *J Biol Chem* 280:17266-74

Gama Sosa MA, De Gasperi R, Elder GA. 2012. Modeling human neurodegenerative diseases in transgenic systems. *Hum Genet* 131:535-63

Garbuzova-Davis S, Haller E, Saporta S, Kolomey I, Nicosia SV, Sanberg PR. 2007a. Ultrastructure of blood-brain barrier and blood-spinal cord barrier in SOD1 mice modeling ALS. *Brain Res* 1157:126-37

Garbuzova-Davis S, Saporta S, Haller E, Kolomey I, Bennett SP, et al. 2007b. Evidence of compromised blood-spinal cord barrier in early and late symptomatic SOD1 mice modeling ALS. *PLoS One* 2:e1205

Ghoddoussi F, Galloway MP, Jambekar A, Bame M, Needleman R, Brusilow WS. 2010. Methionine sulfoximine, an inhibitor of glutamine synthetase, lowers brain glutamine and glutamate in a mouse model of ALS. *J Neurol Sci* 290:41-7

Giess R, Holtmann B, Braga M, Grimm T, Muller-Myhsok B, et al. 2002. Early onset of severe familial amyotrophic lateral sclerosis with a SOD-1 mutation: potential impact of CNTF as a candidate modifier gene. *Am J Hum Genet* 70:1277-86

Gitcho MA, Bigio EH, Mishra M, Johnson N, Weintraub S, et al. 2009. TARDBP 3'-UTR variant in autopsy-confirmed frontotemporal lobar degeneration with TDP-43 proteinopathy. *Acta Neuropathol* 118:633-45

Gonzalez de Aguilar JL, Dupuis L, Oudart H, Loeffler JP. 2005. The metabolic hypothesis in amyotrophic lateral sclerosis: insights from mutant Cu/Zn-superoxide dismutase mice. *Biomed Pharmacother* 59:190-6

Goodall EF, Greenway MJ, van Marion I, Carroll CB, Hardiman O, Morrison KE. 2005. Association of the H63D polymorphism in the hemochromatosis gene with sporadic ALS. *Neurology* 65:934-7

Gordon JW, Ruddle FH. 1981. Integration and stable germ line transmission of genes injected into mouse pronuclei. *Science* 214:1244-6

Gorg B, Qvartskhava N, Voss P, Grune T, Haussinger D, Schliess F. 2007. Reversible inhibition of mammalian glutamine synthetase by tyrosine nitration. *FEBS Lett* 581:84-90

Gowing G, Philips T, Van Wijmeersch B, Audet JN, Dewil M, et al. 2008. Ablation of proliferating microglia does not affect motor neuron degeneration in amyotrophic lateral sclerosis caused by mutant superoxide dismutase. *J Neurosci* 28:10234-44

Graves MC, Fiala M, Dinglasan LA, Liu NQ, Sayre J, et al. 2004. Inflammation in amyotrophic lateral sclerosis spinal cord and brain is mediated by activated macrophages, mast cells and T cells. *Amyotroph Lateral Scler Other Motor Neuron Disord* 5:213-9

Green DR. 1998. Apoptotic pathways: the roads to ruin. *Cell* 94:695-8

Groeneveld GJ, Van Muiswinkel FL, Sturkenboom JM, Wokke JH, Bar PR, Van den Berg LH. 2004. Ovariectomy and 17beta-estradiol modulate disease progression of a mouse model of ALS. *Brain Res* 1021:128-31

Gros-Louis F, Lariviere R, Gowing G, Laurent S, Camu W, et al. 2004. A frameshift deletion in peripherin gene associated with amyotrophic lateral sclerosis. *J Biol Chem* 279:45951-6

Grundstrom E, Askmark H, Lindeberg J, Nygren I, Ebendal T, Aquilonius SM. 1999. Increased expression of glial cell line-derived neurotrophic factor mRNA in muscle biopsies from patients with amyotrophic lateral sclerosis. *J Neurol Sci* 162:169-73

Grundstrom E, Lindholm D, Johansson A, Blennow K, Askmark H. 2000. GDNF but not BDNF is increased in cerebrospinal fluid in amyotrophic lateral sclerosis. *Neuroreport* 11:1781-3

Gruzman A, Wood WL, Alpert E, Prasad MD, Miller RG, et al. 2007. Common molecular signature in SOD1 for both sporadic and familial amyotrophic lateral sclerosis. *Proc Natl Acad Sci U S A* 104:12524-9

Guo H, Lai L, Butchbach ME, Stockinger MP, Shan X, et al. 2003. Increased expression of the glial glutamate transporter EAAT2 modulates excitotoxicity and delays the onset but not the outcome of ALS in mice. *Hum Mol Genet* 12:2519-32

Gurney ME, Pu H, Chiu AY, Dal Canto MC, Polchow CY, et al. 1994. Motor neuron degeneration in mice that express a human Cu,Zn superoxide dismutase mutation. *Science* 264:1772-5

Hall ED, Oostveen JA, Gurney ME. 1998. Relationship of microglial and astrocytic activation to disease onset and progression in a transgenic model of familial ALS. *Glia* 23:249-56

Hanson KA, Kim SH, Wassarman DA, Tibbetts RS. 2010. Ubiquilin modifies TDP-43 toxicity in a Drosophila model of amyotrophic lateral sclerosis (ALS). *J Biol Chem* 285:11068-72

Harraz MM, Marden JJ, Zhou W, Zhang Y, Williams A, et al. 2008. SOD1 mutations disrupt redox-sensitive Rac regulation of NADPH oxidase in a familial ALS model. *J Clin Invest* 118:659-70

Haussinger D. 1987. Hepatic glutamine metabolism. *Beitr Infusionther Klin Ernahr* 17:144-57

Haverkamp LJ, Appel V, Appel SH. 1995. Natural history of amyotrophic lateral sclerosis in a database population. Validation of a scoring system and a model for survival prediction. *Brain* 118 (Pt 3):707-19

Hayashi T, Rizzuto R, Hajnoczky G, Su TP. 2009. MAM: more than just a housekeeper. *Trends Cell Biol* 19:81-8

Hayward C, Colville S, Swingler RJ, Brock DJ. 1999. Molecular genetic analysis of the APEX nuclease gene in amyotrophic lateral sclerosis. *Neurology* 52:1899-901

Hayward LJ, Rodriguez JA, Kim JW, Tiwari A, Goto JJ, et al. 2002. Decreased metallation and activity in subsets of mutant superoxide dismutases associated with familial amyotrophic lateral sclerosis. *J Biol Chem* 277:15923-31

He X, Lu X, Hu J, Xi J, Zhou D, et al. 2011. H63D polymorphism in the hemochromatosis gene is associated with sporadic amyotrophic lateral sclerosis in China. *Eur J Neurol* 18:359-61

Heiman-Patterson TD, Deitch JS, Blankenhorn EP, Erwin KL, Perreault MJ, et al. 2005. Background and gender effects on survival in the TgN(SOD1-G93A)1Gur mouse model of ALS. *J Neurol Sci* 236:1-7

Hensley K, Fedynyshyn J, Ferrell S, Floyd RA, Gordon B, et al. 2003. Message and protein-level elevation of tumor necrosis factor alpha (TNF alpha) and TNF alpha-modulating

cytokines in spinal cords of the G93A-SOD1 mouse model for amyotrophic lateral sclerosis. *Neurobiol Dis* 14:74-80

Higashi S, Tsuchiya Y, Araki T, Wada K, Kabuta T. 2010. TDP-43 physically interacts with amyotrophic lateral sclerosis-linked mutant CuZn superoxide dismutase. *Neurochem Int* 57:906-13

Higgins CM, Jung C, Xu Z. 2003. ALS-associated mutant SOD1G93A causes mitochondrial vacuolation by expansion of the intermembrane space and by involvement of SOD1 aggregation and peroxisomes. *BMC Neurosci* 4:16

Hoffman EK, Wilcox HM, Scott RW, Siman R. 1996. Proteasome inhibition enhances the stability of mouse Cu/Zn superoxide dismutase with mutations linked to familial amyotrophic lateral sclerosis. *J Neurol Sci* 139:15-20

Holmoy T. 2008. T cells in amyotrophic lateral sclerosis. *Eur J Neurol* 15:360-6

Hough MA, Grossmann JG, Antonyuk SV, Strange RW, Doucette PA, et al. 2004. Dimer destabilization in superoxide dismutase may result in disease-causing properties: structures of motor neuron disease mutants. *Proc Natl Acad Sci U S A* 101:5976-81

Howland DS, Liu J, She Y, Goad B, Maragakis NJ, et al. 2002. Focal loss of the glutamate transporter EAAT2 in a transgenic rat model of SOD1 mutant-mediated amyotrophic lateral sclerosis (ALS). *Proc Natl Acad Sci U S A* 99:1604-9

Hubert JP, Doble A. 1989. Ibotenic acid stimulates D-[3H]aspartate release from cultured cerebellar granule cells. *Neurosci Lett* 96:345-50

Hyun DH, Lee M, Halliwell B, Jenner P. 2003. Proteasomal inhibition causes the formation of protein aggregates containing a wide range of proteins, including nitrated proteins. *J Neurochem* 86:363-73

Igaz LM, Kwong LK, Lee EB, Chen-Plotkin A, Swanson E, et al. 2011. Dysregulation of the ALS-associated gene TDP-43 leads to neuronal death and degeneration in mice. *J Clin Invest* 121:726-38

Igaz LM, Kwong LK, Xu Y, Truax AC, Uryu K, et al. 2008. Enrichment of C-terminal fragments in TAR DNA-binding protein-43 cytoplasmic inclusions in brain but not in spinal cord of frontotemporal lobar degeneration and amyotrophic lateral sclerosis. *Am J Pathol* 173:182-94

Iijima K, Takase S, Tsumuraya K, Endo M, Itahara K. 1978. Changes in free amino acids of cerebrospinal fluid and plasma in various neurological diseases. *Tohoku J Exp Med* 126:133-50

Iko Y, Kodama TS, Kasai N, Oyama T, Morita EH, et al. 2004. Domain architectures and characterization of an RNA-binding protein, TLS. *J Biol Chem* 279:44834-40

Ilieva EV, Ayala V, Jove M, Dalfo E, Cacabelos D, et al. 2007. Oxidative and endoplasmic reticulum stress interplay in sporadic amyotrophic lateral sclerosis. *Brain* 130:3111-23

Jaarsma D, Haasdijk ED, Grashorn JA, Hawkins R, van Duijn W, et al. 2000. Human Cu/Zn superoxide dismutase (SOD1) overexpression in mice causes mitochondrial vacuolization, axonal degeneration, and premature motoneuron death and accelerates motoneuron disease in mice expressing a familial amyotrophic lateral sclerosis mutant SOD1. *Neurobiol Dis* 7:623-43

Jaenisch R, Mintz B. 1974. Simian virus 40 DNA sequences in DNA of healthy adult mice derived from preimplantation blastocysts injected with viral DNA. *Proc Natl Acad Sci U S A* 71:1250-4

Jambekar AA, Palma E, Nicolosi L, Rasola A, Petronilli V, et al. 2011. A glutamine synthetase inhibitor increases survival and decreases cytokine response in a mouse model of acute liver failure. *Liver Int*

Jeibmann A, Paulus W. 2009. Drosophila melanogaster as a model organism of brain diseases. *Int J Mol Sci* 10:407-40

Jiang YM, Yamamoto M, Kobayashi Y, Yoshihara T, Liang Y, et al. 2005. Gene expression profile of spinal motor neurons in sporadic amyotrophic lateral sclerosis. *Ann Neurol* 57:236-51

Johnston JA, Dalton MJ, Gurney ME, Kopito RR. 2000. Formation of high molecular weight complexes of mutant Cu, Zn-superoxide dismutase in a mouse model for familial amyotrophic lateral sclerosis. *Proc Natl Acad Sci U S A* 97:12571-6

Jonsson PA, Ernhill K, Andersen PM, Bergemalm D, Brannstrom T, et al. 2004. Minute quantities of misfolded mutant superoxide dismutase-1 cause amyotrophic lateral sclerosis. *Brain* 127:73-88

Joyce PI, Fratta P, Fisher EM, Acevedo-Arozena A. 2011. SOD1 and TDP-43 animal models of amyotrophic lateral sclerosis: recent advances in understanding disease toward the development of clinical treatments. *Mamm Genome* 22:420-48

Kabashi E, Bercier V, Lissouba A, Liao M, Brustein E, et al. 2011. FUS and TARDBP but not SOD1 interact in genetic models of amyotrophic lateral sclerosis. *PLoS Genet* 7:e1002214

Kabashi E, Lin L, Tradewell ML, Dion PA, Bercier V, et al. 2010. Gain and loss of function of ALS-related mutations of TARDBP (TDP-43) cause motor deficits in vivo. *Hum Mol Genet* 19:671-83

Kabashi E, Valdmanis PN, Dion P, Spiegelman D, McConkey BJ, et al. 2008. TARDBP mutations in individuals with sporadic and familial amyotrophic lateral sclerosis. *Nat Genet* 40:572-4

Kachadroka S, Hall AM, Niedzielko TL, Chongthammakun S, Floyd CL. 2010. Effect of endogenous androgens on 17beta-estradiol-mediated protection after spinal cord injury in male rats. *J Neurotrauma* 27:611-26

Kaczynski J, Cook T, Urrutia R. 2003. Sp1- and Kruppel-like transcription factors. *Genome Biol* 4:206

Kamel F, Umbach DM, Hu H, Munsat TL, Shefner JM, et al. 2005. Lead exposure as a risk factor for amyotrophic lateral sclerosis. *Neurodegener Dis* 2:195-201

Kamel F, Umbach DM, Munsat TL, Shefner JM, Hu H, Sandler DP. 2002. Lead exposure and amyotrophic lateral sclerosis. *Epidemiology* 13:311-9

Karpuzoglu E, Ahmed SA. 2006. Estrogen regulation of nitric oxide and inducible nitric oxide synthase (iNOS) in immune cells: implications for immunity, autoimmune diseases, and apoptosis. *Nitric Oxide* 15:177-86

Kasarskis EJ, Berryman S, Vanderleest JG, Schneider AR, McClain CJ. 1996. Nutritional status of patients with amyotrophic lateral sclerosis: relation to the proximity of death. *Am J Clin Nutr* 63:130-7

Kato R, Yamazoe Y. 1992. Sex-specific cytochrome P450 as a cause of sex- and species-related differences in drug toxicity. *Toxicol Lett* 64-65 Spec No:661-7

Kawamata H, Magrane J, Kunst C, King MP, Manfredi G. 2008. Lysyl-tRNA synthetase is a target for mutant SOD1 toxicity in mitochondria. *J Biol Chem* 283:28321-8

Kawamata T, Akiyama H, Yamada T, McGeer PL. 1992. Immunologic reactions in amyotrophic lateral sclerosis brain and spinal cord tissue. *Am J Pathol* 140:691-707

Keeney PM, Bennett JP, Jr. 2010. ALS spinal neurons show varied and reduced mtDNA gene copy numbers and increased mtDNA gene deletions. *Mol Neurodegener* 5:21

Kennedy AJ, Voaden MJ, Marshall J. 1974. Glutamate metabolism in the frog retina. *Nature* 252:50-2

Khare SD, Caplow M, Dokholyan NV. 2006. FALS mutations in Cu, Zn superoxide dismutase destabilize the dimer and increase dimer dissociation propensity: a large-scale thermodynamic analysis. *Amyloid* 13:226-35

Kikuchi H, Almer G, Yamashita S, Guegan C, Nagai M, et al. 2006. Spinal cord endoplasmic reticulum stress associated with a microsomal accumulation of mutant superoxide dismutase-1 in an ALS model. *Proc Natl Acad Sci U S A* 103:6025-30

Kobari M, Obara K, Watanabe S, Dembo T, Fukuuchi Y. 1996. Local cerebral blood flow in motor neuron disease: correlation with clinical findings. *J Neurol Sci* 144:64-9

Kovacevic Z, McGivan JD. 1983. Mitochondrial metabolism of glutamine and glutamate and its physiological significance. *Physiol Rev* 63:547-605

Koyama K, Kaya M, Tsujita J, Hori S. 1998. Effects of decreased plasma glutamine concentrations on peripheral lymphocyte proliferation in rats. *Eur J Appl Physiol Occup Physiol* 77:25-31

Krajewski WW, Collins R, Holmberg-Schiavone L, Jones TA, Karlberg T, Mowbray SL. 2008. Crystal structures of mammalian glutamine synthetases illustrate substrate-induced conformational changes and provide opportunities for drug and herbicide design. *J Mol Biol* 375:217-28

Krebs HA. 1935. Metabolism of amino-acids: The synthesis of glutamine from glutamic acid and ammonia, and the enzymic hydrolysis of glutamine in animal tissues. *Biochem J* 29:1951-69

Krishnaswamy PR, Pamiljans V, Meister A. 1962. Studies on the Mechanism of Glutamine Synthesis: Evidence for the Formation of Enzyme-bound Activated Glutamic Acid. *The Journal of Biological Chemistry* 237:9

Kumada Y, Benson DR, Hillemann D, Hosted TJ, Rochefort DA, et al. 1993. Evolution of the glutamine synthetase gene, one of the oldest existing and functioning genes. *Proc Natl Acad Sci U S A* 90:3009-13

Kwiatkowski TJ, Jr., Bosco DA, Leclerc AL, Tamrazian E, Vanderburg CR, et al. 2009. Mutations in the FUS/TLS gene on chromosome 16 cause familial amyotrophic lateral sclerosis. *Science* 323:1205-8

Lagier-Tourenne C, Polymenidou M, Cleveland DW. 2010. TDP-43 and FUS/TLS: emerging roles in RNA processing and neurodegeneration. *Hum Mol Genet* 19:R46-64

Lamar C, Jr. 1968. The duration of the inhibtion of glutamine synthetase by methionine sulfoximine. *Biochem Pharmacol* 17:636-40

Lang TJ. 2004. Estrogen as an immunomodulator. *Clin Immunol* 113:224-30

Langou K, Moumen A, Pellegrino C, Aebischer J, Medina I, et al. 2010. AAV-mediated expression of wild-type and ALS-linked mutant VAPB selectively triggers death of motoneurons through a Ca2+-dependent ER-associated pathway. *J Neurochem* 114:795-809

Law WJ, Cann KL, Hicks GG. 2006. TLS, EWS and TAF15: a model for transcriptional integration of gene expression. *Brief Funct Genomic Proteomic* 5:8-14

Lee EB, Lee VM, Trojanowski JQ. 2012a. Gains or losses: molecular mechanisms of TDP43-mediated neurodegeneration. *Nat Rev Neurosci* 13:38-50

Lee Y, Morrison BM, Li Y, Lengacher S, Farah MH, et al. 2012b. Oligodendroglia metabolically support axons and contribute to neurodegeneration. *Nature* 487:443-8

Leigh PN, Whitwell H, Garofalo O, Buller J, Swash M, et al. 1991. Ubiquitin-immunoreactive intraneuronal inclusions in amyotrophic lateral sclerosis. Morphology, distribution, and specificity. *Brain* 114 (Pt 2):775-88

Leonardi A, Abbruzzese G, Arata L, Cocito L, Vische M. 1984. Cerebrospinal fluid (CSF) findings in amyotrophic lateral sclerosis. *J Neurol* 231:75-8

Leung CL, He CZ, Kaufmann P, Chin SS, Naini A, et al. 2004. A pathogenic peripherin gene mutation in a patient with amyotrophic lateral sclerosis. *Brain Pathol* 14:290-6

Li M, Ona VO, Guegan C, Chen M, Jackson-Lewis V, et al. 2000. Functional role of caspase-1 and caspase-3 in an ALS transgenic mouse model. *Science* 288:335-9

Li S, Hu GF. 2010. Angiogenin-mediated rRNA transcription in cancer and neurodegeneration. *Int J Biochem Mol Biol* 1:26-35

Li S, Yu W, Hu GF. 2012. Angiogenin inhibits nuclear translocation of apoptosis inducing factor in a Bcl-2-dependent manner. *J Cell Physiol* 227:1639-44

Li X, Decker M, Westendorf JJ. 2010a. TEThered to Runx: novel binding partners for runx factors. *Blood Cells Mol Dis* 45:82-5

Li Y, Ray P, Rao EJ, Shi C, Guo W, et al. 2010b. A Drosophila model for TDP-43 proteinopathy. *Proc Natl Acad Sci U S A* 107:3169-74

Liaw SH, Eisenberg D. 1994. Structural model for the reaction mechanism of glutamine synthetase, based on five crystal structures of enzyme-substrate complexes. *Biochemistry* 33:675-81

Lie-Venema H, Hakvoort TB, van Hemert FJ, Moorman AF, Lamers WH. 1998. Regulation of the spatiotemporal pattern of expression of the glutamine synthetase gene. *Prog Nucleic Acid Res Mol Biol* 61:243-308

Lieschke GJ, Currie PD. 2007. Animal models of human disease: zebrafish swim into view. *Nat Rev Genet* 8:353-67

Lin CL, Bristol LA, Jin L, Dykes-Hoberg M, Crawford T, et al. 1998. Aberrant RNA processing in a neurodegenerative disease: the cause for absent EAAT2, a glutamate transporter, in amyotrophic lateral sclerosis. *Neuron* 20:589-602

Linser P, Moscona AA. 1983. Hormonal induction of glutamine synthetase in cultures of embryonic retina cells: requirement for neuron-glia contact interactions. *Dev Biol* 96:529-34

Liu J, Lillo C, Jonsson PA, Vande Velde C, Ward CM, et al. 2004. Toxicity of familial ALS-linked SOD1 mutants from selective recruitment to spinal mitochondria. *Neuron* 43:5-17

Llorca O, Betti M, Gonzalez JM, Valencia A, Marquez AJ, Valpuesta JM. 2006. The three-dimensional structure of an eukaryotic glutamine synthetase: functional implications of its oligomeric structure. *J Struct Biol* 156:469-79

Lobsiger CS, Boillee S, McAlonis-Downes M, Khan AM, Feltri ML, et al. 2009. Schwann cells expressing dismutase active mutant SOD1 unexpectedly slow disease progression in ALS mice. *Proc Natl Acad Sci U S A* 106:4465-70

Logroscino G, Traynor BJ, Hardiman O, Chio A, Couratier P, et al. 2008. Descriptive epidemiology of amyotrophic lateral sclerosis: new evidence and unsolved issues. *J Neurol Neurosurg Psychiatry* 79:6-11

Mali Y, Zisapels N. 2008. Gain of interaction of ALS-linked G93A superoxide dismutase with cytosolic malate dehydrogenase. *Neurobiol Dis* 32:133-41

Manning JM, Moore S, Rowe WB, Meister A. 1969. Identification of L-methionine S-sulfoximine as the diastereoisomer of L-methionine SR-sulfoximine that inhibits glutamine synthetase. *Biochemistry* 8:2681-5

Maragakis NJ, Dykes-Hoberg M, Rothstein JD. 2004. Altered expression of the glutamate transporter EAAT2b in neurological disease. *Ann Neurol* 55:469-77

Martin D, Thompson MA, Nadler JV. 1993. The neuroprotective agent riluzole inhibits release of glutamate and aspartate from slices of hippocampal area CA1. *Eur J Pharmacol* 250:473-6

Martin LJ, Liu Z, Chen K, Price AC, Pan Y, et al. 2007. Motor neuron degeneration in amyotrophic lateral sclerosis mutant superoxide dismutase-1 transgenic mice: mechanisms of mitochondriopathy and cell death. *J Comp Neurol* 500:20-46

Masu Y, Wolf E, Holtmann B, Sendtner M, Brem G, Thoenen H. 1993. Disruption of the CNTF gene results in motor neuron degeneration. *Nature* 365:27-32

Matsumoto S, Kusaka H, Ito H, Shibata N, Asayama T, Imai T. 1996. Sporadic amyotrophic lateral sclerosis with dementia and Cu/Zn superoxide dismutase-positive Lewy body-like inclusions. *Clin Neuropathol* 15:41-6

Mattiazzi M, D'Aurelio M, Gajewski CD, Martushova K, Kiaei M, et al. 2002. Mutated human SOD1 causes dysfunction of oxidative phosphorylation in mitochondria of transgenic mice. *J Biol Chem* 277:29626-33

McCombe PA, Henderson RD. 2010. Effects of gender in amyotrophic lateral sclerosis. *Gend Med* 7:557-70

McCord JM, Fridovich I. 1969. Superoxide dismutase. An enzymic function for erythrocuprein (hemocuprein). *J Biol Chem* 244:6049-55

McNeill ME. 1997. *Neuroanatomy Primer: Color to learn*. Baltimore, MD: Lippincott Williams & Wilkins

Meister A. 1985. Glutamine synthetase from mammalian tissues. *Methods Enzymol* 113:185-99

Meister A. 1989. Mechanism and regulation of the glutamine-dependent carbamyl phosphate synthetase of Escherichia coli. *Adv Enzymol Relat Areas Mol Biol* 62:315-74

Meister A, Griffith OW, Novogrodsky A, Tate SS. 1979. New aspects of glutathione metabolism and translocation in mammals. *Ciba Found Symp*:135-61

Mellanby E. 1946. Diet and canine hysteria. Experimental production by treated flour. *Br Med J* 2:885-7

Mendonca DM, Chimelli L, Martinez AM. 2006. Expression of ubiquitin and proteasome in motorneurons and astrocytes of spinal cords from patients with amyotrophic lateral sclerosis. *Neurosci Lett* 404:315-9

Meucci G, Rossi G, Bettini R, Montanaro D, Gironelli L, et al. 1993. Laser nephelometric evaluation of albumin, IgG and alpha 2-macroglobulin: applications to the study of alterations of the blood-brain barrier. *J Neurol Sci* 118:73-8

Milani P, Gagliardi S, Cova E, Cereda C. 2011. SOD1 Transcriptional and Posttranscriptional Regulation and Its Potential Implications in ALS. *Neurol Res Int* 2011:458427

Militello A, Vitello G, Lunetta C, Toscano A, Maiorana G, et al. 2002. The serum level of free testosterone is reduced in amyotrophic lateral sclerosis. *J Neurol Sci* 195:67-70

Miller RG, Mitchell JD, Lyon M, Moore DH. 2007. Riluzole for amyotrophic lateral sclerosis (ALS)/motor neuron disease (MND). *Cochrane Database Syst Rev*:CD001447

Miller S, Kesslak JP, Romano C, Cotman CW. 1995. Roles of metabotropic glutamate receptors in brain plasticity and pathology. *Ann N Y Acad Sci* 757:460-74

Mills KI, Walsh V, Gilkes AF, Sweeney MC, Mirza T, et al. 2000. High FUS/TLS expression in acute myeloid leukaemia samples. *Br J Haematol* 108:316-21

Misani F, Reiner L. 1950. Studies on nitrogen trichloride-treated prolamines. VIII. Synthesis of the toxic factor. *Arch Biochem* 27:234-5

Mishra M, Paunesku T, Woloschak GE, Siddique T, Zhu LJ, et al. 2007. Gene expression analysis of frontotemporal lobar degeneration of the motor neuron disease type with ubiquitinated inclusions. *Acta Neuropathol* 114:81-94

Moisse K, Strong MJ. 2006. Innate immunity in amyotrophic lateral sclerosis. *Biochim Biophys Acta* 1762:1083-93

Mong JA, Blutstein T. 2006. Estradiol modulation of astrocytic form and function: implications for hormonal control of synaptic communication. *Neuroscience* 138:967-75

Moreira MC, Klur S, Watanabe M, Nemeth AH, Le Ber I, et al. 2004. Senataxin, the ortholog of a yeast RNA helicase, is mutant in ataxia-ocular apraxia 2. *Nat Genet* 36:225-7

Morey-Holton ER, Globus RK. 2002. Hindlimb unloading rodent model: technical aspects. *J Appl Physiol* 92:1367-77

Morohoshi F, Arai K, Takahashi EI, Tanigami A, Ohki M. 1996. Cloning and mapping of a human RBP56 gene encoding a putative RNA binding protein similar to FUS/TLS and EWS proteins. *Genomics* 38:51-7

Morohoshi F, Ootsuka Y, Arai K, Ichikawa H, Mitani S, et al. 1998. Genomic structure of the human RBP56/hTAFII68 and FUS/TLS genes. *Gene* 221:191-8

Moumen A, Virard I, Raoul C. 2011. Accumulation of wildtype and ALS-linked mutated VAPB impairs activity of the proteasome. *PLoS One* 6:e26066

Muller B, Grossniklaus U. 2010. Model organisms--A historical perspective. *J Proteomics* 73:2054-63

Muqit MM, Feany MB. 2002. Modelling neurodegenerative diseases in Drosophila: a fruitful approach? *Nat Rev Neurosci* 3:237-43

Murakami T, Nagano I, Hayashi T, Manabe Y, Shoji M, et al. 2001. Impaired retrograde axonal transport of adenovirus-mediated E. coli LacZ gene in the mice carrying mutant SOD1 gene. *Neurosci Lett* 308:149-52

Murphy K, Travers P, Walport M. 2008. *Janeway's Immunobiology*. New York, NY: Garland Science

Muyderman H, Hutson PG, Matusica D, Rogers ML, Rush RA. 2009. The human G93A-superoxide dismutase-1 mutation, mitochondrial glutathione and apoptotic cell death. *Neurochem Res* 34:1847-56

Nachreiner T, Esser M, Tenten V, Troost D, Weis J, Kruttgen A. 2010. Novel splice variants of the amyotrophic lateral sclerosis-associated gene VAPB expressed in human tissues. *Biochem Biophys Res Commun* 394:703-8

Nagai M, Aoki M, Miyoshi I, Kato M, Pasinelli P, et al. 2001. Rats expressing human cytosolic copper-zinc superoxide dismutase transgenes with amyotrophic lateral sclerosis: associated mutations develop motor neuron disease. *J Neurosci* 21:9246-54

Nagai M, Re DB, Nagata T, Chalazonitis A, Jessell TM, et al. 2007. Astrocytes expressing ALS-linked mutated SOD1 release factors selectively toxic to motor neurons. *Nat Neurosci* 10:615-22

Nakano Y, Hirayama K, Terao K. 1987. Hepatic ultrastructural changes and liver dysfunction in amyotrophic lateral sclerosis. *Arch Neurol* 44:103-6

Naumenko N, Pollari E, Kurronen A, Giniatullina R, Shakirzyanova A, et al. 2011. Gender-Specific Mechanism of Synaptic Impairment and Its Prevention by GCSF in a Mouse Model of ALS. *Front Cell Neurosci* 5:26

Nelson DL, Cox MM. 2008. *Lehninger Principles of Biochemistry*. New York, NY: W. H. Freeman and Company

Nelson LM, McGuire V, Longstreth WT, Jr., Matkin C. 2000. Population-based case-control study of amyotrophic lateral sclerosis in western Washington State. I. Cigarette smoking and alcohol consumption. *Am J Epidemiol* 151:156-63

Nestler EJ, Hyman SE, Malenka RC, eds. 2001. *Molecular Neuropharmacology: A Foundation for Clinical Neuroscience*. New York, NY: McGraw-Hill Companies, Inc.

Neumann M, Sampathu DM, Kwong LK, Truax AC, Micsenyi MC, et al. 2006. Ubiquitinated TDP-43 in frontotemporal lobar degeneration and amyotrophic lateral sclerosis. *Science* 314:130-3

Newell GW, Erickson TC, et al. 1949a. Studies on human subjects receiving highly agenized food materials. *J Lab Clin Med* 34:239-45

Newell GW, Erickson TC, Gilson WE, Gershoff SN, Elvehjem CA. 1949b. The effect of feeding agene-treated food materials to experimental animals and to human beings. *Trans American Association of Cereal Chemists* VII

Newsholme EA. 1994. Biochemical mechanisms to explain immunosuppression in well-trained and overtrained athletes. *Int J Sports Med* 15 Suppl 3:S142-7

Newsholme EA, Parry-Billings M. 1990. Properties of glutamine release from muscle and its importance for the immune system. *JPEN J Parenter Enteral Nutr* 14:63S-7S

Newsholme P, Lima MM, Procopio J, Pithon-Curi TC, Doi SQ, et al. 2003. Glutamine and glutamate as vital metabolites. *Braz J Med Biol Res* 36:153-63

Nicklin P, Bergman P, Zhang B, Triantafellow E, Wang H, et al. 2009. Bidirectional transport of amino acids regulates mTOR and autophagy. *Cell* 136:521-34

Nishitoh H, Kadowaki H, Nagai A, Maruyama T, Yokota T, et al. 2008. ALS-linked mutant SOD1 induces ER stress- and ASK1-dependent motor neuron death by targeting Derlin-1. *Genes Dev* 22:1451-64

Niwa J, Ishigaki S, Hishikawa N, Yamamoto M, Doyu M, et al. 2002. Dorfin ubiquitylates mutant SOD1 and prevents mutant SOD1-mediated neurotoxicity. *J Biol Chem* 277:36793-8

Norenberg MD, Bender AS. 1994. Astrocyte swelling in liver failure: role of glutamine and benzodiazepines. *Acta Neurochir Suppl (Wien)* 60:24-7

Oosthuyse B, Moons L, Storkebaum E, Beck H, Nuyens D, et al. 2001. Deletion of the hypoxia-response element in the vascular endothelial growth factor promoter causes motor neuron degeneration. *Nat Genet* 28:131-8

Orlowski M, Meister A. 1970. The gamma-glutamyl cycle: a possible transport system for amino acids. *Proc Natl Acad Sci U S A* 67:1248-55

Orrell RW, Habgood J, Rudge P, Lane RJ, de Belleroche JS. 1996. Difficulties in distinguishing sporadic from familial amyotrophic lateral sclerosis. *Ann Neurol* 39:810-2

Ou SH, Wu F, Harrich D, Garcia-Martinez LF, Gaynor RB. 1995. Cloning and characterization of a novel cellular protein, TDP-43, that binds to human immunodeficiency virus type 1 TAR DNA sequence motifs. *J Virol* 69:3584-96

Pace J, McDermott EE. 1952. Methionine sulphoximine and some enzyme systems in volving glutamine. *Nature* 169:415-6

Parkinson N, Ince PG, Smith MO, Highley R, Skibinski G, et al. 2006. ALS phenotypes with mutations in CHMP2B (charged multivesicular body protein 2B). *Neurology* 67:1074-7

Parry-Billings M, Evans J, Calder PC, Newsholme EA. 1990. Does glutamine contribute to immunosuppression after major burns? *Lancet* 336:523-5

Pasinelli P, Belford ME, Lennon N, Bacskai BJ, Hyman BT, et al. 2004. Amyotrophic lateral sclerosis-associated SOD1 mutant proteins bind and aggregate with Bcl-2 in spinal cord mitochondria. *Neuron* 43:19-30

Pasinelli P, Brown RH. 2006. Molecular biology of amyotrophic lateral sclerosis: insights from genetics. *Nat Rev Neurosci* 7:710-23

Pasinelli P, Houseweart MK, Brown RH, Jr., Cleveland DW. 2000. Caspase-1 and -3 are sequentially activated in motor neuron death in Cu,Zn superoxide dismutase-mediated familial amyotrophic lateral sclerosis. *Proc Natl Acad Sci U S A* 97:13901-6

Patel AJ, Hunt A, Tahourdin CS. 1983. Regulation of in vivo glutamine synthetase activity by glucocorticoids in the developing rat brain. *Brain Res* 312:83-91

Patten BM, Harati Y, Acosta L, Jung SS, Felmus MT. 1978. Free amino acid levels in amyotrophic lateral sclerosis. *Ann Neurol* 3:305-9

Pedrini S, Sau D, Guareschi S, Bogush M, Brown RH, Jr., et al. 2010. ALS-linked mutant SOD1 damages mitochondria by promoting conformational changes in Bcl-2. *Hum Mol Genet* 19:2974-86

Philips T, Robberecht W. 2011. Neuroinflammation in amyotrophic lateral sclerosis: role of glial activation in motor neuron disease. *Lancet Neurol* 10:253-63

Pierson DL. 1980. A rapid colorimetric assay for carbamyl phosphate synthetase I. *J Biochem Biophys Methods* 3:31-7

Pocock JM, Kettenmann H. 2007. Neurotransmitter receptors on microglia. *Trends Neurosci* 30:527-35

Polymenidou M, Lagier-Tourenne C, Hutt KR, Huelga SC, Moran J, et al. 2011. Long pre-mRNA depletion and RNA missplicing contribute to neuronal vulnerability from loss of TDP-43. *Nat Neurosci* 14:459-68

Pradat PF, Bruneteau G, Gordon PH, Dupuis L, Bonnefont-Rousselot D, et al. 2010. Impaired glucose tolerance in patients with amyotrophic lateral sclerosis. *Amyotroph Lateral Scler* 11:166-71

Pramatarova A, Laganiere J, Roussel J, Brisebois K, Rouleau GA. 2001. Neuron-specific expression of mutant superoxide dismutase 1 in transgenic mice does not lead to motor impairment. *J Neurosci* 21:3369-74

Prasad DD, Ouchida M, Lee L, Rao VN, Reddy ES. 1994. TLS/FUS fusion domain of TLS/FUS-erg chimeric protein resulting from the t(16;21) chromosomal translocation in human myeloid leukemia functions as a transcriptional activation domain. *Oncogene* 9:3717-29

Prebil M, Jensen J, Zorec R, Kreft M. 2011. Astrocytes and energy metabolism. *Arch Physiol Biochem* 117:64-9

Purves WK, Sadava D, Orians GH, Heller HC. 2001. *Life: The Science of Biology*. Sunderland, MA: W. H. Freeman

Puttaparthi K, Wojcik C, Rajendran B, DeMartino GN, Elliott JL. 2003. Aggregate formation in the spinal cord of mutant SOD1 transgenic mice is reversible and mediated by proteasomes. *J Neurochem* 87:851-60

Pyatibratov MG, Kostyukova AS. 2012. New insights into the role of angiogenin in actin polymerization. *Int Rev Cell Mol Biol* 295:175-98

Pyatibratov MG, Tolkatchev D, Plamondon J, Xu P, Ni F, Kostyukova AS. 2010. Binding of human angiogenin inhibits actin polymerization. *Arch Biochem Biophys* 495:74-81

Rabbitts TH, Forster A, Larson R, Nathan P. 1993. Fusion of the dominant negative transcription regulator CHOP with a novel gene FUS by translocation t(12;16) in malignant liposarcoma. *Nat Genet* 4:175-80

Rakhit R, Robertson J, Vande Velde C, Horne P, Ruth DM, et al. 2007. An immunological epitope selective for pathological monomer-misfolded SOD1 in ALS. *Nat Med* 13:754-9

Rao SL, Meister A. 1972. In vivo formation of methionine sulfoximine phosphate, a protein-bound metabolite of methionine sulfoximine. *Biochemistry* 11:1123-7

Redler RL, Dokholyan NV. 2012. The Complex Molecular Biology of Amyotrophic Lateral Sclerosis (ALS). *Prog Mol Biol Transl Sci* 107:215-62

Redzic Z. 2011. Molecular biology of the blood-brain and the blood-cerebrospinal fluid barriers: similarities and differences. *Fluids Barriers CNS* 8:3

Reiner L, Misani F, Fair W, Weiss P, Cordasco G. 1950. Studies on nitrogen trichloride treated prolamines. IV. Isolation of the neurotoxic principle. *The Journal of the American Chemical Society* 72

Rennie MJ, Edwards RH, Krywawych S, Davies CT, Halliday D, et al. 1981. Effect of exercise on protein turnover in man. *Clin Sci (Lond)* 61:627-39

Richman PG, Orlowski M, Meister A. 1973. Inhibition of gamma-glutamylcysteine synthetase by L-methionine-S-sulfoximine. *J Biol Chem* 248:6684-90

Rizzuto R, Marchi S, Bonora M, Aguiari P, Bononi A, et al. 2009. Ca(2+) transfer from the ER to mitochondria: when, how and why. *Biochim Biophys Acta* 1787:1342-51

Robertson J, Doroudchi MM, Nguyen MD, Durham HD, Strong MJ, et al. 2003. A neurotoxic peripherin splice variant in a mouse model of ALS. *J Cell Biol* 160:939-49

Rodriguez JA, Shaw BF, Durazo A, Sohn SH, Doucette PA, et al. 2005. Destabilization of apoprotein is insufficient to explain Cu,Zn-superoxide dismutase-linked ALS pathogenesis. *Proc Natl Acad Sci U S A* 102:10516-21

Rohde T, MacLean DA, Klarlund Pedersen B. 1996. Glutamine, lymphocyte proliferation and cytokine production. *Scand J Immunol* 44:648-50

Ronzio RA, Meister A. 1968. Phosphorylation of methionine sulfoximine by glutamine synthetase. *Proc Natl Acad Sci U S A* 59:164-70

Rosen DR, Siddique T, Patterson D, Figlewicz DA, Sapp P, et al. 1993. Mutations in Cu/Zn superoxide dismutase gene are associated with familial amyotrophic lateral sclerosis. *Nature* 362:59-62

Rosnow RL, Rosenthal R. 1996. Computing contrasts, effect sizes, and counternulls on other people's published data: Genderal procedures for research consumers. *Psychological Methods* 1:331-40

Rothstein JD, Dykes-Hoberg M, Pardo CA, Bristol LA, Jin L, et al. 1996. Knockout of glutamate transporters reveals a major role for astroglial transport in excitotoxicity and clearance of glutamate. *Neuron* 16:675-86

Rothstein JD, Martin LJ, Kuncl RW. 1992. Decreased glutamate transport by the brain and spinal cord in amyotrophic lateral sclerosis. *N Engl J Med* 326:1464-8

Rothstein JD, Tsai G, Kuncl RW, Clawson L, Cornblath DR, et al. 1990. Abnormal excitatory amino acid metabolism in amyotrophic lateral sclerosis. *Ann Neurol* 28:18-25

Rothstein JD, Van Kammen M, Levey AI, Martin LJ, Kuncl RW. 1995. Selective loss of glial glutamate transporter GLT-1 in amyotrophic lateral sclerosis. *Ann Neurol* 38:73-84

Rowe WB, Meister A. 1970. Identification of L-methionine-S-sulfoximine as the convulsant isomer of methionine sulfoximine. *Proc Natl Acad Sci U S A* 66:500-6

Rowe WB, Ronzio RA, Meister A. 1969. Inhibition of glutamine synthetase by methionine sulfoximine. Studies on methionine sulfoximine phosphate. *Biochemistry* 8:2674-80

Rumfeldt JA, Lepock JR, Meiering EM. 2009. Unfolding and folding kinetics of amyotrophic lateral sclerosis-associated mutant Cu,Zn superoxide dismutases. *J Mol Biol* 385:278-98

Rusinol AE, Cui Z, Chen MH, Vance JE. 1994. A unique mitochondria-associated membrane fraction from rat liver has a high capacity for lipid synthesis and contains pre-Golgi secretory proteins including nascent lipoproteins. *J Biol Chem* 269:27494-502

Salem ML. 2004. Estrogen, a double-edged sword: modulation of TH1- and TH2-mediated inflammations by differential regulation of TH1/TH2 cytokine production. *Curr Drug Targets Inflamm Allergy* 3:97-104

Sargsyan SA, Blackburn DJ, Barber SC, Monk PN, Shaw PJ. 2009. Mutant SOD1 G93A microglia have an inflammatory phenotype and elevated production of MCP-1. *Neuroreport* 20:1450-5

Sasaki S. 2010. Endoplasmic reticulum stress in motor neurons of the spinal cord in sporadic amyotrophic lateral sclerosis. *J Neuropathol Exp Neurol* 69:346-55

Sau D, De Biasi S, Vitellaro-Zuccarello L, Riso P, Guarnieri S, et al. 2007. Mutation of SOD1 in ALS: a gain of a loss of function. *Hum Mol Genet* 16:1604-18

Saxena S, Cabuy E, Caroni P. 2009. A role for motoneuron subtype-selective ER stress in disease manifestations of FALS mice. *Nat Neurosci* 12:627-36

Schiffer D, Cordera S, Cavalla P, Migheli A. 1996. Reactive astrogliosis of the spinal cord in amyotrophic lateral sclerosis. *J Neurol Sci* 139 Suppl:27-33

Schymick JC, Talbot K, Traynor BJ. 2007. Genetics of sporadic amyotrophic lateral sclerosis. *Hum Mol Genet* 16 Spec No. 2:R233-42

Sellinger OZ, Weiler P, Jr. 1963. THE NATURE OF THE INHIBITION IN VITRO OF CEREBRAL GLUTAMINE SYNTHETASE BY THE CONVULSANT, METHIONINE SULFOXIMINE. *Biochem Pharmacol* 12:989-1000

Shan X, Chiang PM, Price DL, Wong PC. 2010. Altered distributions of Gemini of coiled bodies and mitochondria in motor neurons of TDP-43 transgenic mice. *Proc Natl Acad Sci U S A* 107:16325-30

Shaw BF, Valentine JS. 2007. How do ALS-associated mutations in superoxide dismutase 1 promote aggregation of the protein? *Trends Biochem Sci* 32:78-85

Shibata N, Asayama K, Hirano A, Kobayashi M. 1996a. Immunohistochemical study on superoxide dismutases in spinal cords from autopsied patients with amyotrophic lateral sclerosis. *Dev Neurosci* 18:492-8

Shibata N, Hirano A, Kobayashi M, Sasaki S, Kato T, et al. 1994. Cu/Zn superoxide dismutase-like immunoreactivity in Lewy body-like inclusions of sporadic amyotrophic lateral sclerosis. *Neurosci Lett* 179:149-52

Shibata N, Hirano A, Kobayashi M, Siddique T, Deng HX, et al. 1996b. Intense superoxide dismutase-1 immunoreactivity in intracytoplasmic hyaline inclusions of familial amyotrophic lateral sclerosis with posterior column involvement. *J Neuropathol Exp Neurol* 55:481-90

Shinder GA, Lacourse MC, Minotti S, Durham HD. 2001. Mutant Cu/Zn-superoxide dismutase proteins have altered solubility and interact with heat shock/stress proteins in models of amyotrophic lateral sclerosis. *J Biol Chem* 276:12791-6

Siddique T, Deng HX. 1996. Genetics of amyotrophic lateral sclerosis. *Hum Mol Genet* 5 Spec No:1465-70

Sleegers K, Brouwers N, Maurer-Stroh S, van Es MA, Van Damme P, et al. 2008. Progranulin genetic variability contributes to amyotrophic lateral sclerosis. *Neurology* 71:253-9

Slowik A, Tomik B, Wolkow PP, Partyka D, Turaj W, et al. 2006. Paraoxonase gene polymorphisms and sporadic ALS. *Neurology* 67:766-70

Smith DD, Jr., Campbell JW. 1983. Subcellular location of chicken brain glutamine synthetase and comparison with chicken liver mitochondrial glutamine synthetase. *J Biol Chem* 258:12265-8

Smith DD, Jr., Campbell JW. 1987. Glutamine synthetase in liver of the American alligator, Alligator mississippiensis. *Comp Biochem Physiol B* 86:755-62

Smith DD, Jr., Campbell JW. 1988. Distribution of glutamine synthetase and carbamoyl-phosphate synthetase I in vertebrate liver. *Proc Natl Acad Sci U S A* 85:160-4

Smith DD, Jr., Ritter NM, Campbell JW. 1987. Glutamine synthetase isozymes in elasmobranch brain and liver tissues. *J Biol Chem* 262:198-202

Smith QR. 2000. Transport of glutamate and other amino acids at the blood-brain barrier. *J Nutr* 130:1016S-22S

Sondell M, Lundborg G, Kanje M. 1999. Vascular endothelial growth factor has neurotrophic activity and stimulates axonal outgrowth, enhancing cell survival and Schwann cell proliferation in the peripheral nervous system. *J Neurosci* 19:5731-40

Song JH, Huang CS, Nagata K, Yeh JZ, Narahashi T. 1997. Differential action of riluzole on tetrodotoxin-sensitive and tetrodotoxin-resistant sodium channels. *J Pharmacol Exp Ther* 282:707-14

Squire L, Berg D, Bloom F, Lac SD, Ghosh A, Spitzer N, eds. 2008. *Fundamental Neuroscience*. Burlington, MA: Academic Press

Sreedharan J, Blair IP, Tripathi VB, Hu X, Vance C, et al. 2008. TDP-43 mutations in familial and sporadic amyotrophic lateral sclerosis. *Science* 319:1668-72

Straub RH. 2007. The complex role of estrogens in inflammation. *Endocr Rev* 28:521-74

Strong MJ. 2010. The evidence for altered RNA metabolism in amyotrophic lateral sclerosis (ALS). *J Neurol Sci* 288:1-12

Subramanian V, Crabtree B, Acharya KR. 2008. Human angiogenin is a neuroprotective factor and amyotrophic lateral sclerosis associated angiogenin variants affect neurite extension/pathfinding and survival of motor neurons. *Hum Mol Genet* 17:130-49

Subramanian V, Feng Y. 2007. A new role for angiogenin in neurite growth and pathfinding: implications for amyotrophic lateral sclerosis. *Hum Mol Genet* 16:1445-53

Sutedja NA, Sinke RJ, Van Vught PW, Van der Linden MW, Wokke JH, et al. 2007a. The association between H63D mutations in HFE and amyotrophic lateral sclerosis in a Dutch population. *Arch Neurol* 64:63-7

Sutedja NA, Veldink JH, Fischer K, Kromhout H, Wokke JH, et al. 2007b. Lifetime occupation, education, smoking, and risk of ALS. *Neurology* 69:1508-14

Suzuki H, Matsuoka M. 2011. Amyotrophic lateral sclerosis-linked mutant VAPB enhances TDP-43-induced motor neuronal toxicity. *J Neurochem* 119:1099-107

Swarup V, Phaneuf D, Bareil C, Robertson J, Rouleau GA, et al. 2011a. Pathological hallmarks of amyotrophic lateral sclerosis/frontotemporal lobar degeneration in transgenic mice produced with TDP-43 genomic fragments. *Brain* 134:2610-26

Swarup V, Phaneuf D, Dupre N, Petri S, Strong M, et al. 2011b. Deregulation of TDP-43 in amyotrophic lateral sclerosis triggers nuclear factor kappaB-mediated pathogenic pathways. *J Exp Med* 208:2429-47

Talbot K, Ansorge O. 2006. Recent advances in the genetics of amyotrophic lateral sclerosis and frontotemporal dementia: common pathways in neurodegenerative disease. *Hum Mol Genet* 15 Spec No 2:R182-7

Tan CF, Eguchi H, Tagawa A, Onodera O, Iwasaki T, et al. 2007. TDP-43 immunoreactivity in neuronal inclusions in familial amyotrophic lateral sclerosis with or without SOD1 gene mutation. *Acta Neuropathol* 113:535-42

Teng YD, Choi H, Huang W, Onario RC, Frontera WR, et al. 2006. Therapeutic effects of clenbuterol in a murine model of amyotrophic lateral sclerosis. *Neurosci Lett* 397:155-8

Teschendorf D, Link CD. 2009. What have worm models told us about the mechanisms of neuronal dysfunction in human neurodegenerative diseases? *Mol Neurodegener* 4:38

Ticozzi N, LeClerc AL, Keagle PJ, Glass JD, Wills AM, et al. 2010. Paraoxonase gene mutations in amyotrophic lateral sclerosis. *Ann Neurol* 68:102-7

Tiwari A, Hayward LJ. 2005. Mutant SOD1 instability: implications for toxicity in amyotrophic lateral sclerosis. *Neurodegener Dis* 2:115-27

Tomkins J, Usher P, Slade JY, Ince PG, Curtis A, et al. 1998. Novel insertion in the KSP region of the neurofilament heavy gene in amyotrophic lateral sclerosis (ALS). *Neuroreport* 9:3967-70

Topp JD, Gray NW, Gerard RD, Horazdovsky BF. 2004. Alsin is a Rab5 and Rac1 guanine nucleotide exchange factor. *J Biol Chem* 279:24612-23

Tortora GJ, Grabowski SR. 1996. *Principles of anatomy and physiology*. New York, NY: Harper Collins College

Town T, Nikolic V, Tan J. 2005. The microglial "activation" continuum: from innate to adaptive responses. *J Neuroinflammation* 2:24

Troost D, van den Oord JJ, de Jong JM, Swaab DF. 1989. Lymphocytic infiltration in the spinal cord of patients with amyotrophic lateral sclerosis. *Clin Neuropathol* 8:289-94

Tsai G, Lane HY, Yang P, Chong MY, Lange N. 2004. Glycine transporter I inhibitor, N-methylglycine (sarcosine), added to antipsychotics for the treatment of schizophrenia. *Biol Psychiatry* 55:452-6

Turner BJ, Ackerley S, Davies KE, Talbot K. 2010. Dismutase-competent SOD1 mutant accumulation in myelinating Schwann cells is not detrimental to normal or transgenic ALS model mice. *Hum Mol Genet* 19:815-24

Turner BJ, Talbot K. 2008. Transgenics, toxicity and therapeutics in rodent models of mutant SOD1-mediated familial ALS. *Prog Neurobiol* 85:94-134

Turner DA, Adamson DC. 2011. Neuronal-astrocyte metabolic interactions: understanding the transition into abnormal astrocytoma metabolism. *J Neuropathol Exp Neurol* 70:167-76

Turner MR, Cagnin A, Turkheimer FE, Miller CC, Shaw CE, et al. 2004. Evidence of widespread cerebral microglial activation in amyotrophic lateral sclerosis: an [11C](R)-PK11195 positron emission tomography study. *Neurobiol Dis* 15:601-9

Turner MR, Kiernan MC, Leigh PN, Talbot K. 2009. Biomarkers in amyotrophic lateral sclerosis. *Lancet Neurol* 8:94-109

Uchida A, Sasaguri H, Kimura N, Tajiri M, Ohkubo T, et al. 2012. Non-human primate model of amyotrophic lateral sclerosis with cytoplasmic mislocalization of TDP-43. *Brain* 135:833-46

Unno H, Uchida T, Sugawara H, Kurisu G, Sugiyama T, et al. 2006. Atomic structure of plant glutamine synthetase: a key enzyme for plant productivity. *J Biol Chem* 281:29287-96

Vaisman N, Lusaus M, Nefussy B, Niv E, Comaneshter D, et al. 2009. Do patients with amyotrophic lateral sclerosis (ALS) have increased energy needs? *J Neurol Sci* 279:26-9

Valdmanis PN, Kabashi E, Dyck A, Hince P, Lee J, et al. 2008. Association of paraoxonase gene cluster polymorphisms with ALS in France, Quebec, and Sweden. *Neurology* 71:514-20

van Straaten HW, He Y, van Duist MM, Labruyere WT, Vermeulen JL, et al. 2006. Cellular concentrations of glutamine synthetase in murine organs. *Biochem Cell Biol* 84:215-31

Vance C, Rogelj B, Hortobagyi T, De Vos KJ, Nishimura AL, et al. 2009. Mutations in FUS, an RNA processing protein, cause familial amyotrophic lateral sclerosis type 6. *Science* 323:1208-11

Vance JE. 1990. Phospholipid synthesis in a membrane fraction associated with mitochondria. *J Biol Chem* 265:7248-56

Vargas MR, Johnson DA, Johnson JA. 2011. Decreased glutathione accelerates neurological deficit and mitochondrial pathology in familial ALS-linked hSOD1(G93A) mice model. *Neurobiol Dis* 43:543-51

Vermeiren C, Hemptinne I, Vanhoutte N, Tilleux S, Maloteaux JM, Hermans E. 2006. Loss of metabotropic glutamate receptor-mediated regulation of glutamate transport in chemically activated astrocytes in a rat model of amyotrophic lateral sclerosis. *J Neurochem* 96:719-31

Vielhaber S, Kunz D, Winkler K, Wiedemann FR, Kirches E, et al. 2000. Mitochondrial DNA abnormalities in skeletal muscle of patients with sporadic amyotrophic lateral sclerosis. *Brain* 123 (Pt 7):1339-48

Vijayvergiya C, Beal MF, Buck J, Manfredi G. 2005. Mutant superoxide dismutase 1 forms aggregates in the brain mitochondrial matrix of amyotrophic lateral sclerosis mice. *J Neurosci* 25:2463-70

Voigt A, Herholz D, Fiesel FC, Kaur K, Muller D, et al. 2010. TDP-43-mediated neuron loss in vivo requires RNA-binding activity. *PLoS One* 5:e12247

Waldemar G, Vorstrup S, Jensen TS, Johnsen A, Boysen G. 1992. Focal reductions of cerebral blood flow in amyotrophic lateral sclerosis: a [99mTc]-d,l-HMPAO SPECT study. *J Neurol Sci* 107:19-28

Wallace C, Keast D. 1992. Glutamine and macrophage function. *Metabolism* 41:1016-20

Wang HY, Wang IF, Bose J, Shen CK. 2004a. Structural diversity and functional implications of the eukaryotic TDP gene family. *Genomics* 83:130-9

Wang L, Deng HX, Grisotti G, Zhai H, Siddique T, Roos RP. 2009. Wild-type SOD1 overexpression accelerates disease onset of a G85R SOD1 mouse. *Hum Mol Genet* 18:1642-51

Wang X, Arai S, Song X, Reichart D, Du K, et al. 2008. Induced ncRNAs allosterically modify RNA-binding proteins in cis to inhibit transcription. *Nature* 454:126-30

Wang XS, Lee S, Simmons Z, Boyer P, Scott K, et al. 2004b. Increased incidence of the Hfe mutation in amyotrophic lateral sclerosis and related cellular consequences. *J Neurol Sci* 227:27-33

Watanabe M, Dykes-Hoberg M, Culotta VC, Price DL, Wong PC, Rothstein JD. 2001. Histological evidence of protein aggregation in mutant SOD1 transgenic mice and in amyotrophic lateral sclerosis neural tissues. *Neurobiol Dis* 8:933-41

Weisskopf MG, McCullough ML, Calle EE, Thun MJ, Cudkowicz M, Ascherio A. 2004. Prospective study of cigarette smoking and amyotrophic lateral sclerosis. *Am J Epidemiol* 160:26-33

White RM, Sessa A, Burke C, Bowman T, LeBlanc J, et al. 2008. Transparent adult zebrafish as a tool for in vivo transplantation analysis. *Cell Stem Cell* 2:183-9

Wiedemann FR, Manfredi G, Mawrin C, Beal MF, Schon EA. 2002. Mitochondrial DNA and respiratory chain function in spinal cords of ALS patients. *J Neurochem* 80:616-25

Wijesekera LC, Leigh PN. 2009. Amyotrophic lateral sclerosis. *Orphanet J Rare Dis* 4:3

Willard-Mack CL, Koehler RC, Hirata T, Cork LC, Takahashi H, et al. 1996. Inhibition of glutamine synthetase reduces ammonia-induced astrocyte swelling in rat. *Neuroscience* 71:589-99

Williamson TL, Cleveland DW. 1999. Slowing of axonal transport is a very early event in the toxicity of ALS-linked SOD1 mutants to motor neurons. *Nat Neurosci* 2:50-6

Wilms CD, Hausser M. 2009. Lighting up neural networks using a new generation of genetically encoded calcium sensors. *Nat Methods* 6:871-2

Wils H, Kleinberger G, Janssens J, Pereson S, Joris G, et al. 2010. TDP-43 transgenic mice develop spastic paralysis and neuronal inclusions characteristic of ALS and frontotemporal lobar degeneration. *Proc Natl Acad Sci U S A* 107:3858-63

Windmueller HG, Spaeth AE. 1974. Uptake and metabolism of plasma glutamine by the small intestine. *J Biol Chem* 249:5070-9

Wismann J, Willoughby D. 2006. Gender differences in carbohydrate metabolism and carbohydrate loading. *J Int Soc Sports Nutr* 3:28-34

Wong PC, Pardo CA, Borchelt DR, Lee MK, Copeland NG, et al. 1995. An adverse property of a familial ALS-linked SOD1 mutation causes motor neuron disease characterized by vacuolar degeneration of mitochondria. *Neuron* 14:1105-16

Wu C. 1963. GLUTAMINE SYNTHETASE. II. THE INTRACELLULAR LOCALIZATION IN THE RAT LIVER. *Biochim Biophys Acta* 77:482-93

Xu YF, Gendron TF, Zhang YJ, Lin WL, D'Alton S, et al. 2010. Wild-type human TDP-43 expression causes TDP-43 phosphorylation, mitochondrial aggregation, motor deficits, and early mortality in transgenic mice. *J Neurosci* 30:10851-9

Yamamoto M, Mitsuma N, Inukai A, Ito Y, Li M, et al. 1999. Expression of GDNF and GDNFR-alpha mRNAs in muscles of patients with motor neuron diseases. *Neurochem Res* 24:785-90

Yamanaka K, Boillee S, Roberts EA, Garcia ML, McAlonis-Downes M, et al. 2008a. Mutant SOD1 in cell types other than motor neurons and oligodendrocytes accelerates onset of disease in ALS mice. *Proc Natl Acad Sci U S A* 105:7594-9

Yamanaka K, Chun SJ, Boillee S, Fujimori-Tonou N, Yamashita H, et al. 2008b. Astrocytes as determinants of disease progression in inherited amyotrophic lateral sclerosis. *Nat Neurosci* 11:251-3

Yang L, Embree LJ, Tsai S, Hickstein DD. 1998. Oncoprotein TLS interacts with serine-arginine proteins involved in RNA splicing. *J Biol Chem* 273:27761-4

Yang S, Warraich ST, Nicholson GA, Blair IP. 2010. Fused in sarcoma/translocated in liposarcoma: a multifunctional DNA/RNA binding protein. *Int J Biochem Cell Biol* 42:1408-11

Yang Y, Hentati A, Deng HX, Dabbagh O, Sasaki T, et al. 2001. The gene encoding alsin, a protein with three guanine-nucleotide exchange factor domains, is mutated in a form of recessive amyotrophic lateral sclerosis. *Nat Genet* 29:160-5

Yoo YE, Ko CP. 2012. Dihydrotestosterone ameliorates degeneration in muscle, axons and motoneurons and improves motor function in amyotrophic lateral sclerosis model mice. *PLoS One* 7:e37258

Zelko IN, Mariani TJ, Folz RJ. 2002. Superoxide dismutase multigene family: a comparison of the CuZn-SOD (SOD1), Mn-SOD (SOD2), and EC-SOD (SOD3) gene structures, evolution, and expression. *Free Radic Biol Med* 33:337-49

Zetterstrom P, Andersen PM, Brannstrom T, Marklund SL. 2011a. Misfolded superoxide dismutase-1 in CSF from amyotrophic lateral sclerosis patients. *J Neurochem* 117:91-9

Zetterstrom P, Graffmo KS, Andersen PM, Brannstrom T, Marklund SL. 2011b. Proteins that bind to misfolded mutant superoxide dismutase-1 in spinal cords from transgenic amyotrophic lateral sclerosis (ALS) model mice. *J Biol Chem* 286:20130-6

Zetterstrom P, Stewart HG, Bergemalm D, Jonsson PA, Graffmo KS, et al. 2007. Soluble misfolded subfractions of mutant superoxide dismutase-1s are enriched in spinal cords throughout life in murine ALS models. *Proc Natl Acad Sci U S A* 104:14157-62

Zhang X, Chen S, Li L, Wang Q, Le W. 2008. Folic acid protects motor neurons against the increased homocysteine, inflammation and apoptosis in SOD1 G93A transgenic mice. *Neuropharmacology* 54:1112-9

Zhong Z, Deane R, Ali Z, Parisi M, Shapovalov Y, et al. 2008. ALS-causing SOD1 mutants generate vascular changes prior to motor neuron degeneration. *Nat Neurosci* 11:420-2

Zhou H, Huang C, Chen H, Wang D, Landel CP, et al. 2010. Transgenic rat model of neurodegeneration caused by mutation in the TDP gene. *PLoS Genet* 6:e1000887

Zinszner H, Albalat R, Ron D. 1994. A novel effector domain from the RNA-binding protein TLS or EWS is required for oncogenic transformation by CHOP. *Genes Dev* 8:2513-26

Zinszner H, Sok J, Immanuel D, Yin Y, Ron D. 1997. TLS (FUS) binds RNA in vivo and engages in nucleo-cytoplasmic shuttling. *J Cell Sci* 110 (Pt 15):1741-50

Zoccolella S, Beghi E, Palagano G, Fraddosio A, Samarelli V, et al. 2006. Predictors of delay in the diagnosis and clinical trial entry of amyotrophic lateral sclerosis patients: a population-based study. *J Neurol Sci* 250:45-9

Zou J, Wang YX, Dou FF, Lu HZ, Ma ZW, et al. 2010. Glutamine synthetase down-regulation reduces astrocyte protection against glutamate excitotoxicity to neurons. *Neurochem Int* 56:577-84

ABSTRACT

UNDERSTANDING THE GENDER-BASED MECHANISM OF MSO IN ALS MICE: A METABOLIC CHARACTERIZATION OF THE SOD1-G93A MOUSE MODEL

by

MONICA A. BAME

December 2012

Advisor: Dr. William Brusilow

Major: Biochemistry and Molecular Biology

Degree: Doctor of Philosophy

Amyotrophic Lateral Sclerosis (ALS) is a devastating neurodegenerative disease characterized by motor neuron death and a corresponding loss of neuromuscular connections resulting in muscle atrophy. Patients become paralyzed shortly after symptom onset and typically die within one to five years of pulmonary complications. ALS is a relatively rare disease, with an overall incidence of approximately 2 in 100,000 people per year and a prevalence of about 5 in 100,000 people. It is typically associated with increasing age and has a slight male prevalence, with a male to female ratio of approximately 3:2. ALS is classified as either familial (the less common form of the disease that has a hereditary component) or sporadic (the more common form that has no identifiable genetic component), with both forms of the disease exhibiting a great deal of heterogeneity with respect to causes and underlying molecular mechanisms. A wide variety of gene mutations have been associated with both forms of ALS, including mutations in superoxide dismutase 1 (SOD1), TDP-43, and FUS, as well as several other genes that have yet to be identified. These genes encode a variety of proteins that encompass several processes within the cell, leading to an array of molecular

mechanisms that can become dysfunctional during pathogenesis. These mechanisms include, glutamate excitotoxicity, mitochondrial dysfunction and oxidative stress, dysfunctional protein quality control, aberrant mRNA processing, neurotrophic factor dysregulation, and neuroinflammation. ALS is difficult to diagnose due to the heterogeneity of symptoms exhibited by patients and the lack of reliable biomarkers of the disease. As a result, a positive diagnosis typically takes up to a year from symptom onset, at which time a significant amount of irreversible damage has occurred.

Since ALS is a neurodegenerative disease, most research focuses on the central nervous system, however data obtained from ALS patients and animal models suggests that there are metabolic abnormalities associated with the disease. The experiments conducted in this study first examined gender differences in the survival response to an irreversible inhibitor of glutamine synthetase, L-methionine sulfoximine (MSO), which targets excitotoxicity using the SOD1-G93A transgenic mouse model of ALS. Human studies have shown that there are gender differences in basic metabolism, and studies of drug metabolism in rats and humans suggest that males and females may respond differently to treatment. The results of these experiments show that female SOD1 mice respond better to MSO treatment, showing both an extension in the average lifespan as well as improved neuromuscular function with MSO treatment. In addition, ovariectomy removes the beneficial effects of MSO treatment on both survival and neuromuscular function. The second portion of this study was designed to test the hypothesis that the SOD1 mutation disrupts nitrogen metabolism, specifically the urea cycle. The results of these studies show that untreated presymptomatic SOD1 mice have altered nitrogen metabolism and show decreased levels of several urea cycle intermediates in the plasma compared to their wild-type counterparts. These plasma metabolites also show gender-specific differences in wild-type and SOD1 mice, supporting the idea that male and female mice have differences in metabolism. Plasma metabolites change with age and suggest that there

are compensatory mechanisms that aid in normalizing plasma metabolites in SOD1 mice. Again, these metabolites show gender-specificity and MSO treatment normalizes the levels of these metabolites in a gender-specific fashion in SOD1 mice. Studies of nitrogen handling enzymes also show that there are gender-specific differences in CPSI activity levels that are not associated with expression of the transgene. Male SOD1 mice begin to show changes in nitrogen handling enzymes in the liver, specifically glutamine synthetase and CPSI, suggesting that males may begin to experience alterations in nitrogen metabolism prior to symptom onset that may help to explain the gender-specific effects of MSO treatment in this mouse model.

AUTOBIOGRAPHICAL STATEMENT

Monica Bame obtained her B.S. with a major in psychology and a minor in biology from Eastern Michigan University in 2002. While working on her degree she developed an interest in neuroscience and decided to pursue a B.S. in professional biochemistry to gain a better understanding of neurochemistry in order to pursue a career in neuroscience research. She obtained her B.S. in professional biochemistry in 2006 from Eastern Michigan University, working with both Dr. Elizabeth Butch and Dr. Hedeel Evans. In 2007, Monica began her doctoral studies at Wayne State University under the mentorship of Dr. William Brusilow. She graduated with her Ph.D. in Biochemistry and Molecular Biology in 2012.